

**Synthesis and Characterisation of Novel Phenanthroline Quinone Derivatives
and their Evaluation as Alzheimer's Disease Therapeutic Active Ingredients**



Seta Azad Tosonyan

This thesis is submitted in fulfilment of the requirements for the degree of

Doctor of Philosophy

Faculty of Science

School of Mathematical and Physical Sciences

Department of Chemistry

University of Technology Sydney

February 2018

CERTIFICATE OF AUTHORSHIP/ORIGINALITY

I, Seta Tosonyan, certify that the work in this thesis has not been previously submitted for a degree nor has it been submitted as part of requirements for a degree.

I also certify that the thesis has been written by myself. Any assistance that I have received in my research work and the preparation of the thesis itself has been acknowledged. Furthermore, I certify that all information sources and literature used are indicated in the thesis.

Production Note:

Signature removed prior to publication.

Seta Tosonyan

February 2018

ACKNOWLEDGEMENTS

I take this opportunity to express my sincere gratitude and special appreciation to my Principal supervisor, Dr. Shanlin Fu and co supervisor Dr. Ronald Shimmon and Prof. Anthony Baker, Without whose invaluable guidance, motivation and support throughout my research including the drafting of this thesis, the accomplishment of this project would not have been possible. They shown immense patience and have never deterred from sharing their knowledge and support whenever required. Their efforts in improving my skills with proof reading and scientific writing were remarkably fruitful. I could not have imagined having a better advisors and mentors for my PhD study.

Dr. Ronald's guidance and advice during the experimental laboratory part are greatly appreciated. He has been instrumental in getting me trained and competent with advanced analytical techniques mainly in NMR spectroscopy his main field of expertise. He stands for me as an epitome of humility with brains.

I am grateful to Susan Shimmon for her guidance and advice while fulfilling the biological study.

I take this opportunity to express my deepest gratitude to Dr. Costa Conn, for his continuous support and valuable discussions with a keen eye in the prodrug docking investigation guidance,

Thanks are also expressed to Dr. Linda Xiao and to Dr. Regina Verena Taudte and to my postgraduate colleagues for their generous assistance and valuable discussions during my research studies.

Special and sincere thanks are expressed to my husband Surein and My father Azad and all my family, who have standby in my good and bad times and have continuously encouraged and supported me throughout my PhD task. This thesis is dedicated to them.

Finally, the generous financial support and scholarship of the Iraqi ministry of higher education and scientific research and Basra University is sincerely acknowledged.

ABSTRACT

The study is based on the synthesis, characterisation and biological evaluation of series of new derivatives of phen-5,6-dione potentially could act as inhibitors for acetylcholinesterase (AChE) from electric eel and butyrylcholinesterase (BuChE) from equus horse serum and as an active pharmacophore inhibitors of acetylcholinesterase and butyrylcholinesterase.

Twenty four derivatives of phen-5,6-dione were prepared including imine-Schiff based of phen-5,6-dione and 2-amino phenol as mono and di substituted active ingredient, condensation products of phen-5,6-dione with thiosemicarbazide, semicarbazide hydrochloride, hydroxylamine hydrochloride, aminoguanidine hydrochloride, aminoguanidine bicarbonate, 4-methyl-3-thiosemicarbazide, 2-methyl-3-thiosemicarbazide, 4-methyl-3-thiosemicarbazide, 4,4-di methyl-3-thiosemicarbazide, 4-ethyl-3-thiosemicarbazide, 4-phenyl-3-Thiosemicarbazide, ethylenediamine, hydrazine sulfate, o-nitro aniline, diethylamine carbamyl chloride, o-phenylenediamine and benzyl amine. All the prepared compounds were characterised by various advanced techniques: ^1H NMR, ^{13}C NMR, FT-IR, ATR and HRMS and digital melting point.

Ellman Assays were performed with acetylthiocholine iodide (ATCI) and s-butyrylthiocholine iodide (BTCl) as the substrate, using Galantamine and Tacrine, well-known AChE and BuChE inhibitors as the positive controls. IC_{50} for the prepared compounds were determined. The study includes determination of several important kinetic parameters such as type of inhibition (Competitive) and Inhibition constant (K_i). The inhibition mechanism for determination of the activity of both AChE and BuChE inhibitors were extracted from Lineweaver- Burk plots and Dixon plots.

Furthermore the drug-like properties were assessed based on Lipinski five rules and by utilising ADMET properties such as Aqueous solubility, Blood-brain barrier (BBB), CYP2D6 binding, Hepatotoxicity, Intestinal Absorption and PPB descriptors for each of studied compounds. Furthermore all the prepared active ingredients were sent for screening at QLD University.

The simulation studies for molecular modelling of the obtained experimental results were assimilated with implementing Accelrys Discovery Studio 4.5 suite. The obtained data from the docking study were used for analysing the biological properties obtained in this study and some suggestions are stated.

We found ability of the prepared compounds as active ingredient as chelating ligands to form complexes with Cu^{+2} and Zn^{+2} were investigated using UV–Vis spectroscopy. Similarities in absorption spectra including π – π^* intra ligand transitions and a strong metal –ligand charge transfer (MLCT) in the visible region were observed. The obtained results support the idea that the phen-5,6-dione structure and electronic properties of these ligands incorporate features of both diamine and quinone ligands. These characteristics may be beneficial in decreasing the rate of cognitive decline in moderate to severe AD patients.

This technique may provide useful information to investigators with relation to chemical profiling of drug seizures, however its use should be limited to that of a screening method.

This technique demonstrate that a rational structure based on phen-5,6-dione derivatives can generate a molecules that can target modulate multiple factors, and provide a new tool to investigate Alzheimer’s disease.

List of Abbreviations

[M+H] ⁺	Protonated molecular ion
2D-NMR	2 Dimensional Nuclear Magnetic Resonance
3D	3 Dimensional structure
ACh	Acetylcholine
AChE	Acetylcholinesterase
AChEIs	Acetylcholinesterase inhibitors
AD	Alzheimer's disease
APP	Amyloid precursor protein
Ar	Aromatic
A β	Amyloid beta
ATCI	Acetylthiocholine iodide
BBB	Blood-brain barrier
BTCI	S-butyrylthiocholine iodide
BuChE	Butyrylcholinesterase
CAS	Catalytic active site
CDCl ₃	Deuterated chloroform
ChE	Cholinesterase
ChEI	Cholinesterase inhibitor
CNS	Central nervous system
CT	Cerebral tomography
dd	Doublet of doublets (NMR)
d	Doublet (NMR)
DMF	Dimethylformamide
DMSO	Dimethyl sulfoxide
DMSO-d ₆	Deuterated Dimethyl sulfoxide
FDA	Food and Drug Administration
HRMS	High resolution mass spectroscopy
Hz	Hertz
IR	Infrared
<i>J</i>	coupling constant (NMR)

m	Multiplet (NMR)
m.p.	Melting point
m/z	Mass to charge ratio
MAO	Monoamine oxidase
mg	Milligrams
mL	Millilitre
ML	Multifunctional Ligand
mmol	Millimol
MTDLs	Multi-target-directed ligands
MW	Molecular weight
NMR	Nuclear Magnetic Resonance
phen	1,10-phenanthroline
PAS	Peripheral anionic site
phen-5,6-dione	1,10-phenanthroline-5,6-dione
R	Alkyl
Ar	Aryl
ROS	Reactive oxygen species
τ	Tau protein
TcAChE	Torpedo California Acetylcholinesterase
TLC	Thin layer chromatography
δ	Chemical Shift (NMR)
FDA	Food and drug administration
kD	kilo Dalton
q	Quartet
t	Triplet

List of Figures

Figure 1: The amyloid cascade process enhancing the role of metal ions	5
Figure 2: Multifunctional small molecules that can be used to investigate Cu(II)/Zn(II)-associated A β species in AD by combining properties of A β interaction, metal chelation, and ROS regulation	9
Figure 3: Synthetic Route to ML	9
Figure 4: Basic features of resveratrol and clioquinol provides molecules with multifunctionality (metal chelation, A β interaction and antioxidant)	11
Figure 5: Design routes for compounds (3-5)	13
Figure 6: Design strategy for resveratrol derivatives as multi targeted active ingredient for AD treatment	15
Figure 7: Typical Acetylcholinesterase inhibitors	17
Figure 8: Schematic representation for Acetylcholinesterase.....	19
Figure 9: Catalytic triad of AChE formed by serine, histidine and glutamate residues. Note the basicity of the serine OH is increased by the glutamate ion, via the histidine. The product shown as arising from the reaction with acetylcholine is actually the intermediate. A. Hydrolysis of the acetylated serine recycles the enzyme. B. Phosphate ester formed by sarin. C. Carbamoylated serine arising from exposure to neostigmine.....	88
Figure 10: Torpedo AChE showing spatial relationship between PAS, active site and postulated A β binding site.....	89
Figure 11: Lineweaver Burk plot for inhibition of compound ST03.....	102
Figure 12: Lineweaver Burk plot for inhibition of compound ST06.....	102
Figure 13: Lineweaver Burk plot for inhibition of compound ST07.....	103
Figure 14: Lineweaver Burk plot for inhibition of compound ST09.....	103
Figure 15: Lineweaver Burk plot for inhibition of compound ST20.....	104
Figure 16: Lineweaver Burk plot for inhibition of compound ST21.....	104
Figure 17: Lineweaver Burk plot for inhibition of compound ST24.....	105
Figure 18: Lineweaver Burk plot for inhibition of compound ST06.....	105
Figure 19: Lineweaver Burk plot for inhibition of compound ST07.....	106
Figure 20: Lineweaver Burk plot for inhibition of compound ST09.....	106
Figure 21: Lineweaver Burk plot for inhibition of compound ST20.....	107
Figure 22: Lineweaver Burk plot for inhibition of compound ST21.....	107
Figure 23: Lineweaver Burk plot for inhibition of compound ST24.....	108
Figure 24: Dixon plot for the inhibitory effect of compound ST03.....	108
Figure 25: Dixon plot for the inhibitory effect of compound ST06.....	109
Figure 26: Dixon plot for the inhibitory effect of compound ST07.....	109
Figure 27: Dixon plot for the inhibitory effect of compound ST09.....	110
Figure 28: Dixon plot for the inhibitory effect of compound ST20.....	110
Figure 29: Dixon plot for the inhibitory effect of compound ST21.....	111
Figure 30: Dixon plot for the inhibitory effect of compound ST24.....	111
Figure 31: Dixon plot for the inhibitory effect of compound ST06.....	112
Figure 32: Dixon plot for the inhibitory effect of compound ST07.....	112
Figure 33: Dixon plot for the inhibitory effect of compound ST09.....	113
Figure 34: Dixon plot for the inhibitory effect of compound ST20.....	113
Figure 35: Dixon plot for the inhibitory effect of compound ST21.....	114

Figure 36: Dixon plot for the inhibitory effect of compound ST24.....	114
Figure 37: 2D-representation of the highest scoring pose of Aflatoxin B1 with 2xi4 protein.....	126
Figure 38: Binding interactions of the highest scoring pose of Aflatoxin B1 with 2xi4 protein.....	126
Figure 39: 2D-representation of the highest scoring pose of ST-06 with 2xi4 protein.....	127
Figure 40: Binding interactions of the highest scoring pose of ST-06 with 2xi4 protein.....	127
Figure 41: 2D-representation of the highest scoring pose of ST-08 with 2xi4 protein.....	128
Figure 42: Binding interactions of the highest scoring pose of ST-08 with 2xi4 protein.....	128
Figure 43: UV-Vis spectra of the ST01 at 25 uM at different concentration of Cu ⁺²	142
Figure 44: UV-Vis spectra of the ST01 at 25 uM at different concentration of Zn ⁺²	142
Figure 45: UV-Vis spectra of the ST02 at 25 uM at different concentration of Cu ⁺²	143
Figure 46: UV-Vis spectra of the ST02 at 25 uM at different concentration of Zn ⁺²	143
Figure 47: UV-Vis spectra of the ST03 at 25 uM at different concentration of Cu ⁺²	143
Figure 48: UV-Vis spectra of the ST03 at 25 uM at different concentration of Zn ⁺²	144
Figure 49: UV-Vis spectra of the ST04 at 25 uM at different concentration of Cu ⁺²	144
Figure 50: UV-Vis spectra of the ST04 at 25 uM at different concentration of Zn ⁺²	144
Figure 51: UV-Vis spectra of the ST05 at 25 uM at different concentration of Cu ⁺²	145
Figure 52: UV-Vis spectra of the ST05 at 25 uM at different concentration of Zn ⁺²	145
Figure 53: UV-Vis spectra of the ST06 at 25 uM at different concentration of Cu ⁺²	146
Figure 54: UV-Vis spectra of the ST06 at 25 uM at different concentration of Zn ⁺²	146
Figure 55: UV-Vis spectra of the ST07 at 25 uM at different concentration of Cu ⁺²	146
Figure 56: UV-Vis spectra of the ST07 at 25 uM at different concentration of Zn ⁺²	147
Figure 57: UV-Vis spectra of the ST08 at 25 uM at different concentration of Cu ⁺²	147
Figure 58: UV-Vis spectra of the ST08 at 25 uM at different concentration of Zn ⁺²	147
Figure 59: UV-Vis spectra of the ST09 at 25 uM at different concentration of Cu ⁺²	148
Figure 60: UV-Vis spectra of the ST09 at 25 uM at different concentration of Zn ⁺²	148
Figure 61: UV-Vis spectra of the ST10 at 25 uM at different concentration of Cu ⁺²	148
Figure 62: UV-Vis spectra of the ST10 at 25 uM at different concentration of Zn ⁺²	149
Figure 63: UV-Vis spectra of the ST11 at 25 uM at different concentration of Cu ⁺²	149
Figure 64: UV-Vis spectra of the ST11 at 25 uM at different concentration of Zn ⁺²	149
Figure 65: UV-Vis spectra of the ST012 at 25 uM at different concentration of Cu ⁺²	150
Figure 66: UV-Vis spectra of the ST12 at 25 uM at different concentration of Zn ⁺²	150
Figure 67: UV-Vis spectra of the ST13 at 25 uM at different concentration of Cu ⁺²	150
Figure 68: UV-Vis spectra of the ST13 at 25 uM at different concentration of Zn ⁺²	151
Figure 69: UV-Vis spectra of the ST14 at 25 uM at different concentration of Cu ⁺²	151
Figure 70: UV-Vis spectra of the ST14 at 25 uM at different concentration of Zn ⁺²	151
Figure 71: UV-Vis spectra of the ST15 at 25 uM at different concentration of Cu ⁺²	152
Figure 72: UV-Vis spectra of the ST15 at 25 uM at different concentration of Zn ⁺²	152
Figure 73: UV-Vis spectra of the ST16 at 25 uM at different concentration of Cu ⁺²	152
Figure 74: UV-Vis spectra of the ST016 at 25 uM at different concentration of Zn ⁺²	153
Figure 75: UV-Vis spectra of the ST17 at 25 uM at different concentration of Cu ⁺²	153
Figure 76: UV-Vis spectra of the ST017 at 25 uM at different concentration of Zn ⁺²	153
Figure 77: UV-Vis spectra of the ST18 at 25 uM at different concentration of Cu ⁺²	154
Figure 78: UV-Vis spectra of the ST18 at 25 uM at different concentration of Zn ⁺²	154
Figure 79: UV-Vis spectra of the ST19 at 25 uM at different concentration of Cu ⁺²	154
Figure 80: UV-Vis spectra of the ST19 at 25 uM at different concentration of Zn ⁺²	155

Figure 81: UV-Vis spectra of the ST 20 at 25 uM at different concentration of Cu ⁺²	155
Figure 82: UV-Vis spectra of the ST20 at 25 uM at different concentration of Zn ⁺²	155
Figure 83: UV-Vis spectra of the ST21 at 25 uM at different concentration of Cu ⁺²	156
Figure 84: UV-Vis spectra of the ST21 at 25 uM at different concentration of Zn ⁺²	156
Figure 85: UV-Vis spectra of the ST22 at 25 uM at different concentration of Cu ⁺²	157
Figure 86: UV-Vis spectra of the ST22 at 25 uM at different concentration of Zn ⁺²	157
Figure 87: UV-Vis spectra of the ST23 at 25 uM at different concentration of Cu ⁺²	157
Figure 88: UV-Vis spectra of the ST23 at 25 uM at different concentration of Zn ⁺²	158
Figure 89: UV-Vis spectra of the ST24 at 25 uM at different concentration of Cu ⁺²	158
Figure 90: UV-Vis spectra of the ST24 at 25 uM at different concentration of Zn ⁺²	158
Figure 91: Binding interactions of the highest scoring pose of ST-01 with 2xi4 protein	195
Figure 92: Binding interactions of the highest scoring pose of ST-02 with 2xi4 protein	195
Figure 93: Binding interactions of the highest scoring pose of ST-03 with 2xi4 protein	196
Figure 94: Binding interactions of the highest scoring pose of ST-04 with 2xi4 protein	196
Figure 95: Binding interactions of the highest scoring pose of ST-05 with 2xi4 protein	197
Figure 96: Binding interactions of the highest scoring pose of ST-06 with 2xi4 protein	197
Figure 97: Binding interactions of the highest scoring pose of ST-07 with 2xi4 protein	198
Figure 98: Binding interactions of the highest scoring pose of ST-08 with 2xi4 protein	198
Figure 99: Binding interactions of the highest scoring pose of ST-09 with 2xi4 protein	199
Figure 100: Binding interactions of the highest scoring pose of ST-10 with 2xi4 protein	199
Figure 101: Binding interactions of the highest scoring pose of ST-11 with 2xi4 protein	200
Figure 102: Binding interactions of the highest scoring pose of ST-12 with 2xi4 protein	200
Figure 103: Binding interactions of the highest scoring pose of ST-13 with 2xi4 protein	201
Figure 104: Binding interactions of the highest scoring pose of ST-14 with 2xi4 protein	201
Figure 105: Binding interactions of the highest scoring pose of ST-15 with 2xi4 protein	202
Figure 106: Binding interactions of the highest scoring pose of ST-16 with 2xi4 protein	202
Figure 107: Binding interactions of the highest scoring pose of ST-17 with 2xi4 protein	203
Figure 108: Binding interactions of the highest scoring pose of ST-18 with 2xi4 protein	203
Figure 109: Binding interactions of the highest scoring pose of ST-19 with 2xi4 protein	204
Figure 110: Binding interactions of the highest scoring pose of ST-20 with 2xi4 protein	204
Figure 111: Binding interactions of the highest scoring pose of ST-21 with 2xi4 protein	205
Figure 112: Binding interactions of the highest scoring pose of ST-22 with 2xi4 protein	205
Figure 113: Binding interactions of the highest scoring pose of ST-23 with 2xi4 protein	206
Figure 114: Binding interactions of the highest scoring pose of ST-24 with 2xi4 protein	206

List of Schemes

Scheme 1: Showing the action for metal chaperones in AD A β metal interactions mechanism that drive A β aggregation showing the action for metal chaperones in AD A β metal interactions mechanism that drive A β aggregation	10
Scheme 2: Structure scheme of imine resveratrol analogues and chemical structure of the investigated compounds	11
Scheme 3: General Schiff base reaction scheme.....	27
Scheme 4: Chemical mechanism of Ellman's method	32
Scheme 5: Preparation of Mono and Di condensate Schiff base.....	70
Scheme 6: Intermolecular H-bonding of p-aminophenol.....	73
Scheme 7: Reaction scheme for the preparation of di thiosemicarbazone by indirect substitution procedure.....	80
Scheme 8: Hydrolysis of acetylcholine(ACh)catalysed by AChE	90
Scheme 9: Hydrolyses of AChE and BuChE	90

List of Tables

Table 1: Clinical status of cholinesterase inhibitors with putative neuroprotective or disease-modifying actions.....	17
Table 2: The IC_{50} for the 1,10-phenanthroline-5,6-dione derivatives in μM	96
Table 3: Kinetic analysis of active compounds.....	115
Table 4: Estimated physical Drug-Like Properties based on Lipinski five rules for the phen-5,6-dione derivatives	118
Table 5: ADMET results for the phen-5,6-dione derivatives.....	120
Table 6: Docking study of the 1,10-phenanthroline-5,6-dione derivatives to the $2x_4$ receptor protein.	124
Table 7: Typical UV-Vis spectral characteristic of phen-5,6-dione derivatives and there complexes with Cu^{+2} and Zn^{+2} extracted from Figures 43-90.....	159

Contents

Chapter 1 Introduction	1
1.1 Condensed summary of Alzheimer's diseases	1
1.2 Enzymes involved in Alzheimer's disease	4
1.2.1 Cholinesterases	4
1.2.2 Acetylcholinesterase	4
1.2.3 Butyrylcholinesterase	4
1.2.4 Secretases	5
1.3 Blood Brain Barrier	6
1.4 Products used as therapeutic agents to treat Alzheimer's disease	6
1.5 Pharmacological Approach	11
1.6 Multi-target-directed ligands (MTDLs)	12
1.7 Acetylcholinesterase inhibitors	16
1.7.1 Cholinergic Drug Therapy	20
1.7.2 Cholinergic Hypothesis	21
1.7.3 Cholinesterases	21
1.7.4 Clinical use of enzyme inhibitors to Alzheimer's Disease	22
1.7.5 Functions of AChE	23
1.7.6 Binding sites of AChE	23
1.7.7 Butyrylcholinesterase	23
1.7.8 BuChE inhibitors	24
1.8 Structure-based Design	24
1.9 Molecular modelling studies	25
1.10 Applications of Docking	26
2. Coordination studies	26
3. Schiff base	27
3.1 Schiff base reaction	27
4. Chemistry of phen-5,6-dione	28
4.1 Coordination chemistry of phen-5,6-dione complex	29
4.2 The biological study of phen-5,6-dione	30
5. Treatment basis of Alzheimer's disease	31
6. Significance of the project	33
7. Aim of project	33
8. References	34
Chapter 2 Synthesis and characterisation of the new phen-5,6-dione derivatives	48

2.1 Introduction	48
2.2 Materials and techniques	49
2.2.1 Thin Layer Chromatography (TLC)	49
2.2.2 Nuclear Magnetic Resonance (NMR) Spectroscopy :Hydrogen (¹ H) NMR Spectra	49
2.2.3 Carbon (¹³ C) NMR Spectra.....	50
2.2.4 High-Resolution Mass Spectrometry (HRMS).....	50
2.2.5 Infrared Spectroscopy	50
2.2.6 Melting Points.....	50
2.3 Synthesis and characterization	51
2.3.1. Synthesis of phen-5,6-dione (phen-5,6-dione) ST01	51
2.3.2. Synthesis (6 <i>E</i>)-6-[(2-hydroxyphenyl)imino]-1,10-phenanthroline-5(6 <i>H</i>)-one (ST02).....	52
2.3.3. Synthesis of [2,2'-[1,10-phenanthroline-5,6-diylidenedi(<i>E</i>) azanylylidene]diphenol] (ST03)	53
2.3.4. Synthesis of (6 <i>E</i>)-6-(hydroxyimino)-1,10-phenanthroline-5(6 <i>H</i>)-one (ST04).....	54
2.3.5. Synthesis of <i>N,N'</i> -1,10-phenanthroline-5,6-dihyridenedihydroxylamine (ST05).....	54
2.3.6. Synthesis of (2 <i>E</i>)-2-(6-oxo-1,10-phenanthroline-5(6 <i>H</i>)-ylidene) hydrazinecarboxamide (ST06)	55
2.3.7. Synthesis of phen[5,6- <i>e</i>]-1,2,4-triazin-3-one (ST07).....	56
2.3.8. Synthesis of dual function (2 <i>E</i>)-2-[(6 <i>E</i>)-6-(hydroxyimino)-1,10-phenanthroline-5(6 <i>H</i>)-ylidene]hydrazine-1-carboxamide (ST08)	56
2.3.9. Synthesis of (2 <i>E</i>)-2-(6-oxo-6,10b-dihydro-1,10-phenanthroline-5(4 <i>aH</i>)-ylidene)hydrazinecarboximidamide (ST09).....	57
2.3.10. Synthesis of Amino-1,2,4-triazin[5,6- <i>f</i>]1,10-phenanthroline (ST10)	58
2.3.11. Synthesis of (2 <i>E</i>)-2-(6-oxo-1,10-phenanthroline-5(6 <i>H</i>)-ylidene)hydrazinecarbothioamide (ST11)	58
2.3.12. Synthesis of (2 <i>E</i>)- <i>N</i> -methyl-2-(6-oxo-1,10-phenanthroline-5(6 <i>H</i>)-ylidene)hydrazine-1-carbothioamide (ST12)	59
2.3.13. Synthesis of (2 <i>E</i>)-1-methyl-2-(6-oxo-1,10-phenanthroline-5(6 <i>H</i>)-ylidene)hydrazine-1-carbothioamide(ST13)	60
2.3.14. Synthesis of (2 <i>E</i>)- <i>N,N</i> -dimethyl-2-(6-oxo-1,10-phenanthroline-5(6 <i>H</i>)-ylidene)hydrazine-1-carbothioamide (ST14)	61
2.3.15. Synthesis of (2 <i>E</i>)- <i>N</i> -ethyl-2-(6-oxo-1,10-phenanthroline-5(6 <i>H</i>)-ylidene)hydrazinecarbothioamide (ST15).....	62
2.3.16. Synthesis of (2 <i>E</i>)-2-(6-oxo-1,10-phenanthroline-5(6 <i>H</i>)-ylidene)- <i>N</i> -phenylhydrazine-1-carbothioamide(ST16)	63
2.3.17. Synthesis of [1,2,4]triazino[5,6- <i>f</i>][1,10]phenanthroline-3(2 <i>H</i>)-thione (ST17)	64
2.3.18. Synthesis of (2 <i>E</i>)-2-[(6 <i>E</i>)-6-(hydroxyimino)-1,10-phenanthroline-5(6 <i>H</i>)-ylidene]- <i>N</i> -methylhydrazine-1-carbothioamide (ST18).....	64

2.3.19. Synthesis of quinoxalino[2,3-f][1,10]phenanthroline (ST19).....	65
2.3.20. Synthesis of (6 <i>E</i>)-6-[(2-nitrophenyl)imino]-1,10-phenanthroline-5(6 <i>H</i>)-one(ST20).....	66
2.3.21. Synthesis of phen-5,6-diol (ST21)	67
2.3.22. Synthesis of (6 <i>E</i>)-6-(benzylimino)-1,10-phenanthroline-5(6 <i>H</i>)-one(ST22).....	67
2.3.23. Synthesis of (6 <i>Z</i>)-6-[[diethylcarbamoyl]oxy]imino}-1,10-phenanthroline-5(6 <i>H</i>)-one(ST23)	68
2.3.24. Synthesis of pyrazino[2,3-f][1, 10]phenanthroline (ST24).....	69
2.4: Results and discussion:	69
2.4.1: Synthesis of the mono substituted Schiff base (6 <i>E</i>)-6-[(2-hydroxyphenyl) imino]-1,10-phenanthroline-5(6 <i>H</i>)-one (ST02)	69
2.4.2 Preparation of [2,2'-[1,10-phenanthroline-5,6 diylidenedi(<i>E</i>) azanylylidene] diphenol] (ST03)	71
2.4.3 Preparation of quinoxalino[2,3-f][1,10]phenanthroline (ST19).....	74
2.4.4 Preparation of (6 <i>E</i>)-6-[(2-nitrophenyl)imino]-1,10-phenanthroline-5(6 <i>H</i>)-one(ST20).....	74
2.4.5 Preparation of pyrazino[2,3-f][1, 10]phenanthroline (ST24).....	75
2.4.6 Preparation of (6 <i>E</i>)-6-(hydroxyimino)-1,10-phenanthroline-5(6 <i>H</i>)-one (ST04).....	76
2.4.7 Preparation of the condensation product of 5,6-dione with semicarbazide	77
2.4.8 Preparation of dual function (2 <i>E</i>)-2-[(6 <i>E</i>)-6-(hydroxyimino)-1,10-phenanthroline-5(6 <i>H</i>)-ylidene]hydrazine-1-carboxamide (ST08)	78
2.4.9 Preparation of 5,6-dione -thiosemicarbazide derivative	78
2.4.10 Preparation of cyclic thiosemicarbazone derivatives of phen-5,6-dione (ST017).....	81
2.4.11 Preparation of (2 <i>E</i>)-2-(6-oxo-6,10b-dihydro-1,10-phenanthroline-5(4 <i>aH</i>)-ylidene)hydrazinecarboximidamide (ST09).....	82
2.4.12 Preparation of Amino-1,2,4-triazin[5,6-f]1,10-phenanthroline (ST10)	82
2.4.13 Preparation of hetero dual substituted phen-5,6-dione.....	83
2.5 References	85
Chapter 3 Choline esterase inhibitors as anti-AD drugs(ChEI)	87
3.1 Introduction to chemistry and mechanism of Alzheimer's disease	87
3.2 Acetylcholinesterase(AChE) and butyrylcholinesterase (BuChE) inhibitors	90
3.2.1: Method and techniques for evaluation of the Enzyme activity inhibition	91
3.2.2 Review of Ellman Methods.....	92
3.2.3 Experimental part.....	92
3.3 Biological Assays via plate readers	93
3.3.1 Ellman Assay Procedure for inhibition evaluation of AChE	93
3.3.2 Ellman Assay Procedure for BuChE.....	94
3.3.3: Biological Tests according to Ellman Bioassay modified by Ingkaninan et al.....	95
3.4: Ellman bioassay; biological inhibition results and discussion.....	95

3.5: Kinetic analysis of AChE inhibition	101
3.6: Estimation of the Drug-Like Properties based on Lipinski rule	116
3.7: Prediction of BBB penetration of compounds	116
3.8: ADMET Descriptors.....	119
3.8.1: Aqueous Solubility.....	121
3.8.2: BBB Penetration parameters.....	121
3.8.3: Human Intestinal Absorption model	121
3.8.4: CYP2D6 Binding	122
3.8.5: Hepatotoxicity of the like-drug investigation	122
3.8.6: Plasma Protein Binding properties.....	123
3.9: Docking Studies.....	123
3.10 References	129
Chapter 4 Bio metal Complexes of Cu and Zn(chelating) with phen-5,6-dione derivatives	132
4.1: Introduction	132
4.2 Materials and Methods	133
4.2.1 UV–Vis measurements.....	133
4.2.2 Metal-chelating properties of ligands.....	133
4.3 Results and discussion	134
4.4 Conclusions	142
4.5 References	160
4.6 Future research outlines	176
APPENDIX1	177
APPENDIX2 :Docking Results	195

Chapter 1

1. Introduction

1.1 Condensed summary of Alzheimer's diseases (Rashid & Ansari 2014)

The life expectancy is now doubled from the last century in the developed countries due to the revolution progress in medicine and health mainly to chronic diseases.

The Alzheimer's disease (AD) is one of the most fatal and familiar diseases in the modern societies as confirmed by the current statistics and famous type of neurodegenerative disease, characterized by the damage nerve cells in the cerebral cortex tangles (NFTs) in the brain.

AD is the most common form of dementia as was described by Alois Alzheimer in 1906.

Alois who discovered amyloid plaques and neurofibrillary tangles in brain of old woman

Auguste who died of severe dementia. After a century the cause of AD are still not

understood (Berchtold ; Lage 2006; Maurer, Volk & Gerbaldo 1997; Zilka & Novak 2006).

Several health statistics report that AD disease affected more than 50 million people in the world in 2003, it is predictable this number rising to 115 million in 2050 (Mount & Downton

2006; Wimo et al. 2003). It is reported that AD disease affects one in three people over the age 85 (Hebert et al. 2003). The AD is the fourth major cause of death after cardiovascular

disease, cancer, and cerebral accidents. Worldwide there are approximately 35 million

peoples with AD, and that number is promoted to raise to 114 million by 2050 (Berchtold

& Cotman 1998; Wimo et al. 2003).

The symptoms of AD include worry, depression, lack of interest, nervousness, hallucinations, violence, wandering, illusions and unsuitable sexual behaviors (Teri et al. 1992). AD patients

suffer from a decrease in cognitive function and short-term memory. The AD is characterized by the formation of insoluble clumps of protein or plaques, formed by proteins known as β -

amyloids. These proteins attach to the cell surface of neurons and disable the nerve

transmission. These plaques have been demonstrated to contain relatively high levels of Zn^{2+} ,

Cu^{2+} and Fe^{3+} (1 mM, 0.4 mM and 1 mM respectively) (Smith et al. 1997). While the precise

role of these metals is still uncertain, they appear to bind to so-called β -amyloid peptides that

constitute the bulk of plaque deposits. Cu^{2+} and Fe^{3+} , but not Zn^{2+} , The role of these metal ions

appear to play a redox role through the formation of reactive oxygen species (ROS), this has

been confirmed that lead to coupling of monomeric β -amyloid through the formation of dityrosines linkages (Atwood et al. 2004).

Pathogenic beta-amyloids originate through the sequential action of α - and γ -secretases on amyloid precursor protein (APP) a transmembrane glycoprotein (MW 120-200 kD), ubiquitous in glial cells of the CNS. Its precise function has not yet to been elucidated, but it appears to be involved in synapse formation and repair (Priller et al. 2006).

AD results due to neuronal cell death related to many diverse factors like amyloid beta deposits, decreased levels of ACh, aggregation of tau protein, oxidative stress, inflammatory injury, role of free radicals and excitotoxicity (Rashid & Ansari 2014).

One of the key issues for AD drugs and indeed any drug with prospective CNS activity must have the ability to traverse the blood–brain barrier (BBB). There are three general mechanisms by which drug penetrates the BBB; passive diffusion, phagocytosis and active transport. Passive diffusion is largely limited to molecules with MW < 500 approx., is lipophilic, has less than 8 H-bond acceptors and/or donors and less than five hydrogen-bond donors, less than 10 hydrogen bond acceptors, and finally the logP (calculated octanol-water partition coefficient) should be less than five. This is occasionally called the “rule-of-three” and is a modification of Lipinski’s rule of five (Lipinski 2004; Lipinski et al. 2001). This includes many issues that are considered to play significant roles in the pathophysiology of AD such as deposition of amyloid- β ($A\beta$), aggregation of T -protein, oxidative stress and low levels of acetylcholine (ACh) (Querfurth & LaFerla 2010; Tumiatti et al. 2010).

On the other hand, a great deal of development and progress has been taking place in the field AD diagnosis, drugs, medication and related health care. One of the important classes of AD medicines is based on the nitrogen organic derivatives and organometallic derivatives.

The chief hypotheses attempt to explain AD are as following:

- a) (The cholinergic hypothesis) (Bartus et al. 1982b; Cummings & Back 1998; Francis et al. 1999; Garzone 1993; Struble et al. 1982) is the primary and eldest hypothesis which started in mid 1970s. AD related with cholinergic system impairment and neuronal degeneration because of loss of cholinergic neurotransmission.

There is an irreversible deficiency in cholinergic jobs in brain that lead to memory impairment in patients (Tougu 2001).

- b) (amyloid hypothesis) (Haass et al. 1992; Seubert et al. 1992; Shoji et al. 1992 in 1991 amyloid hypothesis was postulated that planned the aggregation of amyloid beta protein in to fibrillar plaques as the important reason of the disease (Carter, Simms & Weaver 2010; Hardy 2009; Hardy & Allsop 1991). Mentioned that these $A\beta$ peptides derivative from secretase-mediated cleavages by (β and γ secretases) of amyloid precursor protein

(APP) in to 40 or 42 amino acid fragment of A β .(Haass et al. 1992; Seubert et al. 1992; Shoji et al. 1992),a peptide (APP) found in the synapse which is required for synapse and neurone growth, the accumulation of the β -amyloid peptide leading to formation of senile plaques and aggregation which triggers pathophysiological change of brain and ultimately chiefs to cognitive dysfunction.

- c) (Tau hypothesis) (Kosik, Joachim & Selkoe 1986)Tau hypothesis study on triple transgenic mice revealed that the deposition of A β plaques contributed to AD by stimulating the hyperphosphorylation of Tau, so increasing the formation of NFTs. Neurofibrillary tangles are put in a hierarchical and systematic fashion starting from the entorhinal cortex and sequentially spread to the hippocampus. Brain damaging tangles that form round axons, dendrites and microglia within the neurones are outcome of the accretion and clumping collected of boundless hyperphosphorylated forms of the *tau* protein. *Tau* proteins are important for healthy cognitive assignment (Wallin et al. 2006a). They are accountable for assembly and stabilisation of axonal microtubules, which supply neurones with a means of intracellular vesicle transmit and structure (Park 2010) and they can be a connection between β -amyloid and increases in the phosphorylation of the *tau* protein (Busciglio et al. 1995). (Oxidative stress hypothesis) which has gained momentum as a possible reason of neuronal death, is oxidative damage of cell membranes, mitochondria, lipids and proteins (Markesbery 1997). The oxidative stress is the imbalance between biochemical processes originating from the free radical theory of aging, it has been associated in the pathogenesis of AD and a literature exist where its role has been studied in AD (Nunomura et al. 2001; Nunomura et al. 1999; Praticò 2005; Sayre et al. 2005; Sayre, Perry & Smith 1999).

- d) (Excitotoxicity) (Danysz & Parsons 1998; Doble 1999; Petrie, Reid & Stewart 2000)has been considered to play a significant role in the neuronal death.

It is triggered by chronic activation of glutamate, a major excitatory neurotransmitter in the brain, in particular of the N-methyl-D-aspartate also known as NMDA as over activation of NMDA, the site disturbance in cellular ion homeostasis (Ca⁺², K⁺, Na⁺) and metabolic activities occur.

- e) (Neuro inflammation) (Wilcock 2012; Zotova et al. 2010) has gained considerable evidence to its contributions to AD pathology. The inflammatory reaction is characterized by activation of glial cells, gliosis and appearance of inflammatory proteins like accompaniment factors, acute phase proteins and pro-inflammatory cytokines.

- f) (Metal ions) (Duce & Bush 2010) are critically involved in the pathogenesis of AD. Assisting the balance of metal ions back to homeostatic levels has been planned as a disease-modifying therapeutic strategy for AD and NDs.
- g) (Mitochondrial dysfunction) (Petersen et al. 2008; Reddy & Beal 2008) is considered as a pivotal module in neurodegeneration. This dysfunction happens early in AD and promotes synaptic damage and apoptosis. APP and A β can be imported into mitochondria, where they can cooperate with mitochondrial components to impair ATP production and increase oxidative damage.

1.2 Enzymes involved in Alzheimer's disease

1.2.1 Cholinesterases

Cholinesterases are a family of enzymes that catalyse the hydrolysis of ACh into choline and acetic acid, an essential process letting for the restoration of the cholinergic neuron. Cholinesterases are divided into acetylcholinesterase and butyrylcholinesterase.

AChE is the key enzyme involved in the metabolic hydrolysis of ACh at cholinergic synapses in the central and peripheral nervous system. This opinion led to the introduction of the acetylcholinesterase inhibitors AChEI (Weinstock & Groner 2008).

1.2.2 Acetylcholinesterase

AChE is expressed in cholinergic neurons and joins in cholinergic transmission by hydrolysing ACh. It is expressed in blood and nerve cells. Inhibition of AChE reasons over stimulation of ACh receptors (Fukuto 1990), the structure of AChE has been studied using AChE from electric eel before the availability of human recombinant AChEs. The electric eel AChEs active site lies on the bottom of a long and narrow cavity (gorge) (Bartolucci et al. 2009).

1.2.3 Butyrylcholinesterase

The BuChE is also known as plasma cholinesterase or pseudocholinesterase. It is called according to its favourite for the artificial substrate butyrylcholine. BuChE is able to hydrolyse acetylcholine-actylthiocholine but much slower than AChE. Although BuChE activity is prevalent in the human body, but its physiological function is not understood entirely.

It lacking individuals are normally healthy with no manifest signs of disease (Manoharan et al. 2007; Rashid & Ansari 2015). There is almost general agreement that changes in BuChE are related to the development of AD. One study has confirmed that in case of AD the level of BuChE increase as that of AChE decreases in the affected parts of brain (Wright, Geula & Mesulam 1993). The action of this enzyme in the temporal cortex has also been shown to associate with the rate of cognitive decline (Greig et al. 2005; Rashid & Ansari 2015).

1.2.4 Secretases

Three cleavage. The sequential enzymatic complexes cleavage of amyloid precursor protein (APP) found on chromosome 21 in humans by α -secretase and γ -secretase leads to formation of small non-toxic and soluble peptide molecules, known as p3 (Selkoe 2001), while the sequential cleavage of APP by β -secretase and γ -secretase form insoluble A β protein (Rashid & Ansari 2015). The insoluble A β has ability to aggregate into oligomer and fibrils in SPs formation in suitable conditions as shown in Figure 1.

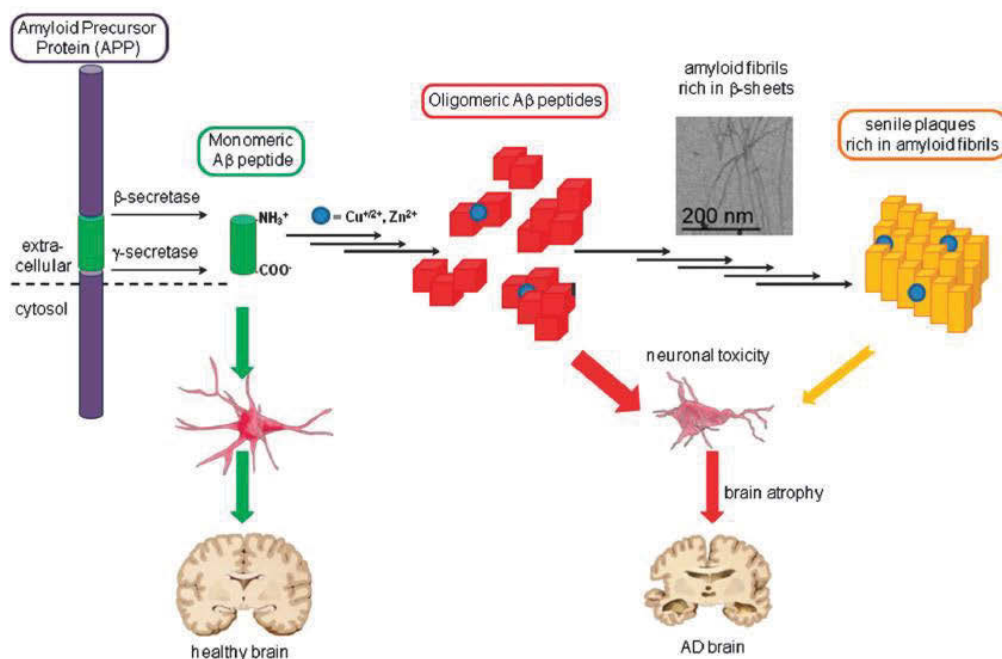


Figure 1: The amyloid cascade process enhancing the role of metal ions (Noël et al. 2013).

The A β peptide is got by cleavage of the Amyloid Precursor Protein (APP) by the β and γ secretases. The non neurotoxic soluble monomeric A β (green arrow) sets in healthy brains. The senile plaques noticed in AD brains are a post-mortem hallmark of the disease. Intermediate species between the A β and amyloid plaques are more toxic (red arrow) than the plaques themselves (orange arrow) which causes major to neuronal death and brain atrophy,

accordingly the metal ions (blue circles) represent a triggering agents for the aggregation process. The reactions forming amyloid plaques has been identified by (Noël et al. 2013).

Who concluded that the reactions involved in this process are equilibrated ones.

1.3 Blood Brain Barrier

The blood brain barrier (BBB) is a separation of circulating blood from the brain extracellular fluid (BECE) in the central nervous system. BBB reasons from tight junctions among capillary endothelial cells. The human BBB contains about 100 billion capillaries estimated to be 640 km in length with a surface part including 20 m² and individual neurons are no more than 8-20 uM normally from a brain capillary. These statistics represent current an enormous and complex biological barrier for both the small and large molecular exchange in and out CNS.

Disruption of the BBB can open entree of the brain to ingredients in the blood by making the tight junction among the endothelial cells of brain capillaries laky. Therefore researchers trying to avoid obstruction the BBB of drug delivery.

The problem is that many of the neurotoxic endogenous materials will enter the brain from blood, therefore disruption of the BBB in the delivery of therapeutics should be controlled carefully (Pardridge 2009b).

1.4 Products used as therapeutic agents to treat AD

Several methods for the treatment of AD are known. The first method is to avoid the neurodegenerative variations that eventually cause irretrievable damage to the brain. As the high formation of tau protein (*T*) and beta-amyloid protein (A β) seems to play a primary role in the neurodegenerative process, efforts have been made to block the synthesis of these proteins.

Local inflammatory factors lead to some secondary changes that may be commenced by beta-amyloid, which leads to slow the decrease of the neuronal degeneration as a sign to treat the symptoms of the disease (Leonard 1998).

The recent research also aimed preventing the beginning of the neuro-pathological processes, such as the deposition of beta-amyloid protein that appears to be causally related to the disease (Gandy & Greengard 1994).

Another reported data has shown potential in slowing the accumulation of A β in transgenic mouse models of AD at this time there is no evidence that such method is active in patients.

The promising treatment of AD requires drugs that can cross the BBB. The BBB is more than a physical barrier, but it represents complex interface that is influenced by peripheral tissues with intimate communication with the central nervous system (CNS). Until now there is no known way to halt or cure the neurodegenerative disease.

To date four drugs are approved by United States to treat the AD (Tacrine, Donepezil, rivastigmine and galanthamine). Nevertheless, the clinical efficiency of these drugs is limited due to the several side effects caused by activation of peripheral cholinergic system and the short half-lives of the concerned tissues.

As a result of these outcomes it is being hypothesized that the action of new Isatin analogues could be due to its penetrating the blood-brain barrier and deliver the active ingredient to the central nervous system. The treatment strategies are being built on the cholinergic hypothesis of cognitive dysfunction (Gualtieri et al. 1995).

This theory is based on the symptoms that the basal forebrain cholinergic neurons are all evidently damaged in patients of AD, together with a defect in choline acetyltransferase, acetylcholinesterase and the choline transporter located on cholinergic neurons (Bartus et al. 1982a; McGeer 1984).

The current diagnosis techniques of AD are based on the identification of the causes of dementia and specific clinical symptoms of AD with other confirmation tests that exclude other causes of dementia by implementing laboratory tests and computerized cerebral tomography (CT) (Wallin et al. 2006b).

The redox-active metals mechanism of toxicity through the formation of (ROS) represents convincing evidence that is etiologically linked to the extensive brain metal build up with aging in other words it reaches its threshold limits (Mitra et al. 2014).

It has been reported by (Kim et al. 2013). That some heavy metals such as Ni causes direct damage to DNA while Cu cause delay of cell growth and promotes apoptosis.

The redox state of Cu and Fe make them biologically important and toxic. Whereas most of the iron in the healthy normal human body is in the haemoglobin, in addition to zinc and copper they serve as important cofactors for the multitude of enzymes and signalling molecules, accordingly they are responsible of different biological pathways, such as synthesis of neurotransmitters, mitochondrial energy production, and transcription / replication of DNA.

The redox activity of Cu²⁺ and Fe³⁺ encourage the genome damage and inhibit the major enzymes in the oxidative process of genome damage via reversibly oxidising cysteine component of these proteins and changing their structure.

Several studies have considered these three metal ions (Fe, Cu, and Zn) as major factors in the pathophysiology treatment of AD (Mitra et al. 2014; Molina-Holgado et al. 2007; Rao, Ney & Herbert 1999), accordingly they can delay the progression of the disease and bring some comfort to the patients and their cares.

Furthermore, in spite the extensive studies that gave convincing evidence for connecting the oligomerisation/ misfolding of tau/ A β , to build-up the Cu/Fe and other metals build-up and reach the threshold limit lead to genomic damage of the brain (Mitra et al. 2014).

The Zn (II) and Cu (I/II) transition metal ions have important role in the brain functions such as transaction of the communication information among neurons at the synapse. The equilibrium of metal ions concentration in the brain tissues is critical for normal healthy brain functioning. These levels are well regulated by (BBB) which is very much dependent on age and the oxidative stresses (Tamano & Takeda 2011).

Investigations and evaluation of different classes of compounds for developing AD therapeutics treatment and metal chelation therapy has been implemented by large number of scholars. Most of the studies were concentrated on general ligands as metal chelating compounds to delete or obstruct these metal ions from interfering with A β to decrease ROS production and accumulate deposition among these chelating ligands are 8-hydroxyquinoline and its derivatives which were basically suggested due to their capability to prevent the associations between these active metal ions and A β .

Most of these studies were carried out in vitro and some of them were performed in vivo to sequester redox active metal ions and migration of the metal ions across the membrane (DeToma et al. 2012); (Scott & Orvig 2009).

Although 8-hydroxyquinoline and its derivatives have several disadvantages such as probing the association between metal ions and A β as related to poor A β functionality interaction.

Which leads to alteration and changing the metal ion homeostasis biology more than inclusion of the metal ions within A β structures (Bandyopadhyay et al. 2010; Bonda et al. 2011; Braymer et al. 2010; Bush & Tanzi 2008a; Hureau et al. 2010; Scott & Orvig 2009).

as shown in Figure 1.

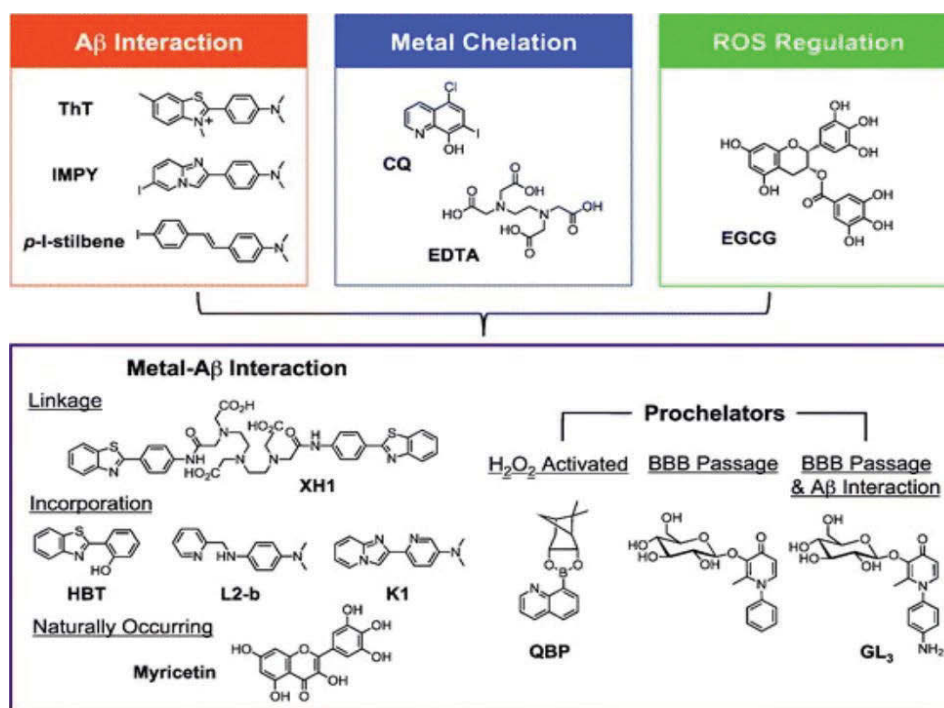


Figure 2: Multifunctional small molecules that can be used to investigate Cu(II)/Zn(II)-associated A β species in AD by combining properties of A β interaction, metal chelation, and ROS regulation (DeToma et al. 2012).

Another study for 2-[(8-quinolinylamino) methyl] phenol indicated that both quinolone and phenolic groups shown in Figure 2 have antioxidant features when integrated into ML as Schiff base condensation followed by transferring imine to amine (Lee et al. 2013).

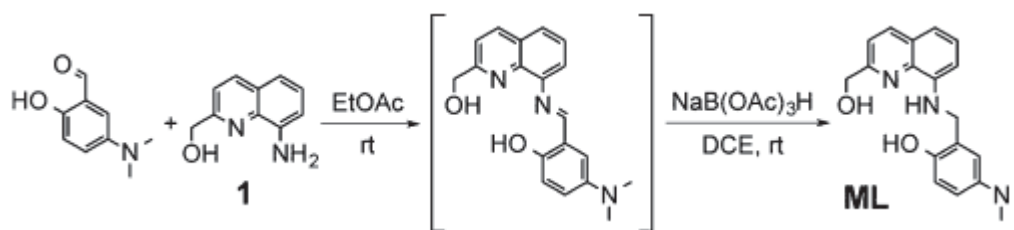
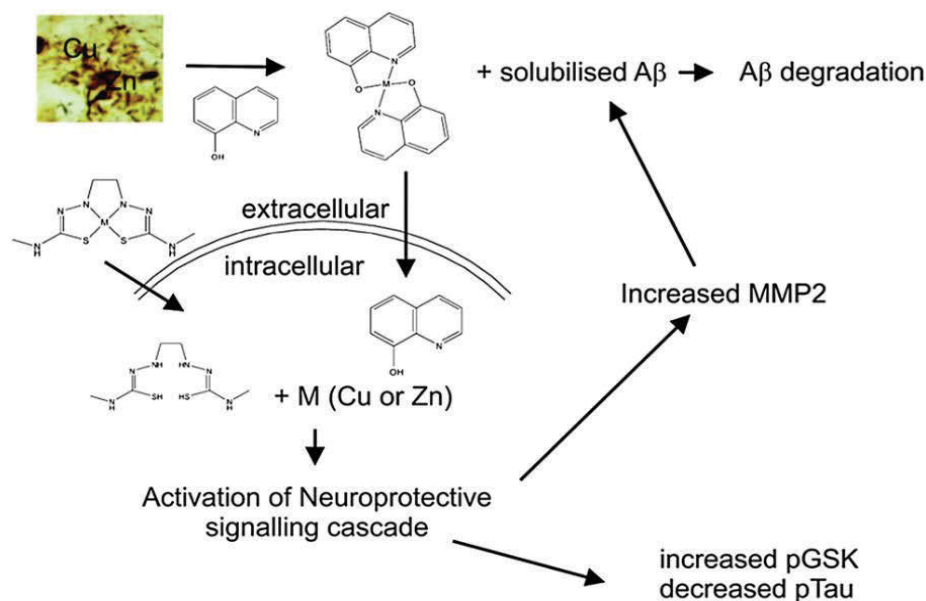


Figure 3: Synthetic Route to ML(Lee et al. 2013).

Further studies based on bis(thiosemicarbazone) derivatives such as glyoxalbis(N(4)-methyl-3-thiosemicarbazonato) copper(II) (Cu^{II}(gtsm)) and diacetyl-bis(N(4)-methyl-3-thiosemicarbazonato) copper(II) (Cu^{II}(atsm)), have shown that these complexes can cross the BBB,(Fodero-Tavoletti et al. 2010) accordingly these class of compounds were selected for evaluation in vivo. The Cu²⁺ oxidation state in both of these complexes is very

stable,(Barnham & Bush 2014) the action of metal ions in this mechanism is shown in Scheme1.



Scheme 1: Showing the action for metal chaperones in AD Aβ metal interactions mechanism that drive Aβ aggregation showing the action for metal chaperones in AD Aβ metal interactions mechanism that drive Aβ aggregation (Barnham & Bush 2014).

On the another hand, series of resveratrol analogies of imines were synthesized by the classical method of imine formation involving condensation between aromatic amine with various aromatic aldehydes in ethanol under reflux condition as show in Scheme 2. Combination of the main features of resveratrol and clioquinol provides molecules with multi functionality (metal chelation, Aβ interaction, and antioxidation). The scheme of imine resveratrol analogues and the chemical structure of compounds investigated in this series are presented in Figure 4. The studies includes also the chelating tendency of all compounds toward metal ions such as Cu^{2+} and Fe^{2+} (Li, Wang & Kong 2014).

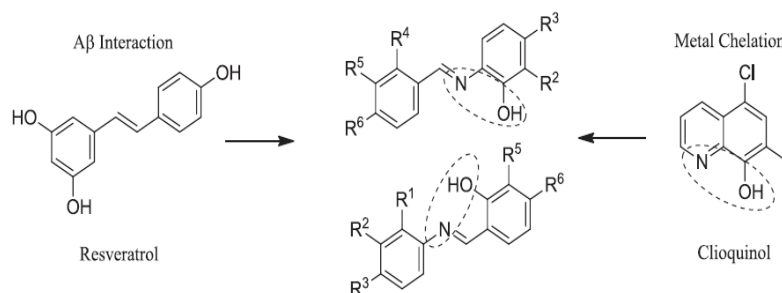
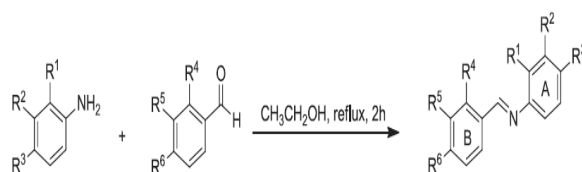


Figure 4: Basic features of resveratrol and clioquinol provides molecules with multifunctionality (metal chelation, A β interaction and antioxidant) (Li, Wang & Kong 2014).



Scheme 2: Structure scheme of imine resveratrol analogues and chemical structure of the investigated compounds (Li, Wang & Kong 2014).

On the other hand, several natural compounds such as curcumin has been extensively investigated due to the wide range of attractive and useful properties that these natural products exhibit such as, antioxidant, anti-inflammatory, chemo preventative and chemotherapeutic. On the other hand, curcumin has shown benefits to AD patients by destabilizing the preformed A β aggregates and inhibiting the production of A β , plus weakening A β -induced neuro inflammation as a therapeutic agent (Park 2010).

1.5 Pharmacological Approach

The pharmacological approach to transit the BBB is based on the notice that same molecules cross the brain freely. This capability to passively enter the BBB depends on molecular weight < 500 Da, charge and lipophilicity. The lipid solubility of a drug has an opposite relationship to the number of hydrogen bonds that the drug create with solvent water, which is 55 M. The H-bonding of any given drug can be specified by check of the molecular structure, and should be measured in tandem with molecular weight (MW) of the drug (Pardridge 2009a, 2010; Perez & Franz 2010).

1.6 Multi-target-directed ligands (MTDLs)

The MTDL design strategy is used to progress single chemical entities that are capable of adjusting multiple targets simultaneously. The MTDLs investigation showed encouraging results based on using multi-target-directed ligands (MTDLs), i.e., single chemical units capable of hitting distinct molecular targets in the neurodegenerative cascade (Csermely, Agoston & Pongor 2005; Espinoza-Fonseca 2006; Youdim & Buccafusco 2005a; Youdim & Buccafusco 2005b).

The investigated compounds consisted multi-functional active groups that have characteristics of anti-oxidants. The substituted phenols and aromatic amine are well known categories of anti-oxidants which are able to terminate chain reactions and act as free radical scavengers.

On the other hand, presences of phenolic and amino groups are active structures to form chelates with various metal ions such as Cu I, Cu II, Fe II, Zn II, Mg II, Mn II, Co II and Ni II. These metal ion complexes represent the core of the recent studies concerning development of drugs for AD.

Other research programs are based on classifying new MTDLs that possesses different effects toward AD-related goals, like Acetylcholinesterase, A β processing, accumulation and oxidative stress. The oxidative damage is considered to be one of the important pathogenic mechanisms in AD that takes place as early pathogenesis (Nunomura et al. 2001).

Although several chemical routes and medical approaches have been targeted to develop MTDLs by combining different pharmacophores with active functionality (Hopkins, Mason & Overington 2006). The design of MTDLs is a complex task, the successful design can be promoted by adequately choosing the starting scaffold that has suitable molecular specificity toward one given target that may represent that may represent the goal via the choice of the better compound.

For example a Tacrine (1) shown in Figure 5 links between the observed cholinergic dysfunction and AD severity providing a therapeutic use of (AChEIs) inhibitors. Two Tacrine units are bonded together by $-(CH_2-CH_2)_n$ -spacer of suitable length to link between the catalytic site and peripheral sites. The formed bivalent ligand -2, has a remarkable affinity toward AChE over the compound -1(Pang et al. 1996). The computational modelling analysis and related crystallographic studies (Rydberg et al. 2006) have demonstrated that ligand -2 is capable to interact with the catalytic active sites and PAS of the enzyme. On the other hand, it has capability to block PAS forming retarded A β assembly but this had not been confirmed experimentally to take place (Bolognesi et al. 2007).

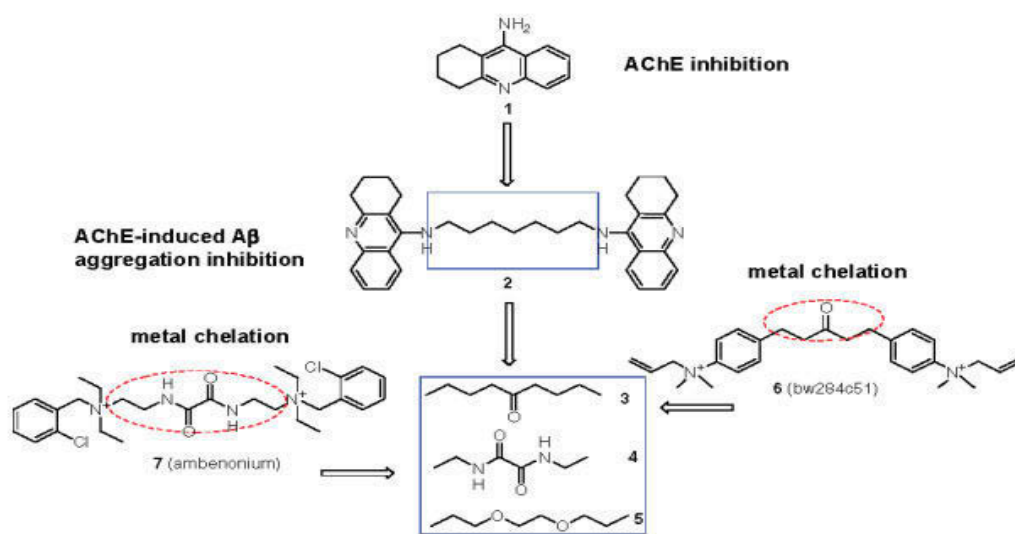


Figure 5: Design routes for compounds (3-5) (Bolognesi et al. 2007)

In conclusion the compounds 3-5 are bis-tacrine derivatives that have a powerful AChE-inhibiting activity (on a nano molar range). These compounds are capable to opposite AChE-induced amyloid fibrillogenesis, and act as metal chelating agent. The new MTDLs form complexes more efficiently than compound -2. These active ingredients have shown in vivo oral activity (Wang et al. 1999).

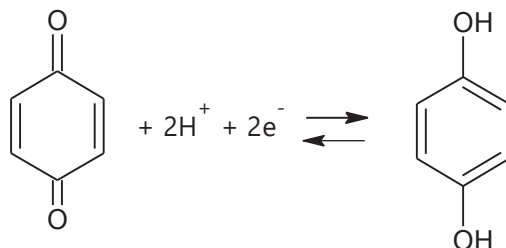
These studies highlight the efficiency of the suggested MTDL as design model concentrating on the unique trifunctional characteristics of bis-tacrines 3–5, accordingly they are promising active ingredient candidates as AD therapeutics.

Polyamines represent a universal class of active reagents that can interact with several protein targets. The affinity of protein targets can be fulfilled by: (a) including suitable substituent on the amino groups; (b) changing spacer chain length between the amine functional groups to fit between the carboxylate groups or the aromatic structure of the biological counterpart. (Bolognesi et al. 1998; Melchiorre et al. 1988). One of the studies based on a series of polyamine derivatives displayed dual action as AChEIs and muscarinic M2 receptor antagonists (Melchiorre et al. 1998).

Another study was based on modifying the structure of polyamines by involving into their backbone an antioxidant structure that acts as the possible chain-breaking antioxidant and free radical scavenger.

The benzoquinone part of the coenzyme Q10 (CoQ) is being considered as a focus because this natural antioxidant offers the promising approach to the AD. The study was performed both together in vitro (Beal 2004) and in vivo (Bragin et al. 2005).

The antioxidant activity of substituted quinones antioxidants are based on a free radical scavenging, retardation, and inhibition according to the reversible redox reaction:



The CoQ and other benzoquinone derivatives showed to be effective to AD molecular targets and inhibiting the A β aggregation (Ono et al. 2005; Tomiyama et al. 1996).

This study represents the first approach to convert AChEIs to MTDLs, via inserting an antioxidant structures into the polyamine chain as a backbone. Several small compounds have also been investigated via a rational structure by integrating the A β framework with a metal chelation moiety forming single designed molecule to modulate the metal ion- associated A β species (DeToma et al. 2012; Liu et al. 2013; Pithadia & Lim 2012; Scott & Orvig 2009; Telpoukhovskaia & Orvig 2013).

The in vitro studies and in living cells showed that these compounds affect the control of metal-induced A β aggregation, and attenuate the reactive oxygen species (ROS) formation by metal-A β , and regulate the metal-A β toxicity (Hindo et al. 2009; Liu et al. 2013).

Other studies relate AD to other multifactorial diseases (Bolea et al. 2011). Based on the monoamine oxidase mechanism (MAO). The flavoenzyme, plays an essential role in the destruction of dopaminergic and serotonergic neurotransmitter components via catalysed enzymatic deamination metabolism of major monoamine neurotransmitters. The MAO is responsible for the regulation and metabolism of major monoamine neurotransmitters.

It presents in two isomeric forms: MAO-A and MAO-B (Desideri et al. 2013). The MAO-A is involved in the psychiatric and depression symptoms, while MAO-B accelerates the oxidative deamination of neurotransmitters, accordingly increasing the rate of production of free radicals which is the main cause of the oxidative stress (Zheng et al. 2012).

According to this assumption studying and evaluation of previously mentioned multifunctional active ingredients that inhibit ChEs, decrease A β aggregation and at the same time inhibit MAOs activity are getting the attention of the researcher as suggested approach for developing AD drugs the following are some of these suggested active ingredients.

The Resveratrol (*trans*-3,4,5-trihydroxystilbene) whose structure is shown in Figure 6 is a natural phenolic compound, was extracted from several plants and also synthesised and evaluated. The molecular modelling of resveratrol derivatives as multi-targeted compounds with anti-ChEs, anti-A β aggregation and MAO inhibition effects as a promising medication rout AD.

The practical investigation both in vitro and in vivo showed that resveratrol has several biological activities such as anti-inflammatory and efficient antioxidant properties (Ge et al. 2012; Yáñez et al. 2006). Recently researchers are focusing on its effectiveness against the AD. Some of these reported studies showed that resveratrol could inhibit A β self-aggregation, and attenuate A β -induced toxicity, promote A β clearance and reduce senile plaques (Rivière et al. 2010; Riviere et al. 2007). Other studies also showed that it has inhibitory effects on MAO activities (Han, Ryu & Han 1990; Yáñez et al. 2006). In conclusion to the outcomes of all these studies, the resveratrol might be used as a target compound in the design of multi-targeted drugs for the treatment of AD.

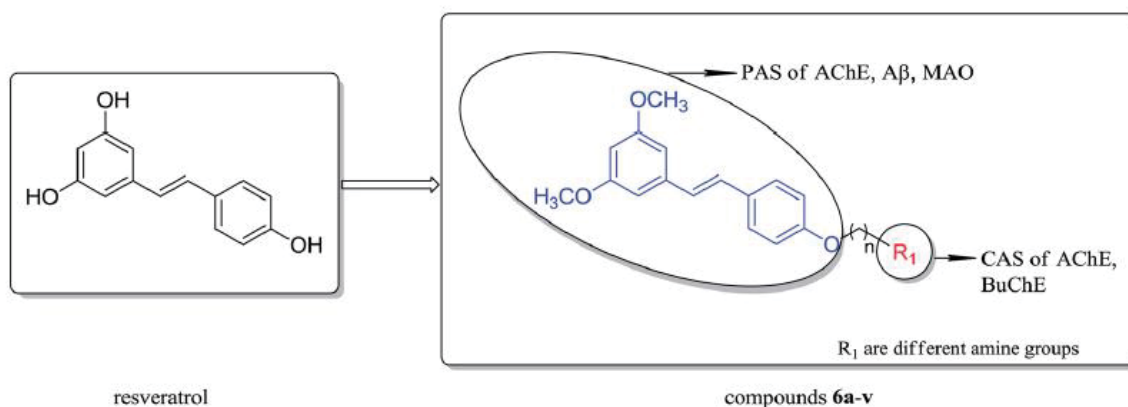


Figure 6: Design strategy for resveratrol derivatives as multi targeted active ingredient for AD treatment (Pan et al. 2014).

1.7 Acetylcholinesterase inhibitors

Several generations of acetylcholinesterase inhibitors (AChEIs) and NMDA antagonists receptors have being developed ,evaluated, and marketed since 1990s and been used to treat AD (Cummings 2003).

AChEIs is one of the ingredients being thoroughly investigated by several researchers, although valuable restoring cholinergic dysfunction have been used as suitable drug for patients who have palliative issues.

Recently several scholars paid great attention to two major proteins; amyloid- β ($A\beta$) (McLaurin et al. 2006) and (τ), (Khlistunova et al. 2006). Which became the focus of research. The $A\beta$ is the major constituent of amyloid plaques and is suggested to be one of the key pathological characteristics of AD. The phosphorylated (τ) is the main component of neurofibrillary tangles as the second major identified factor for AD (Hardy et al. 1998). However, no biochemical pathways of either $A\beta$ or (τ) have so far been commercialised. Typical features of AD-associated plaque deposits displays higher activity than acetylcholinesterase (AChE). This may be responsible for the low levels of ACh in the brain of the AD patients, but it is more likely that loss of neurons and their contribution to biosynthesis of ACh is of greater significance. A closer look at the distribution of AChE indicates that this enzyme is co-localised with $A\beta$ (Fernandez, Moreno & Inestrosa 1996) . Inhibiting the breakdown of ACh by blocking the enzyme AChE is an important step to continue the activity of neurotransmitters. AD is a major cause of dementia which is usually associated with loss of cholinergic neurons in parts of brain.

Several ingredient such as cholinesterase inhibitors (donepezil, galantamine and rivastigmine are known to be effective in retarding the breakdown of acetylcholine released into synaptic clefts which enhance cholinergic neurotransmission (Birks 2012).

Other studies have shown that ChEIs such as (tacrine, donepezil, galantamine, ganstigmine and huperzine A) shown in Figure 7 and Table 1 protect neurons from destruction in patients suffering from the neurodegenerative diseases (Francis, Nordberg & Arnold 2005).

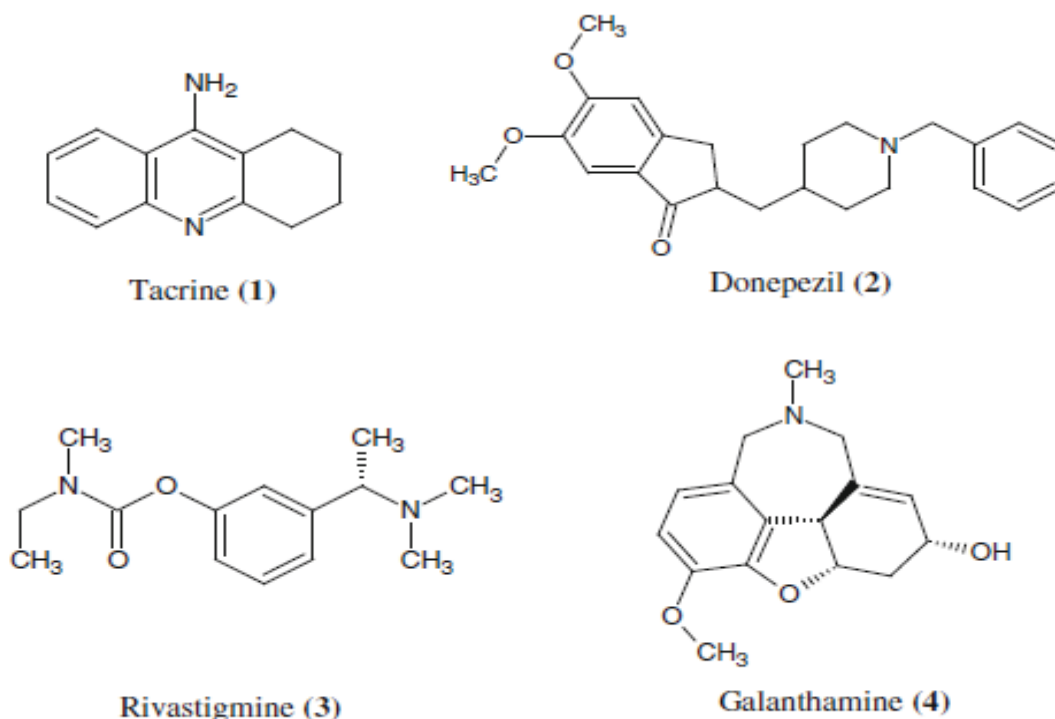


Figure 7: Typical Acetylcholinesterase inhibitors (Anand & Singh 2013).

Table 1: Clinical status of cholinesterase inhibitors with putative neuroprotective or disease-modifying actions (Francis, Nordberg & Arnold 2005).

Compound	Clinical status and other information ^a
Tacrine	First FDA-approved AD therapy (1993); centrally acting reversible ChEI; its therapeutic use is limited as a result of hepatotoxicity
Donepezil	Approved by the FDA in 1997, and now the most widely prescribed AD therapy; piperidine-based, reversible ChEI, with high selectivity for AChE over BuChE; ACh-mediated side-effects tend to be mild and transient
Rivastigmine	Approved as an AD therapy by the FDA in 2000; carbamylating, pseudo-irreversible ChEI and inhibitor of BuChE; dose titration recommended because of common ACh-mediated side-effects during treatment initiation
Galantamine	Latest ChEI to be approved by FDA (2001) as an AD treatment; tertiary alkaloid that is a reversible, competitive ChEI and an allosteric modulator of nicotinic ACh receptors; dose titration is recommended to control mild and transient ACh-mediated side-effects
Ganstigmine	Novel, orally active ChEI in development (Phase II) for the treatment of AD; genserine-derived ChEI with a 115 times higher potency for AChE than BuChE; Phase II trials have been interrupted as a result of the occurrence of severe side-effects in some patients
Physostigmine	Not in clinical use for AD; clinical trial data suggest that its efficacy in AD is hampered by a short half-life, and a high rate of adverse events has led to a significant number of withdrawals from treatment compared with placebo; reversible ChEI, with a higher selectivity for AChE than BuChE, originally extracted from the Calabar bean
Metrifonate	Underwent clinical trials as an AD therapy but did not reach market as a result of side-effects related to muscle weakness; prodrug that spontaneously rearranges into the irreversible ChEI dichlorvos (2,2-dichlorovinyl-dimethyl-phosphate; DDVP), an organophosphate; BuChE is slightly more sensitive to metrifonate-induced inhibition than is AChE
Phenserine	Data from clinical trials in patients with AD not yet released; phenylcarbamate is a derivation of physostigmine and is a pseudo-irreversible ChEI, with a >50-fold greater activity for AChE compared with BuChE
TAK147	Currently in Phase III trials in Japan, data not yet released; a benzylamino inhibitor of AChE, with high CNS selectivity
Huperzine A	Currently in Phase II trials as a treatment for AD; a natural ChEI derived from the Chinese herb <i>Huperzia serrata</i>
Huperzine B	Not under clinical development; also derived from <i>Huperzia serrata</i> , but is a much less potent ChEI than huperzine A
Neostigmine	Used orally to treat myasthenia gravis; not in clinical use for AD; quaternary ammonium compound that binds irreversibly to AChE but is slowly hydrolysed

^aAbbreviations: AChE, acetylcholinesterase; AD, Alzheimer's disease; BuChE, butyrylcholinesterase; ChEI, cholinesterase inhibitor; FDA, Food and Drug Administration.

There are two chief kinds of cholinergic or acetylcholine receptors (AChRs) on which ACh acts, both of which are influenced by declination in AD. For both kinds of receptors, the nerve batch is activated by ACh binding to them after its liberation into the synaptic cleft. These batch are ended by the infection of ACh into the inactive ingredient, choline and acetate, *via* quick hydrolysis by the acetylcholinesterase (AChE) enzyme (Pohanka 2012). Target enzyme contains of a narrow gorge with two separate ligand binding sites: the catalytic active site (CAS) and the peripheral anionic site (PAS) (Bolognesi, Andrisano, Bartolini, Cavalli, et al. 2005; Guo et al. 2004). The gorge itself is a narrow hydrophobic channel with length of about 20°A, linking the PAS to the active site (Sussman et al. 1991). It is encompassed by aromatic amino acids enabling a high selectivity for ACh. The bending of CAS to the quaternary moiety of choline matches to Trp84, which stabilises the positive charge of choline by forming cation- π complex (Wiesner et al. 2007). The peripheral anionic site (PAS) located at the opening of the gorge, has also been specified and assigned to another tryptophan residue ((Trp 279) which is implicated in the enhanced binding of bis-quaternary ligands as detailed in Figure 8.

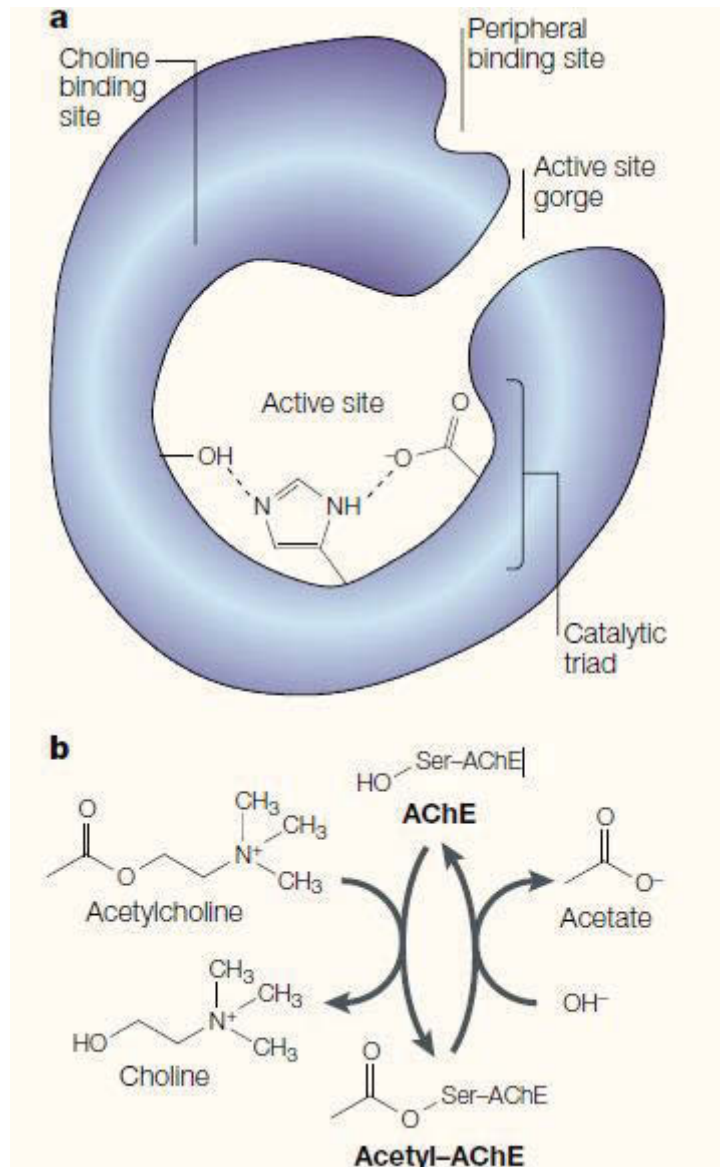


Figure 8: Schematic representation for Acetylcholinesterase

a: structural features of the enzyme
 b: AChE reaction) (Soreq & Seidman 2001)

Acetylcholine hydrolysis can also be catalysed by the butyrylcholinesterase enzyme BuChE (Soreq & Seidman 2001). BuChE also act as molecular destructive for natural anti-AChEs by reacting with these toxins before they reach AChE (Li et al. 2000).

Till now, there is no medication that can finally cure Alzheimer's disease, the primary therapeutic options currently used for the treatment of AD are acetylcholinesterase inhibitors (AChEIs), Food and Drug Administration (FDA) gradually marketed these AChEIs namely, tacrine (1993), donepezil (1997), rivastigmine (2000), and galantamine (2001).

Among them, donepezil is the most effective pharmacological agent for AD treatment (Sugimoto et al. 2000). But, it is effective in reversing the symptoms for only a small period of time.

Tacrine, the first ChEI accepted by the FDA for AD treatment, was withdrawn due to its severe liver toxicity (Watkins et al. 1994). while Galantamine is the latest anticholinesterase drug used in AD which approved in 2001(Rizzo et al. 2010).

Several sub-groups of Cholinesterases (ChE) primary enzymes have been separated and studied based on their catalytic properties.

An enzyme that favours decomposition (hydrolysis) of small substrates, such as ACh is named acetylcholinesterase (AChE).

The enzyme, which is able to adapt to the bulkier substrates such as benzoyl- or butyryl-choline and catalyse their decomposition, is termed as butyrylcholinesterase (BuChE).

AChE and BuChE can both catalyse the hydrolysis of ACh. The adverse effect of neuritic plaques on the neurons producing and releasing acetylcholine (ACh) are linked directly to the enzyme associated with ACh.

Decrease concentration and activity of cholineacetyltransferase concentration and acetylcholinesterase in limbic system and central cortex were associated with the loss of cholinergic neurons in subcortical areas (Frölich 2002), therefore research in an effort to increase ACh brain levels in the synaptic gaps by inhibition AChE. Also Drug should contain functional elements likely to confer biological activity, should Obey Lipinsky's "rule of five".

1.7.1 Cholinergic Drug Therapy

The neuropathology of AD is characterised by the primary loss of basal forebrain cholinergic neurons, chief to a deficiency in cholinergic neurotransmission. This deficiency plays significant role in memory impairment and learning of AD patients.

Through neurotransmission at cholinergic synapsis, acetylcholine (ACh) is released from presynapsis into the synaptic cleft and binds to muscarinic and nicotinic receptors present on postsynapse. This nerve impulse transmission at cholinergic synapsis is ended by acetylcholinesterase (AChE) which catalyses the hydrolysis of ACh.

The phenomenon of cholinergic neurotransmission can be improved by developing following classes of drugs acting at both presynaptic and post-synaptic levels (Contestabile 2011; Dolmella, Bandoli & Nicolini 1994; Greenlee et al. 2001; Maelicke & Albuquerque 1996; McGleenon, Dynan & Passmore 1999).

- a. Blocking AChE enzyme by (AChEIs) which rise the synaptic level of ACh.
- b. Developing drugs as ACh precursor such as phosphatidylcholine that effectively rise the bioavailability of choline.
- c. Developing effective drugs as (ACh releasers) to release the ACh from presynapses.
- d. Developing (Muscarinic agonists) drugs to motivate muscarinic receptors on postsynapse.
- e. (Nicotinic agonists) drugs that motivate muscarinic receptors on postsynapse.

Between these strategies, the only and the most clinically effective therapeutic strategy for treatment of AD is cholinergic improvement by inhibition of AChE. Cholinesterase (ChEs) are collection of chemical compounds which are able to inhibit the hydrolytic activity. There are two types of ChEs acetylcholinesterase (AChE) and butyryl cholinesterase (BuChE).

1.7.2 Cholinergic Hypothesis

The system of cholinergic is created on the neurotransmitter ACh, initially recognized by Loewi in the 1920s and found extensively distributed in central and peripheral nervous system (McCormick 1989).

1.7.3 Cholinesterases

Represent group of enzymes that catalyse the hydrolysis of ACh to choline and acetic acid, this represents important progression allowing for the cholinergic neuron resolution.

Cholinesterase are separated to acetylcholinesterase and butyrylcholinesterase. AChE is the key enzyme involved in the metabolic hydrolysis of ACh at cholinergic synapses in the central and peripheral nervous system. This opinion led to the overview the AChEIs to prolong the duration of action of ACh and provide symptomatic treatment in AD (Weinstock & Groner 2008). BuChE expressed in selected parts of the central and peripheral nervous systems is too accomplished of hydrolysing acetylcholine (Çokuğraş 2003; Mesulam, Guillozet, Shaw & Quinn 2002).

1.7.4 Clinically used enzyme inhibitors to Alzheimer's Disease

Currently there is no confirmed treatment for AD, but managing involves the treatment of cognitive, non-cognitive and behavioural symptoms.

AChE inhibitors became the target of new drugs for AD, for clinical treatment of AD symptoms such as Tacrine, Donepezil, Rivastigmine and Galanthamine which are currently used to increase (ACh) content in the synapse.

AD patients suffer from the reduced availability of ACh is the main neurochemical deficit.

In clinical trials ACh precursors and cholinergic receptor agonists were used, but they were abandoned due to their ineffectiveness or intolerable side effects (Bodick et al. 1997; Patel 1995; Thal et al. 1981).

Increase the levels of ACh in the brain and to facilitate cholinergic neurotransmission is through inhibition of cholinesterase enzymes which are involved in breaking down ACh after it is free from the vesicles. Cholinesterase inhibitors act by inhibiting the enzymes responsible for the breakdown of ACh later its availability increases at the synaptic cleft (Giacobini 2004). Regarding to cholinergic hypothesis, many compounds were studied in preclinical models of cognitive impairment and subsequently tested in clinical trials. Tacrine was the first drug to accept FDA approval in 1993 exactly for the treatment of AD (Tumiatti et al. 2010). It was synthesized in 1949 and has been used after anaesthesia and in combination with morphine because of its analeptic properties. It was used in second world war as a safe intravenous antiseptic, in 1950s was used experimentally to reverse cholinergic coma in animals.

It was non-competitive and reversible ChEI which concentrates in the brain due to its relatively greater lipid solubility it has severe side effects like hepatotoxicity and short biological half-life (1.6-3 hrs).

Galanthamine is a phenanthrene alkaloid was isolated from snowdrop plant *Galanthus nivalis*. After its first extraction in 1952, it was used by Russian and Bulgarian scientists in post-surgery reversal of tubocurarine induced muscle relaxation. In 1972 Soviet researchers prove that it could reverse scopolamine induced amnesia in mice and this was later extended to people till 1986, it was studied for treatment of AD (Heinrich & Teoh 2004).

It can act as reversible inhibitor of AChE with competitive action and approved by FDA in 2001 (Tariot et al. 2000), and it possesses the lowest potency in AChE inhibition.

1.7.5 Functions of AChE

AChE terminates the action of ACh at post-synaptic membrane at the neuromuscular junctions. Really, neural signals pass from cell to cell at synapses, which can be either electrical or chemical. At a chemical synapse, the depolarisation of the presynaptic membrane by an action potential opens voltage gated Ca^{+2} channels, letting an influx of Ca^{+2} to trigger extocytic release of neurotransmitter ACh from synaptic vesicles.

1.7.6 Binding sites of AChE

AChE is a conformational plastic enzyme, is comprised of next five main domains. Initially, an anionic locus, which is used for binding the substrate within AChE molecule. This site determines specificity with respect to the substrate alcohol moiety, it serves as choline-binding pocket.

Secondly as an esteratic locus, comprised of the active site serine and histidine involved in catalysis. This site is the actual catalytic machinery and is similar to the catalytic part of the serine hydrolases such as chymotrypsin (Rosenberry 1975). A third site is a hydrophobic region that is contiguous with or near the esteratic and anionic loci and is important in binding aryl hydrophobic substrates as an active site aromatic cation ligands.

The fourth site is allosteric site which is existing in regulatory subunit but physical remote from the active site of AChE. The allosteric properties of AChE are due to this site (Mabood 1981).

1.7.7 Butyrylcholinesterase

BuChE is a serine hydrolase enzyme, mainly expressed and secreted by glial cells within the human brain. It is also expressed in neuronal somata and their proximal dendrites, such as in amygdala, hippocampus and thalamus of brain areas affected with AD. It has been reported than 10 to 15% of cholinergic neurons in the human hippocampus and amygdala express BuChE in their cell bodies and proximal dendrites, in state of AChE (Darvesh, Grantham & Hopkins 1998).

BuChE has significant role in AD. The activity of AChE decrease as the disease progresses but the activity of BuChE remains unaffected or increase sometimes (Giacobini 2004). In advanced stages of AD, BuChE controls central cholinergic transmission that take place in the brain. BuChE hydrolyses the already depleted levels of ACh. BuChE inhibition has shown potential clinical worth in ameliorating the symptoms of AD.

Restoration of Ach levels by BuChE inhibition appear to occur without apparent adverse effects (Greig et al. 2005).

1.7.8 BuChE inhibitors

The AChE and BuChE vary structurally, genetically and in their substrate specificities and sensitivities to a wide range of inhibitors. Recent research indicates that selective BuChE inhibition approach could help increase in ACh levels and reduce the formation of abnormal amyloid found in AD (Šekutor et al. 2012). Therefore, potent and extremely selective BuChE inhibitors and dual AChE-BuChE inhibitors are synthesised as treatment for AD.

BuChE inhibit the activity of the enzyme which affects the transmission of the neurotransmitter and makes patient inconvenience from blurred vision, dizziness, vomiting fever and death (Pardío et al. 2001; Wang, Timchalk & Lin 2008) BuChEI is improbable to be associated side effects (Greig et al. 2005) and may be considered as an important target for novel drug development to treat AD.

Discovered inhibitors acting on hydrolase activity of BuChE contain cymserine

Analogues, hetero bivalent tacrine derivatives (Elsinghorst, González Tanarro & Gütschow 2006), quinazolinimines (Decker, Kraus & Heilmann 2008), phenothiazines (Darvesh et al. 2007), benzofurans (Rizzo et al. 2008) and isosorbide based compounds (Dillon et al. 2010).

The isosorbide-based compounds show an IC_{50} value 0.15 nM which show highly selective BuChE inhibitor (Carolan et al. 2010).

1.8 Structure-based Design

The 3D structures of drug goal proteins are used in the advance stages, to propose compounds in a way that will improve their selectivity and potency as drugs. There are now drugs in the market that have been planned in this style, (Congreve, Murray & Blundell 2005). One significant aspect includes the identification of parts within the protein where intermolecular connections can take place, therefore molecular modelling is becoming more and more important for defining a potential binding site.

1.9 Molecular modelling studies

Molecular modelling is a promising methodology for analysing the three dimensional structure (3D) of biological macromolecules (Forster 2002).

Knowing the 3D structure of receptor macromolecules is vital to estimate the stability of the drug-receptor complexes. The compatibility of the drug molecule and its receptor is named the active conformation. The active conformation is very important because it reflects the structure activity relationships.

This can be used to estimate the stability of the ligand molecule with arbitrary conformation at arbitrary relative position as indicated by the minimum binding energy. Such approaches are called (docking studies).

Docking is a using computer programs that expects the non-covalent binding of macromolecules or of a receptor and a ligand using their unbound structures obtained from molecular dynamic simulations or homology modelling.

Docking studies are applied to study the mode and stability of binding of drugs to the target receptor in drug design (Wu et al. 2003).

In drug design the mode and stability of binding of drugs to the receptor may be determined by docking studies. In drug design consisting the ligands is require a series of interactive three-dimensional manipulations (translation, rotation and bond rotation) inside the ligand binding site of the protein with docking simulation studies (Lengauer & Rarey 1996).

The docking data can be used to evaluate different inhibitors for specifically targeted proteins, thus assists designing new drugs (Hartmann, Antes & Lengauer 2009).

Acetylcholinesterase (AChE) hydrolyses the acetylcholine (ACh) neurotransmitter at cholinergic synapses (Barnard 1974). This mechanism was the target of the first generation of drugs for the treatment of AD and approved to be as design and development of the new drugs was implemented by determination of the 3D structure of AChE.

The vivo studies showed that the 3D structure of *Torpedo californica* acetylcholinesterase (TcAChE) is very similar to those of both mouse (Bourne et al. 1998) and human AChE (Kryger et al. 1998; Kryger, Silman & Sussman 1999).

1.10 Applications of Docking

A computational method have been advanced to analyse the physical properties of molecules and hypothesise the way they may act in biological systems.

The calculation of polar surface area (PSA), lipophilicity descriptors (such as logP and logD), solubility and pKa, helps to expect attitude like the rate of drug passage into hydrophilic and hydrophobic media. This gives medicinal chemists an suggestion of whether the compound will be capable to cross the BBB or be realize competently by the intestine before it can reach its goal (Dressman et al. 1998).

Also docking studies were estimated which proteins are the most likely goals of AChE and BuChE inhibitors and define the exact binding mechanism of the molecule with its goal protein. CDOCKER applies grid-based molecular dynamics simulated annealing protocol by using CHARMM force field although planning the suitable position of the ligand in the active pocket. The algorithm offers flexible ligand docking where the non-bonded interactions are softened through the docking procedure but taken away during the final minimization process.

2. Coordination studies

From literature survey it is clearly observed that metal chelation is one of the most rational therapeutic methods being focused on treating Alzheimer's amyloid pathogenesis. Enhancing the targeting efficiency metal ion chelating agents depends greatly on the ligand design. The strategy of developing the next generation of metal chelators by modelling design is extremely vital to the researchers (Rodríguez-Rodríguez et al. 2009).

The presence of transition metals in enzyme structures plays a vital role in the reactive oxygen transfer mechanism (ROS), which can damage the cellular components and toxicity.

Their role in the homeostasis has attracted several authors who studied their effect on the neurodegenerative disorders in patients who suffer from AD (Squadrone et al. 2015).

The studies showed that the increased level of oxidative stress in the brain is related to the high levels of copper, iron and zinc in the brain tissues. The Cu and Fe are known to stimulate the free radical formation via the Fenton reaction (Jomova et al. 2010).

The patient of AD are characterised by elevated accumulated levels of iron, zinc and copper in the amyloid tissue. The transition metals like iron, copper, zinc, and manganese are known to be active biochemically are known as functional metals and called biometals.

This is related to the ability of some metal ions like Cu and Fe, to transfer and exchange electrons that lead to free radical formation, on reactive nitrogen and oxygen as reactive

species. The oxidation reaction takes place in the tissue components forming free radicals as by products which are strongly related to aging diseases. In the normal human bodies, the metal ion content of the brain is strictly balanced and controlled to prevent passive flux of metal ions to the brain across what is known BBB. Several studies have shown that iron, zinc and copper are being increasingly involved in the interactions with the major protein components of neurodegenerative diseases (Barnham & Bush 2008).

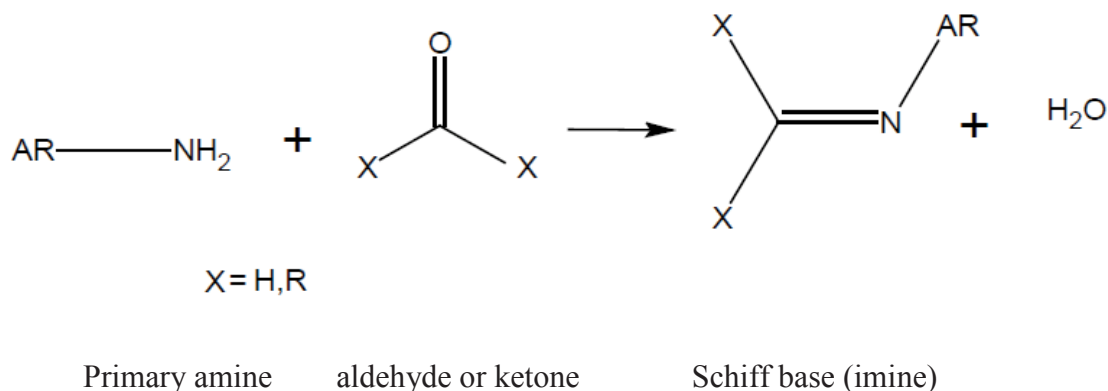
In vivo studies in animals and humans have reported noticeable increase in the levels of copper in the brain tissues from youth to adulthood (Adlard & Bush 2006). On the other hand, the concentration of iron was found to increase in the amyloid plaques in both humans (Zecca et al. 2004) and APP transgenic mice (Falangola et al. 2005).

Accumulating research evidence indicates increase in the level of biometals (Cu, Fe, Zn) in the brain tissues and suggested that their interaction with APP and A β is strongly linked to AD pathology, thus confirming that metal chelation represents another rational therapeutic approach for inhibiting AD pathogenesis (Doraiswamy & Finefrock 2004; Gaeta & Hider 2005; Gaggelli et al. 2006).

3. Schiff base

3.1 Schiff base reaction

The Schiff base chemistry is one of the old chemistry schools well being investigated by thousands of researchers due to their outstanding application and uses in medical science. These developments have being documented in published papers and patents covered by several well-known international journals and conferences. The Schiff base chemistry of imino derivatives of di ketones is one of the important classes of Schiff bases as aliphatic di ketones and aromatic diones.



Scheme 3: General Schiff base reaction scheme

Schiff bases derived from aromatic ketones have been a core of investigation in various fields of chemical industries and pharmaceuticals, the present project which is based on imino derivatives of phen-5,6-dione is linked to the last application.

4. Chemistry of phen-5,6-dione

The current research topic is based on the imino derivative of phen-5,6-dione as starting materials. The phen-5,6-dione has been known since 1947. Several preparation procedures have been reported in the literature from several different starting materials (Gillard & Hill 1974; Hiort, Lincoln & Norden 1993; Yamada et al. 1992) such as (phen). One of documented procedures is based on oxidation of (phen) using $\text{H}_2\text{SO}_4/\text{HNO}_3/\text{KBr}$.

Several chemical reactivity features, properties, reactions and derivatives of phen-5,6-dione have been investigated and are currently attractive and approached by several researchers such as its electrochemical reduction (Vans & Griffith 1982). The synthesis of mono and di substituted compounds based on di ketone functional groups as imino derivatives which are the backbone of the present study.

The imino derivatives of phen-5,6-dione attracted attention of researchers as a result of the presence of two coordination functionalities in the same molecule, the quinonoid and the diimine functional groups, and their strange reactivity as redox system capable of forming Lewis acid-base adducts to metal complexes at high / low oxidation states which let the design of step by step synthesis of wide range of bimetallic compounds.

On the other hand, the presence oxygen and nitrogen atoms with sp^2 -hybridized orbitals as two types of basic centres which contributes to make this molecule an perfect system to study various coordination capability of the two sets of donor atoms (Calderazzo et al. 1999).

The reported literature indicated that the structure of (phen) active ingredient drugs are less toxic to the tissue cells, accordingly the synthesised phen-5,6-dione will be more basic.

On the other hand, its formed complexes with different metal ions like Fe, Cu and Zn as multi-functional active ingredient are expected to show higher activity than the drugs based on (phen) agent against albicans (McCann et al. 2004).

The chemical structure of the phen-5,6-dione indicates two important roles in the present study; firstly it forms an active ligand that is required in the synthesising of the complexes for several metal ions (phen-5,6-dione forms mono dentate or bidentate chelates of different coordination

number according to the chelating metal ion used); secondly it acts as an intermediate reagent in the synthesis of its pendent arm (quinolone).

4.1 Coordination chemistry of phen-5,6-dione complex

The focus of the recent research activities are targeting the coordination properties of the imino derivatives of (phen-5,6-dione) and 2-aminophenol because this ligand has capability to form stable complexes with several metal ions [Cu(II), Fe(II), Zn(II)] and carries as an o-quinone moiety and pH dependent electro activity with abnormal reactivity as a result of the attendance of two functionalities that act as bis-chelating ligands (Binnemans et al. 2004; Boghaei & Behzadian-Asl 2007; Boghaei & Behzadian Asl 2007; Calderazzo et al. 1999; Girgis, Sohn & Balch 1975; Yamada et al. 2002).

The metal ions are fundamentally Lewis acids while the ligands are similar to Lewis bases which have lone pair of electrons that can donate to empty d-orbitals of the metal (Samadi & Salamati 2014). The diketone functionality can also be easily converted to other chelating groups such as a di imine or di oxime (Gillard, Hill & Maskill 1970).

Thus it is a multipurpose organic linker that can form bridges via amine condensation or combination of coordination and condensation reactions which make these derivatives very important ligand in organometallic chemistry (Bodige & MacDonnell 1997a; Constable 1996; Kim et al. 2002; Sauvage et al. 1994).

Several recent investigation studies revealed the importance of phen-5,6-dione, its imino derivatives and complexes with metal cations as oxidizing agents for organic amines and as inorganic reducing agents for biological reluctant (Hilt & Steckhan 1993; Kobetić et al. 2012; Kochius et al. 2012; Mirífico et al. 2004; Wang & Zhu 2002; Xu et al. 2012). The complexes of phen-5,6-dione have been extensively studied by several types of research.

The phen-5,6-dione ligand forms stable complexes with various metal ions. The electro activity of o-quinone moiety depends on pH. The metal complexes of phen-5,6-dione derivatives controls the redox properties over a wide range of pH (Goss & Abruna 1985).

(Phen) derivatives are poor Π acceptors and good Π -donors and have appreciable ability to control orbital energies by proton transfer (Liu et al. 2004) and bidentate N-donors sites of (phen) will coordinate with metal ions (Gomleksiz, Alkan & Erdem 2013; Pansuriya et al. 2007; Wendlandt & Stahl 2014; Zhong 2012) and chelating with metal ions Fe and Cu as

reported in the literatures (Demirhan, Avciata & Gul 2005; Goss & Abruna 1985; Wang & Zhu 2002) co-ordination of Cu^{2+} and/or Fe^{3+} with A β play a role in the deposition of plaque, Cu^{2+} has also been implicated, playing an additional role through oxidative coupling of tyrosine leading to dimerization as stated earlier (Atwood et al. 2004).

Presences of phenolic and amino groups as active groups in the chemical structure of the molecules enable formation of chelates with several metal ions like Fe, Cu and Zn ions. These metal ion complexes represent the core of the recent studies concerning development of drugs for AD. The substituted phenols and aromatic amine are well known categories of anti-oxidants which are able to terminate chain reactions and act as free radical scavengers.

It has been reported that metal-free phen-5,6-dione is more active drug than metal free of (phen) (Coyle et al. 2003; McCann et al. 2000). On the other hand, it has been suggested that the biologically active chelating of phen type ligands is an in situ produced metal complex of the ligand. The Cu (II) complex of phen-5,6-dione ligand are considerably more active than the most active (phen) complexes (Coyle et al. 2003). The results for (metal-free) phen-5,6-dione with Cu(II) complex suggest that the two carbonyl additions on the (phen) skeleton of the ligand play an significant role on its biochemical activity.

In addition, the more electrochemical activity of the phen-5,6-dione ligand, compared to that of (phen), enhance the possibility for phen-5,6-dione to contribute harmfully in cellular redox reactions.

The pseudo tetrahedral structure of metal-free phen-5,6-dione and the Cu (II) phen-5,6-dione complexes are strong anti-Candidate agents and are more active than their (phen) analogues, signifying an effective biochemical role for the carbonyl oxygen atoms of the phen-5,6-dione molecule (McCann et al. 2004).

4.2 The biological study of phen-5,6-dione

The use of Phen-5,6-dione and its derivatives as one of the most multipurpose chelating ligands in the coordination chemistry (Das, Chatterjee & Paine 2013; Sammes & Yahiolu 1994) have stimulating characteristics of the biological activities (Shaik & Ahmed 2014) such as anti-mycobacterial (Yar, Siddiqui & Ali 2007) antimicrobial, anti-tuberculosis (Nayyar & Jain 2008), anti tumorals (Yang et al. 2013), anti-inflammatory (Thirumurugan, Mahalaxmi & Perumal 2010), antimalarial (Franco et al. 2012), anticonvulsant (Sameem, Kumar & Pathak 2012), anti- HIV (Ma et al. 2013) and anticancer (Su et al. 2013). These derivatives have also shown interest in other different areas such as DNA interaction, (Foxon et al. 2011) exhibition

antimicrobial properties, (Coyle et al. 2003; Qizhuang et al. 2006) bind to DNA, (Gao et al. 2007; Holmlin, Dandliker & Barton 1997; Liu, Xu & Li 2009; Ying et al. 2014; Zhang et al. 2004) recognizing and cleave DNA, (Carlson et al. 1993; Jenkins et al. 1992; Poteet et al. 2013) nanotechnology, (Dietrich-Buchecker, Sauvage & Kern 1989; Kern et al. 1997) molecular recognition, photo catalysis, (Ziessel 1991) solar cell devices, (Tyson & Castellano 1999) colorimetric analysis, and self-assembly (Oztekin & Yazicigil 2009).

The non complexed (Phen) has non-agreeable electrochemical characteristic, it does not contribute to any oxidation-reduction reaction system under normal conditions (Gayathri & Senthil Kumar 2014).

5. Treatment basis of AD

The ability of incoming the active site of AChE and BuChE and binding to the esteratic active site. This blocks ACh from incoming and then being broken down, prolonging its presence (Silman & Sussman 2005). Reversible AChE inhibitors should be used for treatment of AD due to irreversible inhibitors outcome in the build-up of ACh and, as an outcome, neurone cell death.

Two key sites, called the catalytic active site (CAS) at the bottom of the gorge and the peripheral anionic site (PAS) near the entering of the gorge, are linked by a narrow groove (Bourne et al. 2003; Sussman & Harel 1991). CAS is responsible for the hydrolysis of ACh over a catalytic triad consisting of Ser200, Glu327, and His440 (Raves et al. 1997).

PAS contains of several aromatic residues, including Tyr70, Tyr121 and Trp279. The goal of treatment AD is the active site of AChE and BuCh due to its high exact activity. If the ligands are too big to departure the complex gorge, they can yet block the entrance by binding to the PAS.

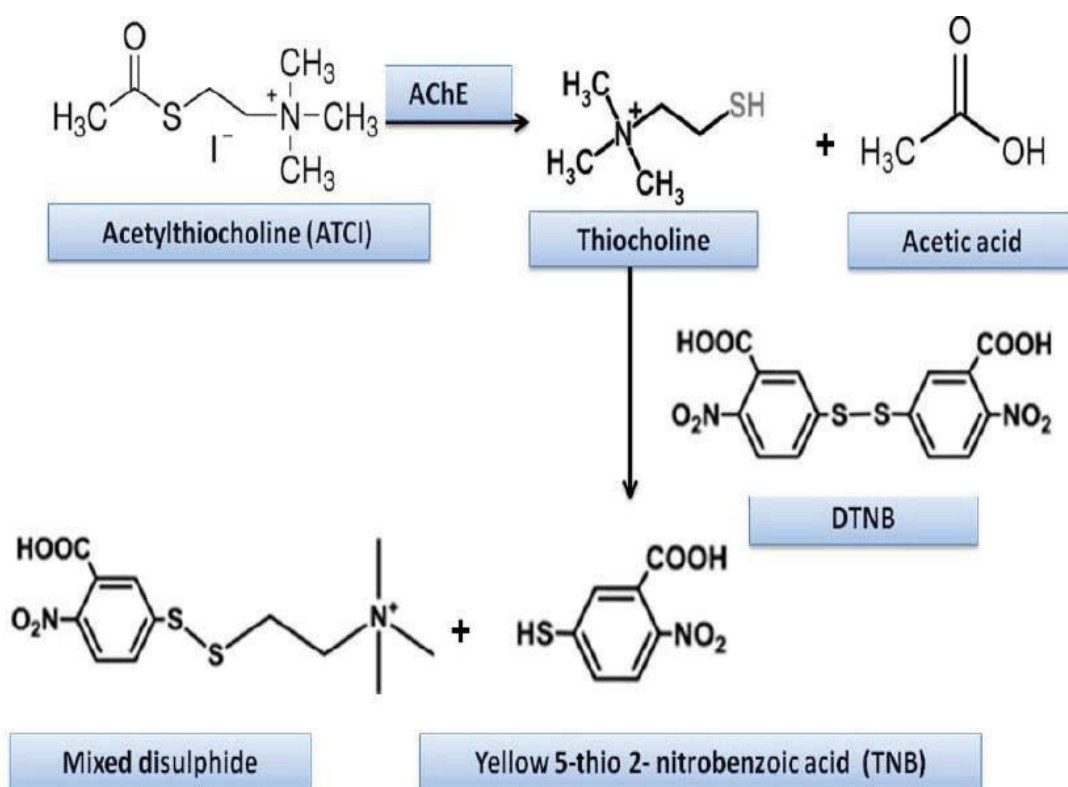
The binding of ligands to the PAS via hydrophobic interactions may block the passing of ACh or alteration the conformation of the active site and inhibit its role (JÄRV, KESVATERA & AAVIKSAAR 1976). Determination of AChE activity has become an important tool in drug design and discovery.

PAS exerts an important occupations regarding to both ACh hydrolysis and A β aggregation (Inestrosa, Sagal & Colombres 2005). Compounds that can cooperate with both CAS and PAS are supposed to use multiple therapeutic effects; this strategy has stimulated the design of multi-target-directed ligands (MTDLs) (Bajda et al. 2011).

The Configuration and form of the active site of BuChE is similar to that of AChE; Though, the volume of the catalytic site in BuChE is larger than that of AChE (Saxena et al. 1997). This alteration provides a chance for the plan of selective BuChE inhibitors.

Assay of AChE, BuChE action plays a significant role in vitro characterization of drugs counting potential treatments for AD.

The most widely used method, is based on Ellman's method (Greig et al. 2005) using the substrate acetylthiocholine iodide (ACTI), S-butyrylthiocholine iodide and the colour reagent 5,5'-dithio-bis-2-nitrobenzoic acid (DTNB) used to produce yellow colour and this yellow colour is read by plate reader at 405 nm. The biological activity of the prepared compounds were determined according to Ellman's methods which is based on the mechanism shown in Scheme 4 (Ali-Shtayeh et al. 2014).



Scheme 4: Chemical mechanism of Ellman's method

6. Significance of the project

Although multiple drugs for AD are now obtainable, none of them are able to slow down, stop, or cure the neurodegeneration in AD. Despite the success at discovering potent AChE inhibitors and A β aggregation, their future clinical usefulness in treating AD is doubtful given that increasing ACh levels in AD sufferers is merely treating symptoms and the doses did not have any prospects of providing a cure.

Thus, if a Multifunctional ligands (ML's) with multi activities toward AD-relevant targets such as (AChE),(BuChE) and A β can be synthesised, mainly with high chelation affinity towards Cu, Fe and Zn ions and decrease A β aggregation.

These active ingredients may reduce the oxidative stress and act as anti-oxidants and free radical scavengers which are able to terminate chain reactions.

On the other hand the successful treatment of AD will require drugs that can penetrate the BBB and have molecular weight below 500g/mol.

7. Aim of project

The project's aims were: synthesis, characterisation, analysis and molecular study and evaluation of novel phen-5,6-dione derivatives having dual inhibitory potency against the acetylcholinesterase and A β aggregation of Alzheimer's disease therapeutics in order to prevent AChE-induced A β aggregation.

Implementing phen-5,6-dione and its derivatives to achieves the dual function of inhibiting the catalytic functions of AChE, BuChE and hindering the A β interaction with AChE by virtue of blocking the PAS.

The first part of the project was focused on synthesis of the novel phen-5,6-dione derivatives through imine formation via condensation between aromatic amine with different aromatic ketone and studying their efficiency for chelating with metal ions like copper, iron and zinc, then characterised all the products by various available techniques. m.p, ^1H , ^{13}C NMR, FT-IR, ATR and HRMS.

The second part of the project consist in vitro evaluation of the new multi-functional active ingredients ligands to monitor the inhibition efficiency as drugs for Alzheimer's disease according to Ellman (Ellman et al. 1961a).

The Last part of the Project consist developing multifunctional active site chelators for targeting multiple categories of Alzheimer's disease by binding and inhibiting (AChE),(BuCh), suppresses oxidative stress, and passivates excess metal ions (Fe, Cu, and Zn) in the brain that have ability to chelate metals.

8. References

- Adlard, P.A. & Bush, A.I. 2006, 'Metals and Alzheimer's disease', *Journal of Alzheimer's disease: JAD*, vol. 10, no. 2-3, pp. 145-63.
- Ali-Shtayeh, M.S., Jamous, R.M., Zaitoun, S.Y.A. & Qasem, I.B. 2014, 'In-vitro screening of acetylcholinesterase inhibitory activity of extracts from Palestinian indigenous flora in relation to the treatment of Alzheimer's disease', *Functional Foods in Health and Disease*, vol. 4, no. 9, pp. 381-400.
- Anand, P. & Singh, B. 2013, 'A review on cholinesterase inhibitors for Alzheimer's disease', *Archives of pharmacal research*, vol. 36, no. 4, pp. 375-99.
- Atwood, C.S., Perry, G., Zeng, H., Kato, Y., Jones, W.D., Ling, K.-Q., Huang, X., Moir, R.D., Wang, D. & Sayre, L.M. 2004, 'Copper mediates dityrosine cross-linking of Alzheimer's amyloid- β ', *Biochemistry*, vol. 43, no. 2, pp. 560-8.
- Bajda, M., Guzior, N., Ignasik, M. & Malawska, B. 2011, 'Multi-target-directed ligands in Alzheimer's disease treatment', *Current medicinal chemistry*, vol. 18, no. 32, pp. 4949-75.
- Bandyopadhyay, S., Huang, X., Lahiri, D.K. & Rogers, J.T. 2010, 'Novel drug targets based on metallobiology of Alzheimer's disease', *Expert Opinion on Therapeutic Targets*, vol. 14, no. 11, pp. 1177-97.
- Barnard, E.A. 1974, 'Neuromuscular transmission—enzymatic destruction of acetylcholine', *The peripheral nervous system*, Springer, pp. 201-24.
- Barnham, K.J. & Bush, A.I. 2008, 'Metals in Alzheimer's and Parkinson's diseases', *Current opinion in chemical biology*, vol. 12, no. 2, pp. 222-8.
- Barnham, K.J. & Bush, A.I. 2014, 'Biological metals and metal-targeting compounds in major neurodegenerative diseases', *Chemical Society Reviews*, vol. 43, no. 19, pp. 6727-49.
- Bartolucci, C., Haller, L.A., Jordis, U., Fels, G. & Lamba, D. 2009, 'Probing Torpedo californica acetylcholinesterase catalytic gorge with two novel bis-functional galanthamine derivatives', *Journal of medicinal chemistry*, vol. 53, no. 2, pp. 745-51.
- Bartus, R.T., Dean, R.L., Beer, B. & Lippa, A.S. 1982a, 'The cholinergic hypothesis of geriatric memory dysfunction', *Science*, vol. 217, no. 4558, pp. 408-14.
- Bartus, R.T., Dean, R.r., Beer, B. & Lippa, A.S. 1982b, 'The cholinergic hypothesis of geriatric memory dysfunction', *Science*, vol. 217, no. 4558, pp. 408-14.
- Beal, M.F. 2004, 'Mitochondrial dysfunction and oxidative damage in Alzheimer's and Parkinson's diseases and coenzyme Q10 as a potential treatment', *Journal of bioenergetics and biomembranes*, vol. 36, no. 4, pp. 381-6.
- Berchtold, N., '8c Cotman, CW.(1998) Evolution in the conceptualization of dementia and Alzheimer's disease: Greco-Roman period to the 1960s', *Neurobiology of Ageing*, pp. 19,173-89.
- Berchtold, N.C. & Cotman, C.W. 1998, 'Evolution in the conceptualization of dementia and Alzheimer's disease: Greco-Roman period to the 1960s', *Neurobiology of aging*, vol. 19, no. 3, pp. 173-89.

- Binnemans, K., Lenaerts, P., Driesen, K. & Gorller-Walrand, C. 2004, 'A luminescent tris(2-thenoyltrifluoroacetato)europium(iii) complex covalently linked to a phen-functionalised sol-gel glass', *Journal of Materials Chemistry*, vol. 14, no. 2, pp. 191-5.
- Birks, J. 2012, 'Cholinesterase inhibitors for Alzheimer's disease (Review)'.
- Bodick, N.C., Offen, W.W., Levey, A.I., Cutler, N.R., Gauthier, S.G., Satlin, A., Shannon, H.E., Tollefson, G.D., Rasmussen, K. & Bymaster, F.P. 1997, 'Effects of xanomeline, a selective muscarinic receptor agonist, on cognitive function and behavioral symptoms in Alzheimer disease', *Archives of neurology*, vol. 54, no. 4, pp. 465-73.
- Bodige, S. & MacDonnell, F.M. 1997, 'Synthesis of Free and Ruthenium Coordinated 5,6-Diamino-1,10-phenanthroline', *Tetrahedron Letters*, vol. 38, no. 47, pp. 8159-60.
- Boghaei, D.M. & Behzadian-Asl, F. 2007, 'Synthesis, characterization and fluorescence spectra of mononuclear Zn(II), Cd(II) and Hg(II) complexes with phen-5,6-dione ligand', *Journal of Coordination Chemistry*, vol. 60, no. 3, pp. 347-53.
- Boghaei, D.M. & Behzadian Asl, F. 2007, 'Synthesis, characterization and fluorescence spectra of mixed ligand Zn(II), Cd(II) and Hg(II) complexes with phen-5,6-dione ligand', *Journal of Coordination Chemistry*, vol. 60, no. 15, pp. 1629-35.
- Bolea, I., Juárez-Jiménez, J., de los Ríos, C., Chioua, M., Pouplana, R., Luque, F.J., Unzeta, M., Marco-Contelles, J. & Samadi, A. 2011, 'Synthesis, Biological Evaluation, and Molecular Modeling of Donepezil and N-[(5-(Benzyloxy)-1-methyl-1H-indol-2-yl)methyl]-N-methylprop-2-yn-1-amine Hybrids as New Multipotent Cholinesterase/Monoamine Oxidase Inhibitors for the Treatment of Alzheimer's Disease', *Journal of Medicinal Chemistry*, vol. 54, no. 24, pp. 8251-70.
- Bolognesi, M.L., Andrisano, V., Bartolini, M., Cavalli, A., Minarini, A., Recanatini, M., Rosini, M., Tumiatti, V. & Melchiorre, C. 2005, 'Heterocyclic inhibitors of AChE acylation and peripheral sites', *Il Farmaco*, vol. 60, no. 6, pp. 465-73.
- Bolognesi, M.L., Cavalli, A., Valgimigli, L., Bartolini, M., Rosini, M., Andrisano, V., Recanatini, M. & Melchiorre, C. 2007, 'Multi-target-directed drug design strategy: from a dual binding site acetylcholinesterase inhibitor to a trifunctional compound against Alzheimer's disease', *Journal of medicinal chemistry*, vol. 50, no. 26, pp. 6446-9.
- Bolognesi, M.L., Minarini, A., Budriesi, R., Cacciaguerra, S., Chiarini, A., Spampinato, S., Tumiatti, V. & Melchiorre, C. 1998, 'Universal template approach to drug design: polyamines as selective muscarinic receptor antagonists', *Journal of medicinal chemistry*, vol. 41, no. 21, pp. 4150-60.
- Bonda, D.J., Lee, H.-g., Blair, J.A., Zhu, X., Perry, G. & Smith, M.A. 2011, 'Role of metal dyshomeostasis in Alzheimer's disease', *Metallomics*, vol. 3, no. 3, pp. 267-70.
- Bourne, Y., Taylor, P., Kanter, J., Bougis, P. & Marchot, P. 1998, 'Crystal Structure of Mouse Acetylcholinesterase', in B. Doctor, P. Taylor, D. Quinn, R. Rotundo & M. Gentry (eds), *Structure and Function of Cholinesterases and Related Proteins*, Springer US, pp. 315-22.
- Bourne, Y., Taylor, P., Radić, Z. & Marchot, P. 2003, 'Structural insights into ligand interactions at the acetylcholinesterase peripheral anionic site', *The EMBO journal*, vol. 22, no. 1, pp. 1-12.
- Bragin, V., Chemodanova, M., Dzhafarova, N., Bragin, I., Czerniawski, J.L. & Aliev, G. 2005, 'Integrated treatment approach improves cognitive function in demented and clinically depressed patients', *American journal of Alzheimer's disease and other dementias*, vol. 20, no. 1, pp. 21-6.
- Braymer, J.J., DeToma, A.S., Choi, J.-S., Ko, K.S. & Lim, M.H. 2010, 'Recent development of bifunctional small molecules to study metal-amyloid- β species in Alzheimer's disease', *International Journal of Alzheimer's Disease*, vol. 2011.
- Busciglio, J., Lorenzo, A., Yeh, J. & Yankner, B.A. 1995, ' β -Amyloid fibrils induce tau phosphorylation and loss of microtubule binding', *Neuron*, vol. 14, no. 4, pp. 879-88.
- Bush, A. & Tanzi, R. 2008, 'Therapeutics for Alzheimer's disease based on the metal hypothesis', *Neurotherapeutics*, vol. 5, no. 3, pp. 421-32.

- Calderazzo, F., Marchetti, F., Pampaloni, G. & Passarelli, V. 1999, 'Co-ordination properties of phen-5,6-dione towards group 4 and 5 metals in low and high oxidation states [dagger]', *Journal of the Chemical Society, Dalton Transactions*, no. 24, pp. 4389-96.
- Carlson, D.L., Huchital, D.H., Mantilla, E.J., Sheardy, R.D. & Murphy Jr, W.R. 1993, 'A new class of DNA metallobinders showing spectator ligand size selectivity: binding of ligand-bridged bimetallic complexes of ruthenium (II) to calf thymus DNA', *Journal of the American Chemical Society*, vol. 115, no. 14, pp. 6424-5.
- Carolan, C.G., Dillon, G.P., Khan, D., Ryder, S.A., Gaynor, J.M., Reidy, S., Marquez, J.F., Jones, M., Holland, V. & Gilmer, J.F. 2010, 'Isosorbide-2-benzyl carbamate-5-salicylate, a peripheral anionic site binding subnanomolar selective butyrylcholinesterase inhibitor', *Journal of medicinal chemistry*, vol. 53, no. 3, pp. 1190-9.
- Carter, M., Simms, G. & Weaver, D. 2010, 'The development of new therapeutics for Alzheimer's disease', *Clinical Pharmacology & Therapeutics*, vol. 88, no. 4, pp. 475-86.
- Çokuğraş, A.N. 2003, 'Butyrylcholinesterase: structure and physiological importance', *Turk J Biochem*, vol. 28, no. 2, pp. 54-61.
- Congreve, M., Murray, C.W. & Blundell, T.L. 2005, 'Keynote review: Structural biology and drug discovery', *Drug discovery today*, vol. 10, no. 13, pp. 895-907.
- Constable, E.C. 1996, *Metals and ligand reactivity: An Introduction to the Organic Chemistry of Metal Complexes*, Verlagsgesellschaft mbH (VCH), Weinheim.
- Contestabile, A. 2011, 'The history of the cholinergic hypothesis', *Behavioural brain research*, vol. 221, no. 2, pp. 334-40.
- Coyle, B., Kavanagh, K., McCann, M., Devereux, M. & Geraghty, M. 2003, 'Mode of anti-fungal activity of 1, 10-phenanthroline and its Cu (II), Mn (II) and Ag (I) complexes', *Biomaterials*, vol. 16, no. 2, pp. 321-9.
- Csermely, P., Agoston, V. & Pongor, S. 2005, 'The efficiency of multi-target drugs: the network approach might help drug design', *Trends in pharmacological sciences*, vol. 26, no. 4, pp. 178-82.
- Cummings, J.L. 2003, 'Treatment of Alzheimer's disease: current and future therapeutic approaches', *Reviews in neurological diseases*, vol. 1, no. 2, pp. 60-9.
- Cummings, J.L. & Back, C. 1998, 'The cholinergic hypothesis of neuropsychiatric symptoms in Alzheimer's disease', *The American Journal of Geriatric Psychiatry*, vol. 6, no. 2, pp. S64-S78.
- Danysz, W. & Parsons, C.G. 1998, 'Glycine and N-methyl-D-aspartate receptors: physiological significance and possible therapeutic applications', *Pharmacological reviews*, vol. 50, no. 4, pp. 597-664.
- Darvesh, S., McDonald, R.S., Darvesh, K.V., Mataija, D., Conrad, S., Gomez, G., Walsh, R. & Martin, E. 2007, 'Selective reversible inhibition of human butyrylcholinesterase by aryl amide derivatives of phenothiazine', *Bioorganic & medicinal chemistry*, vol. 15, no. 19, pp. 6367-78.
- Das, O., Chatterjee, S. & Paine, T. 2013, 'Functional models of α -keto acid dependent nonheme iron oxygenases: synthesis and reactivity of biomimetic iron(II) benzoylformate complexes supported by a 2,9-dimethyl-1,10-phenanthroline ligand', *JBIC Journal of Biological Inorganic Chemistry*, vol. 18, no. 3, pp. 401-10.
- Decker, M., Kraus, B. & Heilmann, J. 2008, 'Design, synthesis and pharmacological evaluation of hybrid molecules out of quinazolinimines and lipoic acid lead to highly potent and selective butyrylcholinesterase inhibitors with antioxidant properties', *Bioorganic & medicinal chemistry*, vol. 16, no. 8, pp. 4252-61.
- Demirhan, N., Avciata, U. & Gul, A. 2005, 'Synthesis and characterisation of 5, 6-bis (salicylideneimino)-1, 10-phenanthroline and its trinuclear complexes', *Indian Journal of Chemistry*, vol. 44, no. 4, pp. 729-32.
- Desideri, N., Fioravanti, R., Monaco, L.P., Biava, M., Yáñez, M., Ortuso, F. & Alcaro, S. 2013, '1, 5-Diphenylpenta-2, 4-dien-1-ones as potent and selective monoamine oxidase-B inhibitors', *European journal of medicinal chemistry*, vol. 59, pp. 91-100.

- DeToma, A.S., Salamekh, S., Ramamoorthy, A. & Lim, M.H. 2012, 'Misfolded proteins in Alzheimer's disease and type II diabetes', *Chemical Society Reviews*, vol. 41, no. 2, pp. 608-21.
- Dietrich-Buchecker, C., Sauvage, J.P. & Kern, J.M. 1989, 'Synthesis and electrochemical studies of catenates: Stabilization of low oxidation states by interlocked macrocyclic ligands', *Journal of the American Chemical Society*, vol. 111, no. 20, pp. 7791-800.
- Dillon, G.P., Gaynor, J.M., Khan, D., Carolan, C.G., Ryder, S.A., Marquez, J.F., Reidy, S. & Gilmer, J.F. 2010, 'Isosorbide-based cholinesterase inhibitors; replacement of 5-ester groups leading to increased stability', *Bioorganic & medicinal chemistry*, vol. 18, no. 3, pp. 1045-53.
- Doble, A. 1999, 'The role of excitotoxicity in neurodegenerative disease: implications for therapy', *Pharmacology & therapeutics*, vol. 81, no. 3, pp. 163-221.
- Dolmella, A., Bandoli, G. & Nicolini, M. 1994, 'Alzheimer's disease: a pharmacological challenge', *Advances in Drug Research*, vol. 25, pp. 203-94.
- Doraiswamy, P.M. & Finefrock, A.E. 2004, 'Metals in our minds: therapeutic implications for neurodegenerative disorders', *The Lancet Neurology*, vol. 3, no. 7, pp. 431-4.
- Dressman, J.B., Amidon, G.L., Reppas, C. & Shah, V.P. 1998, 'Dissolution testing as a prognostic tool for oral drug absorption: immediate release dosage forms', *Pharmaceutical research*, vol. 15, no. 1, pp. 11-22.
- Duce, J.A. & Bush, A.I. 2010, 'Biological metals and Alzheimer's disease: implications for therapeutics and diagnostics', *Progress in neurobiology*, vol. 92, no. 1, pp. 1-18.
- Ellman, G.L., Courtney, K.D., Andres, V. & Featherstone, R.M. 1961, 'A new and rapid colorimetric determination of acetylcholinesterase activity', *Biochemical pharmacology*, vol. 7, no. 2, pp. 88-95.
- Elsinghorst, P.W., González Tanarro, C.M. & Gütschow, M. 2006, 'Novel heterobivalent tacrine derivatives as cholinesterase inhibitors with notable selectivity toward butyrylcholinesterase', *Journal of medicinal chemistry*, vol. 49, no. 25, pp. 7540-4.
- Espinoza-Fonseca, L.M. 2006, 'The benefits of the multi-target approach in drug design and discovery', *Bioorganic & medicinal chemistry*, vol. 14, no. 4, pp. 896-7.
- Falangola, M.F., Lee, S.-P., Nixon, R.A., Duff, K. & Helpert, J.A. 2005, 'Histological Co-Localization of Iron in A β Plaques of PS/APP Transgenic Mice', *Neurochemical research*, vol. 30, no. 2, pp. 201-5.
- Fernandez, H.L., Moreno, R.D. & Inestrosa, N.C. 1996, 'Tetrameric (G4) acetylcholinesterase: structure, localization, and physiological regulation', *Journal of neurochemistry*, vol. 66, no. 4, pp. 1335-46.
- Fodero-Tavoletti, M.T., Villemagne, V.L., Paterson, B.M., White, A.R., Li, Q.-X., Camakaris, J., O'Keefe, G., Cappai, R., Barnham, K.J. & Donnelly, P.S. 2010, 'Bis (thiosemicarbazonato) Cu-64 Complexes for Positron Emission Tomography Imaging of Alzheimer's Disease', *Journal of Alzheimer's Disease*, vol. 20, no. 1, pp. 49-55.
- Forster, M.J. 2002, 'Molecular modelling in structural biology', *Micron*, vol. 33, no. 4, pp. 365-84.
- Foxon, S.P., Green, C., Walker, M.G., Wragg, A., Adams, H., Weinstein, J.A., Parker, S.C., Meijer, A.J. & Thomas, J.A. 2011, 'Synthesis, characterization, and DNA binding properties of ruthenium (II) complexes containing the redox active ligand benzo [i] dipyrdo [3, 2-a: 2', 3'-c] phenazine-11, 16-quinone', *Inorganic chemistry*, vol. 51, no. 1, pp. 463-71.
- Francis, P.T., Nordberg, A. & Arnold, S.E. 2005, 'A preclinical view of cholinesterase inhibitors in neuroprotection: do they provide more than symptomatic benefits in Alzheimer's disease?', *Trends in pharmacological sciences*, vol. 26, no. 2, pp. 104-11.
- Francis, P.T., Palmer, A.M., Snape, M. & Wilcock, G.K. 1999, 'The cholinergic hypothesis of Alzheimer's disease: a review of progress', *Journal of Neurology, Neurosurgery & Psychiatry*, vol. 66, no. 2, pp. 137-47.
- Franco, L.L., de Almeida, M.V., Vieira, P.P.R., Pohlit, A.M. & Valle, M.S. 2012, 'Synthesis and antimalarial activity of dihydroperoxides and tetraoxanes conjugated with bis (benzyl) acetone derivatives', *Chemical biology & drug design*, vol. 79, no. 5, pp. 790-7.

- Frölich, L. 2002, 'The cholinergic pathology in Alzheimer's disease – discrepancies between clinical experience and pathophysiological findings', *Journal of Neural Transmission*, vol. 109, no. 7, pp. 1003-13.
- Fukuto, T.R. 1990, 'Mechanism of action of organophosphorus and carbamate insecticides', *Environmental health perspectives*, vol. 87, p. 245.
- Gaeta, A. & Hider, R.C. 2005, 'The crucial role of metal ions in neurodegeneration: the basis for a promising therapeutic strategy', *British journal of pharmacology*, vol. 146, no. 8, pp. 1041-59.
- Gaggelli, E., Kozłowski, H., Valensin, D. & Valensin, G. 2006, 'Copper homeostasis and neurodegenerative disorders (Alzheimer's, prion, and Parkinson's diseases and amyotrophic lateral sclerosis)', *Chemical reviews*, vol. 106, no. 6, pp. 1995-2044.
- Gandy, S. & Greengard, P. 1994, 'Processing of Alzheimer A β -Amyloid Precursor Protein: Cell Biology, Regulation, and Role in Alzheimer Disease', in J.B. Ronald & R.A. Harris (eds), *International Review of Neurobiology*, vol. Volume 36, Academic Press, pp. 29-50.
- Gao, F., Chao, H., Wang, J.-Q., Yuan, Y.-X., Sun, B., Wei, Y.-F., Peng, B. & Ji, L.-N. 2007, 'Targeting topoisomerase II with the chiral DNA-intercalating ruthenium (II) polypyridyl complexes', *JBIC Journal of Biological Inorganic Chemistry*, vol. 12, no. 7, pp. 1015-27.
- Garzone, P.D. 1993, 'Treatment of Dementias. A New Generation of Progress', *Pharmaceutical Research*, vol. 10, no. 11, p. 1697.
- Gayathri, P. & Senthil Kumar, A. 2014, 'Electrochemical Behavior of the 1, 10-Phenanthroline Ligand on a Multiwalled Carbon Nanotube Surface and Its Relevant Electrochemistry for Selective Recognition of Copper Ion and Hydrogen Peroxide Sensing', *Langmuir*, vol. 30, no. 34, pp. 10513-21.
- Ge, J.-F., Qiao, J.-P., Qi, C.-C., Wang, C.-W. & Zhou, J.-N. 2012, 'The binding of resveratrol to monomer and fibril amyloid beta', *Neurochemistry international*, vol. 61, no. 7, pp. 1192-201.
- GeulaC, M.M. 1993, 'Neurological cholinesterase in the normal brain and in Alzheimer's disease: Relation to plaques, tangles, and patterns of selective vulnerability', *Ann Neurol*, vol. 34, pp. 373-84.
- Giacobini, E. 2004, 'Cholinesterase inhibitors: new roles and therapeutic alternatives', *Pharmacological research*, vol. 50, no. 4, pp. 433-40.
- Gillard, R.D. & Hill, R.E.E. 1974, 'Optically active co-ordination compounds. Part XXXIV. Modification of reaction pathways in phen and its derivatives by metal ions', *Journal of the Chemical Society, Dalton Transactions*, no. 11, pp. 1217-36.
- Gillard, R.D., Hill, R.E.E. & Maskill, R. 1970, 'Optically active co-ordination compounds. Part XX. Reactions of phen co-ordinated to cobalt(III)', *Journal of the Chemical Society A: Inorganic, Physical, Theoretical*, no. 0, pp. 1447-51.
- Girgis, A.Y., Sohn, Y.S. & Balch, A.L. 1975, 'Preparation and oxidation of some quinone adducts of transition metal complexes', *Inorganic Chemistry*, vol. 14, no. 10, pp. 2327-31.
- GomLeksiz, M., Alkan, C. & Erdem, B. 2013, 'Synthesis, characterization and antibacterial activity of imidazole derivatives of phen and their Cu(II), Co(II) and Ni(II) complexes : research article', vol. 66, pp. 107-12,
<http://reference.sabinet.co.za/webx/access/electronic_journals/chem/chem_v66_a17.pdf>.
- Goss, C.A. & Abruna, H.D. 1985, 'Spectral, electrochemical and electrocatalytic properties of phen-5,6-dione complexes of transition metals', *Inorganic Chemistry*, vol. 24, no. 25, pp. 4263-7.
- Greenlee, W., Clader, J., Asberom, T., McCombie, S., Ford, J., Guzik, H., Kozłowski, J., Li, S., Liu, C. & Lowe, D. 2001, 'Muscarinic agonists and antagonists in the treatment of Alzheimer's disease', *Il Farmaco*, vol. 56, no. 4, pp. 247-50.

- Greig, N.H., Utsuki, T., Ingram, D.K., Wang, Y., Pepeu, G., Scali, C., Yu, Q.-S., Mamczarz, J., Holloway, H.W. & Giordano, T. 2005, 'Selective butyrylcholinesterase inhibition elevates brain acetylcholine, augments learning and lowers Alzheimer β -amyloid peptide in rodent', *Proceedings of the National Academy of Sciences of the United States of America*, vol. 102, no. 47, pp. 17213-8.
- Gualtieri, F., Dei, S., Manetti, D., Romanelli, M., Scapecchi, S. & Teodori, E. 1995, 'The medicinal chemistry of Alzheimer's and Alzheimer-like diseases with emphasis on the cholinergic hypothesis', *Farmaco (Società chimica italiana: 1989)*, vol. 50, no. 7-8, p. 489.
- Guo, J., Hurley, M.M., Wright, J.B. & Lushington, G.H. 2004, 'A docking score function for estimating ligand– protein interactions: Application to acetylcholinesterase inhibition', *Journal of medicinal chemistry*, vol. 47, no. 22, pp. 5492-500.
- Haass, C., Schlossmacher, M.G., Hung, A.Y., Vigo-Pelfrey, C., Mellon, A., Ostaszewski, B.L., Lieberburg, I., Koo, E.H., Schenk, D. & Teplow, D.B. 1992, 'Amyloid β -peptide is produced by cultured cells during normal metabolism', *Nature*, vol. 359, no. 6393, pp. 322-5.
- Han, Y., Ryu, S. & Han, B. 1990, 'Antioxidant activity of resveratrol closely correlates with its monoamine oxidase-A inhibitory activity', *Archives of Pharmacal Research*, vol. 13, no. 2, pp. 132-5.
- Hardy, J. 2009, 'The amyloid hypothesis for Alzheimer's disease: a critical reappraisal', *Journal of neurochemistry*, vol. 110, no. 4, pp. 1129-34.
- Hardy, J. & Allsop, D. 1991, 'Amyloid deposition as the central event in the aetiology of Alzheimer's disease', *Trends in pharmacological sciences*, vol. 12, pp. 383-8.
- Hardy, J., Duff, K., Hardy, K.G., Perez-Tur, J. & Hutton, M. 1998, 'Genetic dissection of Alzheimer's disease and related dementias: amyloid and its relationship to tau', *Nature neuroscience*, vol. 1, no. 5, pp. 355-8.
- Hartmann, C., Antes, I. & Lengauer, T. 2009, 'Docking and scoring with alternative side-chain conformations', *Proteins: Structure, Function, and Bioinformatics*, vol. 74, no. 3, pp. 712-26.
- Hebert, L.E., Scherr, P.A., Bienias, J.L., Bennett, D.A. & Evans, D.A. 2003, 'Alzheimer disease in the US population: prevalence estimates using the 2000 census', *Archives of neurology*, vol. 60, no. 8, pp. 1119-22.
- Heinrich, M. & Teoh, H.L. 2004, 'Galanthamine from snowdrop—the development of a modern drug against Alzheimer's disease from local Caucasian knowledge', *Journal of ethnopharmacology*, vol. 92, no. 2, pp. 147-62.
- Hilt, G. & Steckhan, E. 1993, 'Transition metal complexes of phen-5,6-dione as efficient mediators for the regeneration of NAD⁺ in enzymatic synthesis', *Journal of the Chemical Society, Chemical Communications*, no. 22, pp. 1706-7.
- Hindo, S.S., Mancino, A.M., Braymer, J.J., Liu, Y., Vivekanandan, S., Ramamoorthy, A. & Lim, M.H. 2009, 'Small molecule modulators of copper-induced A β aggregation', *Journal of the American Chemical Society*, vol. 131, no. 46, pp. 16663-5.
- Hiort, C., Lincoln, P. & Norden, B. 1993, 'DNA binding of .DELTA.- and .LAMBDA.-[Ru(phen)2DPPZ]2+', *Journal of the American Chemical Society*, vol. 115, no. 9, pp. 3448-54.
- Holmlin, R.E., Dandliker, P.J. & Barton, J.K. 1997, 'Charge transfer through the DNA base stack', *Angewandte Chemie International Edition in English*, vol. 36, no. 24, pp. 2714-30.
- Hopkins, A.L., Mason, J.S. & Overington, J.P. 2006, 'Can we rationally design promiscuous drugs?', *Current opinion in structural biology*, vol. 16, no. 1, pp. 127-36.
- Hureau, C., Sasaki, I., Gras, E. & Faller, P. 2010, 'Two Functions, One Molecule: A Metal-Binding and a Targeting Moiety to Combat Alzheimer's Disease', *ChemBioChem*, vol. 11, no. 7, pp. 950-3.
- Inestrosa, N.C., Sagal, J.P. & Colombres, M. 2005, 'Acetylcholinesterase interaction with Alzheimer amyloid β ', *Alzheimer's Disease*, pp. 299-317.
- JÄRV, J., KESVATERA, T. & AAVIKSAAR, A. 1976, 'Structure-Activity Relationships in Acetylcholinesterase Reactions', *The FEBS Journal*, vol. 67, no. 2, pp. 315-22.

- Jenkins, Y., Friedman, A.E., Turro, N.J. & Barton, J.K. 1992, 'Characterization of dipyridophenazine complexes of ruthenium (II): the light switch effect as a function of nucleic acid sequence and conformation', *Biochemistry*, vol. 31, no. 44, pp. 10809-16.
- Jomova, K., Vondrakova, D., Lawson, M. & Valko, M. 2010, 'Metals, oxidative stress and neurodegenerative disorders', *Molecular and cellular biochemistry*, vol. 345, no. 1-2, pp. 91-104.
- Kern, J.-M., Sauvage, J.-P., Weidmann, J.-L., Armaroli, N., Flamigni, L., Ceroni, P. & Balzani, V. 1997, 'Complexes containing 2, 9-bis (p-biphenyl)-1, 10-phenanthroline units incorporated into a 56-membered ring. Synthesis, electrochemistry, and photophysical properties', *Inorganic Chemistry*, vol. 36, no. 23, pp. 5329-38.
- Khlistunova, I., Biernat, J., Wang, Y., Pickhardt, M., von Bergen, M., Gazova, Z., Mandelkow, E. & Mandelkow, E.-M. 2006, 'Inducible expression of Tau repeat domain in cell models of tauopathy aggregation is toxic to cells but can be reversed by inhibitor drugs', *Journal of Biological Chemistry*, vol. 281, no. 2, pp. 1205-14.
- Kim, M.-J., Konduri, R., Ye, H., MacDonnell, F.M., Puntoriero, F., Serroni, S., Campagna, S., Holder, T., Kinsel, G. & Rajeshwar, K. 2002, 'Dinuclear Ruthenium(II) Polypyridyl Complexes Containing Large, Redox-Active, Aromatic Bridging Ligands: Synthesis, Characterization, and Intramolecular Quenching of MLCT Excited States', *Inorganic Chemistry*, vol. 41, no. 9, pp. 2471-6.
- Kim, S., Cheon, H.-S., Kim, S.-Y., Juhn, Y.-S. & Kim, Y.-Y. 2013, 'Cadmium induces neuronal cell death through reactive oxygen species activated by GADD153', *BMC cell biology*, vol. 14, no. 1, p. 4.
- Kobetić, R., Denžić, M., Zimmermann, B., Rončević, S. & Baranović, G. 2012, 'Preparation and separation of mixed-ligand Fe(II) complexes containing phen-5,6-dione as ligand', *Journal of Coordination Chemistry*, vol. 65, no. 19, pp. 3433-48.
- Kochius, S., Magnusson, A., Hollmann, F., Schrader, J. & Holtmann, D. 2012, 'Immobilized redox mediators for electrochemical NAD(P)⁺ regeneration', *Applied Microbiology and Biotechnology*, vol. 93, no. 6, pp. 2251-64.
- KoSIK, K.S., Joachim, C.L. & Selkoe, D.J. 1986, 'Microtubule-associated protein tau (tau) is a major antigenic component of paired helical filaments in Alzheimer disease', *Proceedings of the National Academy of Sciences*, vol. 83, no. 11, pp. 4044-8.
- Kryger, G., Giles, K., Harel, M., Toker, L., Velan, B., Lazar, A., Kronman, C., Barak, D., Ariel, N., Shafferman, A., Silman, I. & Sussman, J. 1998, '3D Structure at 2.7 Å Resolution of Native and E202Q Mutant Human Acetylcholinesterase Complexed with Fasciculin-II', in B. Doctor, P. Taylor, D. Quinn, R. Rotundo & M. Gentry (eds), *Structure and Function of Cholinesterases and Related Proteins*, Springer US, pp. 323-6.
- Kryger, G., Silman, I. & Sussman, J.L. 1999, 'Structure of acetylcholinesterase complexed with E2020 (Aricept®): implications for the design of new anti-Alzheimer drugs', *Structure*, vol. 7, no. 3, pp. 297-307.
- Lage, J.M.M. 2006, '100 Years of Alzheimer's disease (1906–2006)', *Journal of Alzheimer's Disease*, vol. 9, no. s3, pp. 15-26.
- Lee, S., Zheng, X., Krishnamoorthy, J., Savelieff, M.G., Park, H.M., Brender, J.R., Kim, J.H., Derrick, J.S., Kochi, A. & Lee, H.J. 2013, 'Rational design of a structural framework with potential use to develop chemical reagents that target and modulate multiple facets of Alzheimer's disease', *Journal of the American Chemical Society*, vol. 136, no. 1, pp. 299-310.
- Lengauer, T. & Rarey, M. 1996, 'Computational methods for biomolecular docking', *Current opinion in structural biology*, vol. 6, no. 3, pp. 402-6.
- Leonard, B. 1998, 'Advances in the drug treatment of Alzheimer's disease', *Human Psychopharmacology: Clinical and Experimental*, vol. 13, no. 2, pp. 83-90.

- Li, B., Stribley, J.A., Ticu, A., Xie, W., Schopfer, L.M., Hammond, P., Brimijoin, S., Hinrichs, S.H. & Lockridge, O. 2000, 'Abundant tissue butyrylcholinesterase and its possible function in the acetylcholinesterase knockout mouse', *Journal of neurochemistry*, vol. 75, no. 3, pp. 1320-31.
- Li, S.-Y., Wang, X.-B. & Kong, L.-Y. 2014, 'Design, synthesis and biological evaluation of imine resveratrol derivatives as multi-targeted agents against Alzheimer's disease', *European journal of medicinal chemistry*, vol. 71, pp. 36-45.
- Lipinski, C.A. 2004, 'Lead-and drug-like compounds: the rule-of-five revolution', *Drug Discovery Today: Technologies*, vol. 1, no. 4, pp. 337-41.
- Lipinski, C.A., Lombardo, F., Dominy, B.W. & Feeney, P.J. 2001, 'Experimental and computational approaches to estimate solubility and permeability in drug discovery and development settings', *Advanced drug delivery reviews*, vol. 46, no. 1-3, pp. 3-26.
- Liu, F., Wang, K., Bai, G., Zhang, Y. & Gao, L. 2004, 'The pH-Induced Emission Switching and Interesting DNA-Binding Properties of a Novel Dinuclear Ruthenium(II) Complex', *Inorganic Chemistry*, vol. 43, no. 5, pp. 1799-806.
- Liu, X., Xu, L. & Li, H. 2009, 'H. Chao, KC Zheng and LN Ji', *J. Mol. Struct*, vol. 920, pp. 163-71.
- Liu, Y., Kochi, A., Pithadia, A.S., Lee, S., Nam, Y., Beck, M.W., He, X., Lee, D. & Lim, M.H. 2013, 'Tuning reactivity of diphenylpropynone derivatives with metal-associated amyloid- β species via structural modifications', *Inorganic chemistry*, vol. 52, no. 14, pp. 8121-30.
- Ma, X., Li, L., Zhu, T., Ba, M., Li, G., Gu, Q., Guo, Y. & Li, D. 2013, 'Phenylspirodrimanones with anti-HIV activity from the sponge-derived fungus *Stachybotrys chartarum* MXH-X73', *Journal of natural products*, vol. 76, no. 12, pp. 2298-306.
- Maelicke, A. & Albuquerque, E.X. 1996, 'New approach to drug therapy in Alzheimer's dementia Alfred Maelicke and Edson X. Albuquerque', *Drug Discovery Today*, vol. 1, no. 2, pp. 53-9.
- Manoharan, I., Boopathy, R., Darvesh, S. & Lockridge, O. 2007, 'A medical health report on individuals with silent butyrylcholinesterase in the Vysya community of India', *Clinica chimica acta*, vol. 378, no. 1, pp. 128-35.
- Markesbery, W.R. 1997, 'Oxidative stress hypothesis in Alzheimer's disease', *Free Radical Biology and Medicine*, vol. 23, no. 1, pp. 134-47.
- Maurer, K., Volk, S. & Gerbaldo, H. 1997, 'Auguste D and Alzheimer's disease', *The Lancet*, vol. 349, no. 9064, pp. 1546-9.
- McCann, M., Coyle, B., McKay, S., McCormack, P., Kavanagh, K., Devereux, M., McKee, V., Kinsella, P., O'connor, R. & Clynes, M. 2004, 'Synthesis and X-ray crystal structure of [Ag (phendio) 2] ClO₄ (phendio= 1, 10-phenanthroline-5, 6-dione) and its effects on fungal and mammalian cells', *Biometals*, vol. 17, no. 6, pp. 635-45.
- McCann, M., Geraghty, M., Devereux, M., O'Shea, D., Mason, J. & O'Sullivan, L. 2000, 'Insights into the mode of action of the anti-Candida activity of 1, 10-phenanthroline and its metal chelates', *Metal-Based Drugs*, vol. 7, no. 4, p. 185.
- McCormick, D.A. 1989, 'Acetylcholine: distribution, receptors, and actions', *Semin Neurosci*, vol. 1, pp. 91-101.
- McGeer, P.L. 1984, 'The 12th J. A. F. Stevenson Memorial Lecture: Aging, Alzheimer's disease, and the cholinergic system', *Canadian Journal of Physiology and Pharmacology*, vol. 62, no. 7, pp. 741-54.
- McGleenon, B., Dynan, K. & Passmore, A. 1999, 'Acetylcholinesterase inhibitors in Alzheimer's disease', *British journal of clinical pharmacology*, vol. 48, no. 4, p. 471.
- McLaurin, J., Kierstead, M.E., Brown, M.E., Hawkes, C.A., Lambermon, M.H., Phinney, A.L., Darabie, A.A., Cousins, J.E., French, J.E. & Lan, M.F. 2006, 'Cyclohexanehexol inhibitors of A β aggregation prevent and reverse Alzheimer phenotype in a mouse model', *Nature medicine*, vol. 12, no. 7, pp. 801-8.

- Melchiorre, C., Andrisano, V., Bolognesi, M.L., Budriesi, R., Cavalli, A., Cavrini, V., Rosini, M., Tumiatti, V. & Recanatini, M. 1998, 'Acetylcholinesterase noncovalent inhibitors based on a polyamine backbone for potential use against Alzheimer's disease', *Journal of medicinal chemistry*, vol. 41, no. 22, pp. 4186-9.
- Melchiorre, C., Angeli, P., Brasili, L., Giardinà, D., Pigni, M. & Quaglia, W. 1988, 'Polyamines: a possible "passe-partout" for receptor characterization', *Actual. Chim. Ther*, pp. 149-68.
- Mesulam, M., Guillozet, A., Shaw, P. & Quinn, B. 2002, 'Widely spread butyrylcholinesterase can hydrolyze acetylcholine in the normal and Alzheimer brain', *Neurobiology of disease*, vol. 9, no. 1, pp. 88-93.
- Mirífico, M.V., Svartman, E.L., Caram, J.A. & Vasini, E.J. 2004, 'Partial electrooxidation of nitrogenated heterocycles: novel synthesis of phen-5,6-quinone by electrooxidation of phen', *Journal of Electroanalytical Chemistry*, vol. 566, no. 1, pp. 7-13.
- Mitra, J., Guerrero, E.N., Hegde, P.M., Wang, H., Boldogh, I., Rao, K.S., Mitra, S. & Hegde, M.L. 2014, 'New perspectives on oxidized genome damage and repair inhibition by pro-oxidant metals in neurological diseases', *Biomolecules*, vol. 4, no. 3, pp. 678-703.
- Molina-Holgado, F., Hider, R.C., Gaeta, A., Williams, R. & Francis, P. 2007, 'Metals ions and neurodegeneration', *Biometals*, vol. 20, no. 3-4, pp. 639-54.
- Mount, C. & Downton, C. 2006, 'Alzheimer disease: progress or profit?', *Nature medicine*, vol. 12, no. 7, pp. 780-4.
- Nayyar, A. & Jain, R. 2008, 'Synthesis and anti-tuberculosis activity of 2, 4-disubstituted quinolines', *Indian journal of chemistry. Section B, Organic including medicinal*, vol. 47, no. 1, p. 117.
- Noël, S., Cadet, S., Gras, E. & Hureau, C. 2013, 'The benzazole scaffold: a SWAT to combat Alzheimer's disease', *Chemical Society Reviews*, vol. 42, no. 19, pp. 7747-62.
- Nunomura, A., Perry, G., Aliev, G., Hirai, K., Takeda, A., Balraj, E.K., Jones, P.K., Ghanbari, H., Wataya, T. & Shimohama, S. 2001, 'Oxidative damage is the earliest event in Alzheimer disease', *Journal of Neuropathology & Experimental Neurology*, vol. 60, no. 8, pp. 759-67.
- Nunomura, A., Perry, G., Pappolla, M.A., Wade, R., Hirai, K., Chiba, S. & Smith, M.A. 1999, 'RNA oxidation is a prominent feature of vulnerable neurons in Alzheimer's disease', *Journal of Neuroscience*, vol. 19, no. 6, pp. 1959-64.
- Ono, K., Hasegawa, K., Naiki, H. & Yamada, M. 2005, 'Preformed β -amyloid fibrils are destabilized by coenzyme Q 10 in vitro', *Biochemical and biophysical research communications*, vol. 330, no. 1, pp. 111-6.
- Oztekin, Y. & Yazicigil, Z. 2009, 'Preparation and characterization of a 1, 10-phenanthroline-modified glassy carbon electrode', *Electrochimica Acta*, vol. 54, no. 28, pp. 7294-8.
- Pan, L.-F., Wang, X.-B., Xie, S.-S., Li, S.-Y. & Kong, L.-Y. 2014, 'Multitarget-directed resveratrol derivatives: anti-cholinesterases, anti- β -amyloid aggregation and monoamine oxidase inhibition properties against Alzheimer's disease', *MedChemComm*, vol. 5, no. 5, pp. 609-16.
- Pang, Y.-P., Quiram, P., Jelacic, T., Hong, F. & Brimijoin, S. 1996, 'Highly Potent, Selective, and Low Cost Bis-tetrahydroaminacrine Inhibitors of Acetylcholinesterase Steps toward Novel Drugs for Treating Alzheimer's Disease', *Journal of Biological Chemistry*, vol. 271, no. 39, pp. 23646-9.
- Pansuriya, P.B., Dhandhukia, P., Thakkar, V. & Patel, M.N. 2007, 'Synthesis, spectroscopic and biological aspects of iron (II) complexes', *Journal of enzyme inhibition and medicinal chemistry*, vol. 22, no. 4, pp. 477-87.
- Pardío, V.T., Ibarra, N., Rodríguez, M.A. & Waliszewski, K.N. 2001, 'Use of cholinesterase activity in monitoring organophosphate pesticide exposure of cattle produced in tropical areas', *Journal of agricultural and food chemistry*, vol. 49, no. 12, pp. 6057-62.
- Pardridge, W.M. 2009, 'Alzheimer's disease drug development and the problem of the blood-brain barrier', *Alzheimer's & dementia*, vol. 5, no. 5, pp. 427-32.
- Pardridge, W.M. 2010, 'Biopharmaceutical drug targeting to the brain', *Journal of drug targeting*, vol. 18, no. 3, pp. 157-67.

- Park, S.-Y. 2010, 'Potential therapeutic agents against Alzheimer's disease from natural sources', *Archives of pharmacal research*, vol. 33, no. 10, pp. 1589-609.
- Patel, S.V. 1995, 'Pharmacotherapy of cognitive impairment in Alzheimer's disease: a review', *Journal of geriatric psychiatry and neurology*, vol. 8, no. 2, pp. 81-95.
- Perez, L.R. & Franz, K.J. 2010, 'Minding metals: tailoring multifunctional chelating agents for neurodegenerative disease', *Dalton Transactions*, vol. 39, no. 9, pp. 2177-87.
- Petersen, C.A.H., Alikhani, N., Behbahani, H., Wiehager, B., Pavlov, P.F., Alafuzoff, I., Leinonen, V., Ito, A., Winblad, B. & Glaser, E. 2008, 'The amyloid β -peptide is imported into mitochondria via the TOM import machinery and localized to mitochondrial cristae', *Proceedings of the National Academy of Sciences*, vol. 105, no. 35, pp. 13145-50.
- Petrie, R.X., Reid, I.C. & Stewart, C.A. 2000, 'The N-methyl-D-aspartate receptor, synaptic plasticity, and depressive disorder: a critical review', *Pharmacology & therapeutics*, vol. 87, no. 1, pp. 11-25.
- Pithadia, A.S. & Lim, M.H. 2012, 'Metal-associated amyloid- β species in Alzheimer's disease', *Current opinion in chemical biology*, vol. 16, no. 1, pp. 67-73.
- Pohanka, M. 2012, 'Acetylcholinesterase inhibitors: a patent review (2008–present)', *Expert Opinion on Therapeutic Patents*, vol. 22, no. 8, pp. 871-86.
- Poteet, S.A., Majewski, M.B., Breitbach, Z.S., Griffith, C.A., Singh, S., Armstrong, D.W., Wolf, M.O. & MacDonnell, F.M. 2013, 'Cleavage of DNA by Proton-Coupled Electron Transfer to a Photoexcited, Hydrated Ru (II) 1, 10-Phenanthroline-5, 6-dione Complex', *Journal of the American Chemical Society*, vol. 135, no. 7, pp. 2419-22.
- Praticò, D. 2005, 'Peripheral biomarkers of oxidative damage in Alzheimer's disease: the road ahead', *Neurobiology of Aging*, vol. 26, no. 5, pp. 581-3.
- Priller, C., Bauer, T., Mitteregger, G., Krebs, B., Kretschmar, H.A. & Herms, J. 2006, 'Synapse formation and function is modulated by the amyloid precursor protein', *Journal of Neuroscience*, vol. 26, no. 27, pp. 7212-21.
- Qizhuang, H., Jing, Y., Hui, M. & Hexing, L. 2006, 'Studies on the spectra and antibacterial properties of rare earth dinuclear complexes with L-phenylalanine and o-phenanthroline', *Materials Letters*, vol. 60, no. 3, pp. 317-20.
- Querfurth, H.W. & LaFerla, F.M. 2010, 'Mechanisms of disease', *N Engl J Med*, vol. 362, no. 4, pp. 329-44.
- Rao, G.N., Ney, E. & Herbert, R.A. 1999, 'Changes associated with delay of mammary cancer by retinoid analogues in transgenic mice bearing c-neu oncogene', *Breast cancer research and treatment*, vol. 58, no. 3, pp. 239-52.
- Raves, M.L., Harel, M., Pang, Y.-P., Silman, I., Kozikowski, A.P. & Sussman, J.L. 1997, 'Structure of acetylcholinesterase complexed with the nootropic alkaloid,(-)-huperzine A', *Nature Structural & Molecular Biology*, vol. 4, no. 1, pp. 57-63.
- Reddy, P.H. & Beal, M.F. 2008, 'Amyloid beta, mitochondrial dysfunction and synaptic damage: implications for cognitive decline in aging and Alzheimer's disease', *Trends in molecular medicine*, vol. 14, no. 2, pp. 45-53.
- Rivière, C., Papastamoulis, Y., Fortin, P.-Y., Delchier, N., Andriamanarivo, S., Waffo-Teguo, P., Kapche, G.D.W.F., Amira-Guebalia, H., Delaunay, J.-C., Mérillon, J.-M., Richard, T. & Monti, J.-P. 2010, 'New stilbene dimers against amyloid fibril formation', *Bioorganic & Medicinal Chemistry Letters*, vol. 20, no. 11, pp. 3441-3.
- Rivière, C., Richard, T., Quentin, L., Krisa, S., Mérillon, J.-M. & Monti, J.-P. 2007, 'Inhibitory activity of stilbenes on Alzheimer's β -amyloid fibrils in vitro', *Bioorganic & medicinal chemistry*, vol. 15, no. 2, pp. 1160-7.
- Rizzo, S., Bartolini, M., Ceccarini, L., Piazzini, L., Gobbi, S., Cavalli, A., Recanatini, M., Andrisano, V. & Rampa, A. 2010, 'Targeting Alzheimer's disease: Novel indanone hybrids bearing a pharmacophoric fragment of AP2238', *Bioorganic & medicinal chemistry*, vol. 18, no. 5, pp. 1749-60.

- Rizzo, S., Rivière, C.I., Piazzini, L., Bisi, A., Gobbi, S., Bartolini, M., Andrisano, V., Morroni, F., Tarozzi, A. & Monti, J.-P. 2008, 'Benzofuran-based hybrid compounds for the inhibition of cholinesterase activity, β amyloid aggregation, and A β neurotoxicity', *Journal of medicinal chemistry*, vol. 51, no. 10, pp. 2883-6.
- Rodríguez-Rodríguez, C., Sánchez de Groot, N., Rimola, A., Alvarez-Larena, A., Lloveras, V., Vidal-Gancedo, J., Ventura, S., Vendrell, J., Sodupe, M. & González-Duarte, P. 2009, 'Design, selection, and characterization of thioflavin-based intercalation compounds with metal chelating properties for application in Alzheimer's disease', *Journal of the American Chemical Society*, vol. 131, no. 4, pp. 1436-51.
- Rydberg, E.H., Brumshtein, B., Greenblatt, H.M., Wong, D.M., Shaya, D., Williams, L.D., Carlier, P.R., Pang, Y.-P., Silman, I. & Sussman, J.L. 2006, 'Complexes of Alkylene-Linked Tacrine Dimers with Torpedo californica Acetylcholinesterase: Binding of Bis (5)-tacrine Produces a Dramatic Rearrangement in the Active-Site Gorge', *Journal of medicinal chemistry*, vol. 49, no. 18, pp. 5491-500.
- Samadi, N. & Salamati, M. 2014, 'Determination of complex stabilities with 1, 10-phenanthroline-5, 6-dione as ligand for the complexation of several transition metallic cations using chemometrics methods', *Bulletin of the Chemical Society of Ethiopia*, vol. 28, no. 3, pp. 373-82.
- Sameem, S., Kumar, N. & Pathak, D. 2012, 'Synthesis and anticonvulsant activity of some newer semicarbazone derivatives', *IJPSDR*, vol. 4, no. 3, pp. 195-8.
- Sammes, P.G. & Yahioğlu, G. 1994, '1, 10-Phenanthroline: a versatile ligand', *Chem. Soc. Rev.*, vol. 23, no. 5, pp. 327-34.
- Sauvage, J.P., Collin, J.P., Chambron, J.C., Guillerez, S., Coudret, C., Balzani, V., Barigelletti, F., De Cola, L. & Flamigni, L. 1994, 'Ruthenium (II) and osmium (II) bis (terpyridine) complexes in covalently-linked multicomponent systems: synthesis, electrochemical behavior, absorption spectra, and photochemical and photophysical properties', *Chemical Reviews*, vol. 94, no. 4, pp. 993-1019.
- Saxena, A., Redman, A.M., Jiang, X., Lockridge, O. & Doctor, B. 1997, 'Differences in active site gorge dimensions of cholinesterases revealed by binding of inhibitors to human butyrylcholinesterase', *Biochemistry*, vol. 36, no. 48, pp. 14642-51.
- Sayre, L.M., Moreira, P.I., Smith, M.A. & Perry, G. 2005, 'Metal ions and oxidative protein modification in neurological disease', *Annali dell'Istituto superiore di sanita*, vol. 41, no. 2, pp. 143-64.
- Sayre, L.M., Perry, G. & Smith, M.A. 1999, '[10] In situ methods for detection and localization of markers of oxidative stress: Application in neurodegenerative disorders', *Methods in enzymology*, vol. 309, pp. 133-52.
- Scott, L.E. & Orvig, C. 2009, 'Medicinal inorganic chemistry approaches to passivation and removal of aberrant metal ions in disease', *Chemical reviews*, vol. 109, no. 10, pp. 4885-910.
- Šekutor, M., MLinarić-Majerski, K., Hrenar, T., Tomić, S. & Primožič, I. 2012, 'Adamantane-substituted guanidylhydrazones: novel inhibitors of butyrylcholinesterase', *Bioorganic chemistry*, vol. 41, pp. 28-34.
- Selkoe, D.J. 2001, 'Alzheimer's Disease: Genes, Proteins, and Therapy', *Physiological reviews*, vol. 81, no. 2, pp. 741-66.
- Seubert, P., Vigo-Pelfrey, C., Esch, F., Lee, M., Dovey, H., Davis, D., Sinha, S., Schiossmacher, M., Whaley, J. & Swindlehurst, C. 1992, 'Isolation and quantification of soluble Alzheimer's β -peptide from biological fluids', *Nature*, vol. 359, no. 6393, pp. 325-7.
- Shaik, K.A. & Ahmed, A. 2014, 'An Environmentally Benign Solvent Free Novel Methods for the Synthesis of Metal Complexes Using Imidazo [4, 5-F] 1, 10-Phenanthroline and their Derivatives and Biological Activities', *International Journal of Advanced Research in Chemical Science*, vol. 1, no. 4, pp. 29-34.

- Shoji, M., Golde, T.E., Ghiso, J., Cheung, T.T., Estus, S., Shaffer, L.M., Cai, X.-D., McKay, D.M., Tintner, R. & Frangione, B. 1992, 'Production of the Alzheimer amyloid β protein by normal proteolytic processing', *Science*, pp. 126-9.
- Silman, I. & Sussman, J.L. 2005, 'Acetylcholinesterase: 'classical' and 'non-classical' functions and pharmacology', *Current opinion in pharmacology*, vol. 5, no. 3, pp. 293-302.
- Smith, M.A., Harris, P.L.R., Sayre, L.M. & Perry, G. 1997, 'Iron accumulation in Alzheimer disease is a source of redox-generated free radicals', *Proceedings of the National Academy of Sciences*, vol. 94, no. 18, pp. 9866-8.
- Soreq, H. & Seidman, S. 2001, 'Acetylcholinesterase—new roles for an old actor', *Nature Reviews Neuroscience*, vol. 2, no. 4, pp. 294-302.
- Squadrone, S., Brizio, P., Mancini, C., Pozzi, E., Cavalieri, S., Abete, M.C. & Brusco, A. 2015, 'Blood metal levels and related antioxidant enzyme activities in patients with ataxia telangiectasia', *Neurobiology of disease*.
- Struble, R.G., Cork, L.C., Whitehouse, P.J. & Price, D.L. 1982, 'Cholinergic innervation in neuritic plaques', *Science*, vol. 216, no. 4544, pp. 413-5.
- Su, W., Qian, Q., Li, P., Lei, X., Xiao, Q., Huang, S., Huang, C. & Cui, J. 2013, 'Synthesis, Characterization, and Anticancer Activity of a Series of Ketone-N4-Substituted Thiosemicarbazones and Their Ruthenium(II) Arene Complexes', *Inorganic Chemistry*, vol. 52, no. 21, pp. 12440-9.
- Sugimoto, H., Yamanish, Y., Iimura, Y. & Kawakami, Y. 2000, 'Donepezil hydrochloride (E2020) and other acetylcholinesterase inhibitors', *Current medicinal chemistry*, vol. 7, no. 3, pp. 303-39.
- Sussman, J.L. & Harel, M. 1991, 'Atomic structure of acetylcholinesterase from *Torpedo californica*: a prototypic acetylcholine-binding protein', *Science*, vol. 253, no. 5022, p. 872.
- Sussman, J.L., Harel, M., Frolow, F., Oefner, C., Goldman, A., Toker, L. & Silman, I. 1991, 'Atomic structure of acetylcholinesterase from *Torpedo californica*: a prototypic acetylcholine-binding protein', *Science*, vol. 253, no. 5022, pp. 872-9.
- Tamano, H. & Takeda, A. 2011, 'Dynamic action of neurometals at the synapse', *Metallomics*, vol. 3, no. 7, pp. 656-61.
- Tariot, P.N., Solomon, P., Morris, J., Kershaw, P., Lilienfeld, S., Ding, C. & Group, G.U.-S. 2000, 'A 5-month, randomized, placebo-controlled trial of galantamine in AD', *Neurology*, vol. 54, no. 12, pp. 2269-76.
- Telpoukhovskaia, M.A. & Orvig, C. 2013, 'Werner coordination chemistry and neurodegeneration', *Chemical Society Reviews*, vol. 42, no. 4, pp. 1836-46.
- Teri, L., Rabins, P., Whitehouse, P., Berg, L., Reisberg, B., Sunderland, T., Eichelman, B. & Phelps, C. 1992, 'Management of behavior disturbance in Alzheimer disease: current knowledge and future directions', *Alzheimer Disease & Associated Disorders*, vol. 6, no. 2, pp. 77-88.
- Thal, L., Rosen, W., Sharpless, N. & Crystal, H. 1981, 'Choline chloride fails to improve cognition in Alzheimer's disease', *Neurobiology of aging*, vol. 2, no. 3, pp. 205-8.
- Thirumurugan, P., Mahalaxmi, S. & Perumal, P.T. 2010, 'Synthesis and anti-inflammatory activity of 3-indolyl pyridine derivatives through one-pot multi component reaction', *Journal of chemical sciences*, vol. 122, no. 6, pp. 819-32.
- Tomiyama, T., Shoji, A., Kataoka, K.-i., Suwa, Y., Asano, S., Kaneko, H. & Endo, N. 1996, 'Inhibition of Amyloid Protein Aggregation and Neurotoxicity by Rifampicin ITS POSSIBLE FUNCTION AS A HYDROXYL RADICAL SCAVENGER', *Journal of Biological Chemistry*, vol. 271, no. 12, pp. 6839-44.
- Tougu, V. 2001, 'Acetylcholinesterase: mechanism of catalysis and inhibition', *Current Medicinal Chemistry-Central Nervous System Agents*, vol. 1, no. 2, pp. 155-70.
- Tumiatti, V., Minarini, A., Bolognesi, M., Milelli, A., Rosini, M. & Melchiorre, C. 2010, 'Tacrine derivatives and Alzheimer's disease', *Current medicinal chemistry*, vol. 17, no. 17, pp. 1825-38.

- Tyson, D.S. & Castellano, F.N. 1999, 'Light-harvesting arrays with coumarin donors and MLCT acceptors', *Inorganic chemistry*, vol. 38, no. 20, pp. 4382-3.
- Umer Rashid and Farzana L. Ansari. 2014, 'Drug Design and Discovery in Alzheimer's disease' Chapter 2 - Challenges in designing therapeutic agents for treating Alzheimer's disease-from Serendipity to Rationality, 40-141.
- Vans, D.H. & Griffith, D.A. 1982, 'Effect of pH on the electrochemical reduction of some heterocyclic quinones', *Journal of Electroanalytical Chemistry and Interfacial Electrochemistry*, vol. 134, no. 2, pp. 301-10.
- Wallin, Å., Blennow, K., Andreasen, N. & Minthon, L. 2006a, 'CSF biomarkers for Alzheimer's Disease: levels of β -amyloid, tau, phosphorylated tau relate to clinical symptoms and survival', *Dementia and geriatric cognitive disorders*, vol. 21, no. 3, pp. 131-8.
- Wallin, A.K., Blennow, K., Andreasen, N. & Minthon, L. 2006b, 'CSF biomarkers for Alzheimer's Disease: levels of beta-amyloid, tau, phosphorylated tau relate to clinical symptoms and survival', *Dementia and Geriatric Cognitive Disorders*, vol. 21, no. 3, pp. 131-8.
- Wang, H., Carlier, P.R., Ho, W.L., Wu, D.C., Lee, N.T.K., Li, C.P., Pang, Y.P. & Han, Y.F. 1999, 'Effects of bis (7)-tacrine, a novel anti-Alzheimer's agent, on rat brain AChE', *Neuroreport*, vol. 10, no. 4, pp. 789-93.
- Wang, J., Timchalk, C. & Lin, Y. 2008, 'Carbon nanotube-based electrochemical sensor for assay of salivary cholinesterase enzyme activity: an exposure biomarker of organophosphate pesticides and nerve agents', *Environmental science & technology*, vol. 42, no. 7, pp. 2688-93.
- Wang, P. & Zhu, G.-Y. 2002, 'Sol-Gel Derived Carbon Ceramic Electrode Bulk-Modified with Tris (1, 10-phenanthroline-5, 6-dione) iron (II) Hexafluorophosphate and Its Use as an Amperometric Iodate Sensor', *Chinese Journal of Chemistry*, vol. 20, no. 2, pp. 153-9.
- Watkins, P.B., Zimmerman, H.J., Knapp, M.J., Gracon, S.I. & Lewis, K.W. 1994, 'Hepatotoxic effects of tacrine administration in patients with Alzheimer's disease', *Jama*, vol. 271, no. 13, pp. 992-8.
- Weinstock, M. & Groner, E. 2008, 'Rational design of a drug for Alzheimer's disease with cholinesterase inhibitory and neuroprotective activity', *Chemico-biological interactions*, vol. 175, no. 1, pp. 216-21.
- Wendlandt, A.E. & Stahl, S.S. 2014, 'Bioinspired Aerobic Oxidation of Secondary Amines and Nitrogen Heterocycles with a Bifunctional Quinone Catalyst', *Journal of the American Chemical Society*, vol. 136, no. 1, pp. 506-12.
- Wiesner, J., Kříž, Z., Kuča, K., Jun, D. & Koča, J. 2007, 'Acetylcholinesterases—the structural similarities and differences', *Journal of enzyme inhibition and medicinal chemistry*, vol. 22, no. 4, pp. 417-24.
- Wilcock, D.M. 2012, 'A changing perspective on the role of neuroinflammation in Alzheimer's disease', *International journal of Alzheimer's disease*, vol. 2012.
- Wimo, A., Winblad, B., Aguero-Torres, H. & von Strauss, E. 2003, 'The magnitude of dementia occurrence in the world', *Alzheimer Disease & Associated Disorders*, vol. 17, no. 2, pp. 63-7.
- Wright, C.I., Geula, C. & Mesulam, M. 1993, 'Neuroglial cholinesterases in the normal brain and in Alzheimer's disease: relationship to plaques, tangles, and patterns of selective vulnerability', *Annals of neurology*, vol. 34, no. 3, pp. 373-84.
- Wu, G., Robertson, D.H., Brooks, C.L. & Vieth, M. 2003, 'Detailed analysis of grid-based molecular docking: A case study of CDOCKER—A CHARMM-based MD docking algorithm', *Journal of computational chemistry*, vol. 24, no. 13, pp. 1549-62.
- Xu, H.-H., Tao, X., Li, Y.-Q., Shen, Y.-Z. & Wei, Y.-H. 2012, 'Synthesis and characterization of a series of transition metal polypyridyl complexes and the pH-induced luminescence switch of Zn(II) and Ru(II) complexes', *Polyhedron*, vol. 33, no. 1, pp. 347-52.

- Yamada, M., Tanaka, Y., Yoshimoto, Y., Kuroda, S. & Shima, I. 1992, 'Synthesis and Properties of Diamino-Substituted Dipyrro (3, 2-a: 2', 3'-c) phenazine', *Bulletin of the Chemical Society of Japan*, vol. 65, no. 4, pp. 1006-11.
- Yamada, Y., Sakurai, H., Miyashita, Y., Fujisawa, K. & Okamoto, K.-i. 2002, 'Crystal structures, electronic absorption and reflectance spectral behaviors, and electrochemical properties of five-coordinated chlorocopper (II) complexes with 5, 6-disubstituted-1, 10-phenanthroline', *Polyhedron*, vol. 21, no. 21, pp. 2143-7.
- Yáñez, M., Fraiz, N., Cano, E. & Orallo, F. 2006, 'Inhibitory effects of cis- and trans-resveratrol on noradrenaline and 5-hydroxytryptamine uptake and on monoamine oxidase activity', *Biochemical and biophysical research communications*, vol. 344, no. 2, pp. 688-95.
- Yang, F., Nickols, N.G., Li, B.C., Marinov, G.K., Said, J.W. & Dervan, P.B. 2013, 'Antitumor activity of a pyrrole-imidazole polyamide', *Proceedings of the National Academy of Sciences*, vol. 110, no. 5, pp. 1863-8.
- Yar, S.M., Siddiqui, A.A. & Ali, A.M. 2007, 'Synthesis and antimycobacterial activity of novel heterocycles', *Journal of the Serbian Chemical Society*, vol. 72, no. 1, pp. 5-11.
- Ying, P., Tian, X., Zeng, P., Lu, J. & Chen, H. 2014, 'Synthesis, DNA-binding, Photocleavage and in vitro Cytotoxicity of Novel Imidazole [4, 5-f][1, 10] phenanthroline-based Oxovanadium Complexes', *Med chem*, vol. 4, pp. 549-57.
- Youdim, M. & Buccafusco, J. 2005a, 'CNS Targets for multi-functional drugs in the treatment of Alzheimer's and Parkinson's diseases', *Journal of neural transmission*, vol. 112, no. 4, pp. 519-37.
- Youdim, M.B. & Buccafusco, J.J. 2005b, 'Multi-functional drugs for various CNS targets in the treatment of neurodegenerative disorders', *Trends in Pharmacological Sciences*, vol. 26, no. 1, pp. 27-35.
- Zecca, L., Youdim, M.B., Riederer, P., Connor, J.R. & Crichton, R.R. 2004, 'Iron, brain ageing and neurodegenerative disorders', *Nature Reviews Neuroscience*, vol. 5, no. 11, pp. 863-73.
- Zhang, Q.-L., Liu, J.-H., Liu, J.-Z., Zhang, P.-X., Ren, X.-Z., Liu, Y., Huang, Y. & Ji, L.-N. 2004, 'DNA-binding and photoactivated enantiospecific cleavage of chiral polypyridyl ruthenium (II) complexes', *Journal of inorganic biochemistry*, vol. 98, no. 8, pp. 1405-12.
- Zheng, H., Amit, T., Bar-Am, O., Fridkin, M., Youdim, M.B. & Mandel, S.A. 2012, 'From anti-Parkinson's drug rasagiline to novel multitarget iron chelators with acetylcholinesterase and monoamine oxidase inhibitory and neuroprotective properties for Alzheimer's disease', *Journal of Alzheimer's Disease*, vol. 30, no. 1, p. 1.
- Zhong, K.-L. 2012, 'Tris (1, 10-phenanthroline-κ2N, N') iron (II) bis (2, 4, 5-tricarboxybenzoate) monohydrate and tris (2, 2'-bipyridine-κ2N, N') iron (II) 2, 5-dicarboxybenzene-1, 4-dicarboxylate-benzene-1, 2, 4, 5-tetracarboxylic acid-water (1/1/2)', *Acta Crystallographica Section C: Crystal Structure Communications*, vol. 68, no. 9, pp. 259-64.
- Ziessel, R. 1991, 'Photocatalysis of the Homogeneous Water-Gas Shift Reaction under Ambient Conditions by Cationic Iridium (III) Complexes', *Angewandte Chemie International Edition in English*, vol. 30, no. 7, pp. 844-7.
- Zilka, N. & Novak, M. 2006, 'The tangled story of Alois Alzheimer', *Bratislavské lekárske listy*, vol. 107, no. 9/10, p. 343.
- Zotova, E., Nicoll, J.A., Kalaria, R., Holmes, C. & Boche, D. 2010, 'Inflammation in Alzheimer's disease: relevance to pathogenesis and therapy', *Alzheimers Res Ther*, vol. 2, no. 1, p. 1.

Chapter 2 Synthesis and characterisation of the new phen-5, 6 dione derivatives

2.1 Introduction

The published literature covered extensive number of active ingredients and starting materials investigated for developing AD drugs .1,10-phenanthroline (phen) was the backbone of several studies as a main molecule for developing drugs to AD with dual functions for AChE esterase inhibition and against AChE-induced A β aggregation, via inhibiting the catalytic functions of AChE and retarding the A β interaction with AChE by virtue of blocking the PAS (Chitra et al. 2013).

Based on the published research carried out on phen and the encouraging results obtained the outlines of this research project were planned to synthesise series of derivatives of phen-5,6-dione and evaluate their efficiency as AD drugs .The new derivatives were designed to act as multifunctional antioxidants via amino, phenolic, and quinone groups. On the other hand phen-5,6-dione may display a significant anti-Alzheimer role with or without a coordinated metals.

The capability of the active ingredients to coordinate with the targeted metal ions such as Cu, Zn and Fe has been proved to be directly linked to AD as detailed in Chapter.1 chelation with such metal ions Cu, Fe and Zn decrease the A β aggregation and retard AChE from production of ROS in the assays.

This class of multifunctional group ligands and substituted derivatives may interact with DNA by aromatic π stacking between the Lewis base pair of electrons whether they are free or coordinated to the central metal ions. The biological activity of such system is enhanced or reduced according to its state of coordination with the metal central ion even at its planar geometry. These chemical features and the electronic characteristics of both central metal ion and the phen-5,6-dione indicate the vital role of the metal moiety as crucial factor leading to remarkable differences in the biological activity (Ying et al. 2014); (Deegan et al. 2006).

The present research goal was based on the coordination chemistry of series of Schiff bases derived from phen-5,6-dione and 2-aminophenol aiming to synthesis and study of mono and di substituted derivatives shown in scheme 7 as potential a novel imines and biologically active chelating agents with several metal ions like Cu, Zn and Fe as multi-functional active ingredients.

2.2 Materials and techniques

Reagents and analytical grade solvents were purchased from Sigma–Aldrich Chem.-supply Chemical Co. All the reactions made the use of magnetic stirring bars.

Purity of compounds was determined by ^1H NMR, GC/High resolution MS, FT-IR (ATR) and m.p. Low-resolution mass spectra were obtained on an Agilent 6890GC fitted with 5% polysilphenylene, 95% polydimethylsiloxane column, and an Agilent 5973n MS (EI) spectrometer. High-resolution mass spectra were obtained on an Agilent 6510 Accurate Mass Q-TOF MS with an ESI source, Infrared spectra (IR)(ATR) were recorded in the range 4000-600 cm^{-1} using Nicolet 6700 spectrophotometer. Solid samples measured as KBr pellets Melting points were determined on a GALLENKAMP Electrothermal melting point apparatus and U.V.

2.2.1 Thin Layer Chromatography (TLC)

Progress of reactions was monitored by TLC analysis, performed on aluminium backed Merck 60 GF₂₅₄ silica gel or Merck 60 GF₂₅₄ neutral alumina gel with UV detection at 254 nm. TLC analysis was performed using aluminium backed Merck 60 GF₂₅₄ neutral alumina gel TLC plates and separation methods were developed with the stated chromatography solvent system. UV detection at 254 nm and I₂ atmosphere staining was used to develop the plates.

2.2.2 Nuclear Magnetic Resonance (NMR) Spectroscopy: Hydrogen (^1H) NMR Spectra

^1H NMR spectra were recorded on an Agilent 500 MHz spectrometer at 25⁰ C in deuterated chloroform (CDCl_3) containing 0.03% v/v tetramethylsilane (TMS) and deuterated dimethyl sulfoxide (DMSO-d_6), unless otherwise specified.

All samples were referenced relative to the TMS chemical shift at 0 ppm. Proton resonances were assigned as: chemical shift (multiplicity, coupling constant(s), the number of protons, proton assignment). The following abbreviations were used in the splitting pattern:

m for (multiplet), s for (singlet), br s for (broad singlet), d for (doublet), t for (triplet), q for (quartet), dd for (doublet of doublets), dt for (doublet of triplet). NMR assignments were based on HSQC and DEPT experiments and are numbered according to the systematic name.

2.2.3 Carbon (¹³C) NMR Spectra

¹³C NMR spectra were recorded on an Agilent 125 MHz spectrometer in deuterated chloroform (CDCl₃) containing 0.03% v/v tetramethylsilane (TMS), unless otherwise specified. All samples were referenced relative to the CDCl₃ chemical shift at 77.36 ppm and DMSO 93.7 ppm. Carbon resonances were assigned as chemical shift (carbon assignment). The NMR assignments were based on HSQC and DEPT experiments and are numbered according to the systematic name.

2.2.4 High-Resolution Mass Spectrometry (HRMS)

High-resolution mass spectra were obtained on an Agilent 6510 Accurate-Mass Q-TOF Mass Spectrometer, equipped with an electrospray ionisation source using an acetonitrile:water (70:30) solvent system with 0.1% v/v formic acid. HRMS were obtained in lieu of elemental analysis, with NMR used to determine purity.

2.2.5 Infrared Spectroscopy

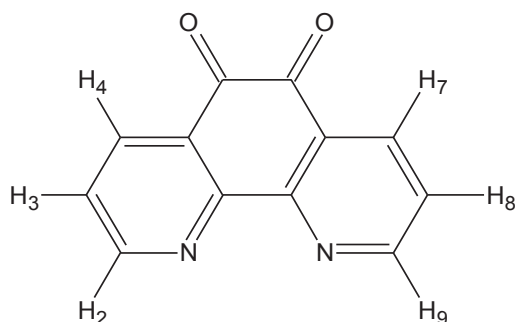
Infrared spectra were collected using a Thermo Scientific FT-IR(ATR) spectrometer Nicolet 6700 spectrometer in the range of 4000-600 cm⁻¹. Signals are given as (cm⁻¹).

2.2.6 Melting Points

Melting points were measured on a Gallenkamp Electrothermal melting point apparatus. The Melting Point Apparatus was corrected using benzoic acid as reference.

2.3 Synthesis and characterization

2.3.1. Synthesis of 1,10-phenanthroline-5,6-dione ST01

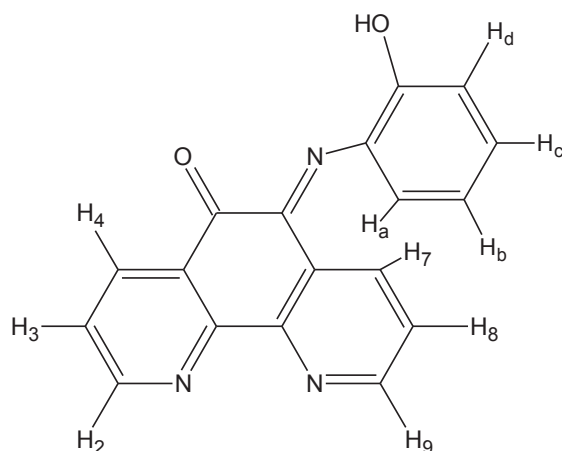


The procedure was performed by (Gillard & Hill 1974; Hiort, Lincoln & Norden 1993; McCann et al. 2004; Yamada et al. 1992) with some modification was implemented in this synthesis and as following:

A mixture of 1,10-phenanthroline (0.0166 mol, 3 g) and potassium bromide (0.159 mol, 19 g) was ground in a mortar, the ground powder was transferred to 1 liter round bottom flask and allowed to cool in ice bath. 60 mL of concentrated sulphuric acid was added drop wise over one hour with vigorously stirring using mechanical stirrer, then slowly 30 mL of nitric acid was added until the mixture became homogeneous and red coloured solution was obtained.

The reaction mixture was refluxed for 10 hours, then the orange solution was allowed to cool to room temperature. The mixture was poured into 700 mL of ice/water and neutralised with 10 M sodium hydroxide solution to pH 6-8. The product was extracted from the aqueous solution with a chloroform, dried with anhydrous Na_2SO_4 , then filtered the solution was evaporated at reduced pressure using rotary evaporator. The crude product was initially characterised by NMR then it was recrystallised from methanol to give yellow needle crystals. The yield was 65%, m.p. -255-257 °C (lit. Hiort, Lincoln & Norden 1993 m.p. 257 °C). ^1H NMR (CDCl_3) δ 9.11, 2H (dd $J=2,7.5\text{Hz}$) **H2;H9**; 8.50 (2H, dd $J=2,8\text{Hz}$) **H4;H7**; 7.6 (2H dd $J=4.5,7.5\text{Hz}$) **H3;H8**; ^{13}C (CDCl_3) δ (154.8, 157.3, 166.6, 182.1, 185.7, 207.9). FT-IR (ATR) ($\nu_{\text{max}}/\text{cm}^{-1}$): 3074 (C-H), 1689 (C=O), 1565 (C=N), 1461 (C=C), 1316 (C-N). HRMS: $[\text{M}+\text{H}]^+$, m/z Calcd: 211.0502 g/mol for $\text{C}_{12}\text{H}_6\text{N}_2\text{O}_2$ Found: 211.0503 g/mol.

2.3.2. Synthesis (6E)-6-[(2-hydroxyphenyl)imino]-1,10-phenanthroline-5(6H)-one (ST02)



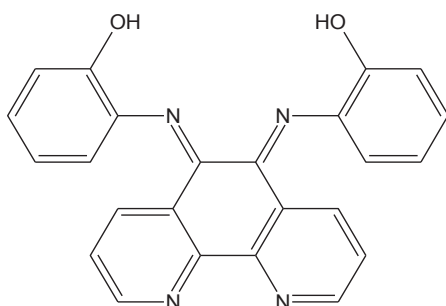
1,10-phenanthroline-5,6-dione (0.5mmol, 105 mg) was dissolved in absolute ethyl alcohol (5 mL). Then solution of 2-amino phenol (0.5mmol, 54.5 g) in ethyl alcohol (5 mL) was added to the mixture. The reaction was refluxed for 21 hours, monitored by Alumina TLC plate and mobile phase consist of 30% methanol and 70% ethyl acetate. The mixture was allowed to cool, the resultant yellow precipitate was filtered, washed with cold ethanol and recrystallised with ethanol then dried. The yield was 57%; decomposed at 220 °C.

$^1\text{H NMR}$ (DMSO- d_6) δ 8.93 (1H, dd $J=1.5, 4.5$ Hz) phen **H2**; 8.85 (1H, dd $J=1.5, 4.5$ Hz) phen **H9**; 8.73 (1H, dd $J=1.5, 8$ Hz) phen **H4**; 8.49 (1H, dd $J=1.5, 8$ Hz) phen **H7**; 7.99, **OH**; 7.65 (3H, m) phen **H3**; **H8**; ph **Ha**; 7.41 (1H, t $J= 8.5$ Hz) ph **Hb**; 7.30 (1H, d $J=7.5$ Hz) ph **Hd**; 7.21 (1H, t $J=7.5$ Hz)ph **Hc**; ^{13}C (DMSO- d_6) δ (86.6, 117.3, 123, 124.8, 125.1, 126.8, 128, 130.1, 132.7, 132.8, 134.1, 134.2, 143.2, 146.8, 149.8, 151.1,152.8, 153.1)

AT-IR ($\nu_{\text{max}}/\text{cm}^{-1}$): 3464 (O-H), 3208 (C-H), 1682 (C=O), 1669 (C=N), 1473 (C=C).

HRMS: $[\text{M}+\text{H}]^+$, m/z Calcd: 302.0930 g/mol for $\text{C}_{18}\text{H}_{12}\text{N}_3\text{O}_2$ Found: 302.0931g/mol.

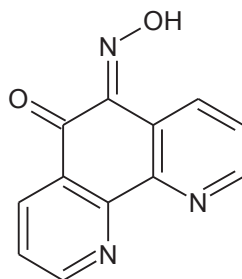
2.3.3. Synthesis of [2,2'-[1,10-phenanthroline-5,6-diylidenedi(*E*) azanylylidene]diphenol] (ST03)



1,10-phenanthroline-5,6-dione (1 mmol, 210 mg) was dissolved in absolute ethyl alcohol (5mL) .A solution of 2-mino phenol (2.2 mmol, 239.8 mg) in absolute ethyl alcohol (5 mL) was added to the mixture. The reaction was refluxed for 21 hours checked by TLC using alumina plate and mobile phase consists 30% methanol + 70% ethyl acetate. The crude mono substitute 2-aminopheonl was added to 2 mL of acetic acid, and the mixture was refluxed for further 15 hours to prepare di substitution compound. The reaction progress was followed up by TLC in alumina plate and mobile phase consisting 5% methanol and 95% ethyl acetate. The mixture was allowed to cool, the resultant red precipitate was filtered, washed with cold ethanol and recrystallised with ethanol then dried. The yield was 62%; decomposition melting point

265 °C. ¹H NMR(DMSO-d₆) δ 8.69(2H, dd $J= 1.5, 5$ Hz) phen**H2; H9**; 7.94(2H, dd($J=1.5, 7.5$ Hz) phen**H4; H7**; 7.5(2H,s) **OH**; 7.43 (2H, m) phen **H3;H8**; 6.95 (2H, dd $J=1.5, 7.5$ Hz) ph **Ha; Ha'**; 6.68 (4H, m) ph **Hb; Hc; Hb'; Hc'**; 6.5 (2H, dd $J=2, 7$ Hz)ph **Hd; Hd'**; ¹³C (DMSO-d₆) δ (72.4, 80.5, 114.3, 116.5, 117, 119.4, 121.8, 124.2, 133.4,150, 150.2, 188.8) FT-IR(ATR) ($\nu_{\max}/\text{cm}^{-1}$): 3447(OH), 3061 (C-H), 1496 (C=N), 1420 (C=C), 1225(C-N). HRMS:[M+H]⁺,m/z Calcd: 393.1346 for C₂₄H₁₇N₄O₂ Found: 393.1349.

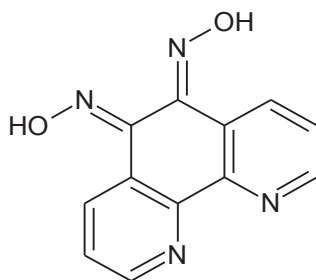
2.3.4. Synthesis of (6*E*)-6-(hydroxyimino)-1,10-phenanthroline-5(6*H*)-one (ST04)



A mixture of 210 mg (1 mmol) 1, 10- phenanthroline 5,6-dione , 76.43mg (1.1 mmol) of hydroxylamine hydrochloride and 15 mL of ethanol in a flask, heated within 1 h to 50°C, stirred at reflux for 3 h, the progress of the reaction was followed up by TLC in alumina plate and mobile phase consisting 90% methanol and 10% ethyl acetate cooled, filtered. Washed with chloroform and recrystallised with ethanol dried to give a yellow powdered solid and the yield was 79%, m.p. 221-222 °C.

¹HNMR(DMSO-*d*₆) δ 9.31(1H, d *J*=7.5Hz) **H9**; 9.05(1H, d *J*=4.5 Hz) **H2**; 8.85(1H, d *J*=4.5 Hz) **H4**; 8.48 (1H, d *J*= 7.5) **H7**; 7.72(2H, m) **H3**; **H8**; 4.5(1H,s, br) **OH**. ¹³C (DMSO-*d*₆) δ (124, 125.7, 126, 126.2, 128.3, 136.1, 146.2, 150.2, 150.5, 151.8, 155.2, 181.4) FT-IR(ATR) (ν_{\max} /cm⁻¹): 3500(O-H), 1616(C=O), 1596 (C=N), 1492 (C=C), 1376 (C-N). HRMS:[M+H]⁺,m/z Calcd: 226.0611 g/mol for C₁₂H₈N₃O₂ Found: 226.0618 g/mol.

2.3.5. Synthesis of *N,N'*-1,10-phenanthroline-5,6dihydrilidenedihydroxylamine (Kleineweischede & Mattay 2006) (ST05)



A mixture of phen-5,6-dione (210 mg, 1.00 mmol) and Na₂CO₃ (296 mg, 1.50mmol) were dissolved in ethanol (15 mL) and heated to reflux. To this solution hydroxylamine hydrochloride (243 mg, 3.50 mmol) in ethanol (5 mL) was added dropwise and the reaction mixture was then refluxed for 5 hours. After completion of the reaction, the mixture was cooled to room temperature and the solvent was evaporated under reduced pressure.

The residue yellow to green powder was washed successively with water and ether and dried under vacuum at 80 °C the yield was 85% as a light yellow solid. Decomposed at 233-235 °C (lit Bodige & MacDonnell 1997, Dec. 230°C).

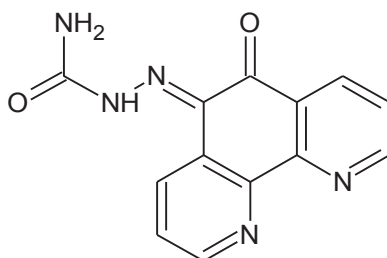
¹H NMR (CDCl₃) δ 13.2 (2H, s, OH) 8.89(2H, dd $J=1.5, 5.5$ Hz) **H2;H9**; 8.57(2H, dd $J=1, 8$ Hz) **H4;H7**; 7.83(2H, dd $J=5, 8$ Hz) **H3;H8**.

¹³C(CDCl₃) δ (124.2, 125.9, 126.6, 126.9, 130.1,130.4, 135.7, 139.8, 141.5, 144, 148.2, 148.8).

AT-IR ($\nu_{\max}/\text{cm}^{-1}$): 3087 and 3038 (OH), 1621(C=O), 1577 (C=N), 1453 (C=C), 1347

(C-N). HRMS:[M+H]⁺, m/z Calcd: 241.0720 g/mol for C₁₂H₉N₄O₂ Found: 241.0721 g/mol.

2.3.6. Synthesis of (2E)-2-(6-oxo-1,10-phenanthrolin-5(6H)-ylidene)hydrazinecarboxamide(Murali, Sastri & Maiya 2002) (ST06)

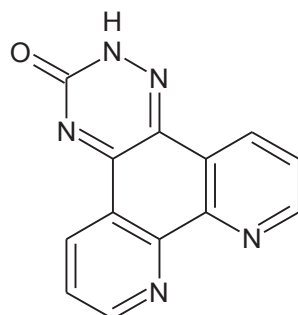


This method has modified from the paper mentioned above phen-5,6-dione(210 mg, 1 mmol) and semicarbazide hydrochloride (133.8 mg, 1.2 mmol) were dissolved in 15 mL of methanol and refluxed for 5 hours. The progress of the reaction was followed up by TLC in alumina plate and mobile phase consisting 5% methanol and 95% dichloromethane. Reduced the solvent to half, and the yellow solid product was obtained by suction while hot and Filtration. The filtrate was further concentrated to obtain additional product. The product was recrystallised to obtain 84% yield and the filtrate was concentrated to give product yellow powder again and the yield was 90%. Decomposed at 216 °C.

¹H NMR(DMSO-d₆) δ 13.66 (s,1 H) **NH**; 9.37 (d, 1 H, $J = 8\text{Hz}$)**H2**; 9.18 (dd, 1 H, $J=1.5, 4.5$ Hz)**H4**; 8.93 (dd, 1 H, $J = 1, 4.5\text{Hz}$) **H7**; 8.76 (dd, 1 H, $J=1.5, 8.5$ Hz)**H9**; 7.95 (m,2 H)**H3;8**; 7.58 (br, s, 2 H)**NH2**; ¹³C (DMSO-d₆) δ (126.6, 126.7, 127.3, 128.5, 130.8, 137.2, 137.4, 140.3, 145.8, 147.2, 154.2, 154.6, 178.8. FT-IR(ATR) ($\nu_{\max}/\text{cm}^{-1}$): 3326 and 3148 (NH+NH₂), 1747 (C=O), 1620 and 1576 (C=N), 1502 (C=C), 1495(C-N).

HRMS:[M+H]⁺, m/z Calcd: 268.0829g/mol for C₁₃H₁₀N₅O₂ Found: 268. 0829 g/mol.

2.3.7. Synthesis of phen[5,6-e]-1,2,4-triazin-3-one(Murali, Sastri & Maiya 2002) (ST07)

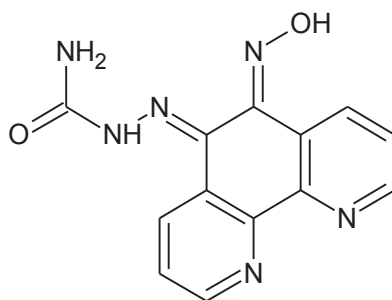


Semicarbazone (200 mg, 0.749 mmol) dissolved in ammonium acetate (2 g, 7.49 mmol) and (2.8) mL of acetic acid and refluxed for 7 hours. Then filtrate to get yellow to green precipitate and washed several times with water to remove the acetic acid and the yield was 28%. Decomposed at 310 °C.

^1H NMR(DMSO- d_6) δ 14.12 (br, s, 1 H) **NH**; 9.18 (dd, 1 H, $J = 1.5, 4.5$ Hz) **H2**; 9.07 (dd, 1 H, $J = 1.5, 7.5$ Hz) **H4**; 9.01 (dd, 1 H, $J = 1.5, 4.5$ Hz) **H9**; 8.81 (d, 1 H, $J = 8$ Hz) **H7**; 7.82 (dd, 1 H, $J = 4.5, 8$ Hz) **H3**; 7.76 (dd, 1 H, $J = 4.5, 8.5$ Hz) **H8**; ^{13}C (DMSO- d_6) δ (121.5, 123.3, 124.8, 124.9, 127.8, 129.8, 133.7, 143.6, 148.6, 152.4, 153.2, 154.6, 165.2). FT-IR(ATR) ($\nu_{\text{max}}/\text{cm}^{-1}$): 2820 (NH), 1614 (C=O), 1570 (C=N), 1492 (C=C), 1287 (C-N).

HRMS: $[\text{M}+\text{H}]^+$, m/z Calcd: 250.0723 g/mol for $\text{C}_{13}\text{H}_8\text{N}_5\text{O}$ Found: 250.0727 g/mol.

2.3.8. Synthesis of dual function (2E)-2-[(6E)-6-(hydroxyimino)-1,10-phenanthroline-5(6H)-ylidene]hydrazine-1-carboxamide (ST08)

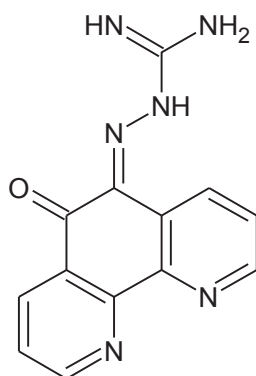


(2E)-2-(6-oxo-1,10-phenanthroline-5(6H)-ylidene)hydrazinecarboxamide (267mg, 1mmol) and hydroxylamine hydrochloride (69.49 mg, 1 mmol) were dissolved in 12 mL of ethanol and 6 mL water. The reaction was heated to reflux for 8 hours and the reaction was monitored using Alumina plate and mobile phase consisting 95% methanol and 5% ethyl acetate to

monitor the reaction completion. With recrystallization the crude sample in butanol to get yellow precipitate the yield was 83%. Decomposed at 227 °C.

$^1\text{H NMR}$ (DMSO- d_6) δ 13.65 (s, 1 H) **NH**; 9.12 (dd, 2 H, $J=1.5, 4.5$ Hz) **H2; H9**; 8.86 (d, 1 H, $J=3.5$ Hz) **H4**; 8.66 (dd, 1 H, $J=1.5, 9$ Hz) **H7**; 7.81 (dd, 1 H, $J=4.5, 8$ Hz) **H3**; 7.73 (dd, 1 H, $J=4.5, 8$ Hz) **H8**; 7.49 (br, s, 2 H) **NH2**; 4.5 (1H, s, br) OH. ^{13}C (DMSO- d_6) δ (125.4, 125.5, 127.9, 128.3, 129.5, 133.9, 148.6, 150.5, 154.9, 155, 172.3, 179.9, 222.9). FT-IR(ATR) ($\nu_{\text{max}}/\text{cm}^{-1}$): 3010, (O-H) 2820 and 2619 (NH+NH₂) 1614 (C=O), 1590 (C=N), 1492 (C=C), 1346 (C-N). HRMS: [M+H]⁺, m/z Calcd: 283.0938 g/mol for C₁₃H₁₁N₆O₂ Found: 283.0937 g/mol.

2.3.9. Synthesis of (2E)-2-(6-oxo-6,10b-dihydro-1,10-phenanthroline-5(4aH)-ylidene)hydrazinecarboximidamide (ST09)

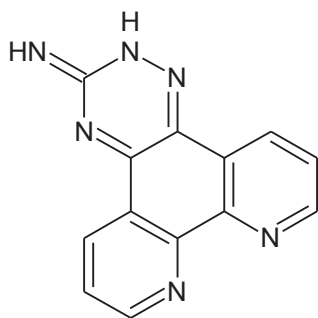


1,10-phenanthroline-5,6-dione (231 mg, 1.1 mol) and aminoguanidine hydrochloride (110.5 mg, 1 mol) were dissolved in 15 mL of MeOH. The reaction was heated to reflux for 24 hours and TLC in alumina plate and mobile phase consisting 80% methanol and 20% ethyl acetate was used to monitor whether the reaction was complete, the yellow precipitate wash with methanol and CHCl₃. The yield was 65%. Decomposed at 188 °C.

$^1\text{HNMR}$ (DMSO- d_6) δ 9.5 (1H, dd $J=1, 8$ Hz) **H9**; 9.24 (1H, dd $J=1.5, 5$ Hz) **H2**; 9.08 (1H, br) **NH**; 9.03 (1H, dd $J=1, 4.5$ Hz) **H4**; 8.81 (1H, dd $J=1.5, 7.5$) **H7**; 8.69 (2H, br) **NH2**; 8.04 (2H, m) **H3; H8**; 7.84 (1H, br) **NH**; ^{13}C (DMSO- d_6) δ (126.6, 126.9, 128.4, 129.9, 132.8, 137.4, 137.6, 142.4, 147.7, 148, 154.4, 156, 179.6) FT-IR(ATR) ($\nu_{\text{max}}/\text{cm}^{-1}$): 3287 and 2988 (NH+NH₂) 1637 (C=O) 1578 (C=N) 1450 (C=C), 1306 (C-N).

HRMS: [M+H]⁺, m/z Calcd: 267.0988 g/mol for C₁₃N₆OH₁₁ Found :267.0985 g/mol.

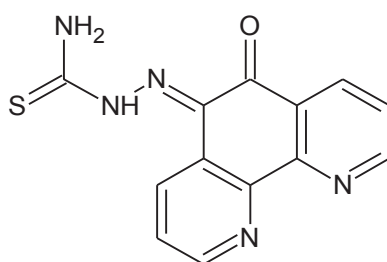
2.3.10. Synthesis of Amino-1,2,4-triazin[5,6-f]1,10-phenanthroline (ST10)



A mixture of phen-5,6-dione (105 mg, 0.5 mmol) and aminoguanidine bicarbonate (86 mg, 0.5 mmol) in ethanol in presence of 3 drops of HCl concentration reflux for 18 hours then cool to room temperature and filtrate to get yellow precipitate recrystallised in methanol with yield was 71%. Decomposed at 338 °C.

^1H NMR(DMSO- d_6) δ 11.14 (1H, br) **NH**; 9.5 (1H, br) **NH**; 9.19 (1H, d $J=8$ Hz) **H2**; 9.11 (1H, dd ($J=1.5, 4.5$ Hz) **H9**; 8.98 (1H, s br) **NH**; 8.90 (1H, dd $J=1.5, 5$ Hz) **H4**; 8.69 (1H, s br) **NH**; 8.61 (1H, dd $J=1.5, 8$ Hz) **H7**; 7.79 (1H, dd $J=4.5, 8$ Hz) **H3**; 7.73 (1H, dd $J=4.5, 8$ Hz) **H8**; ^{13}C (DMSO- d_6) δ (125.7, 126.1, 126.4, 127.1, 133.5, 134.9, 136.4, 140.3, 143, 145.6, 148.1, 152.8, 162.8). FT-IR(ATR)($\nu_{\text{max}}/\text{cm}^{-1}$): 3290 and 3078(2 NH), 1577(C=N), 1468(C=C), 1379(C-N). HRMS:[M+H] $^+$, m/z Calcd: 249.0883 g/mol for $\text{C}_{13}\text{N}_6\text{H}_9$ Found: 249.0885.

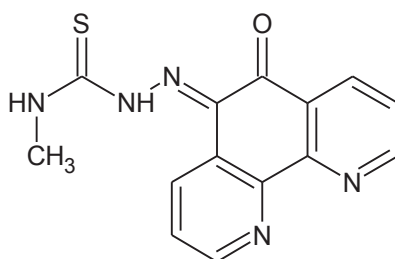
2.3.11. Synthesis of (2E)-2-(6-oxo-1,10-phenanthrolin-5(6H)-ylidene)hydrazinecarbothioamide (ST11)



phen-5,6-dione (105 mg, 0.5 mmol) and thiosemicarbazide (45.5 mg, 0.5 mmol) were added to a dry flask. The mixture was dissolved in 15 mL of anhydrous MeOH and 1% acetic acid (0.1 mL) was also added to the reaction. The reaction was heated to reflux for 26 hours under nitrogen. TLC using alumina plate and mobile phase consists 10% methanol and 90% dichloromethane was used to monitor whether the reaction was complete. The reaction time

ranged to overnight to complete. The solvent was removed in vacuum, and the yellow resulting solid was recrystallised in methanol and the yield was 75%. Decomposed at 298°C. $^1\text{H NMR}$ (CDCl_3) δ 10.19 (1H, br) **NH**; 9.58(1H, dd $J=2, 8$ Hz) **H4**; 9.31(1H, dd $J=1.5, 8$ Hz) **H7**; 9.25(2H, m) **H2**; **H9**; 7.77 (1H, dd $J=4.5, 8$ Hz) **H8**; 7.67 (1H, dd $J=4, 8$ Hz) **H3**; 3.5 2H, s **NH₂**. ^{13}C (CDCl_3) δ (124.5, 124.7, 125, 132.4, 134.4, 142.9, 143.7, 147, 150, 153.5, 155.1, 169, 190.7). FT-IR(ATR) ($\nu_{\text{max}}/\text{cm}^{-1}$): 3436(NH_2), 2969(NH), 1616($\text{C}=\text{O}$), 1587($\text{C}=\text{N}$), 1494($\text{C}=\text{C}$), 1060($\text{C}=\text{S}$). HRMS: $[\text{M}+\text{H}]^+$, m/z Calcd: 284.06005 g/mol for $\text{C}_{13}\text{H}_{10}\text{N}_5\text{OS}$ Found: 284.0601 g/mol.

2.3.12. Synthesis of (2E)-N-methyl-2-(6-oxo-1,10-phenanthrolin-5(6H)-ylidene)hydrazine-1-carbothioamide (ST12)

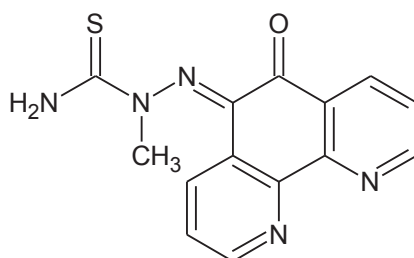


4-methyl-3-Thiosemicarbazide (105 mg, 1mmol) dissolved in warm ethanol (5 mL) was added to a ethanol solution (10 mL) containing phen-5,6-dione (210 mg, 1mmol) and 1 mL acetic acid. The mixture was refluxed for 20 hours the progress of the reaction was followed up by TLC in alumina plate and mobile phase consisting 30% dichloromethane and 70% ethyl acetate. The reaction mixture was then cooled to room temperature and the solid yellow precipitate was formed. It was then recrystallization in ethanol the yield was 57 %. Decomposed at 303 °C.

$^1\text{HNMR}$ (DMSO-d_6) δ 10.29 (1H, br) **NH**; 9.01(1H, dd $J=1.5, 8$ Hz) **H2**; 8.9(1H, dd $J=1.5, 4.5$ Hz) **H9**; 8.7(1H, dd($J=1.5, 5$ Hz) **H4**; 8.16(1H, dd $J=1.5, 5$ Hz) **H7**; 7.65 (1H, br) **NH**; 7.62(1H, dd $J=4.5, 8$ Hz) **H3**; 7.5(1H, dd $J=4.5, 8$ Hz) **H8**; 2.5(3H, s) **CH₃**.

^{13}C (DMSO-d_6) δ (31.2, 121.4, 123.5, 126.3, 127.6, 128.5, 134.3, 143.8, 152.4, 152.6, 153.1, 154.7, 179.2, 183.8). FT-IR(ATR) ($\nu_{\text{max}}/\text{cm}^{-1}$): 2820 (NH), 1614 ($\text{C}=\text{O}$), 1570 ($\text{C}=\text{N}$), 1492 ($\text{C}=\text{C}$), 1363(CH_3), 1309($\text{C}-\text{N}$), 1116 ($\text{C}=\text{S}$). HRMS: $[\text{M}+\text{H}]^+$, m/z Calcd: 298.0757 g/mol for $\text{C}_{14}\text{N}_5\text{OSH}_{12}$ Found: 298.0759 g/mol.

2.3.13. Synthesis of (2E)-1-methyl-2-(6-oxo-1,10-phenanthrolin-5(6H)-ylidene)hydrazine-1-carbothioamide(ST13)

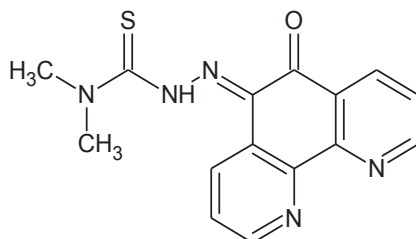


2-methyl-3-Thiosemicarbazide (105 mg, 1mmol) dissolved in warm ethanol (5 mL) was added to a methanol solution (10 mL) containing phen-5,6-dione(210 mg, 1 mmol) and 1 mL acetic acid. The mixture was refluxed for 16 hours the progress of the reaction was followed up by TLC in alumina plate and mobile phase consisting 95% methanol and 5% ethyl acetate. The reaction mixture was then cooled to room temperature and the solid red precipitate was formed. It was then recrystallization in ethanol the yield was 67 %. Decomposed at 277° C.

^1H NMR(DMSO- d_6) δ 9.5 2H,s **NH2**; 9.32(1H, d J = 3, 8 Hz) **H2**; 9.29(1H, dd J =2, 4.5 Hz) **H9**; 9.19 (1H, dd J =1.5, 4.5 Hz) **H4**; 8.92 (1H, dd J =2, 8.5 Hz) **H7**; 7.72 (2H, m) **H3**; **H8**; 4.44 (3H, s) **CH3**; ^{13}C (DMSO- d_6) δ (49.8, 124 ,142.2, 124.8, 124.9, 131.4, 135.4,135.6, 146.9 ,147.4, 151.4, 153.2, 155.9, 179.8) FT-IR(ATR) ($\nu_{\text{max}}/\text{cm}^{-1}$): 3007 (NH₂), 1614 (C=O), 1590 (C=N), 1492 (C=C), 1346(CH₃), 1309 (C-N), 1059 (C=S).

HRMS:[M+H]⁺,m/z Calcd: 298.0757 g/mol for C₁₄N₅OSH₁₂ Found:298.0750 g/mol.

2.3.14. Synthesis of (2E)-N,N-dimethyl-2-(6-oxo-1,10-phenanthrolin-5(6H)-ylidene)hydrazine-1-carbothioamide (ST14)



4,4-di methyl-3-Thiosemicarbazide (119 mg, 1mmol) dissolved in warm ethanol (5 mL) was added to a ethanol solution (10 mL) containing phen-5,6-dione (210 mg, 1mmol) and some 1mL of acetic acid was added. The mixture was refluxed for 24 hours the progress of the reaction was followed up by TLC in alumina plate and mobile phase consisting 95% methanol and 5% ethyl acetate.

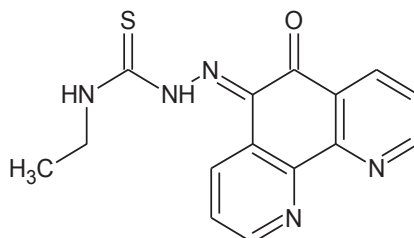
The reaction mixture was then cooled to room temperature and the solid yellow compound was filtered. It was then recrystallization in ethanol the yield was 49%. Decomposed at 292 °C.

^1H NMR(DMSO- d_6) δ 10.199(1H, s) **NH**; 8.97 (2H, dd $J=1.5, 4.5$ Hz) **H2; H9**; 8.38(2H, dd $J=1.5, 7.5$ Hz) **H4; H7**; 7.67(2H, dd $J=5, 8$ Hz) **H5; H8**; 3.73(6H, s) **CH₃; CH₃**;

^{13}C (DMSO- d_6) δ (56.4, 55.9, 121.5, 123.2, 125.6, 128.3, 129.5, 130.5, 136.1, 152.7, 152.9, 153, 154.7, 178.1, 186.8) FT-IR(ATR) ($\nu_{\text{max}}/\text{cm}^{-1}$): 2820 (NH), 1614 (C=O), 1590 (C=N), 1416 (C=C), 1346 and 1363(CH₃), 1309 (C-N), 1116 (C=S).

HRMS:[M+H]⁺,m/z Calcd: 312.0913 g/mol for C₁₅N₅OSH₁₄ found 312.0910 g/mol.

2.3.15. Synthesis of (2E)-N-ethyl-2-(6-oxo-1,10-phenanthrolin-5(6H)-ylidene) hydrazinecarbothioamide (ST15)



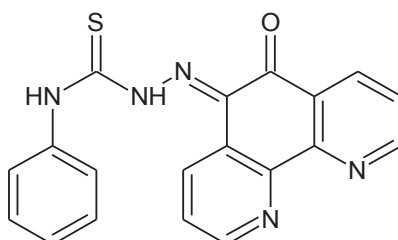
4-ethyl-3-Thiosemicarbazide (59.5 mg, 0.5mmol) dissolved in warm ethanol (5 mL) was added to a ethanol solution (10 mL) containing phen-5,6-dione(105 mg, 0.5 mmol) and 1 mL acetic acid. The mixture was refluxed for 22 hours the progress of the reaction was followed up by TLC in alumina plate and mobile phase consisting 10% methanol and 90% toluene. The reaction mixture was then cooled to room temperature and the solid yellow precipitate was formed. It was then recrystallization in ethanol the yield was 51%. Decomposed at 297 °C.

^1H NMR(DMSO- d_6) δ 10.07(1H, s) **NH**; 8.96 (2H, dd $J=1.5, 4.5$ Hz) **H2; H9**; 8.58(1H, dd $J=1.5, 7.5$ Hz) **H4**; 8.1(1 H, dd $J=1.5, 7.5$ Hz) **H7**;7.64(2H, dd $J=5, 8$ Hz) **H3;H8**; 7.5 (1H, s) **NH**; 3.15(3H ,q $J=7.5$ Hz)**CH₃**;1.2(2H, t, $J=7.5$ Hz)**CH₂**.

^{13}C (DMSO- d_6) δ (14.1, 39.6, 121.5, 123.2, 126.6, 127.5, 128.3, 134.8, 134.5, 151.2, 152.3, 153.5, 154.6, 179.1, 185.8). FT-IR(ATR) ($\nu_{\text{max}}/\text{cm}^{-1}$): 2820 (NH), 1614 (C=O), 1590 (C=N), 1492 (C=C),1404 (CH₂) 1363(CH₃), 1309(C-N), 1059 (C=S).

HRMS:[M+H]⁺,m/z Calcd: 312.0913 g/mol for C₁₅N₅OSH₁₂ Found 312.0914 g/mol.

2.3.16. Synthesis of (2E)-2-(6-oxo-1,10-phenanthrolin-5(6H)-ylidene)-N-phenylhydrazine-1-carbothioamide(ST16)

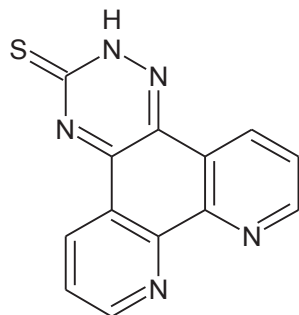


4-phenyl-3-Thiosemicarbazide (167 mg, 1mmol) dissolved in warm ethanol (5 mL) was added to a ethanol solution (10 mL) containing phen-5,6-dione(105 mg, 1 mmol) and 1 mL acetic acid. The mixture was refluxed for 20 hours the progress of the reaction was followed up by TLC in alumina plate and mobile phase consisting 10% methanol and 90% toluene. The reaction mixture was then cooled to room temperature and the solid yellow precipitate was formed. It was then recrystallization in ethanol the yield was 35%. Decomposed at 300°C.

^1H NMR(DMSO- d_6) δ 11.17 (1H, s) **NH**; 10.08 (1H, s) **NH**; 9.01 (2H, dd $J=1.5, 7.5$ Hz) **H2**; **H9**;8.5(1H, dd $J=1.5, 4.5$ Hz) **H4**; 8.1(1H, dd $J=1.5, 4.5$ Hz) **H7**;7.61(2H, dd $J=5, 8$ Hz) **H3**;**H8**; 7.3(4H ,dddd 8,7.5,1.5,1) 6.949(1H, tt $J =7,1.5$). ^{13}C (DMSO- d_6) δ (121.5, 123.9, 122.1,123.2, 123.9, 124.5, 126.7, 127.8, 128.3, 129.1, 128.8, 134.7, 134.8, 139, 152.4, 153.7, 154.6, 179, 185.7). FT-IR(ATR) ($\nu_{\text{max}}/\text{cm}^{-1}$): 2820 (NH), 1614 (C=O), 1570 (C=N), 1492 (C=C), 1346(C-N), 1116 (C=S).

HRMS:[M+H] $^+$,m/z Calcd: 360.0913 g/mol for $\text{C}_{19}\text{N}_5\text{OSH}_{14}$ Found: 360.0914 g/mol.

2.3.17. Synthesis of [1,2,4]triazino[5,6-*f*][1,10]phenanthroline-3(2*H*)-thione (ST17)

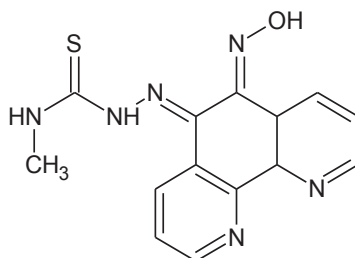


The mixture of phen-5,6-dione (105 mg, 0.5 mmol) and thiosemicarbazide (45.5 mg, 0.5 mmol) was dissolved in 15 mL of anhydrous MeOH and acetic acid (0.1 mL) was also added to the reaction. The reaction was heated to reflux for 40 hours TLC using alumina plate and mobile phase consists 10% methanol and 90% dichloromethane was used to monitor whether the reaction was complete. The reaction time ranged to overnight to complete. The solvent was removed in vacuo, and the resulting yellow solid was recrystallized in methanol and the yield was 79%. Decomposed at 287 °C.

$^1\text{H NMR}$ (CDCl_3) δ 11.12 (1H, br) **NH**; 9.65 (1H, d $J=8$ Hz) **H4**; 9.37 (1H, d $J=8.5$ Hz) **H7**; 9.31 (2H, m) **H2**; **H9**; 7.83 (1H, d $J=3.5$ Hz) **H8**; 7.74 (1H, , d $J=4$ Hz) **H3**.

^{13}C (CDCl_3) δ (175.9, 165.3, 164.1, 154.4, 152.4, 152.2, 127.9, 127.6, 123.4, 121.5, 121.2, 154.6, 123.1). FT-IR(ATR) ($\nu_{\text{max}}/\text{cm}^{-1}$): 2964(NH), 1596 (C=N), 1478 (C=C), 1376(C-N), 1175(C=S). HRMS: $[\text{M}^+]$, m/z Calcd: 265.0422 g/mol for $\text{C}_{13}\text{N}_5\text{SH}_7$ Found: 265.0429 g/mol.

2.3.18. Synthesis of (2*E*)-2-[(6*E*)-6-(hydroxyimino)-1,10-phenanthroline-5(6*H*)-ylidene]-*N*-methylhydrazine-1-carbothioamide (ST18)

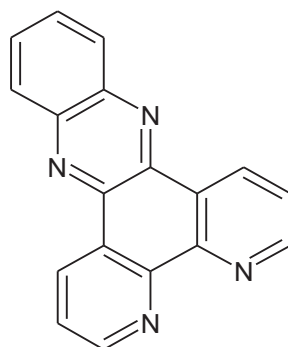


4-methyl-3-thiosemicarbazide (52.5 mg, 0.5 mmol) dissolved in warm ethanol (5 mL) was added to a ethanol solution (10 mL) containing (6*E*)-6-(hydroxyimino)-6a,10a-dihydro-1,10-phenanthroline-5(6*H*)-one (112.5 mg, 0.5 mmol) and some drops of acetic acid was added.

The mixture was refluxed for 20 hours the progress of the reaction was followed up by TLC in alumina plate and mobile phase consisting 95% methanol and 5% ethyl acetate . The reaction mixture was then cooled to room temperature and the solid yellow compound was filtered. It was then recrystallization in ethanol the yield was **35 %**. Decomposed at 303 °C.

$^1\text{H NMR}$ (DMSO- d_6) δ 11.28 (1H , br) **NH**; 8.47 (2H, dd $J=1.5,8$ Hz) **H2; H9**; 8.12(1H, dd($J=1.5,5$ Hz) **H4; H7**; 7.32 (1H , br) **NH**; ,7.52(1H, dd $J= 4.5, 8$ Hz) **H3; H8**; 2.5(3H ,s) **CH₃** ; ^{13}C (DMSO- d_6) δ (31.1, 121.4, 120.8, 123.4,122.7, 127.6,127.4, 152.3, 153.8, 154.6, 154.4, 165.5, 168.4,179). FT-IR(ATR) ($\nu_{\text{max}}/\text{cm}^{-1}$): 3004(OH), 2820 (NH), 1614 (C=O), 1570 (C=N), 1492 (C=C), 1363(CH₃), 1309(C-N), 1116 (C=S). HRMS:[M+H]⁺,m/z Calcd: 299.0709 g/mol for C₁₃N₆SOH₁₁ Found: 299.0703.

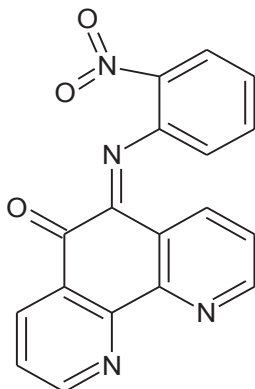
2.3.19. Synthesis of quinoxalino[2,3-f][1,10]phenanthroline (ST19)



A reported procedure (Travis et al. 2016) with some modification was implemented in this study and as following:

1,10-phenanthroline-5,6-dione (250 mg, 1.19 mmol) in 10 mL of absolute ethanol added o-phenylenediamine (193 mg, 1.785 mmol). The reaction solution was reflux for 6 hours then cool in room temperature. The solid yellow precipitate which formed was filtered and recrystallized from ethanol. The yield was 73 %. m.p. -251-252 °C. $^1\text{H NMR}$ (CDCl₃- d_6) δ 9.65 (2H, dd $J= 2, 8$ Hz), 9.27 (2H, dd $J= 1.5, 4$ Hz), 8.36 (2H m), 7.93 (2H m) 7.8 (2H, dd $J=4, 8$ Hz). ^{13}C (CDCl₃- d_6) δ (124.1, 127.5, 129.5, 130.6, 133.7, 141.1, 142.5, 148.4, 152.5).FT-IR(ATR) ($\nu_{\text{max}}/\text{cm}^{-1}$): 1596 (C=N), 1478 (C=C), 1347 (C-N). HRMS:[M+H]⁺,m/z Calcd: 283.0978 g/mol for C₁₈N₄H₁₀ 283.0979 g/mol.

2.3.20. Synthesis of (6*E*)-6-[(2-nitrophenyl)imino]-1,10-phenanthrolin-5(6*H*)-one(ST20)



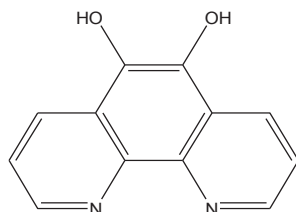
o-nitro aniline (69.065 mg, 0.5 mmol) in 10 mL of ethanol was added to the solution containing phen-5,6-dione (105 mg, 0.5 mmol) and 1 mL acetic acid reflux for 50 hours the progress of the reaction was followed up by TLC in alumina plate and mobile phase consisting 10% methanol and 90% toluene and kept at room for 24 hr to get orange precipitate filtrate and recrystallized from ethanol. The yield was 45%. m.p -181-182° C.

$^1\text{H NMR}$ (DMSO- d_6) δ 8.97(1H, d $J=3.5$ Hz) , **H2**; 8.38(1H, dd $J=1, 7.5$ Hz) **H9**; 7.92(1H, dd $J=1.5, 9$ Hz) **H4**; 7.66 (2H, dd $J= 4.5, 7.5$) **H3**; **H8**; 7.37 (3H, m) **H7**, **Hb**, **Hd**; 6.98(1H d $J=9$ Hz) **Ha**; 6.59(1H, d.t $J=1, 8.5$ Hz) **Hc**; ^{13}C (DMSO- d_6) δ (115.7, 119.3, 121.5, 123.3, 125.4, 125.5, 126.7, 128.3, 129.2, 130.5, 134.8, 135.8, 135.9, 140.5, 146.4, 152.4, 154.5, 177.9).

FT-IR(ATR) ($\nu_{\text{max}}/\text{cm}^{-1}$):1614(C=O), 1590 (C=N), 1570 (N=O), 1492(C=C), 1363(C-N).

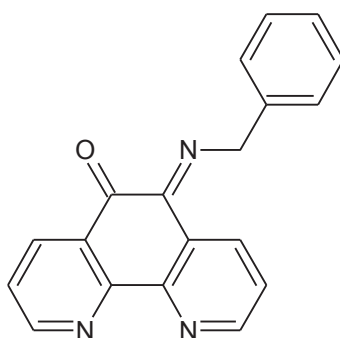
HRMS:[M+H] $^+$, m/z Calcd: 331.0825 g/mol for $\text{C}_{18}\text{O}_3\text{N}_4\text{H}_{10}$ Found: 331.0823 g/mol.

2.3.21. Synthesis of phen-5,6-diol (Wu et al. 2002)(ST21)



1,10-Phenanthroline-5,6-dione (105 mg, 0.5 mmol) and hydrazine sulfate (237.6 mg, 1.826 mmol) were dissolved in water (15 mL) and kept in a boiling water bath for 2 min, until the vigorous evolution of the gas had ceased. Then cooling the yellow solid was removed and washed with ethanol thoroughly to yield was 86%. The compound decomposed at 390 °C (lit. Wu et al. 2002 decomposed at 390 °C. ¹H NMR(DMSO-d₆) δ 10.30 (1H, br s) **OH**; 9.08 (2H, d *J*=3.5 Hz) **H2**; **H9**; 9.00 (2H, d *J*=8.5 Hz) **H4**; **H7**; 8.1 (2H, dd *J*= 5, 8.5) **H3**; **H8**; 4.09 (1H, br s) **OH**. ¹³C(DMSO-d₆) δ (125.1, 125.8, 133.8, 135.1, 135.7, 145) AT-IR (ν_{max}/cm⁻¹): 3036 and 2894 (OH), 1540 (C=N), 1499 (C=C), 1310 (C-N). HRMS: [M+H]⁺, *m/z* Calcd: 213.0658 for C₁₂N₂O₂H₈ Found: 213.0656.

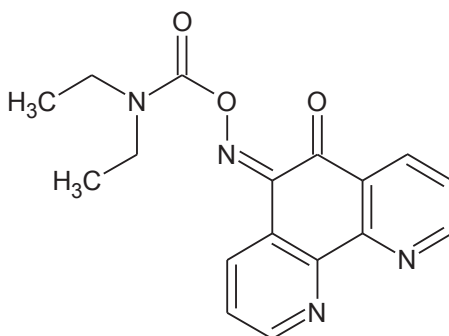
2.3.22. Synthesis of (6*E*)-6-(benzylimino)-1,10-phenanthroline-5(6*H*)-one (ST22)



1,10-phenanthroline-5,6-dione (105 mg, 0.5 mmol) in 15 mL of toluene was added (56.3 mg, 1.05 mmol) benzyl amine and 4-toluene sulfonic acid (3.5 mg, 0.0188 mmol) and reflux use dean and stark for (45) hrs. The progress of the reaction was followed up by TLC in alumina plate and mobile phase consisting 30% methanol and 70% toluene, wash with petroleum ether and the yield was 47%. Decomposed at 276 °C.

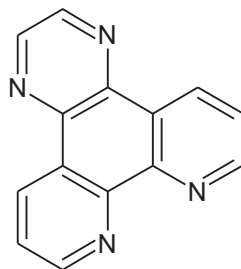
^1H NMR(DMSO- d_6) δ 9.24 (2H dd J = 2.5, 4.5 Hz) **H2**; **H9**; 8.97 (1H, dd J = 1.5, 8 Hz) **H4**; 8.71(1H, dd J = 1.5, 8 Hz) **H7**; 8.38 (2H, 2H dd J = 4, 8 Hz) **H3**; **H8**; 7.78 (2H, m) , 7.59 (3 H dd J = 3.5, 5 Hz) 3.88 (1H , s) **CH2**; ^{13}C (DMSO- d_6) δ (50.4, 121.6, 123.4, 126.6, 127.7, 128.1, 128.3, 128.5, 128.7, 128.9, 134.5, 138.9, 139.5, 152.3, 152.5, 153.1, 153.7, 154.4, 185.7) FT-IR(ATR) (ν_{max} /cm-1): 1614 (C=O), 1590 (C=N), 1492(C=C), 1404(CH₂), 1346 (C-N). HRMS:[M⁺],m/z Calcd:299.1058 for C₁₉H₁₃N₃O g/mol Found: 299.1051 g/mol.

2.3.23. Synthesis of (6Z)-6-(Rashid & Ansari)-1,10-phenanthrolin-5(6H)-one(ST23)



(6E)-6-(hydroxyimino)-1,10-phenanthroline-5(6H)-one (225mg, 1mmol) and *N,N*-diethylamine carbamyl chloride (271.1 mg , 2 mmol) were stirred at room temperature in anhydrous DMF for 18 hours in presence of sodium hydride (60 mg, 2.5 mmol). The yellow precipitate obtained was filtered, washed with cold water and dried under reduced pressure to obtain the products the yield was 30%. Decomposed at 240°C. ^1H NMR(DMSO- d_6) δ 9.24 1H, d(J = 8 Hz) **H2**; 9.03 1H, dd(J = 1.5, 4 Hz) **H9**; 8.83 (1H, dd J = 1, 4.5 Hz) **H4**; 8.44 (1H m) **H7**; 7.6 (1H dd J = 4.5,8 Hz) **H3**; 7.61 (1H dd J =4.5,8 Hz) **H8**; 3.31(4 H q J =7) **CH2**;1.22 (6H t J =7) **CH3**; ^{13}C (DMSO- d_6) δ (11.2, 41.5, 123.4, 124.9, 125.1, 127.9, 131.6, 135.1, 135.8, 137.2, 146.9, 150.8, 150.9,152.6, 155.1,155.2, 181.3) FT-IR(ATR) (ν_{max} /cm-1):1598 (C=O), 1540(C=N), 1499(C=C), 1469(CH₂), 1420 (CH₃), 1308(C-N). HRMS:[M+H]⁺,m/z Calcd: 325.1295g/mol for C₁₇N₄O₃H₁₆ Found: 325.1298 g/mol.

2.3.24. Synthesis of pyrazino[2,3-f][1, 10]phenanthroline (ST24)



A reported procedure (Xu et al. 2015) with some modification was implemented in this study and as following:

1,10-phenanthroline-5,6-dione (420 mg, 2 mmol) in 10 mL of absolute ethanol added ethylenediamine (147mg, 2.2 mmol). The reaction solution was heated gently for (18) hours at 50 °C, then cool in room temperature for 5 hours. The orange precipitate which formed was filtered and recrystallized from ethanol. The yield was 57%. Decomposed at 270° C.

^1H NMR(DMSO- d_6) δ 9.46 dd, 2H, (J = 2, 8 Hz), 9.23 dd, 2H, (J = 2, 4.5 Hz), 9.16 (s,2H), 7.96 (dd, 2H, (J = 4, 8 Hz) ^{13}C (DMSO- d_6) δ (124.5, 126.6, 132.7, 139.7, 145.6, 146.9, 152.2) FT-IR(ATR) ($\nu_{\text{max}}/\text{cm}^{-1}$): 1587(C=N), 1416(C=C), 1312(C-N).

HRMS:[M+H] $^+$, m/z Calcd: 233.0821 g/mol for $\text{C}_{14}\text{N}_4\text{H}_8$ Found 233.0829.

2.4: Results and discussion:

2.4.1: Synthesis of the mono substituted Schiff base (6E)-6-[(2-hydroxyphenyl) imino]-1,10-phenanthroline-5(6H)-one (ST02)

One of the potential problems faced in this research project was related to the preparation, characterisation and analysis of the basic starting material phen-5,6-dione although it can be supplied by international laboratories on demand, but the purity of the ingredients could not be confirmed in addition to the high cost, accordingly all the starting material phen-5,6-dione was prepared and analysed according to published procedure. The preparation was carried out by oxidation of (phen) using $\text{H}_2\text{SO}_4/\text{HNO}_3/\text{KBr}$. The preparation was carried out on small scale batches (2-3g/batch) due to the hazardous nature of the oxidation reactions involved in the preparation.

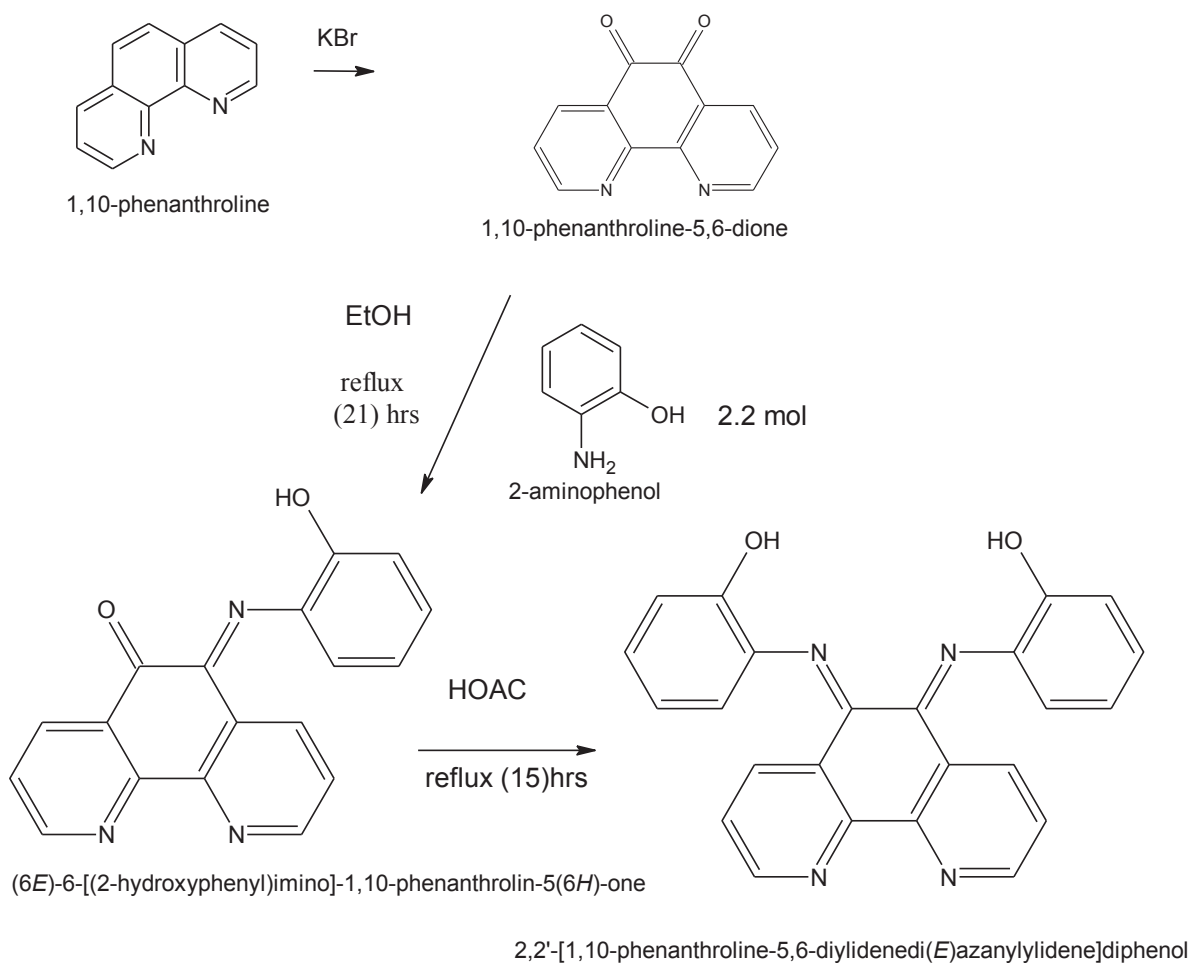
The oxidation step of phen was followed by neutralisation of the of the reaction mixture to obtain the phen-5,6-dione.

The neutralisation step is very critical step in the preparation to avoid the side reaction of forming 4,5-diazafluoren-9-one that is usually formed under basic conditions (Inglett & Smith 1950).

The yield in the reported procedure is low (45%) (Lincoln & Norden 1993) accordingly several modification and various trials were adopted to increase the yield and enhance the purity. Among the attempts changing the physical state to fine powder to increase its solubility, increase the reflux time, modifying the oxidant mixture composition, changing the reaction conditions, the best yield obtained was 65 %.

The Structure of the product was verified by ^1H NMR, ^{13}C NMR, FTIR, ATR and UV visible as UV visible detailed in chapter 4.

Applying the modified procedure, bulk quantity of phen-5,6-dione, was prepared and characterised. The imine derivatives were prepared by condensation reaction of phen-5,6-dione with 2- aminophenol to prepare mono and di substituted derivatives as novel imines compounds as detailed in the experimental part and represented in Scheme 5.



Scheme 5: Preparation of Mono and Di condensate Schiff base

Different trials were attempted to prepare the mono condensate of 2-aminophenol with phen-5,6-dione using different stoichiometric ratios of 2-aminophenol. The reaction conditions were also investigated to find the best reaction conditions such as reaction temperature, solvents, reaction time, separation and purification procedures. The detailed and optimum conditions explained in 2.3 represent the best and suitable conditions for the preparation of the mono substituted compound. The product was confirmed using ^1H NMR to demonstrate the phenol group at δ 7.99ppm. Furthermore ^{13}C NMR spectra consisted of eighteen peaks supporting assigned structure, and the infrared spectrum clearly showed a broad intense peak at 3464 cm^{-1} due to the O-H stretch in other words all the obtained spectral data confirmed and supported the assigned chemical structure of compound (6E)-6-[(2-hydroxyphenyl)imino]-1,10-phenanthroline-5(6H)-one (ST02).

2.4.2 Preparation of [2,2'-[1,10-phenanthroline-5,6 diylidenedi(*E*) azanylylidene] diphenol] (ST03)

The attention was turned to next step in the sequence of the preparation to establish a satisfactory method to synthesise the di substituted, condensation product of 2-aminophenol with phen-5,6-dione. The preparation of the di substituted Schiff base structure (Scheme -7) was one of the hardest tasks of this project. In spite of the extensive experimental work and trials that has been carried out, this could be possibly due to steric hindrance. Finally it was possible to prepare the required product. In the following paragraphs summary for some of the not successful trials are listed:

Different trials were fulfilled under different reaction conditions such as using different stoichiometric ratios of 2-amino phenol, different solvents with various solubility parameters such as ethanol, mixture of ethanol and methanol (1:1 ratio), DMSO, DMF, varying the reaction pH , acidic and basic medium aiming of getting the desired Product [2,2'-[1,10-phenanthroline-5,6-diylidenedi(*E*)azanylylidene]diphenol] (di substituted ST03).

Other experiments were based on replacing 2-amino phenol with o-anisidine. Due to difficulties to prepare the di substitution and the acidity of 2-amino phenol which is expected to form some ionic adducts which was thought to be one of the barriers that prevent the condensation of amino phenol with phen -5,6-dione to form di substituted products.

To overcome intermolecular ionic bonding between the *p*-aminophenol molecules 2-amino phenol was replaced with *o*-anisidine substituting phenolic hydrogen with methyl group as non-acidic intermediate then to cleave the phenyl methyl ether group to recover the phenolic hydroxyl functional group. Adopting different previously mentioned reaction conditions applied to this experiment and the negative results obtained ;the assumption of intermolecular ionic bonding may not be valid reason for the not formation of the di substituted product.

The other unsuccessful trial was carried out in the presence of ammonium acetate as standard neutral buffer to adjust pH 7 for the condensation of phen-5,6-dione with *o*-anisidine and *p*-anisidine in glacial acetic acid medium, without any traces of the mono or di substituted as indicated from ¹H NMR and HRMS spectra analysis .

Another trial to condense *o*-anisidine and *p*- anisidine with phenanthroline 5,6-dione to prepare mono and di substituted using *p*-toluenesulfonic acid was added to toluene with the zeotropic removal of water using a Dean and Stark apparatus in order to drive the reaction to the desired product side, but unfortunately neither changing solvent nor acid had any influence on outcome of the reaction.

Another experiment was carried out for the reaction of *o* -anisidine and *p* - anisidine with phen 5,6-dione to prepare mono and di substituted ligands without solvent (as solid state reaction) in the presence of SnCl₂.2H₂O. The reaction mixture was grinded in a mortar at room temperature unfortunately no product was obtained. This trial was based on the reported literature on the preparation of some Schiff bases in solid state conditions (solvent free).

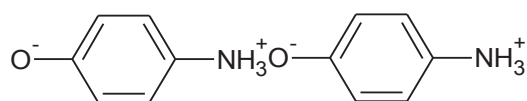
Another trial was carried out in the presence of molecular sieves to absorb water formed as by product, thoughtfully that the reversible condensation reaction of the Schiff base will be forced to forward according to Le chatelier principle. The reaction product was worked out and analysed by NMR and HRMS, no indication for the di substituted was found.

The same trial was repeated in the presence of other drying agents such as calcium oxide, and anhydrous magnesium sulphate as an attempt to retard the hydrolysis of the di substituted imine if it is formed as probably unstable product. Other experiment was planned and fulfilled based on removing the by-product water by azeotrope technique using Dean-Stark apparatus in the presence of toluene under nitrogen atmosphere, but again the desired compound was not obtained.

Other unsuccessful trials were based on preparation of iron complexes with phen-5,6-dione, before condensing it with 2-amino phenol or p- anisidine as another approach to prepare desired product.

As a results of these extended experiments it was noticed that two stage reaction; firstly forming the mono substituted then fulfilling the second stage under reflux in the presence of glacial acetic acid which react with the by product water to force the equilibrium reaction to forward. The di substituted targeted product was obtained as indicated from the NMR, FTIR and HRMS analysis, in ^1H NMR spectrum showed singlets peak at δ 7.5(2H,s) due to OH, and the infrared spectrum clearly showed a broad intense peak at 3447 cm^{-1} due to the O-H stretch. In addition, infrared spectrum and ^{13}C NMR of the product showed no peak in the characteristic carbonyl region, which support the proposed structure as detailed in 2.3.3.

After all these trials that covered almost all the factors might one think of based on the chemistry of Schiff bases to synthesise the targeted di substituted product. Three main outcomes can be made as reasons for this reaction not to take place either to the steric hindrance. As being adjacent to carbonyl group of the mono substituted product. The steric hindrance factor in the preparation of some aromatic Schiff based has been also reported by (Moody, Rees & Thomas 1992), or the intramolecular ionic bonding explained before or the equilibrium condensation reaction that form water as by product which reverse the reaction and hydrolyse the formed di substituted product. To prove any of these outcomes are affecting the reaction progress from mono substituted product to di substituted product the following experiment was planned by replacing p-amino phenol with o-amino phenol the later do not form intermolecular hydrogen bonds but rather form intramolecular hydrogen bonding as shown in Scheme 6.



Scheme 6: Intermolecular H-bonding of p-aminophenol

This di substituted derivative was prepared by condensation of phen-5,6-dione with 2-amino phenol using glacial acetic acid as detailed in the experimental part section 2.3.3. The structure of this compound was confirmed by various advanced techniques: M.P, ^1H NMR, ^{13}C NMR, FTIR, UV and HRMS. The ^1H NMR spectrum presented in section 2.3.3 showed singlets peak at δ 7.5(2H,s) related to OH, the infrared spectrum clearly showed a broad intense absorption peak at 3447 cm^{-1} related to O-H stretching.

In addition the infrared spectrum and ^{13}C NMR spectrum of the product did not show characteristic band at the carbonyl region, So all the analysis data support the proposed structure.

The attempt was tune on use the *m*-aminophenol and *p*-aminophenol to condense phen-5,6-dione. However several trial had been attempted to synthesis the meta and para, mono and di substituted condensation of phen-5,6-dione , but all these trials were unsuccessful. Furthermore, another trial was attempted using K_2CO_3 and stirring under nitrogen in anhydrous DMF then extracted in toluene and washed with water, but unfortunately once more it was not the desired result for this reaction. The most properly reason that the meta aminophenol failed to condense with phen-5,6-dione is due to the amino is in position meta which will be in week of electro density and will be week to react as electron donner,

while the para- aminophenol could be due to extremal hydrogen bonding between the OH and NH_2 . Once the trial of (*m* and *p*-aminophenol) was discontinued.

2.4.3 Preparation of quinoxalino[2,3-f][1,10]phenanthroline (ST 19)

Condensation of phen-5,6-dione with o-phenylenediamine get desired product characterised by various techniques ^1H NMR, ^{13}C NMR, FTIR, UV and HRMS. The infrared spectrum and ^{13}C NMR of the product showed no peak in the characteristic carbonyl region, which support the proposed structure and the ^{13}C NMR spectrum consisted of nine peaks supporting assigned structure symmetric supporting strongly the compound has been prepared as shown in section 2.3.19

2.4.4 Preparation of (6E)-6-[(2-nitrophenyl)imino]-1,10-phenanthroline-5(6H)-one(ST20)

Condensation product of phen-5,6-dione and O-nitroaniline compound. The compound was prepared by condensation of phen-5,6-dione with O-nitroanline according to the detailed procedure in section 2.3.20 , the product was characterised by ^1H NMR, ^{13}C NMR, FTIR, UV and HRMS. The absorption band at 1570 cm^{-1} of the IR spectrum is related to (N=O). The ^{13}C NMR spectrum consisted of eighteen peaks supporting assigned chemical structure.

2.4.5 Preparation of pyrazino[2,3-f][1, 10]phenanthroline (ST24)

Fortunately, stirring phen-5,6-dione with ethylenediamine get desired product characterised by various techniques ^1H NMR, ^{13}C NMR, FTIR, UV and HRMS. The infrared spectrum and ^{13}C NMR of the product showed no peak in the characteristic carbonyl region, which support the proposed structure as shown in section 2.3.24.

Several other condensation product were planned to be prepared in this study under various reaction conditions unfortunately the trials were not successful as indicated from the analysis of NMR and HRMS:

- a. Condensation of phen-5,6-dione with 2,4-dinitro phenyl hydrazine, various reaction conditions were investigated. The obtained product was insoluble in most commonorganic solvents therefore it has not been fully characterized due to solubility issues.
- b. Condensation phen-5,6-dione with phenyl hydrazine using few drops of H_2SO_4 .
- c. Condensation of phen-5,6-dione with 2,4-dinitroaniline in ethanol in acetic acid medium.
- d. Condensation phen-5,6-dione with 2,6-dichloro-4-nitroaniline in ethanol in presence of acetic acid.
- e. Condensation of phen-5,6-dione with o-toulidine in methanol in the presence of acetic acid and another trail in presence of formic acid.
- f. Condensation of phen-5,6-dione with 4-Chloro-2-methylanline in ethanol with and without acetic acid.
- g. Condensation phen-5,6-dione with 2-amino thiophene-3-carboxylic acid amide after work up on reaction concluded not get desire product.
- h. Condensation of the mono substituted compound ST02 with diethylcarbamoyl chloride

in the presence of anhydrous acetonitrile and repeated the experiment in the presence of sodium hydride in ice bath for 30 min then at ambient temperature for 24 h with gentle mixing and under nitrogen adopting various reaction conditions the analysis of the product were negative.

2.4.6 Preparation of (6*E*)-6-(hydroxyimino)-1,10-phenanthroline-5(6*H*)-one (ST04)

The attention was focused on small molecules such as oxime to synthesis the new pathway of the aliphatic group, such as reactants ratio, reaction time, reaction pH conditions to prepare the mono and di derivatives of phenanthroline-5,6 dione.

The reactive ingredient was synthesised by condensation phen-5,6-dione with hydroxylamine hydrochloride, purified and characterised by ^1H NMR, ^{13}C NMR, FTIR, UV and HRMS. The ^1H NMR spectrum showed singlets peak at δ 4.5(1H,s,br) due to OH also the infrared spectrum clearly showed a broad intense absorption peak at 3500 cm^{-1} related to the O-H stretch.

Another trial was attempted by condensation phenanthroline 5,6-dione with methoxyamine hydrochloride in presence of ethanol with and without K_2CO_3 . The reaction was monitored by TLC, did not give any indication of forming the mono substitute product as indicated from NMR and HRMS. It appeared that no desired compound was obtained and the phenanthroline 5,6-dione was not consumed. This elucidate that either the metoxyamine less reactive than the hydroxylamine or the condensation was not occurred due to reaction condition was week for such condensation.

Different trials were fulfilled under different reaction conditions such as: reactant ratio of hydroxyl amine hydrochloride: Phen-5,6-dione, solvents, reaction temperature and reaction time. The conditions and reactant ratio listed in sect.2.3.6, represent the optimum conditions for the preparation of 5,6-dione di oxime substituted product (compound ST05)

To increase the yield and purity of the oxime derivatives of the 5,6-di one, a series of experiments were carried out under different reaction conditions; reactant ratio of hydroxyl amine hydrochloride, solvents, reaction time and reaction temperature. The optimum reaction conditions obtained to give 85% yield were carrying the reaction under slight basic conditions using Na_2CO_3 and 3.5:1 molar ratio of hydroxyl amine hydrochloride:5,6-dione.

According to literature (Kleineweischede & Mattay 2006) the dioxime (ST05) can react under acidic and basic conditions to form the 1,2,5-oxadiazole as by product. Therefore the reaction of phen-5,6-dione with hydroxylamine hydrochloride, without addition of sodium carbonate led to the formation of the 1,2,5-oxadiazole side product.

It is therefore important to minimize the concentration of the free base in the reaction medium by adding hydroxylamine hydrochloride as a solution in absolute ethanol to the solution of the phen-5,6-dione dropwise with mixing and to neutralise the hydrogen chloride, produced during the condensation reaction in situ, by addition of a weak base NaCO_3 .

On the other hand it was found that optimising the reflux time to minimum required time was critical to avoid formation of 1,2,5-oxidazole. The purification step was also found to be critical accordingly the purification and washing up was fulfilled using small portion of cold water to remove the by product salts then washed with small portion of ether before drying it under vacuum at 80 °C.

It was noticed that applying the published procedure for preparation of dioxime for other diones (Bodige & MacDonnell 1997b) did not work with this new series of dioximes.

This may be due to the solubility of the by-product 1,2,5-oxadiazolo[3,4-*f*]-1,10-phenanthroline or the solubility of the phendioxime in ethanol, ether and in diluted mineral acids as reported by (Inglett & Smith 1950).

2.4.7 Preparation of the condensation product of 5,6-dione with semicarbazide

The other category of the suggested active ingredient prepared in this study are based on derivatives of phen-5,6-dione with some aliphatic active groups as active ligands that contain O and N, O and S, O,N and S, and N,N and S as donor atoms which are notable for their great biological activities.

Using semicarbazide hydrochloride salt instead of free base, as the acidity and stability of salt of semicarbazide was achievable to synthesis the mono semicarbazone of phenanthroline 5,6-dione gave positive results of forming mono semicarbazone (ST06) as indicated by various techniques ^1H NMR, ^{13}C NMR, FTIR, UV and HRMS details are presented in 2.3.6.

A literature procedure (Murali, Sastri & Maiya 2002) was used in the preparation of cyclic semicarbazone (ST07) by doing the reaction in ammonium acetate and reflux for 7 hours gave positive results as characterised by ^1H NMR, ^{13}C NMR, FTIR, UV and HRMS. All the analysis obtained data confirmed the formation of cyclic semicarbazone as detailed in section 2.3.7.

The attempts to prepare di substituted of semicarbazone at different reaction conditions were investigated: reactants ratio, reaction time, reaction pH were not successful this could be also related to steric hindrance as noticed with previous derivatives.

Due to successful reaction with semicarbazide family, and due to well known that this group has a major effect on cancer, malaria and AD disease, a new trial of condensation 4-phenylsemicarbazide hydrochloride with phenanthroline 5,6-dione in ethanol was attempted with and without acetic acid and other trial in the presence K_2CO_3 under nitrogen in anhydrous DMF. The product was separated, purified and analysed by NMR and HRMS. No indication for the formation of the product were noticed.

2.4.8 Preparation of dual function (2*E*)-2-[(6*E*)-6-(hydroxyimino)-1,10-phenanthroline-5(6*H*)-ylidene]hydrazine-1-carboxamide (ST08)

The dual functionality derivatives of phen-5,6-dione as semicarbazone and oxime by condensation mono semicarbazone of phen-5,6-dione with hydroxylamine hydrochloride were successfully prepared and characterised by various techniques 1H NMR, ^{13}C NMR, FTIR, UV and HRMS. To confirm that, the NH signal at 13.65 (s, 1 H) in the NMR solution disappeared when D_2O was added. The 1H NMR peak at 4.5 (1H, s, br) due to OH also confirm the product formation. The infrared spectrum clearly showed a broad intense peak at 3010 cm^{-1} due to the O-H stretching.

Also several attempts to mimicking the dual method to condensate mono semicarbazone of phen-5,6-dione with methoxy amine hydrochloride under various reaction conditions did not give any positive results.

2.4.9 Preparation of 5,6-dione -thiosemicarbazide derivative

Various reaction conditions were investigated: reactant stoichiometric ratio, reaction time, temperature, solvents, reaction medium pH, and working out procedures.

The optimum reaction conditions found for the preparation of mono-derivatives of thiosemicarbazone were: reacting equal molar ratios of thiosemicarbazide with phen-5,6-dione in the presence of a few drops of glacial acetic acid in anhydrous MeOH as a solvent under reflux and nitrogen stream.

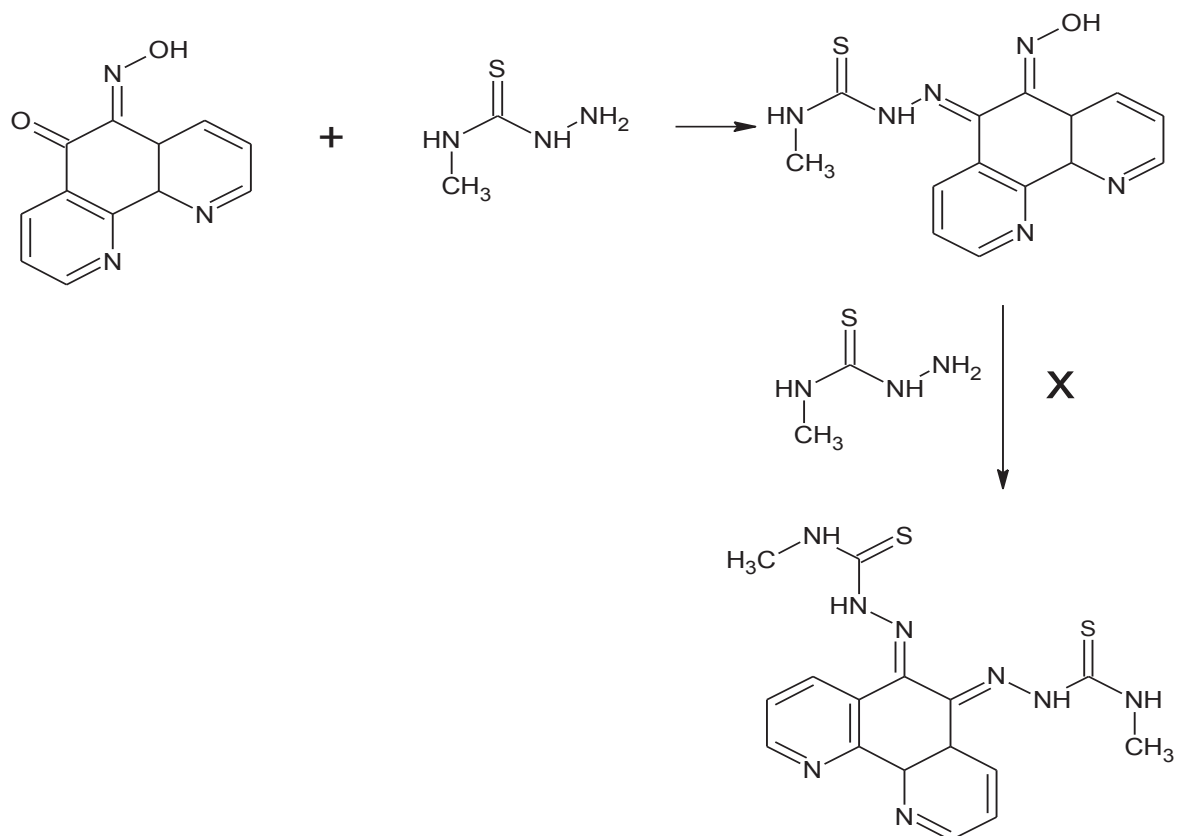
The compound was fully characterised by ^1H NMR, ^{13}C NMR, FTIR, UV and HRMS as detailed in 2.3.11. The infrared spectrum clearly showed a peak at 1060 cm^{-1} due to the(C=S)

Several experiments were carried out to optimise the reaction conditions such as; reactants ratio, reaction pH, solvents reaction time and others to prepare di substituted thiosemicarbazone.

The analysis of the reaction products by HRMS and NMR did not give evidence of forming the di substitute derivatives of 5,6,-dione with thiosemicarbazide.

The reaction was repeated using different polar anhydrous solvents such as DMF and DMSO in the presence of different acidic catalysts such as acetic anhydride, HCl (as gas bubbles). The separated and analysed product showed to be mono substituted derivative due to possibility that the second carbonyl in phenanthroline 5,6-dione become more acidic and difficult to react with amino group.

The other indirect procedure to prepare the di substituted derivative was experimented via condensation of mono oxime (ST04) with thiosemicarbazide then exchange of the oxime group with second thiosemicarbazide and /or displacement of the oxime with other reactive displacing groups to prepare the di substituted 5,6-dione derivatives as detailed in the reaction scheme 7 .The reaction products were separated, purified by standard procedures and analysed by NMR,HRMS. The analysis did not gave any evidence for the formation of the di substitute derivatives based NMR and HRMS.



Scheme 7: Reaction scheme for the preparation of di thiosemicarbazone by indirect substitution procedure

The reaction was implemented on another analogous phen-5,6-dione to condense with 4-methyl-3-Thiosemicarbazide gave desired product as detailed in section 2.3.12 as characterised by various techniques ^1H NMR, ^{13}C NMR, FTIR, UV and HRMS. In ^1H NMR the single spectrum of δ 2.5(3H,s) indicates CH_3 spectrum. Other absorption bands were present at 1363 cm^{-1} indicating (CH_3) spectrum. The ^{13}C NMR spectrum consisted of fourteen peaks supporting assigned structure as detailed in section 2.3.12.

Fortunately, condensation of phen-5,6-dione with 2-methyl-3-Thiosemicarbazide gave desired product characterised by various techniques ^1H NMR, ^{13}C NMR, FTIR, UV and HRMS.

In ^1H NMR the single spectrum of δ 4.44 (3H,s) indicates CH_3 spectrum. Also, bands were present at 1346 cm^{-1} indicating (CH_3) spectrum. The ^{13}C NMR spectrum consisted of fourteen peaks supporting assigned structure as detailed in section 2.3.13.

phen-5,6-dione to condense with 4,4-di methyl-3-Thiosemicarbazide gave desired product characterised by various techniques ^1H NMR, ^{13}C NMR, FTIR, UV and HRMS. In ^1H NMR the single spectrum of δ 3.73(6H, s) indicates two CH_3 spectra in the compound.

The ^{13}C NMR spectrum consisted of fifteen peaks supporting assigned structure. Also, bands were present at (1346 and 1363) cm^{-1} indicating two (CH_3) spectra and bands at 1116 cm^{-1} indicating ($\text{C}=\text{S}$) spectrum as detailed in section 2.3.14.

phen-5,6-dione to condense with 4-ethyl-3-Thiosemicarbazide gave desired product characterised by various techniques ^1H NMR, ^{13}C NMR, FTIR, UV and HRMS. In NMR the spectra of δ 3.15(3H, q $J=7.5$ Hz) for CH_3 and δ 1.2(2H, t, $J=7.5$ Hz) for CH_2 and bands were present at 1404 cm^{-1} for (CH_2) 1363 cm^{-1} for (CH_3) and the ^{13}C NMR spectrum consisted of fifteen peaks supporting assigned structure supporting strongly the compound has been prepared as detailed in 2.3.15.

phen-5,6-dione to condense with 4-phenyl-3-Thiosemicarbazide gave desired product characterised by various techniques ^1H NMR, ^{13}C NMR, FTIR, UV and HRMS. In NMR the spectra at δ 7.3(4H, dddd 8,7.5,1.5,1) and δ 6.949(1H, tt $J=7,1.5$) indicated phenyl group and the ^{13}C NMR spectrum consisted of nineteen peaks supporting assigned structure supporting strongly the compound has been prepared as detailed in section 2.3.16.

Unfortunately, phen-5, 6-dione to condense with 4-(2-Methylphenyl)-3 thiosemicarbazide in ethanol in presence of acetic acid after work up on reaction did not show formation of the desired product as indicated from the NMR and HRMS.

2.4.10 Preparation of cyclic thiosemicarbazone derivatives of phen-5,6-dione (ST017)

Experimental procedure was tried for the preparation of cyclic thiosemicarbazone by refluxing mono thiosemicarbazone dissolved in ammonium acetate in the presence of acetic acid. The procedure was also repeated by carrying the reaction in 5% KOH solution.

The obtained product was worked up, purified and analysed by NMR and HRMS, no indication of forming the designed products were obtained.

Condensation of phen-5,6-dione with thiosemicarbazide in anhydrous MeOH in the presence of acetic acid after reflux for 40 hours gave the desired product as confirmed by various techniques; ^1H NMR, ^{13}C NMR, FTIR, UV and HRMS. ^{13}C NMR. The FTIR spectrum of the product showed no characteristic carbonyl absorption peak, which support the proposed

structure. The infrared spectrum showed peak at 1175 cm^{-1} due to (C=S) and in ^{13}C δ 175.9 as detailed in section 2.3.17.

2.4.11 Preparation of (2*E*)-2-(6-oxo-6,10b-dihydro-1,10-phenanthroline-5(4*aH*)-ylidene)hydrazinecarboximidamide (ST09)

Condensation of phen-5,6-dione with aminoguanidine hydrochloride gave desire product as detailed in 2.3.9. The ^{13}C NMR spectrum consisted of thirteen peaks supporting assigned structure. To confirm that the single peak of NH signal at 9.08 (s,1H) disappeared when D_2O was added to the solution.

Once the mono aminoguanidine phen-5,6-dione was synthesised, the trials were carried out to obtain di substitution, through optimising the reaction conditions using different reactants ratio, reaction pH conditions and reaction time to prepare di substituted of aminoguanidine hydrochloride. The trials carried out to optimise the reaction conditions of to prepare the di substituted of aminoguanidine hydrochloride were unsuccessful.

2.4.12 Preparation of Amino-1,2,4-triazin[5,6-*f*]1,10-phenanthroline (ST10)

Once the mono aminoguanidine phen-5,6-dione was synthesised, the trials were carried out to obtain di substitution, through optimising the reaction conditions using different reactants ratio, reaction pH conditions and reaction time to prepare di substituted of aminoguanidine hydrochloride.

The reaction was worked and a new product was observed, the product was subjected to ^1H NMR, ^{13}C NMR, FTIR, UV and HRMS, and it indicated that instead of di substitution on Phen-5,6-dione a cyclic aminoguanidine was prepared detailed in section 2.3.10. To confirm that the single peak of NH signal at δ 11.14 (1H, br) **NH**; 9.5(1H, br) **NH**; disappeared when D_2O was added to the solution.

This product was confirmed by ^{13}C NMR spectra, and the product showed no peak in the characteristic carbonyl region. In addition no bands were present in infrared at 1630 cm^{-1} - 1800 cm^{-1} indicating the absence of a carbonyl group.

2.4.13 Preparation of hetero dual substituted phen-5,6-dione

The other target of this project was to prepare hetero di substituted phen-5,6-dione with different substituent groups ; The reactions were carried out under various reaction conditions (stoichiometry, solvents, addition rate and heating). Unfortunately, the results on the products separated, purified and analysed by NMR and HRMS did not confirm the formation of the proposed products.

a. New trials were carried out to prepare dual function group of semicarbazone and thiosemicarbazone under various reaction conditions using Amberlite-IR 120 resin as an efficient heterogeneous catalyst.

b. Preparation of dual function group consisting semicarbazone and thiosemicarbazone by condensation ST08 with thiosemicarbazide by replacing the oxime hydroxyl group with thiosemicarbazide to form the dual function group.

c. Preparation of hetero dual function group of aminoguanidine hydrochloride and thiosemicarbazone under various reaction conditions such as basic, acidic conditions and using various solvents were also unsuccessful.

d. Prepare dual function group of semicarbazone and aminoguanidine hydrochloride by condensation ST08 with aminoguanidine hydrochloride by replacing oxime hydroxide group with aminoguanidine to obtain dual functional group .

e. Preparation of dual function group of (6*E*)-6-(hydroxyimino)-1,10-phenanthroline-5(6*H*)-one (ST04) with aminoguanidine hydrochloride .

Several other condensation product were planned to be prepared in this study under various reaction conditions unfortunately the trials were not successful as indicated from the analysis of NMR and HRMS:

a. Stirred phen-5,6-dione with Triethylenetetramine over night in 60 ° C after work up on reaction concluded not get desire product.

b. Condensation phen-5,6-dione with thiocarbohydrazide with and without of acetic acid after work up on reaction were also unsuccessful.

- c. Condensation phen-5,6-dione with Formamid in sulfinic acid in ethanol after work up on reaction concluded not get desire product.
- d. Stirred phen-5,6-dione with Diethylenetriamine over night in 60° C.
- e. Stirred phen-5,6-dione with Phenylethylamine hydrochloride in methanol for 24 hours.
- f. Condensation phen-5,6-dione with Phenylethylamine hydrochloride using toluene with the azeotropic removal of water using a Dean and Stark apparatus in order to drive the reaction to the product side but unfortunately had not any influence on outcome of the reaction.

Fortunately, reacting phen-5,6-dione with hydrazine sulfate get desired product of phen-5,6-diol characterised by various techniques ¹H NMR, ¹³C NMR, FTIR, UV and HRMS. In ¹H NMR the spectra of δ 10.30 (1H, br s) indicating OH spectrum and δ 4.09(1H, br) indicating OH spectrum. In addition the infrared bands were present at (3036 and 2894) cm⁻¹ indicating 2 (OH) spectra.

In addition no bands were present at 1630 cm⁻¹-1800 cm⁻¹ indicating the absence of a carbonyl group supporting strongly the compound has been prepared.

New approach was implemented by stirred (6*E*)-6-(hydroxyimino)-1,10-phenanthrolin-5(6*H*)-one (ST04) with *N,N*-diethylamine carbamyl chloride at room temperature in anhydrous DMF for 18 hours in presence of sodium hydride to prepare new compound characterised by various techniques ¹H NMR, ¹³C NMR, FTIR, UV and HRMS. In ¹H NMR the spectra of δ 3.31(4 H q *J*=7) indicating (CH₂) spectrum and δ 1.22 (6H t *J*=7) indicating (CH₃) spectrum and the ¹³C NMR spectrum consisted of seventeen peaks supporting assigned structure in addition The infrared bands were present at 1469 cm⁻¹ indicating (CH₂) spectrum and 1420 cm⁻¹ indicating (CH₃) spectrum supporting strongly the compound has been prepared.

However rather than trial new reactions, conditions were fulfilled aiming of getting the desired Product (6*E*)-6-(benzylimino)-1,10-phenanthrolin-5(6*H*)-one under different conditions such as using different solvents such as methanol, dichloromethane using phen-5,6-dione with benzyl amine with TiCl₄ as reagent stirred under nitrogen in ice and filtrate on celite and wash with dichloromethane and ether. Another trial repeated reaction under argon after work up on reaction and did not produce the desired product.

But fortunately another trail using 4-toluene sulfonic acid as weak acid in toluene changing the solvent and conditions using Dean and Stark had influence on the outcome of the reaction characterised by various techniques ^1H NMR, ^{13}C NMR, FTIR, UV and HRMS. In ^1H NMR the spectra of δ 3.88 (1H, s) indicating (CH₂) spectrum and in the infrared spectrum at 1404 cm^{-1} indicating (CH₂) spectrum and the ^{13}C NMR spectrum consisted of nineteen peaks supporting assigned structure supporting strongly the compound has been prepared.

2.5 References

- BODIGE, S. & MACDONNELL, F. M. 1997. Synthesis of free and ruthenium coordinated 5, 6-diamino-1, 10-phenanthroline. *Tetrahedron letters*, 38, 8159-8160.
- CHITRA, L., KUMAR, C. R., BASHA, H. M., PONNE, S. & BOOPATHY, R. 2013. Interaction of metal chelators with different molecular forms of acetylcholinesterase and its significance in Alzheimer's disease treatment. *Proteins: Structure, Function, and Bioinformatics*, 81, 1179-1191.
- DEEGAN, C., COYLE, B., MCCANN, M., DEVEREUX, M. & EGAN, D. A. 2006. In vitro anti-tumour effect of phen-5,6-dione (phendione), [Cu(phendione)₃](ClO₄)₂·4H₂O and [Ag(phendione)₂]ClO₄ using human epithelial cell lines. *Chemico-Biological Interactions*, 164, 115-125.
- Gillard, R.D. & Hill, R.E.E. 1974, 'Optically active co-ordination compounds. Part XXXIV. Modification of reaction pathways in phen and its derivatives by metal ions', *Journal of the Chemical Society, Dalton Transactions*, no. 11, pp. 1217-36.
- Hiort, C., Lincoln, P. & Norden, B. 1993, 'DNA binding of .DELTA.- and .LAMBDA.-[Ru(phen)2DPPZ]2+', *Journal of the American Chemical Society*, vol. 115, no. 9, pp. 3448-54.
- INGLETT, G. E. & SMITH, G. F. 1950. The Formation of a New Nitrogen Heterocyclic Ring System by the Loss of Carbon Monoxide from 1, 10-Phenanthroline-5, 6-quinone. *Journal of the American Chemical Society*, 72, 842-844.
- Kleineweischede, A. & Mattay, J. 2006, 'Synthesis of amino- and bis (bromomethyl)-substituted bi- and tetradentate N-Heteroaromatic ligands: building blocks for pyrazino-functionalized fullerene dyads', *European journal of organic chemistry*, vol. 2006, no. 4, pp. 947-57.
- Murali, S., Sastri, C. & Maiya, B.G. 2002, 'New mixed ligand complexes of ruthenium (II) that incorporate a modified phenanthroline ligand: Synthesis, spectral characterization and DNA binding', *Journal of Chemical Sciences*, vol. 114, no. 4, pp. 403-15.
- MOODY, C. J., REES, C. W. & THOMAS, R. 1992. The synthesis of ascididemin. *Tetrahedron*, 48, 3589-3602.
- Travis, W., Knapp, C.E., Savory, C.N., Ganose, A.M., Kafourou, P., Song, X., Sharif, Z., Cockcroft, J.K., Scanlon, D.O. & Bronstein, H. 2016, 'Hybrid Organic-Inorganic Coordination Complexes as Tunable Optical Response Materials', *Inorganic chemistry*, vol. 55, no. 7, pp. 3393-400.
- Wu, J.-Z., Li, H., Zhang, J.-G. & Xu, J.-H. 2002, 'Synthesis and DNA binding behavior of a dipyrrocatecholate bridged dicopper (II) complex', *Inorganic Chemistry Communications*, vol. 5, no. 1, pp. 71-5.
- Xu, S., Wang, J., Zhao, F., Xia, H. & Wang, Y. 2015, 'Photophysical properties of copper (I) complexes containing pyrazine-fused phenanthroline ligands: a joint experimental and theoretical investigation', *Journal of molecular modeling*, vol. 21, no. 12, p. 313.

- Yamada, M., Tanaka, Y., Yoshimoto, Y., Kuroda, S. & Shimao, I. 1992, 'Synthesis and Properties of Diamino-Substituted Dipyrdo (3, 2-a: 2', 3'-c) phenazine', *Bulletin of the Chemical Society of Japan*, vol. 65, no. 4, pp. 1006-11.
- YING, P., TIAN, X., ZENG, P., LU, J. & CHEN, H. 2014. Synthesis, DNA-binding, Photocleavage and in vitro Cytotoxicity of Novel Imidazole [4, 5-f][1, 10] phenanthroline-based Oxovanadium Complexes. *Med chem*, 4, 549-557.

Chapter 3 Choline esterase inhibitors as anti-AD drugs (ChEI)

3.1 Introduction to chemistry and mechanism of AD

The well-established hypothesis that AD patients have usually irregular level of acetylcholine (ACh) compared to normal healthy people. According to cholinergic hypothesis, the AD is accompanied by drop of ACh level. The decrease in ACh level has being related to its rapid hydrolysis to acetic acid and Choline by cholinesterase (ChEs) enzymes such as acetylcholinesterase (AChE) and butyrylcholinesterase (BuChE) (Luo et al. 2011).

ACh was synthesised in 1867 and detected in the adrenal gland of human tissue in 1906 as a neuro transmitter (Hunt & De M. Taveau 1906). The physiological role of ACh was known by Dale in 1914, he suggested the hypothesis of enzymatic hydrolysis of ACh in nerves (Marminon et al. 2003). A chemical step in transmission of electric signals between nerves and muscles at neuromuscular junction was shown by Loewi in 1921 and Navratil in 1926 (Kelly et al. 1997).

ACh formation starts with reaction of choline with acetate in neurons. Acetate is activated by enzymes and co-enzyme A, thus it converts to Acetyl Co-enzyme A. The Acetyl Co-Enzyme A reacts with choline; the reaction is catalysed by enzymes of choline transferase. ACh is occupied into synaptic vesicles by vascular transporter.

ACh must be quickly removed from the synapse if repolarisation occurs. The removal of ACh takes place by hydrolysis of ACh to choline and acetic acid. The reaction is catalysed by acetylcholine esterase (Ganong & Ganong 1995).

AChE is widely spreadable enzyme located in CNS and muscles of several living organisms. AChE plays significant role in nerve single transmission. Its inhibition chiefs to death of an organism like human beings (Massoulié et al. 1993).

AChE participates in cholinergic transmission by hydrolysing ACh and cholinergic neurons in the nerves and blood cells. AChE breaks down the plasma's ACh (Fujii et al. 1997). Accordingly it is suggested that AChE inhibition is prioritised over the simulation of ACh receptors (Fukuto 1990).

Several types of AChE inhibitors are known and used as insecticides and chemical warfare agents. In both two cases, the inhibitors act as irreversible or “suicide” inhibitors. The active site of AChE, at the bottom of the 20Å gorge, consists of a so-called catalytic triad (Figure 9). The nucleophilicity of the serine is enhanced by H-bonding to the histidine, which is itself H-bonded to the glutamate, thus the serine OH is effectively electronically connected to the glutamate via the imidazole ring of histidine.

AChE inhibitors have broad range of structural types; however, the most potent inhibitors are those which block the serine OH by forming a phosphate ester (e.g. sarin) (Figure 9 B) or a carbamate derivative (Figure 9 C) or the active site serine OH. The phosphorylated enzyme is completely resistant to hydrolysis while the carbamoylated enzyme is hydrolysable but at very slow rate that kinetically it appears to be irreversible.

Other group of AChE inhibitors are not bonded to the active site of the catalytic triad, but are bonded to the so-called peripheral anionic site (PAS). These inhibitors tend to be related to di-, tri- and tetra-ammonium azaphenanthracenes, e.g. propidium. As might be expected, π - π interactions, represent a key feature of binding these polycyclic aromatics to the PAS region particularly involving the tryptophan ring of Trp279. Figure 10 reveals the interaction of PAS and the A β binding site of coloured aqua. Figure shows also how PAS surrounds the opening of the active site triad, indicating the distance between the PAS and the enzyme’s exterior surface, in the presence of adhesion tendency between PAS and AChE.

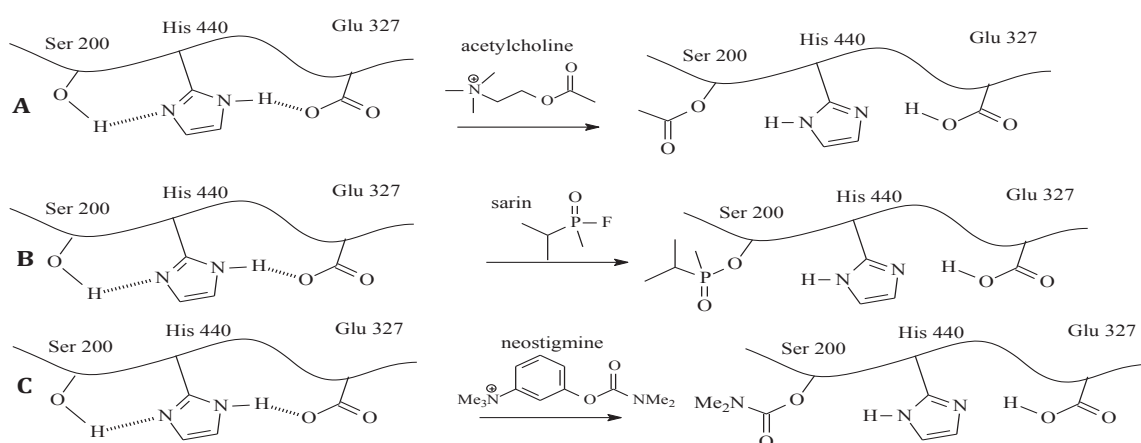


Figure 9: Catalytic triad of AChE formed by serine, histidine and glutamate residues. Note the basicity of the serine OH is increased by the glutamate ion, via the histidine. The product shown as arising from the reaction with acetylcholine is actually the intermediate. A. Hydrolysis of the acetylated serine recycles the enzyme. B. Phosphate ester formed by sarin. C. Carbamoylated serine arising from exposure to neostigmine.

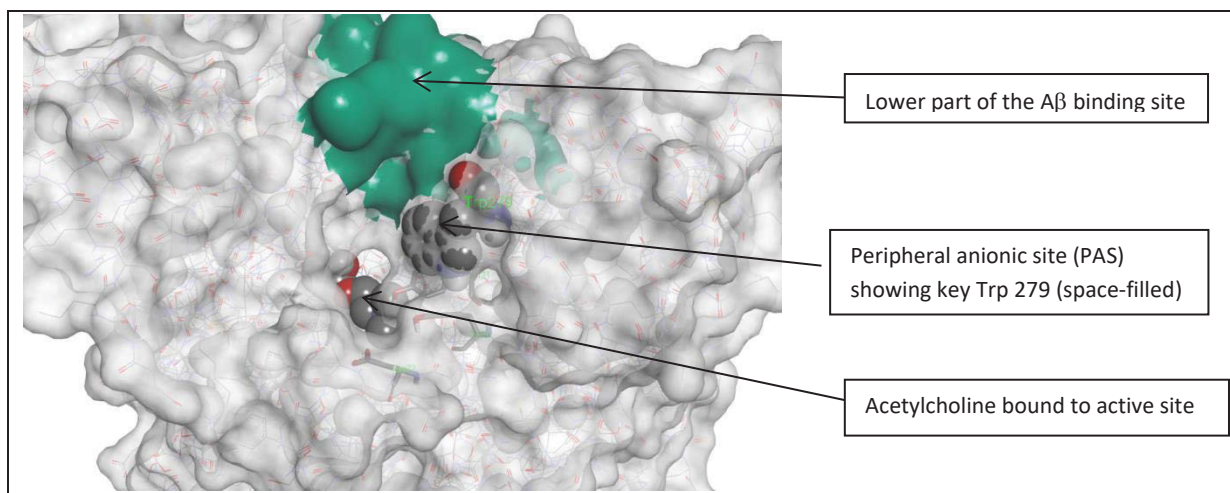


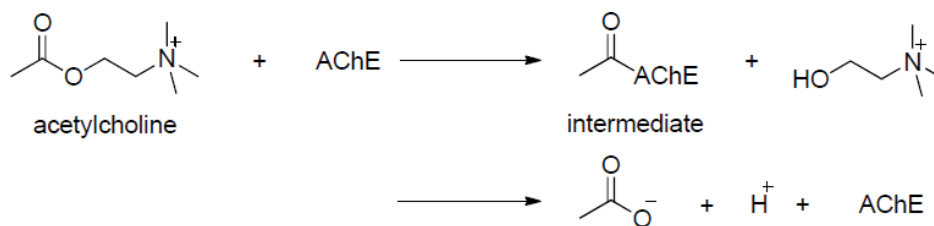
Figure 10: Torpedo AChE showing spatial relationship between PAS, active site and postulated A β binding site.

The AChE of (20 °A) gorge consists of two binding sites: a catalytic active site (CAS) at the bottom of the gorge and a peripheral anionic site (PAS) near the entry of the gorge. (Chen et al. 2012; Sussman & Harel 1991), accordingly the inhibitors can inhibit the AChE that bind to either sites.

Recent researches showed that in addition to the hydrolysis of ACh as main symptoms of AD, the PAS has strong effect to prevent A β aggregation (Bolognesi, Andrisano, Bartolini, Banzi, et al. 2005; Fernández-Bachiller et al. 2012). On the other hand it has also been reported that BuChE becomes main modulator in adjusting the ACh level in AD (Luo et al. 2011; Mesulam, Guillozet, Shaw, Levey, et al. 2002).

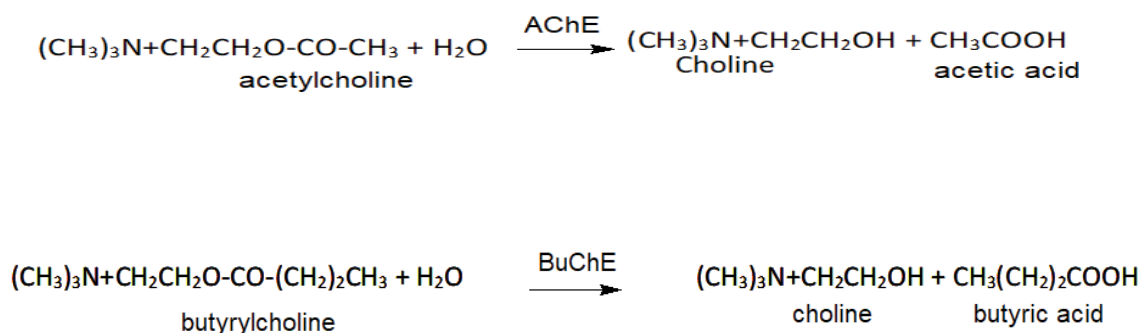
The AChE and BuChE enzymes control the level and duration of ACh's action. These enzymes Catalyses the hydrolysis of ACh and BuCh to inactive choline and acetic acid or butyric acid respectively as shown in the reaction schemes 5 and 6. The inhibition of AChE and BuChE extends the duration of ACh's action which is vital for the treatment of AD.

AChE also contains a peripheral anionic sites of PAS that has been identified as being responsible for enhancing A β fibrillisation.



Scheme 8: Hydrolysis of acetylcholine (ACh) catalysed by AChE Acetylcholinesterase, online accessed <http://en.wikipedia.org/wiki/acetylcholinesterase>

AChE enzyme accelerate the hydrolyses of the acetyl choline esters, whereas BuChE enzyme hydrolyses butyrylcholine esters as shown in Scheme 9.



Scheme 9: Hydrolyses of AChE and BuChE

3.2 Acetylcholinesterase (AChE) and butyrylcholinesterase (BuChE) inhibitors

Based on the mechanism and chemistry of AD explained in 3.1, several types of ChEI inhibitors have being evaluated and extensively studied and as following:

Dual binding site inhibitors that block both the active site and the peripheral anionic site are being sought as they potentially could alleviate cognitive symptoms associated with acetylcholine deficiency while simultaneously reducing A β fibrillisation, which is believed to be central to the disease mechanism. One of the important classes of these inhibitors involves incorporating with metals that exhibits lower cytotoxicity (Perez & Franz 2010).

A treatment to the Alzheimer's disease patients consists inhibition of the (AChE) and (BuChE), which are responsible for the acetylcholine control level in the synapses.

(AChE) and (BuChE) inhibitors have been used as drugs for the symptomatic treatment of Alzheimer's disease patients.

One of the interesting classes of inhibitors are those based on phen and its derivatives that can interact with PAS and may retard formation of "AChE-A β peptide" complex. Phen and its derivatives represent important class of inhibitors with dual inhibiting functionality to AChE plus their ability to hinder the interaction of A β with AChE via blocking the active centres of PAS. Hence, phen and its derivatives represent the backbone for developing new classes of single chemical composition drugs for AD with dual inhibiting functionality as inhibitor for AChE and retards A β aggregation (Chitra et al., 2013).

The current research project is based on the synthesis, characterisation and biological evaluation of this series of new phen-5,6-dione derivatives whose chemical structures are listed in Table 2.

3.2.1: Method and techniques for evaluation of the enzyme activity inhibition

Several methods and techniques have been adopted for the evaluation of the activity inhibition of the cholinesterase enzymes mainly AChE and BuChE.

One of the most widely and commonly used method is Ellman's colorimetric method in 96-welled microplates which has been tested by several researchers. The method was proved to be excellent for the evaluation of the enzyme activity inhibition (Chitra et al. 2013; Gutiérrez et al. 2013; Ingkaninan et al. 2003; Rahim et al. 2015; Rajasree, Singh & Sankar 2012; Sinha & Shrivastava 2013). Ellman method favourite features are simplicity, accuracy, continuous increase in colour density as a function of incubation time, and relatively low cost. It is simply flexible for automated analysers or plate readers for the rapid processing of large number of samples (Miao, He & Zhu 2010). There are different published methods for evaluation the inhibition activity of AChE by novel compounds.

The Ellman method was introduced by (Ellman et al. 1961b) which is based on photometric analysis using spectrophotometer to measure the absorbance of light at 405 nm as yellow coloured solutions. The yellow colour characteristic of aromatic nitro compounds is due to formation of 2-nitro-5-sulfanyl-benzoic acid (TNB) (Dyachenko & Rusanov 2003).

The coloured reagent TNB is the reaction product of the colour reagent 5,5'-dithiobis-(2-nitrobenzoic acid) (DTNB) with thiocholine; the product of the enzymatic hydrolysis of the acetylthiocholine (ATCI) substrate by AChE (Bizyaev, Gatilov & Tkachev 2015) (Shreevidhyaa Suresh et al. 2014).

The intensity of the measured absorbance is directly related to the progress of the enzymatic reaction. The ATCI is used as a substitute for its analogue acetylcholine which gives the same related enzymatic kinetic results. In the presence of AChE inhibitor, there will be a significant reduction in the formation of TNB and hence a lower absorbance at 405 nm for the assayed solution. From the obtained inhibition data at different concentrations, the concentration-response curve can be plotted and used to determine the inhibitors IC_{50} . This method was implemented by several researchers for the determination of the IC_{50} for large number of the suggested active ingredients for AD. The assay procedure implemented for Galantamine was used in the present study as a control and for comparison adopting the same procedure (Ingkaninan et al. 2003).

3.2.2 Review of Ellman Methods

Review of the literature listed two modified methods to Ellman's original paper (Ellman et al. 1961b) using the same experimental procedure for implementing the Ellman assay. The modification of the procedure was justified by the authors because each enzymatic reaction has various kinetic parameters and as a result, the reported IC_{50} values cannot be contrasted across different methods. Instead, K_i (the equilibrium constant for the binding of the substrate with the active site) should be applied in order to represent the actual inhibition potency. If the kinetic parameters across the experiments are preserved the same, then the IC_{50} values should be similar.

3.2.3 Experimental part

Two methods were implemented in this biological study for evaluation the inhibition efficiency of the new series of phen-5,6-dionederivatives prepared in this study; a. (Ingkaninan et al. 2003) method, using Galantamine as a control to test the comparability of the obtained IC_{50} values for AChE inhibition and b. (Xie et al. 2013) method using Tacrine as a control to test the comparability of IC_{50} values for BuChE.

The assay using Galantamine as a control, gave average IC_{50} obtained value was 1.9715 μ M. The method was implemented for its validity by commitment kinetics experiments, where the assay was performed with different concentrations of the substrate [S], in the presence and other set of experiments in the absence of inhibitor. The Michael's constant (K_m) and maximum reaction rate (V_{max}) were determined for the consumption of the [S] by AChE using a Lineweaver-Burk Plot, where the inverse of the reaction rate ($1/V$) was plotted versus ($1/[S]$). The plot should also validate the type of inhibition. In the case of a reversible competitive inhibitor such as Galantamine, the extrapolated lines of the reaction in the presence and absence of inhibitor should both cross the y-axis. This point is $1/V_{max}$, as shown in the Lineweaver-Burk Plot Figures (12-24).

Several millimolar mM concentrations of acetylthiocholine iodide and s-butyrylthiocholine iodide solutions were prepared: 0.0156, 0.0312, 0.0625, 0.125, 0.25 mM for the assay run in the presence of different inhibitor concentrations (2.5, 5, 10, 20, 30) nM. Other series of experiments were carried out without inhibitor for blank evaluation. At each concentration, the velocity (V) was determined from the gradient of average of the triplicate biological absorbance triplicate plot against time. The calculated reciprocals of velocity $1/V$ was plotted versus substrate concentration [S] to give the Lineweaver-Burk Plots, typical plots are shown in Figures (11-23). As stated before, $1/V_{max}$ should have the same value with inhibitor and without the inhibitor.

3.3 Biological Assays via plate readers

For the Ellman assay, the absorbance was read with a BIO-TEK Synergy HT plate reader Falcon Polystyrene 96-well Flat-bottom plates was used. For the MTS assay, the absorbance data were obtained with a Tecan Infinite M1000 PRO plate reader using Falcon Polystyrene 96-well Flat-bottom plates.

3.3.1 Ellman Assay Procedure for inhibition evaluation of AChE

The assay used to determine the IC_{50} values of AChE inhibition was adjusted version of the Ellman method, as described by (Ingkaninan et al. 2003). Tris-buffer was prepared using Tris-HCl and Tris-Base to give pH 8 at 37 °C. The enzyme stock solution was prepared as 0.28 U/mL from electric eel AChE (eeAChE) using the Tris-buffer with 0.1% bovine serum

albumin. The colour reagent was prepared as 3 mM stock solution of DTNB in Tris-buffer containing (0.1M) Na Cl and (0.02 M) $MgCl_2 \cdot 6H_2O$.

The substrate was prepared by making a stock solution of 15 mM ATCI in Millipore water. The inhibitor samples were dissolved in Tris-buffer containing 1% DMSO at 1mg/mL and diluted to different concentrations:

(0.97, 1.953, 3.906, 7.812, 15.62, 31.25, 62.5, 125, 250) μ M.

Falcon Polystyrene 96-well, flat-bottom plates were used for each concentration of inhibitor. Each well contained, 125 μ L of colour reagent solution (DTNB), 25 μ L of acetylthiocholine iodide substrate (ATCI) solution, 50 μ L of buffer, 25 μ L of inhibitor solution and 25 μ L of enzyme solution. The BIO-TEK Synergy HT plate reader was used to read the absorbance for each well at 405 nm. The absorbance at each concentration was measured in triplicate in addition to the assay while using the buffer without any inhibitor for the blank assay. Galantamine hydrobromide was used as a positive control.

3.3.2 Ellman Assay Procedure for BuChE

The assay used to determine the IC_{50} values for BuChE inhibition was adjusted version of the Ellman method, as described by (Xie et al. 2013).

Tris-buffer solution was prepared using Tris-HCl and Tris-Base to give pH 8 at 37 °C. The 0.12 U/mL BuChE (from equine serum) enzyme stock solution was prepared using Tris-buffer with 0.1% bovine serum albumin. The colour reagent was prepared at concentration of 1.5 mM stock solution of DTNB in Tris-buffer containing (0.1 M) NaCl and (0.02 M). $MgCl_2 \cdot 6H_2O$ The substrate was prepared as a stock solution of 15 mM s-butrylthiocholine iodide (BTCl) in Millipore water. The inhibitor samples were dissolved in Tris-buffer at 1mg/mL solution containing 1% DMSO diluted to several different concentrations :(0.0001, 0.001, 0.01, 1, 5, 10, 50, 100, 250) μ M.

Falcon Polystyrene 96-well, flat-bottom plates were used for each concentration of inhibitor. Each well contained 160 μ L of colour reagent solution, with concentration of 1.5 mM(DTNB) 50 μ L of enzyme solution, 10 μ L of inhibitor solution, incubated at 37 °C for 6 min before the reaction was started by the addition of 30 μ L of substrate s-butrythiocholine iodide(BTCl) solution of concentration 15 mM. BIO-TEK Synergy HT plate reader was used to read the absorbance in each well at 405 nm at 37 °C. The absorbance at each concentration was measured in triplicate in addition to the assay using the buffer without any inhibitor as blank assay. Tacrine was used as a positive control.

3.3.3: Biological Tests according to Ellman Bioassay modified by Ingkaninan et al.

(Chitra et al. 2013; Gutiérrez et al. 2013; Ingkaninan et al. 2003; Rahim et al. 2015; Rajasree, Singh & Sankar 2012; Sinha & Shrivastava 2013)

To evaluate the potential application of the target compounds synthesised phen-5,6-dione derivatives for the treatment of AD. The level of activity for inhibiting the AChE and BuChE implementing Ellman's method.(Ellman et al. 1961b) using Galtamine and Tacrine as reference standards .The obtained activity data are listed in (Table 3.1).

The results obtained from the eeAChE and BuChE (from equine serum) showed higher activities than the values obtained for the control as shown in (Table3.1) to obtained IC₅₀ values for the investigated samples ST01 to ST24 respectively.

3.4: Ellman bioassay; biological inhibition results and discussion

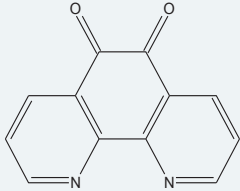
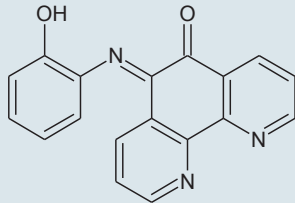
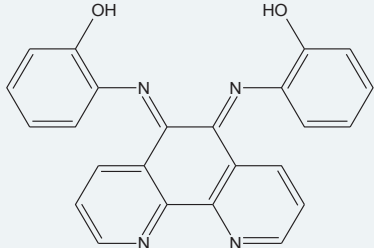
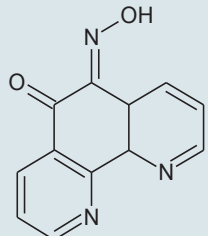
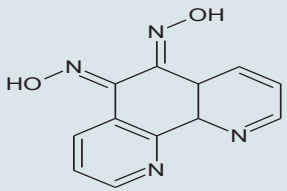
The evaluation results IC₅₀ for the activity inhibition of the new phen-5,6-dione derivatives for AChE and BuChE measured in section 3.3 are listed in Table 2.

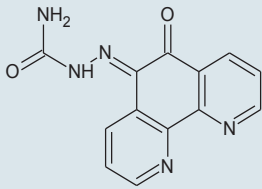
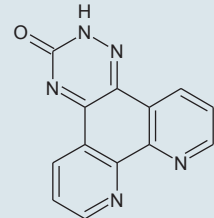
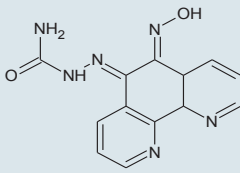
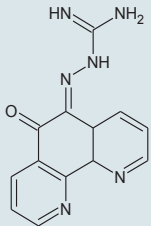
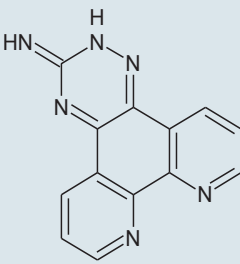
Also BuChE evaluation was also included in this biological study because it also plays a significant role in the metabolism of ACh in the central nervous system (CNS). BuChE is richer in the peripheral system (Zheng, Youdim & Fridkin 2009),on the other hand BuChE specific inhibition may show efficacy without remarkable side effects (Greig et al. 2005). (BuChE) inhibition in AD has important role in both medicinal chemistry and from the clinical points of view (Giacobini et al. 2002; Greig et al. 2001) .The attention to BuChE role in AD drug design has being rising due to its possible role in Alzheimer disease via introducing anticholinesterase treatments for this disease (Darvesh, Hopkins & Geula 2003).

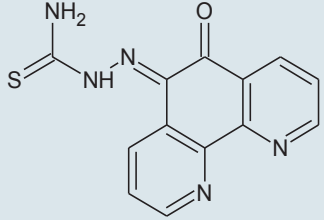
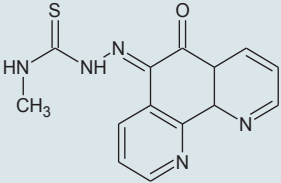
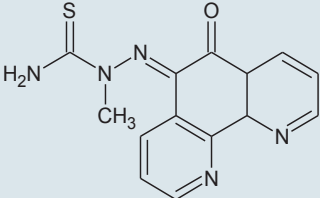
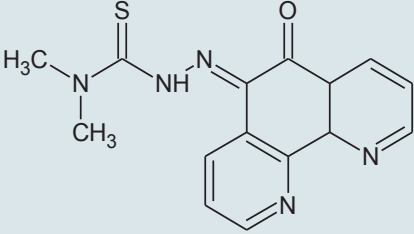
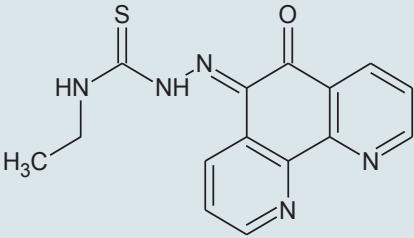
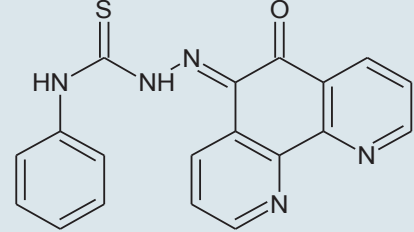
Taking into consideration that BuChE specific inhibition is unlikely to be related to the adverse events and can show efficacy without extraordinary side effects. Recently it was found that BuChE also regulates acetylcholine levels, and concurrent inhibition of both ACh and BuCh leading to additional benefits in Alzheimer's disease treatment.

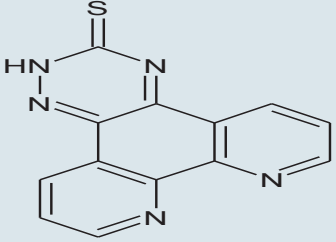
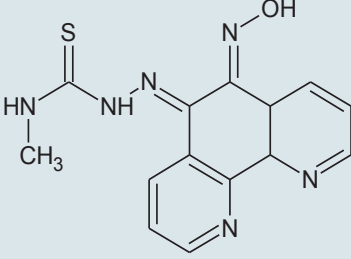
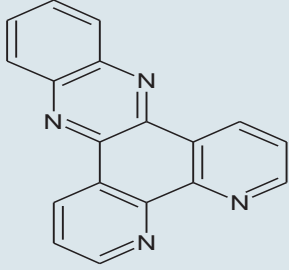
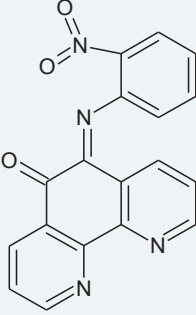
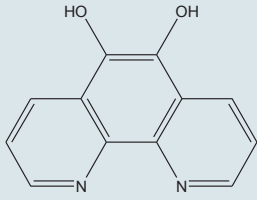
Among all our compounds, we found ST08 has the best activity in inhibition of AChE, and ST21 has the best activity in inhibition of BuChE because they have competitive small IC₅₀ values. ST01 and ST22 tend to have no activity on AChE (1683 uM and 717.607 uM) sequentially. ST01, ST04, ST05, ST12, ST14, ST16, ST17, ST18, ST22 and ST23 have no activity on BuChE due to their high value of IC₅₀.

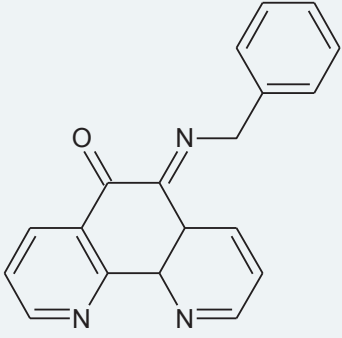
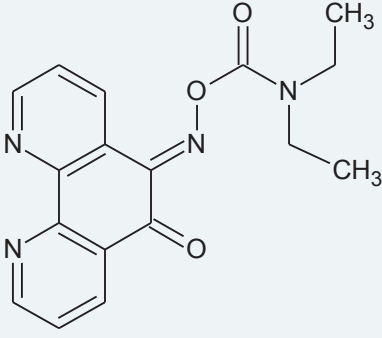
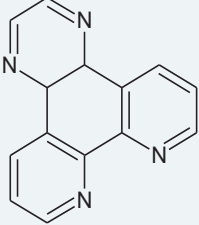
Table 2: The IC₅₀ for the 1,10-phenanthroline-5,6-dione derivatives in uM.

Compounds	IC ₅₀ uM AChE	IC ₅₀ uM BuChE
 (ST01)	1683 ± 14.79	1014 ± 12.25
 (ST02)	0.296 ± 0.007	1.222 ± 0.09
 (ST03)	0.0834 ± 0.061	5.631 ± 0.15
 (ST04)	0.845 ± 0.015	221.855 ± 3.6
 (ST05)	0.2608 ± 0.01	183.426 ± 5.0

 <p>(ST06)</p>	0.0601 ± 0.045	0.277 ± 0.023
 <p>(ST07)</p>	0.5005 ± 0.009	0.0384 ± 0.005
 <p>(ST08)</p>	0.0108 ± 0.003	0.484 ± 0.015
 <p>(ST09)</p>	0.0575 ± 0.067	2.444 ± 0.08
 <p>(ST10)</p>	0.245 ± 0.04	0.174 ± 0.026

 <p>(ST11)</p>	0.305 ± 0.07	34.222 ± 2.8
 <p>(ST12)</p>	0.2107 ± 0.005	317.951 ± 6.2
 <p>(ST13)</p>	0.256 ± 0.008	92.999 ± 1.13
 <p>(ST14)</p>	1.0418 ± 0.14	792.867 ± 8.0
 <p>(ST15)</p>	0.0528 ± 0.032	95.297 ± 2.7
 <p>(ST16)</p>	0.120 ± 0.039	306.379 ± 2.92

 <p>(ST17)</p>	0.154 ± 0.061	193.9 ± 2.25
 <p>(ST18)</p>	0.0959 ± 0.043	175.0 ± 3.1
 <p>(ST19)</p>	0.4248 ± 0.018	6.0 ± 0.16
 <p>(ST20)</p>	0.0486 ± 0.054	0.009125 ± 0.002
 <p>(ST21)</p>	0.845 ± 0.066	0.000291 ± 0.001

 (ST22)	717.607± 9.63	1043.264 ±13.1
 (ST23)	91.145 ± 0.87	168.161± 0.91
 (ST24)	0.0436±0.035	0.923 ± 0.074
Tacrine (control)	0.548 ± 0.012	0.10708 ± 0.016
Galtamine (control)	1.9715 ± 0.1	13.1 ±0.3

3.5: Kinetic analysis of AChE inhibition

In order to know the mechanism of action of these derivatives on AChE, the compounds (ST03, ST06, ST07, ST09, ST20, ST21 and ST24) were selected for kinetic measurements because it showed the highest inhibitory activity against AChE. The graphical presentation of the steady-state inhibition data for AChE is shown in Figs 11-17. The compounds (ST06, ST07, ST09, ST20, ST21 and ST24) were selected for kinetic measurements inhibition studies for BuChE due to their highest inhibitory activity against BuChE as shown in Figs 18-23.

The results indicated that slopes and intercepts increased with increasing the concentration of the inhibitor. The trend of the obtained results is in line with results found by other researchers (Pan et al. 2014).

To obtain of the mechanism of act inhibitor mutual plots of $1/\text{velocity}$ versus $1/[\text{substrate}]$ were made at different concentrations of the substrate acetylthiocholine iodide (0.0156, 0.0312, 0.0625, 0.125,0.25) mM and butyrylthiocholine iodide (0.0156, 0.0312, 0.0625, 0.125,0.25) mM .Using Ellman's method different concentrations of inhibitor were selected in this study (2.5, 5, 10, 20, 30) nM. The plots were assessed by a weighted least-squares analysis that assumed the variance of velocity (v) to be a constant percentage of v for the entire data set and we estimated that the inhibition constants K_i values was determined as the intercept on the negative x-axis (Xie et al. 2013).

Compounds ST03, ST06, ST07, ST09, ST20, ST21 and ST24 had better inhibitory activities with IC_{50} values of 0.0834 μM , 0.0601 μM , 0.5005 μM , 0.0575 μM , 0.0486 μM , 0.845 μM and 0.0436 μM respectively than the reference compound Galtamine (IC_{50} : 1.9715 μM) for AChE. and ST06, ST07, ST09, ST20, ST21 and ST24 had better inhibitory activity with IC_{50} values of 0.0384 μM , 0.009125 μM , 0.000291 μM respectively based on the reference compound Tacrine (IC_{50} : 0.10708 μM). To explore the mechanism, the kinetics of inhibition in the presence of the most active compounds was examined, the obtained data are shown in Table 3. As the concentrations of active inhibitors increased, K_m values gradually increased, but V_{max} values did not change, thereby indicating that the inhibitors act as competitive inhibitors for AChE as shown in (Figure 11,12,13,14, 15,16 and 17) and inhibitors that act as competitive inhibitors for BuChE are shown in (figures18,19, 20, 21,22 and 23).

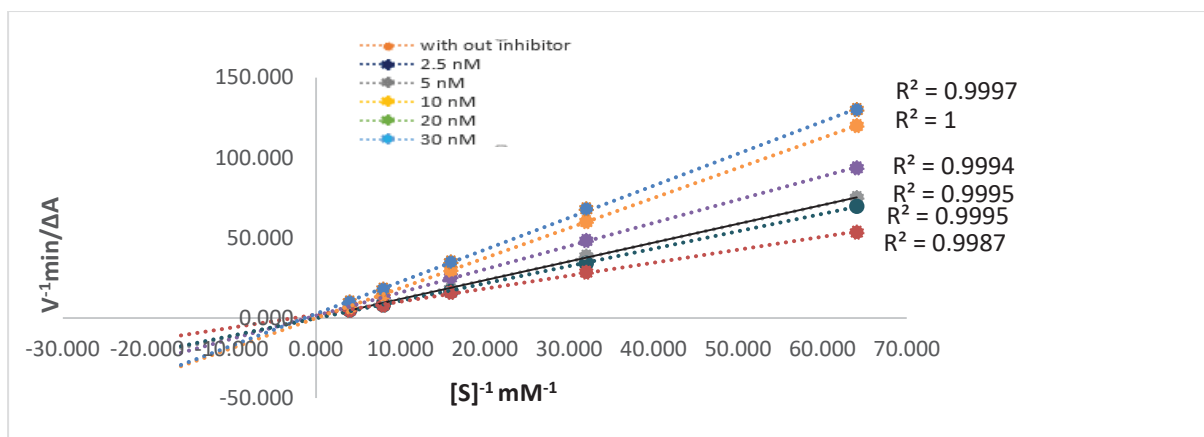


Figure 11: Lineweaver Burk plot for inhibition of compound ST03

Data were obtained as mean values of $1/V$, the inverse of the absorbance increase at a wavelength of 405 nm per min of five independent tests with different concentrations of ATCI as a substrate. The concentration of compounds ST03, ST06, ST07, ST09, ST20, ST21 and ST24 from top to bottom is (30, 20, 10, 5 and 2.5) nM, respectively for AChE.

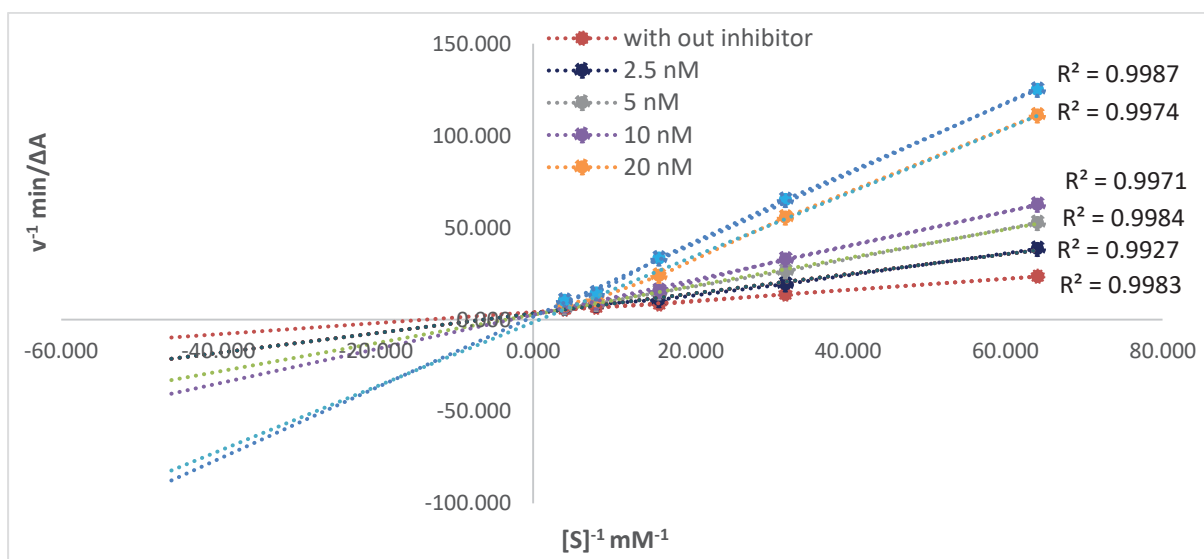


Figure 12: Lineweaver Burk plot for inhibition of compound ST06

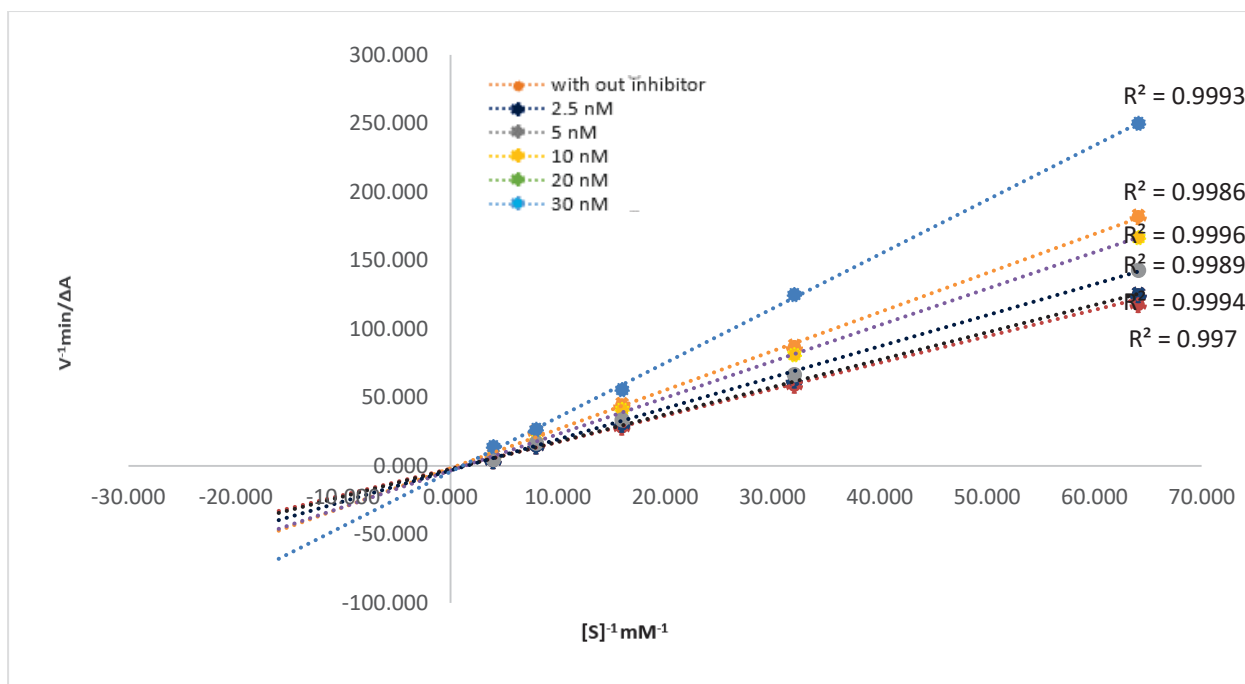


Figure 13: Lineweaver Burk plot for inhibition of compound ST07

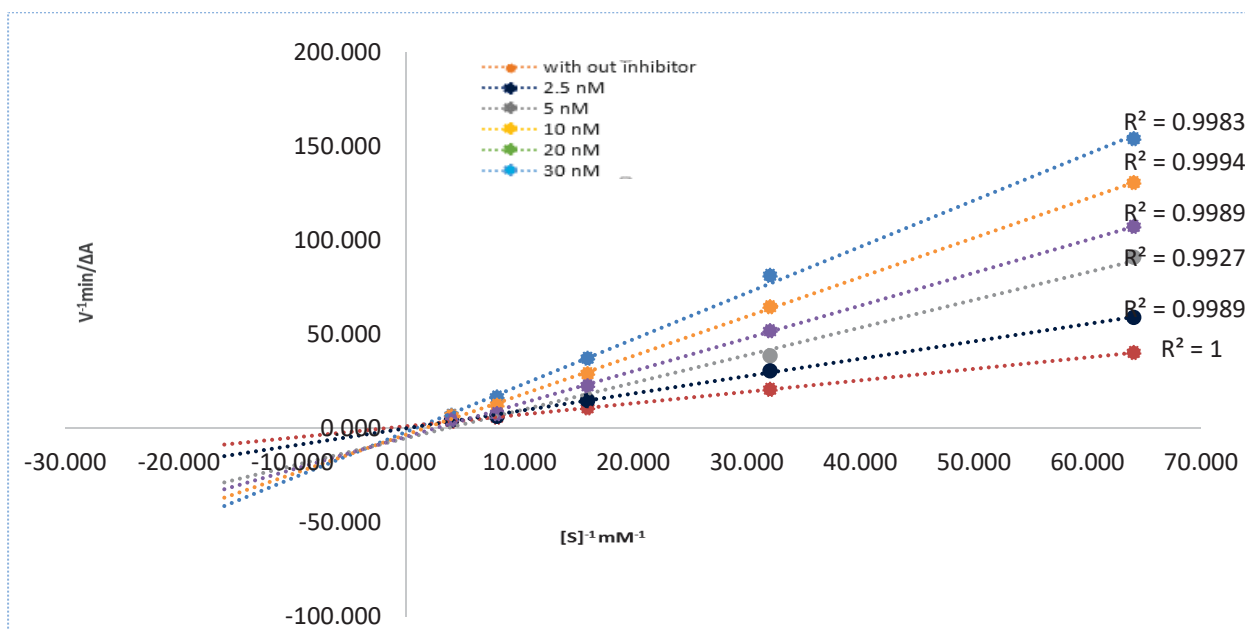


Figure 14: Lineweaver Burk plot for inhibition of compound ST09

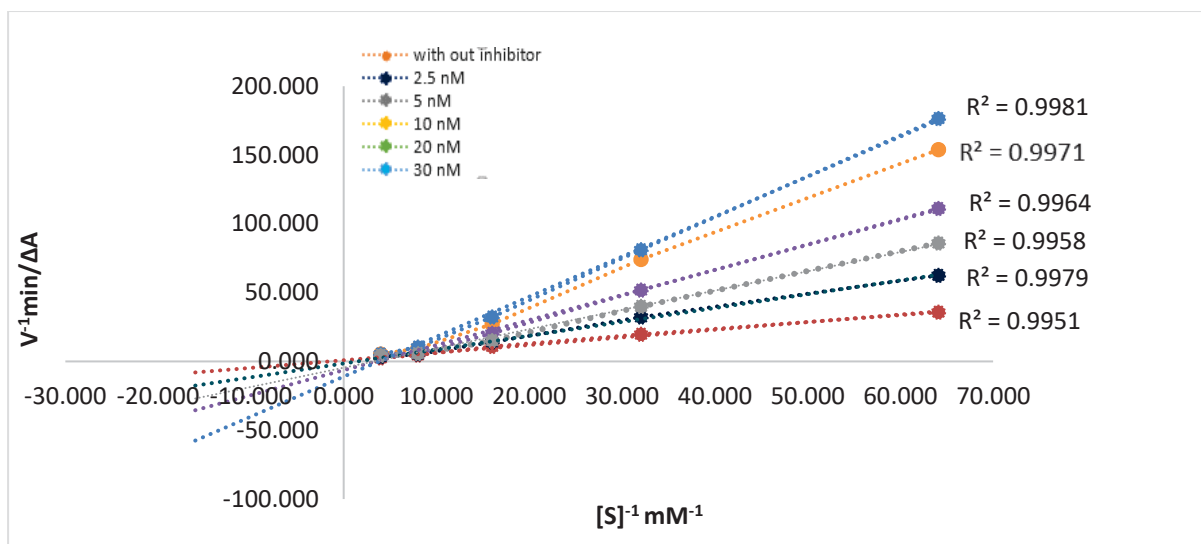


Figure 15: Lineweaver Burk plot for inhibition of compound ST20

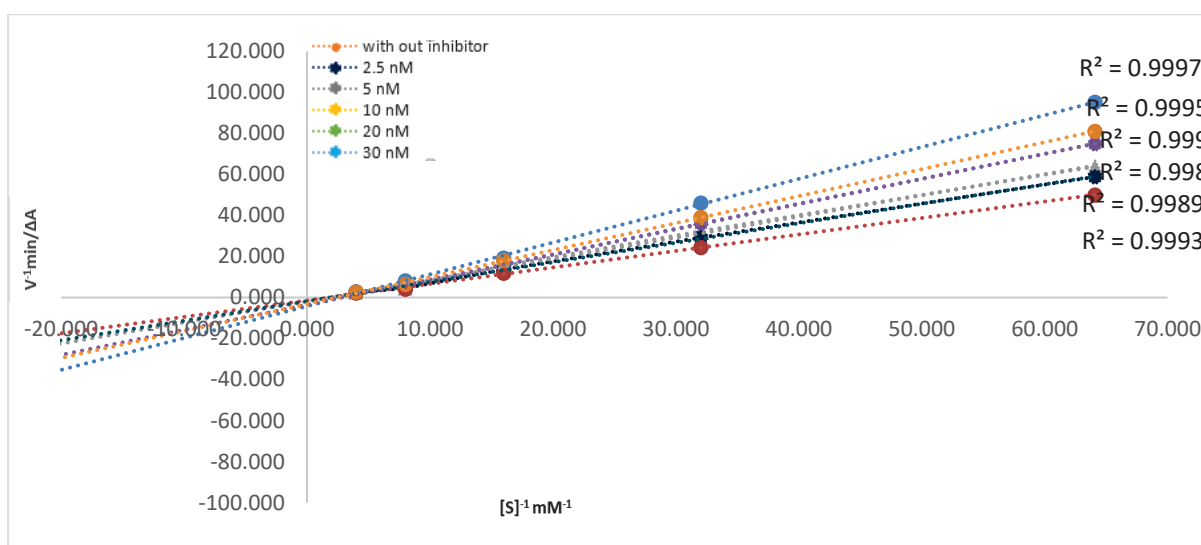


Figure 16: Lineweaver Burk plot for inhibition of compound ST21

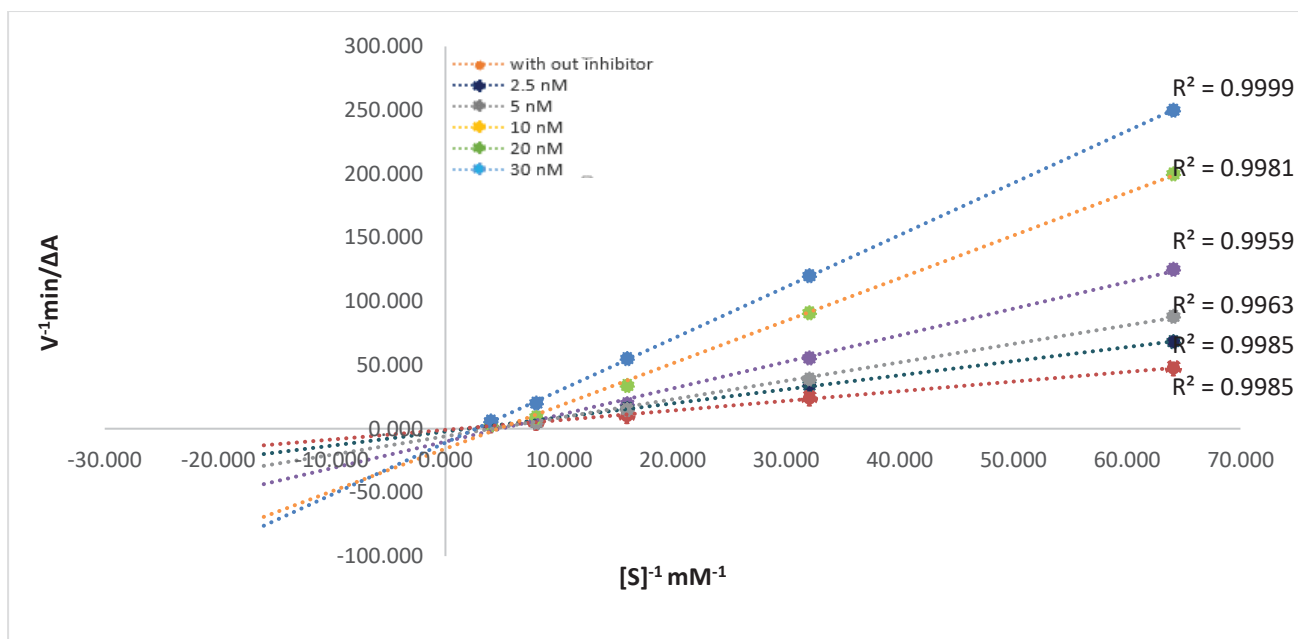


Figure 17: Lineweaver Burk plot for inhibition of compound ST24

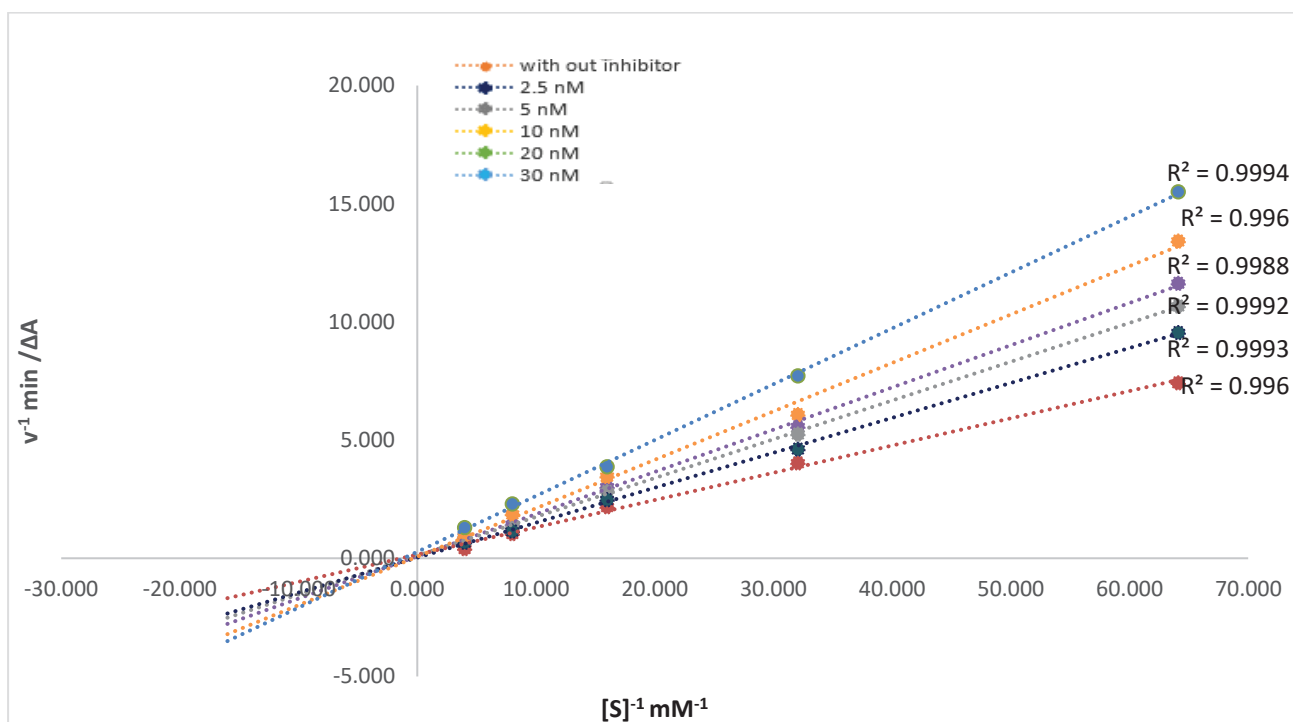


Figure 18: Lineweaver Burk plot for inhibition of compound ST06

Data were obtained as mean values of $1/V$, the inverse of the absorbance increase at a wavelength of 405nm per min of five independent tests with different concentrations of BTCI as a substrate. The concentration of compounds ST06, ST07, ST09, ST20, ST21 and ST24 from top to bottom is (30, 20, 10, 5 and 2.5) nM respectively for BuChE.

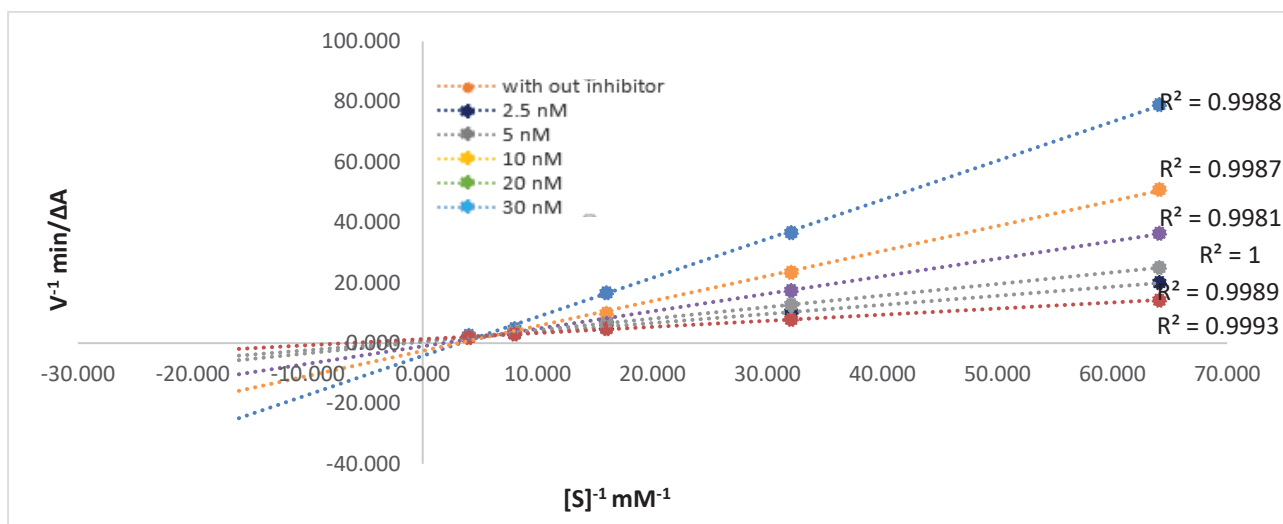


Figure 19: Lineweaver Burk plot for inhibition of compound ST07

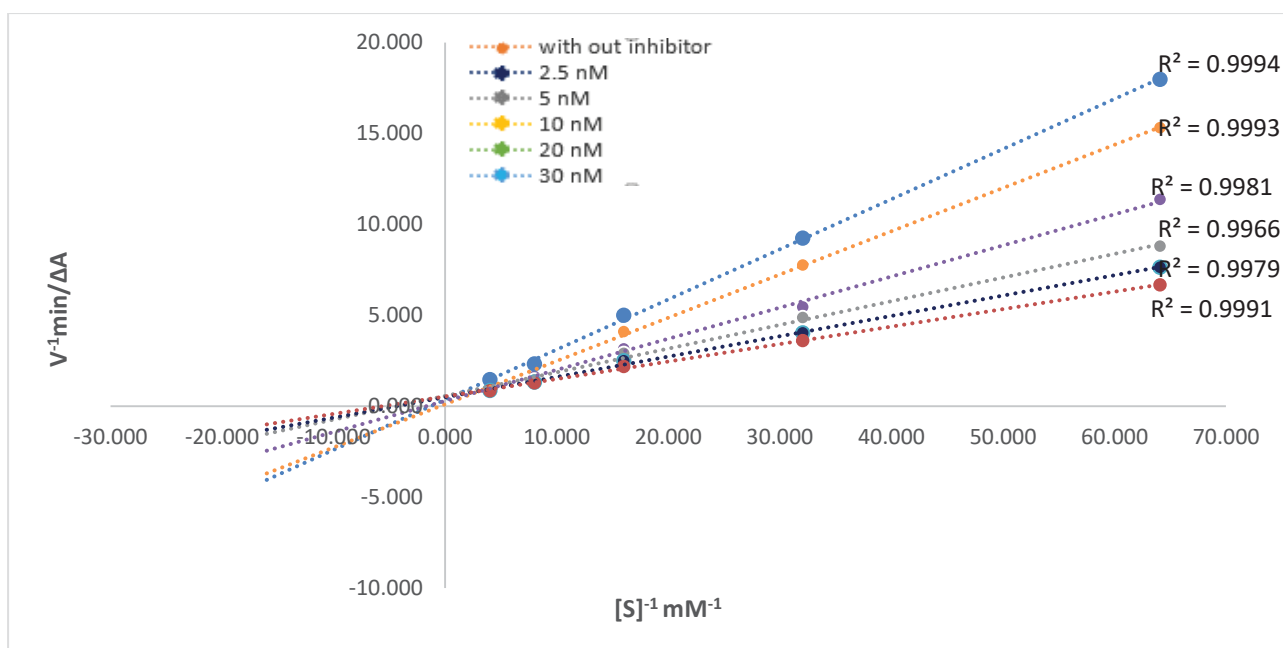


Figure 20: Lineweaver Burk plot for inhibition of compound ST09

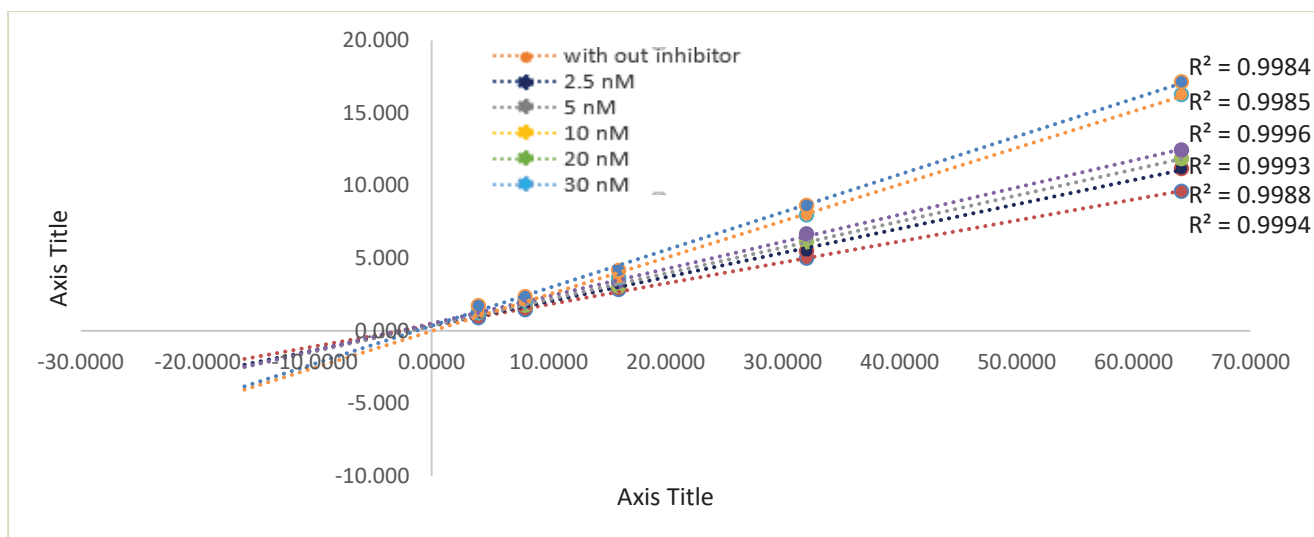


Figure 21: Lineweaver Burk plot for inhibition of compound ST20

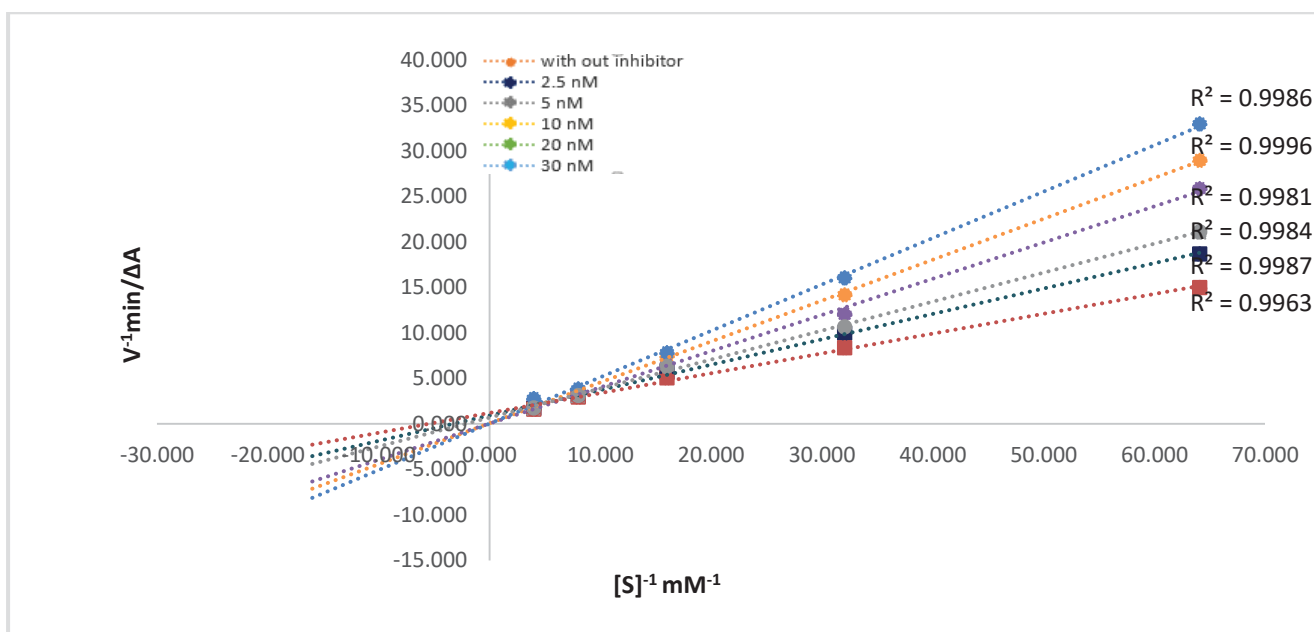


Figure 22: Lineweaver Burk plot for inhibition of compound ST21

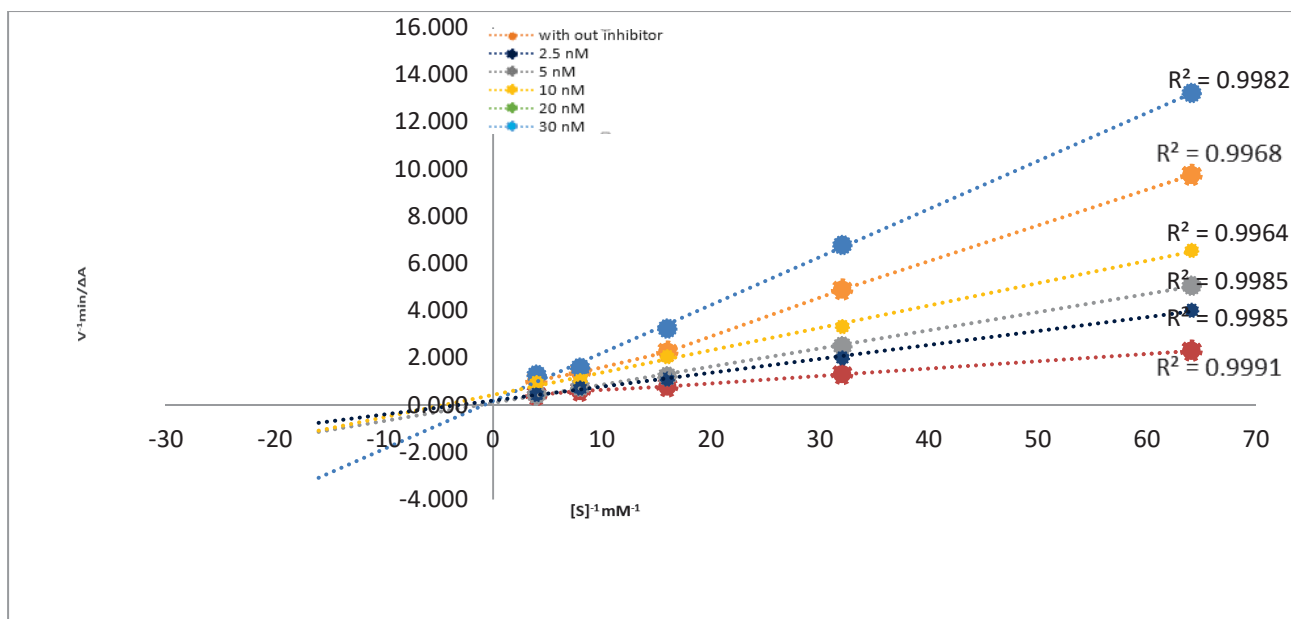


Figure 23: Lineweaver Burk plot for inhibition of compound ST24

The inhibition kinetics were demonstrated by Dixon plots, which were obtained by plotting $1/V$ versus $[I]$ with varying concentrations of substrate. Dixon plots gave a family of straight lines passing through the same point at the second quadrant, giving the inhibition constant (K_i) (Figures 24, 25, 26, 27, 28, 29 and 30) for AChE

The inhibitor concentrations were 0, 5, 10, 20 and 30 nM respectively. The substrate ATCI concentrations were 0.0156, 0.0312 and 0.0625 mM.

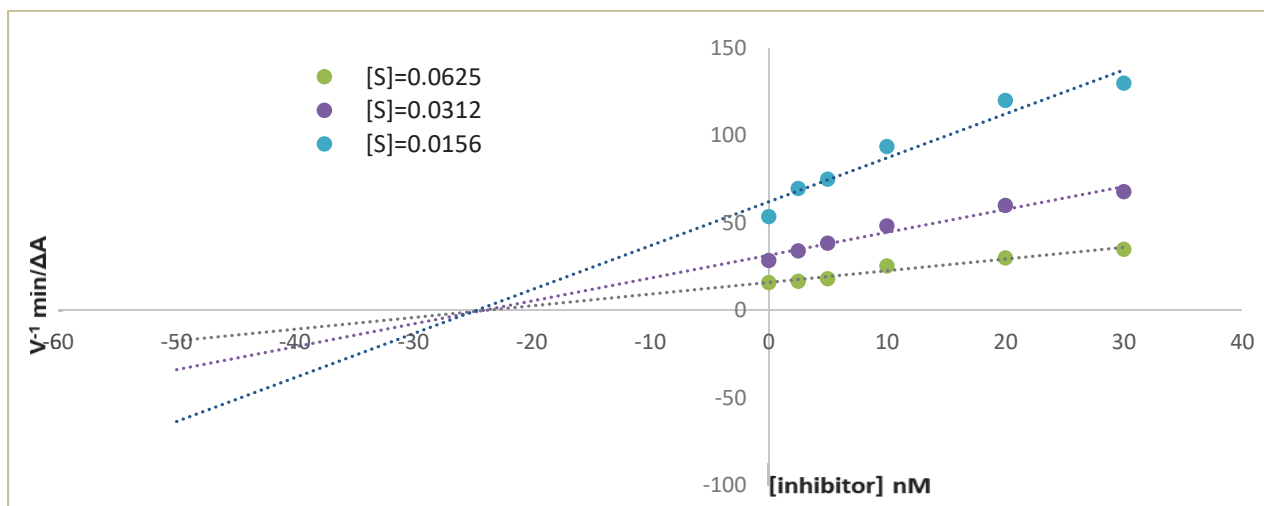


Figure 24: Dixon plot for the inhibitory effect of compound ST03

As shown in Figure 24 the K_i value estimated from this Dixon plot was $K_i=25.3716$ nM for the compounds ST03. A comparison of the K_i values of the compounds with that of Tacrine and Galantamine revealed that they possess much higher affinity to AChE than Tacrine and Galantamine as shown in (Table 3).

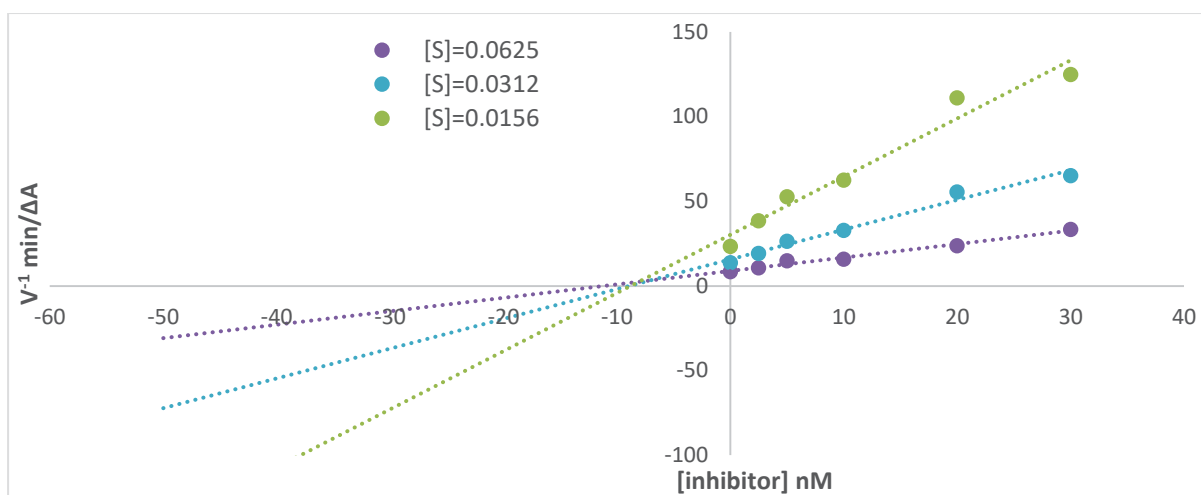


Figure 25: Dixon plot for the inhibitory effect of compound ST06

As shown in Figure 25 the K_i value estimated from this Dixon plot was $K_i = 7.0778 \text{ nM}$ for the compounds ST06. A comparison of the K_i values of the compounds with that of Tacrine and Galantamine revealed that they possess much higher affinity to AChE than Tacrine and Galantamine as shown in (Table 3).

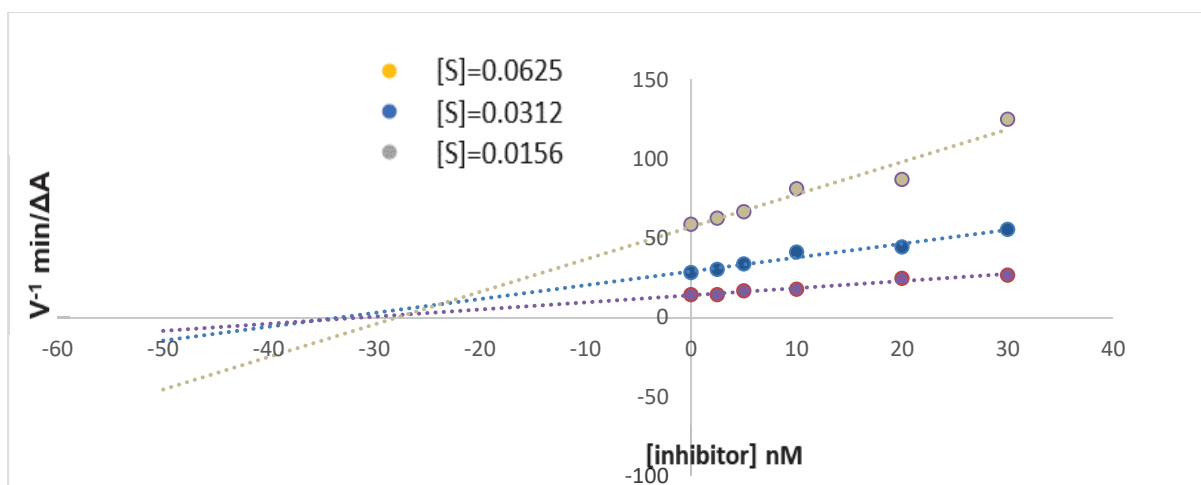


Figure 26: Dixon plot for the inhibitory effect of compound ST07

As shown in Figure 26 the K_i value estimated from this Dixon plot was $K_i = 23.8013 \text{ nM}$ for the compounds ST07. A comparison of the K_i values of the compounds with that of Tacrine and Galantamine revealed that they possess much higher affinity to AChE than Tacrine and Galantamine as shown in (Table 3).

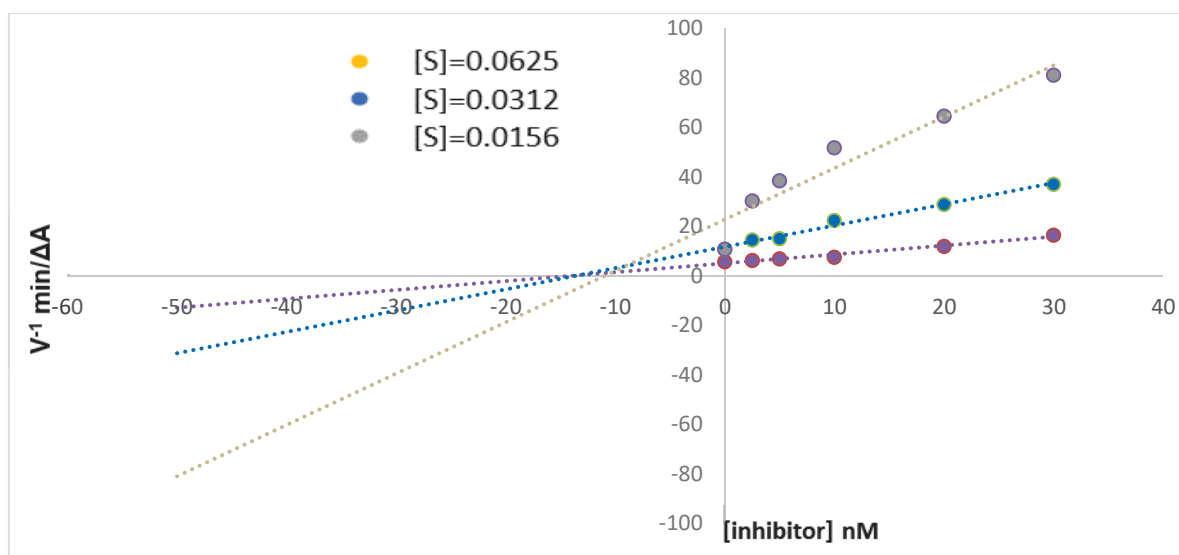


Figure 27: Dixon plot for the inhibitory effect of compound ST09

As shown in Figure 27 the K_i value estimated from this Dixon plot was $K_i = 9.0858 \text{ nM}$ for the compounds ST09. A comparison of the K_i values of the compounds with that of Tacrine and Galantamine revealed that they possess much higher affinity to AChE than Tacrine and Galantamine as shown in (Table 3).

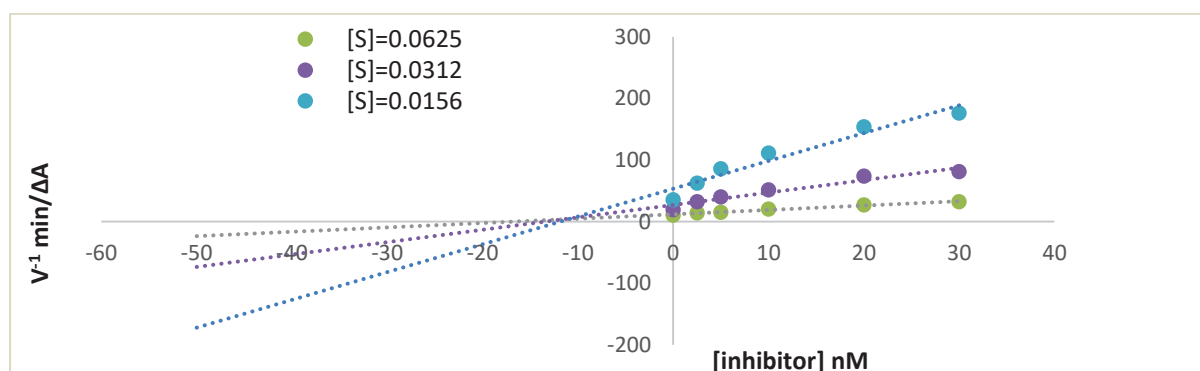


Figure 28: Dixon plot for the inhibitory effect of compound ST20

As shown in Figure 28 the K_i value estimated from this Dixon plot was $K_i = 10.5518 \text{ nM}$ for the compounds ST20. A comparison of the K_i values of the compounds with that of Tacrine and Galantamine revealed that they possess much higher affinity to AChE than Tacrine and Galantamine as shown in (Table 3).

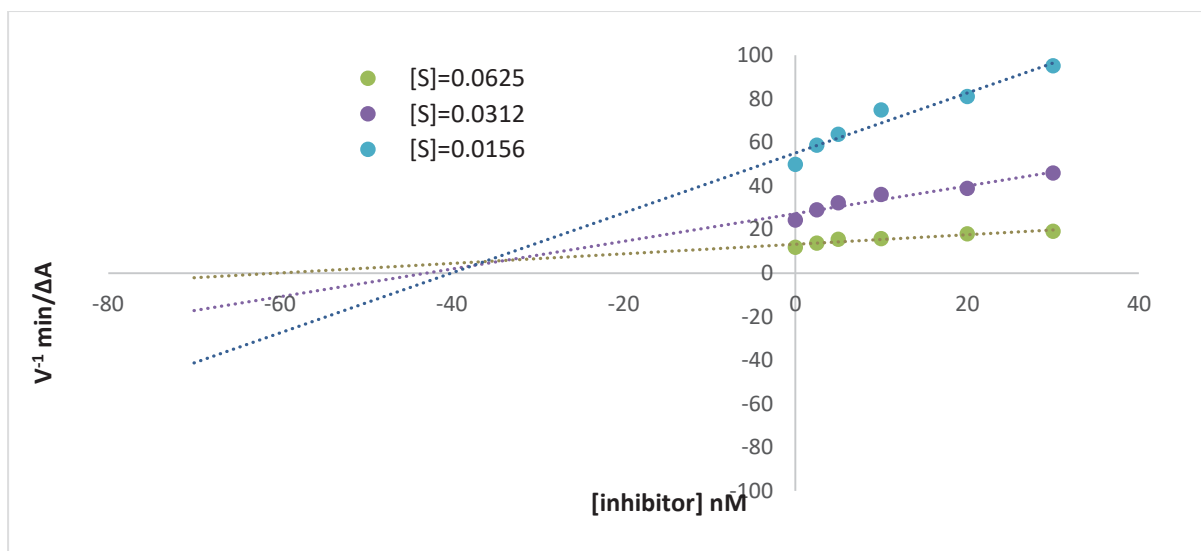


Figure 29: Dixon plot for the inhibitory effect of compound ST21

As shown in Figure 29 the K_i value estimated from this Dixon plot was $K_i = 33.7878 \text{ nM}$ for the compounds ST21. A comparison of the K_i values of the compounds with that of Tacrine and Galantamine revealed that they possess much higher affinity to AChE than Tacrine and Galantamine as shown in (Table 3).

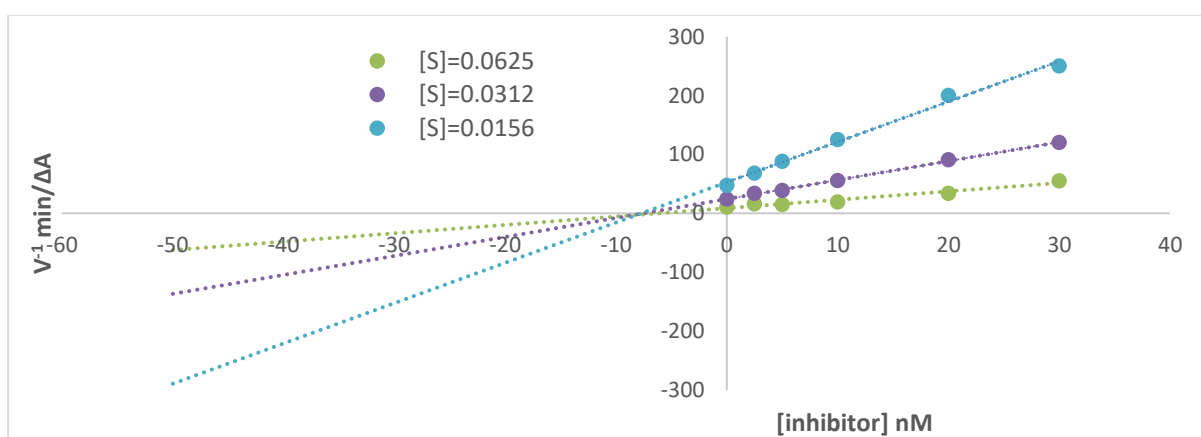


Figure 30: Dixon plot for the inhibitory effect of compound ST24

As shown in Figure 30 the K_i value estimated from this Dixon plot was $K_i = 7.8719 \text{ nM}$ for the compounds ST24. A comparison of the K_i values of the compounds with that of Tacrine and Galantamine revealed that they possess much higher affinity to AChE than Tacrine and Galantamine as shown in (Table 3).

The inhibition kinetics were demonstrated by Dixon plots, which were obtained by plotting $1/V$ versus $[I]$ with varying concentrations of substrate. Dixon plots gave a family of straight lines passing through the same point at the second quadrant, giving the inhibition constant (K_i) (Figures 30, 31, 32, 33, 34, 35 and 36) for BuChE. The inhibitor concentrations were 0, 5, 10, 20 and 30 nM respectively. The substrate BTCI concentrations were 0.0156, 0.0312 and 0.0625 mM.

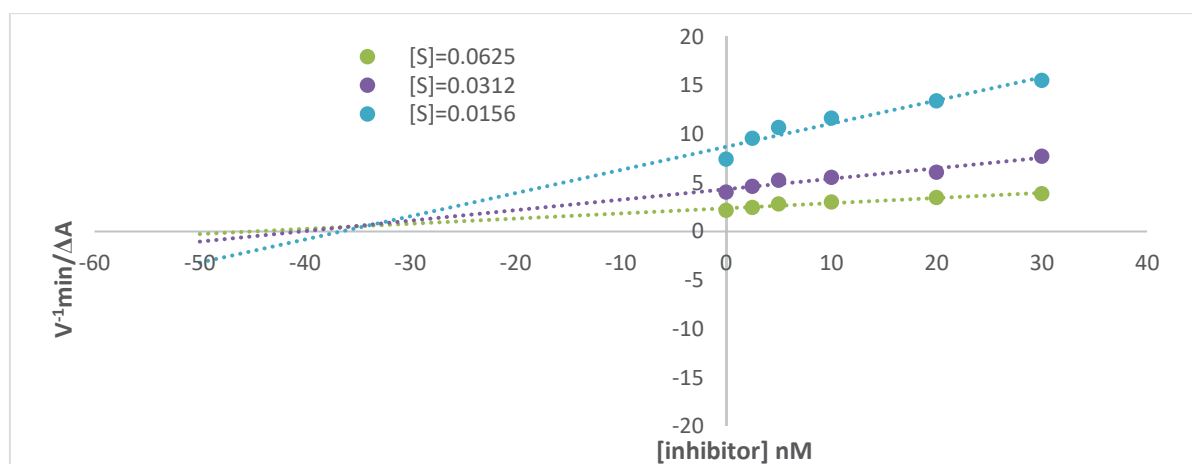


Figure 31: Dixon plot for the inhibitory effect of compound ST06

As shown in Figure 31 the K_i value estimated from this Dixon plot was $K_i = 33.4205$ nM for the compounds ST06. A comparison of the K_i values for the compounds with that of Tacrine and Galantamine revealed that they possess much higher affinity to AChE than Tacrine and Galantamine as shown in (Table 3).

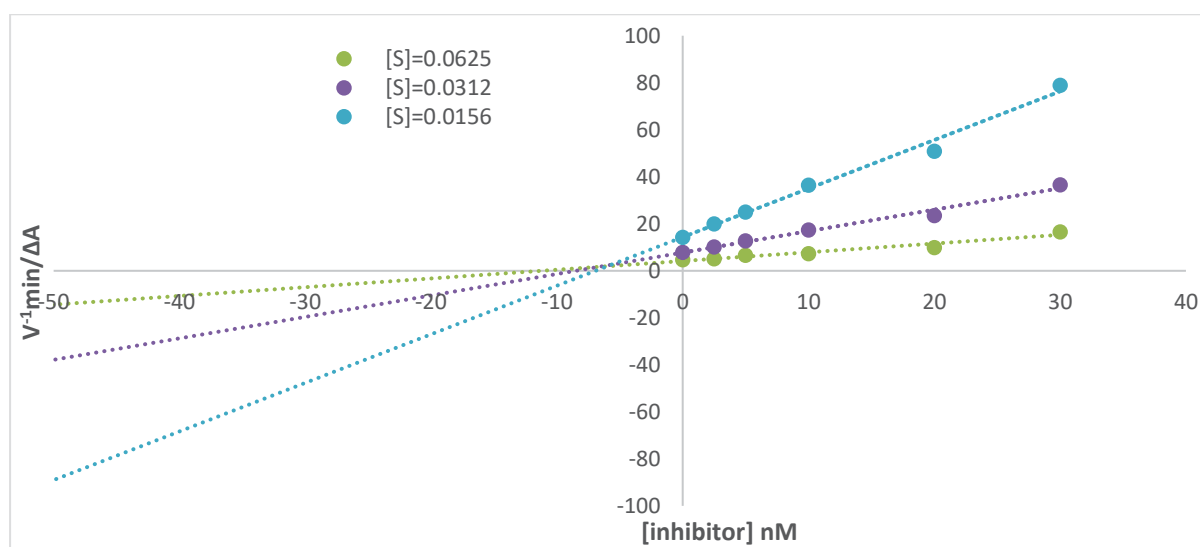


Figure 32: Dixon plot for the inhibitory effect of compound ST07

As shown in Figure 32 the K_i value estimated from this Dixon plot was $K_i = 5.687$ nM for the compounds ST07. A comparison of the K_i values of the compounds with that of Tacrine and Galantamine revealed that they possess much higher affinity to AChE than Tacrine and Galantamine as shown in (Table 3).

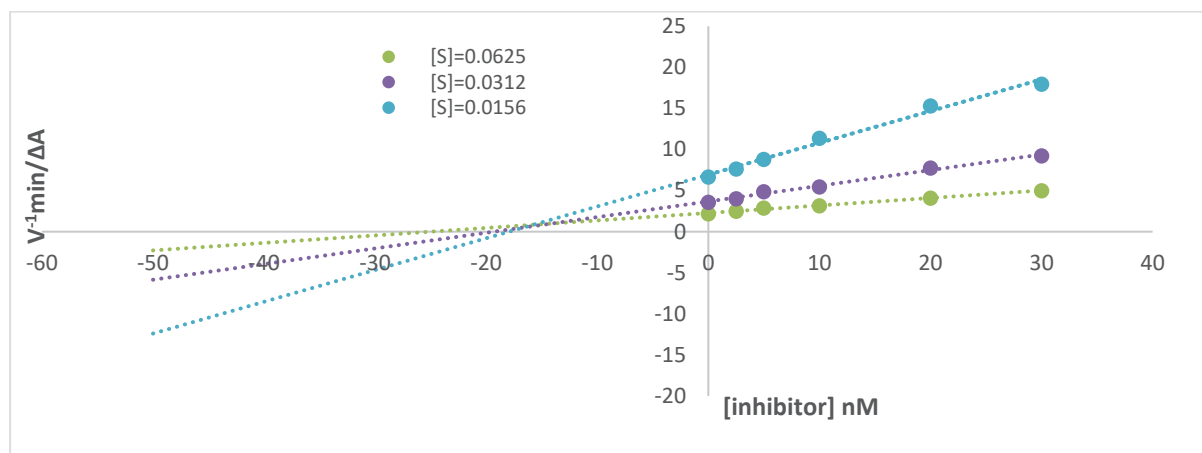


Figure 33: Dixon plot for the inhibitory effect of compound ST09

As shown in Figure 33 the K_i value estimated from this Dixon plot was $K_i = 16.6257$ nM for the compounds ST09. A comparison of the K_i values of the compounds with that of Tacrine and Galantamine revealed that they possess much higher affinity to AChE than Tacrine and Galantamine as shown in (Table 3).

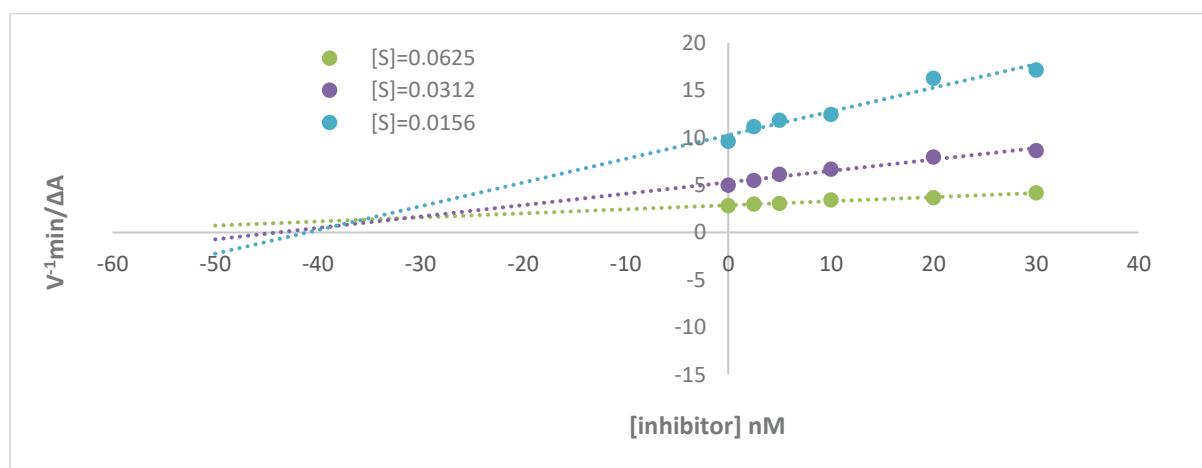


Figure 34: Dixon plot for the inhibitory effect of compound ST20

As shown in Figure 34 the K_i value estimated from this Dixon plot was $K_i = 31.2425$ nM for the compounds ST20. A comparison of the K_i values of the compounds with that of Tacrine and Galantamine revealed that they possess much higher affinity to AChE than Tacrine and Galantamine as shown in (Table 3).

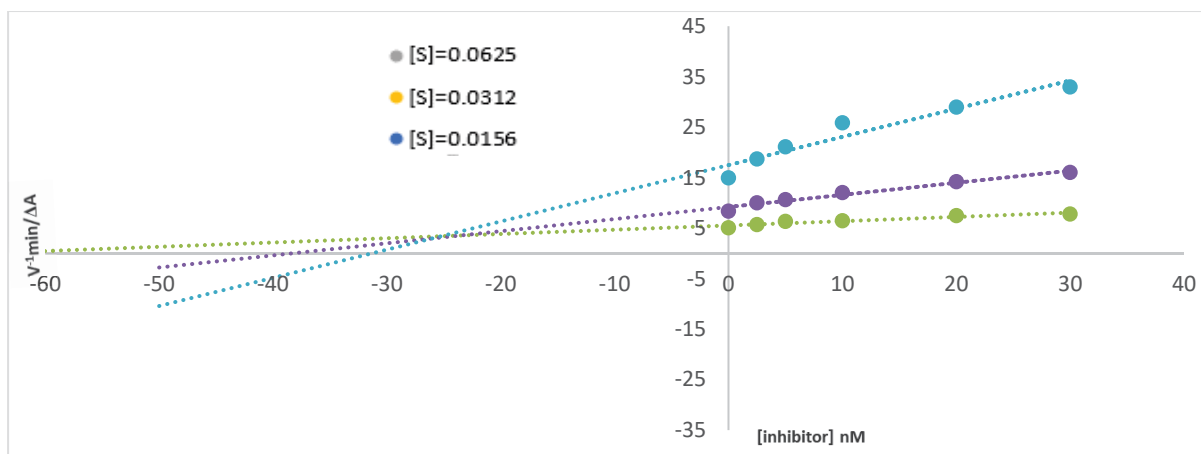


Figure 35: Dixon plot for the inhibitory effect of compound ST21

As shown in Figure 35 the K_i value estimated from this Dixon plot was $K_i = 23.5672$ nM for the compounds ST21. A comparison of the K_i values of the compounds with that of Tacrine and Galantamine revealed that they possess much higher affinity to AChE than Tacrine and Galantamine as shown in (Table 3).

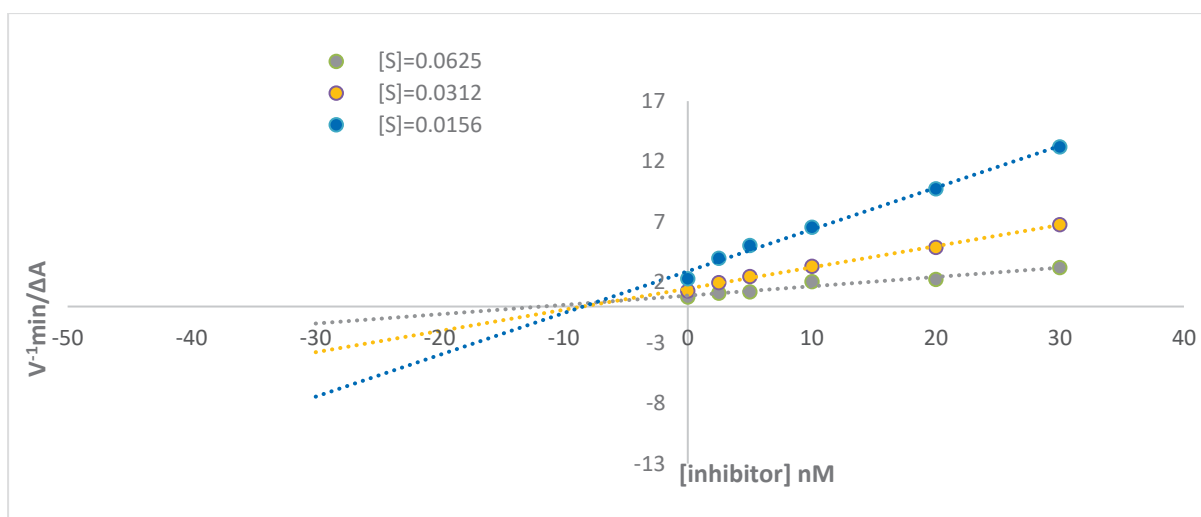


Figure 36: Dixon plot for the inhibitory effect of compound ST24

As shown in Figure 36 the K_i value estimated from this Dixon plot was $K_i = 8.3982$ nM for the compounds ST24. A comparison of the K_i values of the compounds with that of Tacrine and Galantamine revealed that they possess much higher affinity to AChE than Tacrine and Galantamine as shown in (Table 3).

Table 3: Kinetic analysis of active compounds

Compound	Type of inhibition*	Ki (nM) in AChE[!]	Ki (nM) in BuChE[!]
ST03	Competitive	25.371± 0.98	—
ST06	Competitive	7.077 ±0.65	33.420 ± 1.24
ST07	Competitive	23.801± 0.87	5.687±0.43
ST09	Competitive	9.085± 0.68	16.625±0.64
ST20	Competitive	10.551 ±0.72	31.242± 1.08
ST21	Competitive	33.787±1.17	23.567 ±0.81
ST24	Competitive	7.871± 0.54	8.3982±0.61
Tacrine	Competitive	34.250±1.26	33.810± 1.20
Galantamine	Competitive	450.100±5.1	530.730 ±6.3

* Lineweaver- Burk plot for AChE and BuChE of active compounds :Data are presented as mean values of $1/V_i$, which is the inverse of the increase in absorbance at wavelength 405 nm/min ($\Delta A_{405}/\text{min}$), for three independent tests with different concentrations of ATCI and BTCl as the substrate.

! K_i is the (inhibitor constant) of active compounds

3.6: Estimation of the Drug-Like Properties based on Lipinski rule

Design of new drugs for Alzheimer's disease treatment are usually tested for Lipinski rule of five (Lipinski et al. 1997) which is very important evaluation scheme for drug development. The lipophilic drugs cross the Blood Brain Barrier by passive diffusion and the hydrogen bonding properties of the drugs that can significantly influence the Central Nervous System uptake profiles.

The Size, ionization properties and molecular flexibility and molecular weight are other factors that were found to influence the transport of an organic compound across the Blood Brain Barrier (Borra & Kuna 2013; Mouritsen & Jørgensen 1998). The range of these properties are of importance in the pharmacological activity screening of drugs are as following :

1-The molecular weight which represent the size of the molecules should be equal or less than 500 Dalton.

2-The number of hydrogen bonding formed by nitrogen and oxygen acceptors to be equal or less than ten.

3-The number of hydrogen bond donors as NH and OH, SH or others to be equal or less than five.

4-The log of the calculated logarithm of the octanol: water partition coefficient (Clog P) (solubility parameters) to be equal or less than five.

5-The number of rotatable bonds that represent the extend of the molecular flexibility to be equal or less than ten (Borra & Kuna 2013; Kalidasu & Kuna 2012).

Typical characteristic properties estimated for the new compounds prepared and evaluated in this study are listed in Table 4.

3.7: Prediction of BBB penetration of compounds

The blood brain barrier (BBB) represents transportation of active ingredients from the circulating blood from brain extracellular fluid to the central nervous system. An active delivery of a drug across BBB represent essential step in the design and development AD drugs crossing the BBB depends on the same five rules mentioned in section 3.5 Lipinski's in addition to the previous five rules; the molecule's surface area to be less than 90 square angstrom (\AA^2) (Borra & Kuna 2013; Li, Wang & Kong 2014).

The lipid solubility of drug has an opposite relationship to the number of hydrogen bonds that makes the drug soluble in water. The H-bonding of any drug can be known by inspection of the molecular structure, and can be measured relative to the MW of the drug. (Rishton et al. 2006) (Paterson & Donnelly 2011). The BBB penetration values can be calculated from logBB using the following equation as defined by terms of Lipinski's five rules. The calculated logBB are important for potential applications in brain drug design.

The logBB is equal to the logarithm of the ratio between the concentration of a drug in the brain and that in the blood). The data obtained for the novel phen-5,6-dione derivatives that fulfil drug-like criteria and possible brain penetration characteristics are listed in (Table 4).

$\log BB = -0.0148 \times PSA + 0.152 \times Clog P + 0.139$ (Li, Wang & Kong 2014). ($\log BB < -1.0$, poorly distributed in the brain).

Table 4: Estimated physical Drug-Like Properties based on Lipinski five rules for the phen-5,6-dione derivatives

Compounds	Log p	MW	HBD	HBA	Num- H Rotatable Bonds	Total Num- H of Rings	Num- H of Aromatic Rings	PSA	Log BB
ST01	1.364	210	0	4	0	3	2	0.303	0.340
ST02	2.959	301	1	5	1	4	3	0.262	0.577
ST 03	4.554	392.409	2	6	2	5	4	0.24	0.815
ST04	1.431	225.203	1	5	0	3	2	0.354	0.349
ST05	1.498	240.218	2	6	0	3	2	0.398	0.357
ST06	0.583	267.243	2	5	1	3	2	0.43	0.223
ST07	1.46	249.228	1	5	0	4	2	0.351	0.353
ST08	0.651	282.257	3	6	1	3	2	0.462	0.233
ST09	0.638	266.258	3	5	2	3	2	0.446	0.231
ST10	1.515	248.243	2	5	0	4	2	0.371	0.360
ST 11	1.574	283.308	2	5	2	3	2	0.464	0.367
ST12	2.778	297.335	2	5	3	3	2	0.382	0.545
ST13	2.552	297.335	1	5	2	3	2	0.392	0.512
ST14	3.314	311.362	1	5	3	3	2	0.322	0.637
ST15	3.127	311.362	2	5	4	3	2	0.361	0.597
ST16	4.633	359.404	2	5	4	4	3	0.327	0.820
ST17	1.976	265.273	3	6	0	4	2	0.453	0.426
ST18	2.073	312.35	3	6	3	3	2	0.414	0.441
ST19	3.432	282.299	0	4	0	5	5	0.194	0.650
ST20	3.867	330.297	0	6	2	4	3	0.321	0.708
ST21	1.718	212.204	2	4	0	3	3	0.328	0.391
ST22	3.208	299.326	0	4	2	4	3	0.186	0.617
ST23	2.926	324.334	0	6	4	3	2	0.252	0.508
ST24	1.666	232.24	0	4	0	4	4	0.23	0.386

MW, molecular weight; cLog p, calculated logarithm of the octanol– water partition coefficient; HBA, the number of hydrogen bond acceptor atoms; HBD, the number of hydrogen bond donor atoms; PSA, polar surface area.

The Lipinski five rules parameter listed in Table 4 shows that all the phen-5,6-dione derivatives prepared in this study apply the Lipinski's five rules explained in section 3.6, accordingly these new phenanthroline derivatives fulfil one of the essential drug like requirements and are possible drug like promoters. The molecular of all the prepared phen-5,6-dione derivatives are less than 500 Dalton.

3.8: ADMET Descriptors

The term ADMET is an abbreviation for five biological phenomena; Metabolism, Excretion, Absorption, Distribution, and Toxicity. These characteristics are important for the design and developing drugs. Evaluating, optimising and integration of these properties during the drug discovery process enhance the chance of developing active ingredients with wanted pharmaceutical kinetic properties, which will promote them to be good drug candidates otherwise will be discarded at initial stages of the drug developing pipeline. ADMET descriptors values can be calculated by the program known by Discovery Studio 4.5 which also covers the evaluation of the drug like properties detailed in section 3.6 such as aqueous solubility, (BBB) penetration, intestinal absorptivity, hepatotoxicity, plasma protein binding PPB and CYP2D6 binding. Several types of models were developed based on training standard sets of compounds to include the prediction range and the category to which the investigated compounds belong.

Each of these models that investigate particular organ are the results of integrative efforts of several researchers. For example (Egan, Merz & Baldwin 2000) and (Egan & Lauri 2002) developed the intestinal absorption model modified from BBB penetration model. The aqueous solubility model was developed by Cheng and Merz (Egan & Lauri 2002), while Susnow and Dixon developed both cytochrome P450 2D6 (or CYP2D6 binding) and hepatotoxicity mod.

Table 5: ADMET results for the phen-5,6-dione derivatives

Compound	Aqueous solubility	BBB Penetration	CYP2D6 binding	Hepatotoxicity	Intestinal Absorption	PPB
ST01	3	3	false	True	0	true
ST02	2	2	false	True	0	true
ST03	2	3	false	True	0	true
ST04	3	3	false	True	0	false
ST05	3	3	false	True	0	false
ST06	3	3	false	True	0	false
ST07	2	3	false	True	0	true
ST08	3	3	false	True	0	false
ST09	3	3	false	True	0	false
ST10	3	3	false	True	0	false
ST11	2	3	false	True	0	false
ST12	3	3	false	True	0	false
ST13	2	3	false	True	0	false
ST14	3	2	false	True	0	true
ST15	2	3	false	True	0	true
ST16	2	2	false	True	0	true
ST17	2	2	false	True	0	true
ST18	3	3	false	True	0	false
ST19	1	1	false	True	0	true
ST20	2	3	false	True	0	true
ST21	3	3	false	True	0	false
ST22	2	1	false	True	0	true
ST23	3	2	false	True	0	true
ST24	2	2	false	True	0	false

3.8.1: Aqueous Solubility

The aqueous solubility parameter is used to evaluate the solubility of the drug promoted compounds in water, in order to determine their hydrophilicity and lipophilicity while they are in the blood stream.

The solubility assessment implements the linear regression model to estimate the solubility of the compounds in water at pH seven and 25 °C. The other level of the solubility scores from 1-5 correspond to the predicted solubility based on the drug- likeness similarity: thus zero is given to extremely low solubility or non-soluble, no.1 indicates to very low solubility but possible under specific conditions, no.2 indicates low solubility, no.3 good solubility, no.4 optimal solubility, and no.5 too soluble. The solubility scales for active drug ingredients were also implemented by other researchers.

As shown in Table 5 most of the compounds were predicted to be soluble drug-like and scored two or three. The predicted solubility scaling for the prepared phen-5,6-dione derivatives are listed in Table 5. The scored level two and three for the solubility promotes the compounds to be drug-like ingredients.

3.8.2: BBB Penetration parameters

The BBB model predict and estimate the optimum concentration of an orally administered drug that passes from the blood to the brain tissues *via* the blood-brain barrier. The scale used for BBB ranges between 0-4, zero indicate very high penetration ,1; high penetration,2; medium penetration,3; low penetration and 4; Undefined – if the range of prediction is outside 95% - 99% confidence. The obtained data are listed in Table 5 for the studied compounds which ranged between high to low BBB penetration.

3.8.3: Human Intestinal Absorption model

The second important model estimates the level of absorption of the compound under investigation at the intestinal tissues after the compound is being administered orally. This parameter is of significant importance because it represents the amount of the orally taken dose that will be absorbed and goes to the blood stream. For humans; if the active ingredient is at least 90% absorbed it is called well-absorbed.

The following estimated scores are commonly used for indicating intestinal absorption levels: 0 = Good adsorption, 1 = Moderate adsorption, 2 = Poor adsorption, and 3 = Very poor absorption.

The estimated values of the intestinal absorption for the studied phen-5,6-dionederivatives are listed in Table 5 the predicted scores for the studied compounds are zero, that means they have good intestinal absorption in the human body.

3.8.4: CYP2D6 Binding

In human body the gen CYP2D6 encodes the cytochrome enzyme P450 2D6, one of the liver delivered enzymes that account for the metabolism of the administered active drug ingredients. The binding characteristics of the clinically administered drug are very important thus if the drug bind to the liver enzymes as a result of such binding properties it will inhibits the function of the enzyme, accordingly binding may change the metabolism of other drugs this action is known as drug interactions (Wang et al. 2009). Binding the drug to the enzyme represents one of the drawbacks for controlling the required therapeutic dose of the drug in the blood stream, accordingly testing for CYP2D6 enzyme inhibition is a fundamental aspect for any new drug design based on these rules for drug selection. Taking into consideration the genetic difference of people that may act differently toward specific drug outcomes. Trials are usually implemented to investigate and test the genetic variations of peoples response toward the investigated drugs (Teh & Bertilsson 2012).

Discovery Studio 4.5 software program scores the screened like-drug compounds by this module to show how well the chemical structure of the drug fits the model. This score is commonly known by CYP2D6 inhibitor as a score cut-off threshold. The prediction is expressed by either true or falls as indication of whether it is calculated or not calculated respectively.

3.8.5: Hepatotoxicity of the like-drug investigation

The liver is the responsible organ in the body for the metabolism of the drugs and their fragments, some of the drugs and their fragments damage the liver cells, this drawback of the drugs is known by Hepatotoxicity. Such drug side effect may cause liver failure which leads to accumulation of the drugs and their chemical fragments in the body. This is one of the critical issues appears during the use of the drug for definite period of time which may lead to suspend the drugs from use or put limits and restrictions on their use due to their hepatotoxicity.

Therefore, for the explained reasons the hepatotoxicity must be identified and investigated during the drug design and stages of development. In the present study the new phen derivatives are scored against a model drugs and a cut-off represents the type of hepatotoxicity either ‘true’ or ‘falls’ if the hepatotoxicity is predicted or not.

The obtained data for the investigated compounds are presented in Table 5. All the compounds showed to be hepatotoxic.

3.8.6: Plasma Protein Binding properties

Transportation and migration of the drug in the body takes place via blood plasma. The drugs are bonded to the transporter proteins, thus the capability of the binding of drugs to transporter proteins in blood plasma plays an important role in drug pharmacokinetics. The metabolism of the drug is important characteristic that determine its efficiency in addition to its negative pharmacological effect upon the intended target while it is bound to blood plasma proteins. Which is important to be considered while determining the drug’s therapeutic dosing as balanced between the toxicity and pharmacological effects. Estimating the high binding probability of the drug to plasma protein (equal or more than 90%) this determines the threshold scoring for compound which is expressed by “True” or scored as ‘Falls” for lower binding percentages. The estimated scores for the compounds prepared and investigated in this study are listed in Table 5. Twelve of the analysed compounds are predicted to have high plasma protein binding as scored by term ‘True’.

3.9: Docking Studies

In order to predict the binding interactions of 1,10-phenathroline-5,6-dione derivatives to the active site of 2xi4 receptor protein docking studies were performed using the GOLD docking software, accessed *via* the Accelrys Discovery Studio software package. Each compound was sketched in DS 4.0 using Small Molecule Tools. Input conformations were generated by energy minimization using the Force Field CHARMM with default parameter settings, followed by conformational search with the following settings: Conformation Method BEST, Maximum Conformations 255, Energy Threshold 20.0 kcal/mol. Docking of the minimized ligands into the binding pocket sub-unit E of the crystal structure of the 2xi4 was performed using GOLD (Cambridge Crystallography Data Centre, UK) through the DS interface. The protocol was run with default settings with the following changes: Poses – 100; Detect cavity – False; Early termination – False.

The docking pose in the largest, highest scoring cluster between at 2 Å root mean-square-deviation (RMSD) of ligand heavy atoms was then selected for the GOLD score.

The GOLD docking software was then being employed to optimize a protocol for obtaining possible binding modes of the proposed scaffolds within the 2xi4 binding site, as well as to generate Goldscore values to indicate the relative affinity of each potential ligand. Predicted binding interactions such as hydrogen bonding, π and hydrophobic interactions between the highest scored pose for each compound and the 2xi4 receptor are presented in Table 6.

Table 6: Docking study of the 1,10-phenanthroline-5,6-dione derivatives to the 2xi4 receptor protein.

Compound	Gold score fitness	Interaction from selected pose	
		H-bond Interactions	Hydrophobic and π Interactions
ST-01	43.86	Phe288, Arg289	Trp279, Tyr70, Tyr121, Leu282
ST-02	51.35	Trp279, Tyr70, Tyr121	Trp279, Tyr70, Tyr121
ST-03	58.54	--	Trp279
ST-04	47.67	--	Trp279, Tyr70
ST-05	46.39	Tyr121	Tyr279
ST-06	51.41	Phe288, Arg289	Tyr234, Trp279, Tyr70
ST-07	51.19	Tyr121	Trp279, Tyr70
ST-08	50.74	Phe288, Ser286, Arg289	Tyr334, Trp279
ST-09	53.05	Phe288, Arg289, Tyr121	Trp279, Leu282

ST-10	51.75	Phe288	Trp279, Tyr121, Ser286, Ile287, Leu282
ST-11	53.04	Phe288, Arg289, Tyr121	Trp279, Tyr70, Tyr121
ST-12	51.14	Phe288, Arg289, Tyr121	Trp279
ST-13	53.50	Phe288, Arg289,	Tyr334, Trp279, Tyr70, Leu282
ST-14	50.51	Tyr70	Trp279, Tyr334
ST-15	52.78	Tyr70	Trp279
ST-16	54.31	Tyr70	Trp279
ST-17	55.65	Tyr70, Arg289	Trp279, Tyr334
ST-18	51.75	Arg289, Trp279, Ser286	Trp279, Tyr70
ST-19	56.19	Phe288	Trp279, Tyr70, Tyr121, Ser286, Leu282
ST-20	52.51	Phe288, Arg289	Trp279, Tyr70, Tyr334, Leu282
ST-21	46.12	Tyr121, Ser286	Trp279, Tyr70
ST-22	55.43	Ser286	Trp279, Tyr334, Leu282
ST-23	48.94	--	Trp279, Tyr70,
ST-24	49.63	--	Trp279, Tyr70, Tyr121
Aflatoxin B1	60.48	Phe288, Arg289,	Trp279, Tyr70, Tyr121, Trp279, Tyr334

The docking poses and interactions formed between Aflatoxin B1 and 2xi4 receptor are shown in Figure 37.

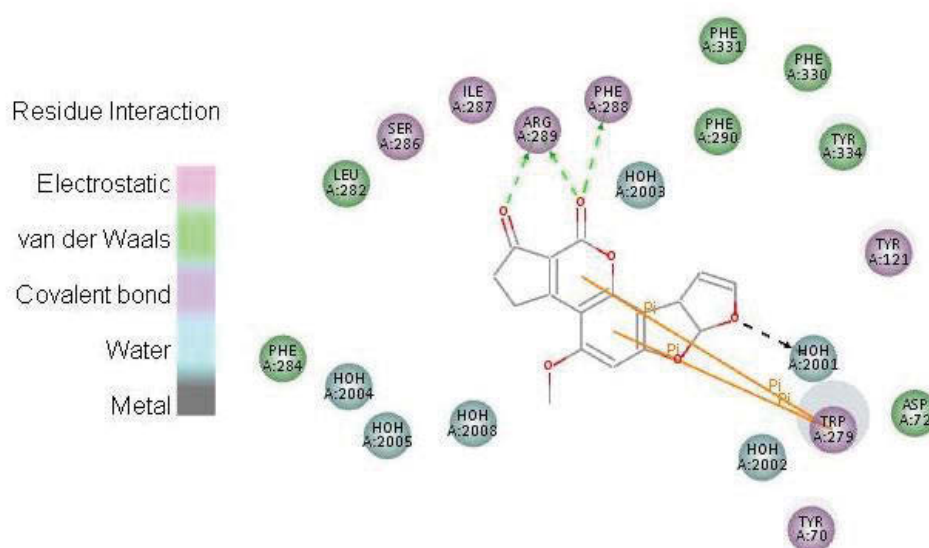


Figure 37: 2D-representation of the highest scoring pose of Aflatoxin B1 with 2xi4 protein.

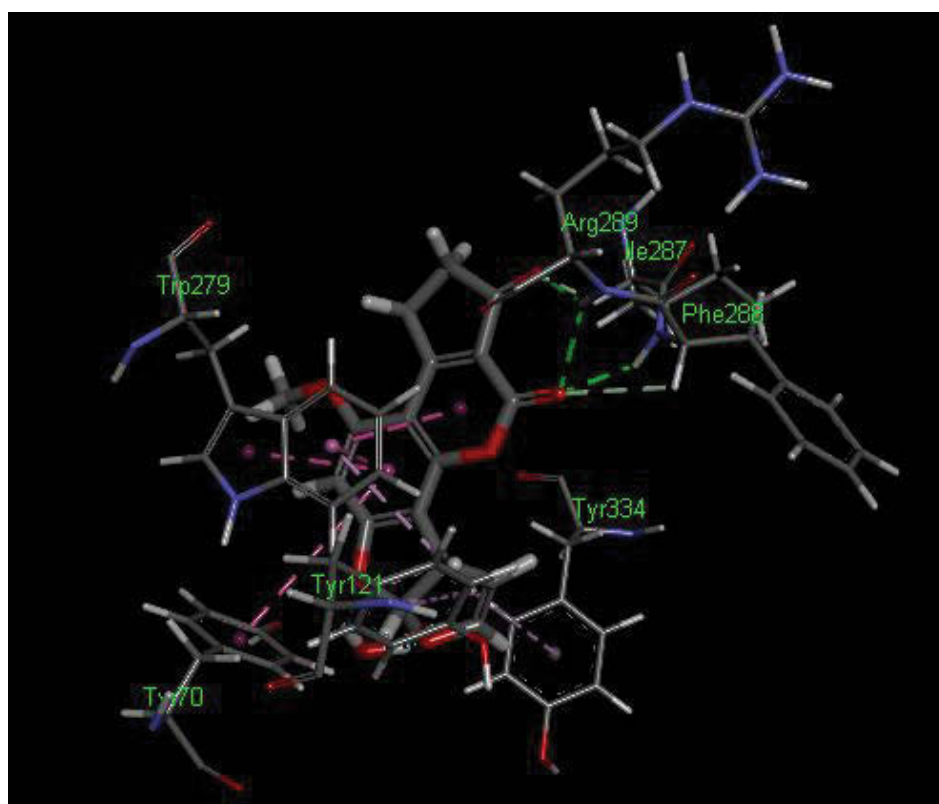


Figure 38: Binding interactions of the highest scoring pose of Aflatoxin B1 with 2xi4 protein.

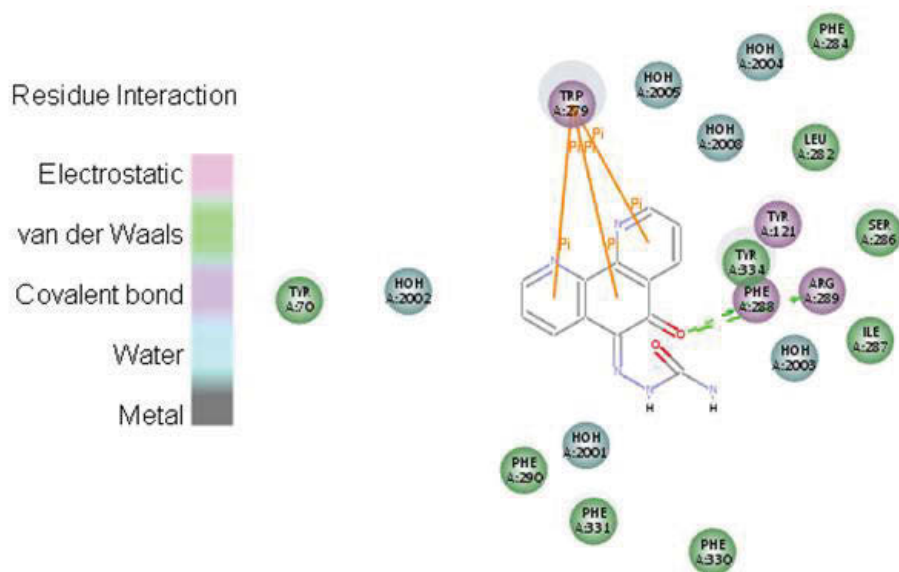


Figure 39: 2D-representation of the highest scoring pose of ST-06 with 2xi4 protein.

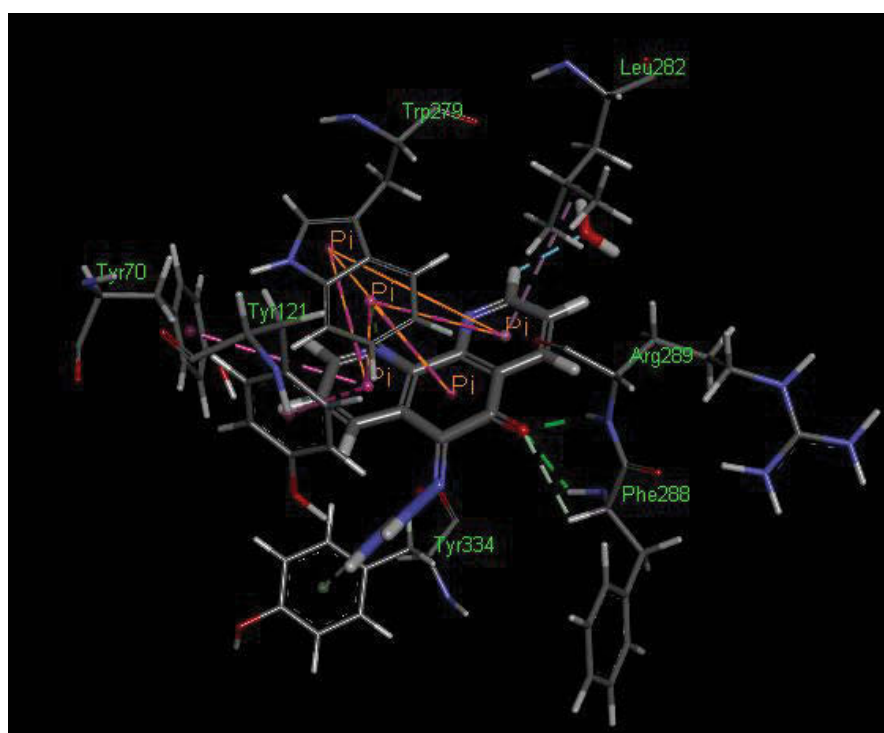


Figure 40: Binding interactions of the highest scoring pose of ST-06 with 2xi4 protein.

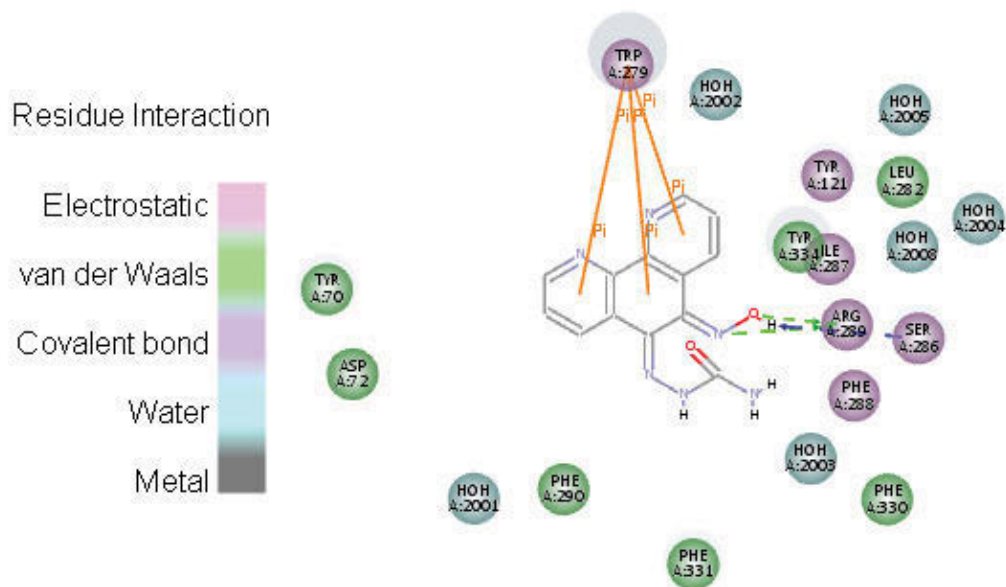


Figure 41: 2D-representation of the highest scoring pose of ST-08 with 2xi4 protein.

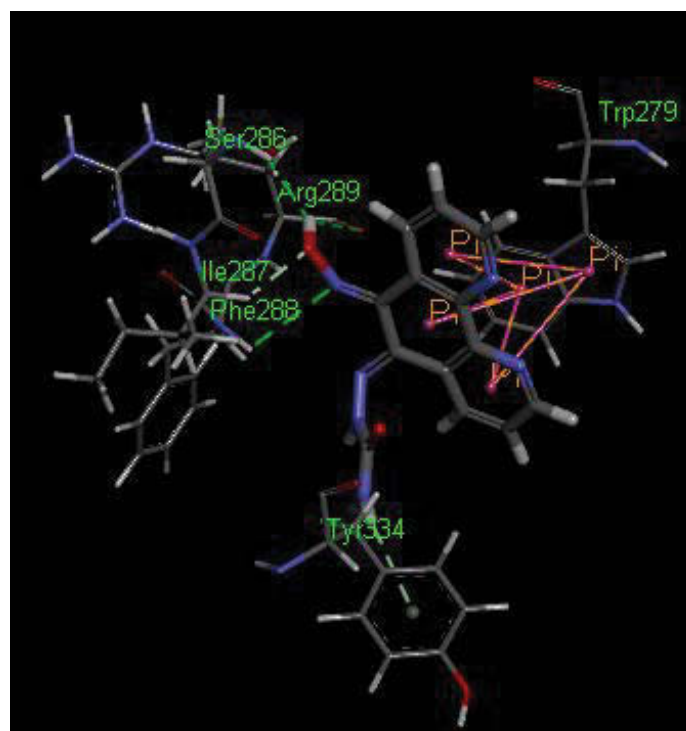


Figure 42: Binding interactions of the highest scoring pose of ST-08 with 2xi4 protein.

3.10 References

- BIZYAEV, S. N., GATILOV, Y. V. & TKACHEV, A. V. 2015. Syntheses of α -cyano substituted oximes from terpenic hydrocarbons via nitroso chlorides: X-ray structures of 3-cyanocarane-4-one oxime, 2-cyanopinane-3-one oxime and 1-cyano-p-menth-8-en-2-one oxime. *Mendeleev Communications*, 25, 93-95.
- BOLOGNESI, M. L., ANDRISANO, V., BARTOLINI, M., BANZI, R. & MELCHIORRE, C. 2005. Propidium-based polyamine ligands as potent inhibitors of acetylcholinesterase and acetylcholinesterase-induced amyloid- β aggregation. *Journal of medicinal chemistry*, 48, 24-27.
- BORRA, N. K. & KUNA, Y. 2013. Evolution of toxic properties of Anti Alzheimer's Drugs through Lipinski's rule of five. *Int. J. Pure App. Biosci*, 1, 28-36.
- CHEN, Y., SUN, J., FANG, L., LIU, M., PENG, S., LIAO, H., LEHMANN, J. & ZHANG, Y. 2012. Tacrine-ferulic acid-nitric oxide (NO) donor trihybrids as potent, multifunctional acetyl- and butyrylcholinesterase inhibitors. *Journal of medicinal chemistry*, 55, 4309-4321.
- CHITRA, L., KUMAR, C. R., BASHA, H. M., PONNE, S. & BOOPATHY, R. 2013. Interaction of metal chelators with different molecular forms of acetylcholinesterase and its significance in Alzheimer's disease treatment. *Proteins: Structure, Function, and Bioinformatics*, 81, 1179-1191.
- DARVESH, S., HOPKINS, D. A. & GEULA, C. 2003. Neurobiology of butyrylcholinesterase. *Nature reviews. Neuroscience*, 4, 131.
- DYACHENKO, V. & RUSANOV, E. 2003. Synthesis and Crystal Structure of 5-Amino-4-cyano-8-isobutyl-7-isopropyl-6-thiocarbonyl-2-azabicyclo [2.2. 2] oct-5-en-3-thione. *Chemistry of Heterocyclic Compounds*, 39, 645-690.
- EGAN, W. J. & LAURI, G. 2002. Prediction of intestinal permeability. *Advanced drug delivery reviews*, 54, 273-289.
- EGAN, W. J., MERZ, K. M. & BALDWIN, J. J. 2000. Prediction of drug absorption using multivariate statistics. *Journal of medicinal chemistry*, 43, 3867-3877.
- ELLMAN, G. L., COURTNEY, K. D., ANDRES, V. & FEATHERSTONE, R. M. 1961. A new and rapid colorimetric determination of acetylcholinesterase activity. *Biochemical pharmacology*, 7, 881-9095.
- FERNÁNDEZ-BACHILLER, M. I., PÉREZ, C. N., MONJAS, L., RADEMANN, J. R. & RODRÍGUEZ-FRANCO, M. I. 2012. New Tacrine-4-Oxo-4 H-chromene Hybrids as Multifunctional Agents for the Treatment of Alzheimer's Disease, with Cholinergic, Antioxidant, and β -Amyloid-Reducing Properties. *Journal of medicinal chemistry*, 55, 1303-1317.
- FUJII, T., MORI, Y., TOMINAGA, T., HAYASAKA, I. & KAWASHIMA, K. 1997. Maintenance of constant blood acetylcholine content before and after feeding in young chimpanzees. *Neuroscience letters*, 227, 21-24.
- FUKUTO, T. R. 1990. Mechanism of action of organophosphorus and carbamate insecticides. *Environmental health perspectives*, 87, 245.
- GANONG, W. F. & GANONG, W. 1995. *Review of medical physiology*, Appleton & Lange Norwalk, CT.
- GIACOBINI, E., SPIEGEL, R., ENZ, A., VEROFF, A. & CUTLER, N. 2002. Inhibition of acetyl- and butyrylcholinesterase in the cerebrospinal fluid of patients with Alzheimer's disease by rivastigmine: correlation with cognitive benefit. *Journal of Neural Transmission*, 109, 1053-1065.
- GREIG, N. H., UTSUKI, T., INGRAM, D. K., WANG, Y., PEPEU, G., SCALI, C., YU, Q.-S., MAMCZARZ, J., HOLLOWAY, H. W. & GIORDANO, T. 2005. Selective butyrylcholinesterase inhibition elevates brain acetylcholine, augments learning and lowers Alzheimer β -amyloid peptide in rodent. *Proceedings of the National Academy of Sciences of the United States of America*, 102, 17213-17218.

- GREIG, N. H., UTSUKI, T., YU, Q.-S., ZHU, X., HOLLOWAY, H. W., PERRY, T., LEE, B., INGRAM, D. K. & LAHIRI, D. K. 2001. A new therapeutic target in Alzheimer's disease treatment: attention to butyrylcholinesterase. *Current medical research and opinion*, 17, 159-165.
- GUTIÉRREZ, M., MATUS, M. F., POBLETE, T., AMIGO, J., VALLEJOS, G. & ASTUDILLO, L. 2013. Isoxazoles: synthesis, evaluation and bioinformatic design as acetylcholinesterase inhibitors. *Journal of Pharmacy and Pharmacology*, 65, 1796-1804.
- HUNT, R. & DE M. TAVEAU, R. 1906. On the physiological action of certain cholin derivatives and new methods for detecting cholin. *The British Medical Journal*, 1788-1791.
- INGKANINAN, K., TEMKITTHAWON, P., CHUENCHOM, K., YUYAEM, T. & THONGNOI, W. 2003. Screening for acetylcholinesterase inhibitory activity in plants used in Thai traditional rejuvenating and neurotonic remedies. *Journal of Ethnopharmacology*, 89, 261-264.
- KALIDASU, S. & KUNA, Y. 2012. Validation of selected Anti-Alzheimer's drugs through Lipinski rule of five. *Journal of Pharmacy Research Vol*, 5, 2174-2177.
- KELLY, T. A., MCNEIL, D. W., ROSE, J. M., DAVID, E., SHIH, C.-K. & GROB, P. M. 1997. Novel non-nucleoside inhibitors of huMan immunodeficiency virus type 1 reverse transcriptase. 6. 2-Indol-3-yl-and 2-azaindol-3-yl-dipyridodiazepinones. *Journal of Medicinal Chemistry*, 40, 2430-2433.
- LI, S.-Y., WANG, X.-B. & KONG, L.-Y. 2014. Design, synthesis and biological evaluation of imine resveratrol derivatives as multi-targeted agents against Alzheimer's disease. *European journal of medicinal chemistry*, 71, 36-45.
- LIPINSKI, C. A., LOMBARDO, F., DOMINY, B. W. & FEENEY, P. J. 1997. Experimental and computational approaches to estimate solubility and permeability in drug discovery and development settings. *Advanced drug delivery reviews*, 23, 3-25.
- LUO, W., LI, Y.-P., HE, Y., HUANG, S.-L., TAN, J.-H., OU, T.-M., LI, D., GU, L.-Q. & HUANG, Z.-S. 2011. Design, synthesis and evaluation of novel tacrine-multialkoxybenzene hybrids as dual inhibitors for cholinesterases and amyloid beta aggregation. *Bioorganic & medicinal chemistry*, 19, 763-770.
- MARMINON, C., PIERRÉ, A., PFEIFFER, B., PÉREZ, V., LÉONCE, S., JOUBERT, A., BAILLY, C., RENARD, P., HICKMAN, J. & PRUDHOMME, M. 2003. Syntheses and antiproliferative activities of 7-azarebeccamycin analogues bearing one 7-azaindole moiety. *Journal of medicinal chemistry*, 46, 609-622.
- MASSOULIÉ, J., PEZZEMENTI, L., BON, S., KREJCI, E. & VALLETTE, F.-M. 1993. Molecular and cellular biology of cholinesterases. *Progress in neurobiology*, 41, 31-91.
- MESULAM, M.-M., GUILLOZET, A., SHAW, P., LEVEY, A., DUYSSEN, E. & LOCKRIDGE, O. 2002. Acetylcholinesterase knockouts establish central cholinergic pathways and can use butyrylcholinesterase to hydrolyze acetylcholine. *neuroscience*, 110, 627-639.
- MIAO, Y., HE, N. & ZHU, J.-J. 2010. History and new developments of assays for cholinesterase activity and inhibition. *Chemical reviews*, 110, 5216-5234.
- MOHAMED, T., YEUNG, J. C., VASEFI, M. S., BEAZELY, M. A. & RAO, P. P. 2012. Development and evaluation of multifunctional agents for potential treatment of Alzheimer's disease: application to a pyrimidine-2, 4-diamine template. *Bioorganic & medicinal chemistry letters*, 22, 4707-4712.
- MOURITSEN, O. G. & JØRGENSEN, K. 1998. A new look at lipid-membrane structure in relation to drug research. *Pharmaceutical research*, 15, 1507-1519.
- PAN, L.-F., WANG, X.-B., XIE, S.-S., LI, S.-Y. & KONG, L.-Y. 2014. Multitarget-directed resveratrol derivatives: anti-cholinesterases, anti- β -amyloid aggregation and monoamine oxidase inhibition properties against Alzheimer's disease. *MedChemComm*, 5, 609-616.
- PATERSON, B. M. & DONNELLY, P. S. 2011. Copper complexes of bis (thiosemicarbazones): from chemotherapeutics to diagnostic and therapeutic radiopharmaceuticals. *Chemical Society Reviews*, 40, 3005-3018.

- PEREZ, L. R. & FRANZ, K. J. 2010. Minding metals: tailoring multifunctional chelating agents for neurodegenerative disease. *Dalton Transactions*, 39, 2177-2187.
- RAHIM, F., JAVED, M. T., ULLAH, H., WADOOD, A., TAHA, M., ASHRAF, M., KHAN, M. A., KHAN, F., MIRZA, S. & KHAN, K. M. 2015. Synthesis, molecular docking, acetylcholinesterase and butyrylcholinesterase inhibitory potential of thiazole analogs as new inhibitors for Alzheimer disease. *Bioorganic chemistry*, 62, 106-116.
- RAJASREE, P., SINGH, R. & SANKAR, C. 2012. Screening for acetylcholinesterase inhibitory activity of methanolic extract of *Cassia fistula* roots. *International Journal of Pharmacy & Life Sciences*, 3.
- RISHTON, G. M., LABONTE, K., WILLIAMS, A. J., KASSAM, K. & KOLOVANOV, E. 2006. Computational approaches to the prediction of blood-brain barrier permeability: A comparative analysis of central nervous system drugs versus secretase inhibitors for Alzheimer's disease. *Current opinion in drug discovery & development*, 9, 303-313.
- SHREEVIDHYA SURESSH, V., SATHYA, S., AKILA, A., PONNUSWAMY, S. & USHA, G. 2014. Crystal structure of 1-[2, 4-bis (4-methoxyphenyl)-3-azabicyclo [3.3. 1] nonan-3-yl] ethanone. *Acta Crystallographica Section E: Structure Reports Online*, 70, o1171-o1172.
- SINHA, S. K. & SHRIVASTAVA, S. K. 2013. Synthesis, evaluation and molecular dynamics study of some new 4-aminopyridine semicarbazones as an anti-amnesic and cognition enhancing agents. *Bioorganic & medicinal chemistry*, 21, 5451-5460.
- SUSNOW, R. G. & DIXON, S. L. 2003. Use of robust classification techniques for the prediction of human cytochrome P450 2D6 inhibition. *Journal of chemical information and computer sciences*, 43, 1308-1315.
- SUSSMAN, J. L. & HAREL, M. 1991. Atomic structure of acetylcholinesterase from *Torpedo californica*: a prototypic acetylcholine-binding protein. *Science*, 253, 872.
- TEH, L. K. & BERTILSSON, L. 2012. Pharmacogenomics of CYP2D6: molecular genetics, interethnic differences and clinical importance. *Drug metabolism and pharmacokinetics*, 27, 55-67.
- VOTANO, J. R., PARHAM, M., HALL, L. M., HALL, L. H., KIER, L. B., OLOFF, S. & TROPSHA, A. 2006. QSAR modeling of human serum protein binding with several modeling techniques utilizing structure-information representation. *Journal of medicinal chemistry*, 49, 7169-7181.
- WANG, B., YANG, L.-P., ZHANG, X.-Z., HUANG, S.-Q., BARTLAM, M. & ZHOU, S.-F. 2009. New insights into the structural characteristics and functional relevance of the human cytochrome P450 2D6 enzyme. *Drug metabolism reviews*, 41, 573-643.
- WOO, T., MARGL, P., DENG, L., CAVALLO, L. & ZIEGLER, T. 1999. Towards more realistic computational modeling of homogeneous catalysis by density functional theory: combined QM/MM and ab initio molecular dynamics. *Catalysis Today*, 50, 479-500.
- XIE, S.-S., WANG, X.-B., LI, J.-Y., YANG, L. & KONG, L.-Y. 2013. Design, synthesis and evaluation of novel tacrine-coumarin hybrids as multifunctional cholinesterase inhibitors against Alzheimer's disease. *European journal of medicinal chemistry*, 64, 540-553.
- ZHENG, H., YODIM, M. B. & FRIDKIN, M. 2009. Site-Activated Multifunctional Chelator with Acetylcholinesterase and Neuroprotective-Neurorestorative Moieties for Alzheimer's Therapy. *Journal of medicinal chemistry*, 52, 4095-4098.

Chapter 4 Bio metal Complexes of Cu and Zn (chelating) with phen-5,6-dione derivatives

4.1: Introduction

The capability of drugs to form complexes with metal ions such as Cu, Zn and Fe represents one of the essential characteristics for AD like-drugs according to the hypothesis named “metal hypothesis”. This hypothesis indicated that the metals (Cu , Zn and Fe) play an important role in pathogenesis of AD (Bush & Tanzi 2008b).

Biometal's of (Cu and Zn) ions may be crucial members in the pathological processes of the AD. The well-known chelating active ingredient is phen-5,6-dione. Phen-5,6-dione derivatives may serve as a bridging ligand in the construction of multi nuclear complexes. The structure and electronic properties of this ligand incorporate features of both diamine and quinone ligands, which may play a significant role to decrease the rate of cognitive and decline in moderately severe AD patients.

Furthermore the relatively high concentrations of copper and zinc found in the amyloid deposits in the AD affected brains, and it was hypothesised that metal-mediated chelators could help control the concentration of the oxidised metals in the 40-43 polypeptides accordingly further investigations for this hypothesis is vital in AD drug development (Iwata et al. 2004) the formation of these metals or reactive oxygen species (ROS) was goal as the chief concern in decrease the oxidative stress (Iwata et al. 2004).

Oxidative stress is believed to enhance the cleaving of the amyloid protein from the generation of high level of ROS, currently this represents attractive research interest to controlling AD. Formation of the metal chelators is promising attempt to reduce oxidative stress and control the neurotoxicity in the brain (Spencer et al. 2008) different from the previous inhibitors, the metal-based compounds are smaller and more appropriate to cross the BBB and display more compatible oral bioavailability. There are two methods currently being researched in design of these bi functional compounds. Direct incorporation of the metal-binding atom donors into the interacting peptide, and linking the chelating element to amyloid beta binding fragments (Huang et al. 2006). These metals-based compounds showed high binding affinities to the metals found in the brain and significantly reduced the levels of Hydrogen peroxide, suggesting that a reduction in the oxidizing conditions diffuse in the AD (Wang et al. 2012).

Metal ion chelators have been recommended as potential therapies for a disease relating issues. A β interacts with biogenic elements such as copper and zinc and together form cytotoxic aggregates (Cuajungco, Frederickson & Bush 2005; Duce & Bush 2010; Schrag et al. 2011). A novel strategy to develop site-activated multifunctional chelators for targeting multiple etiologies of Alzheimer's disease is activated by binding and inhibiting acetylcholinesterase (AChE), suppresses oxidative stress, and passivates excess of metal ions (Cu and Zn) in the brain . A novel prochelators were designed to inhibit AChE with a concurrent release in the brain of multifunctional metal chelators possessing the neuroprotective and neurorestorative propargylamine moiety (Zheng, Youdim & Fridkin 2009).

4.2 Materials and Methods

4.2.1 UV–Vis measurements

Samples were prepared by dissolving the active ingredient in 1%DMSO and buffer (20 μ M 4-(2-hydroxyethyl)-1-piperazineethanesulfonic acid (HEPES), pH 7.4, 150 μ M Na Cl) .The prepared stock solution was diluted to appropriate concentrations before transferring the solutions to a 10mm quartz cuvette HELLMA and analysed.

Absorption spectra in the ultraviolet region were obtained in the range 200–500 nm using an Agilent Technologies Cary 60 spectrometer (Santa Clara, CA, USA). Spectra were recorded at the rate of 500 nm/min and baseline corrections were achieved for all spectral measurements. The ligands and the complex properties were studied and several complex characteristic parameters were determined as detailed in section 4.3.

4.2.2 Metal-chelating properties of ligands

The complexation abilities for the investigated compounds phen-5,6-dione derivatives ST01 ST24 for bio metals complexes such as Cu⁺² and Zn⁺² in 1% DMSO at room temperature at the physiological pH 7.4 buffer solution (20 μ M 4-(2-hydroxyethyl)-1-piperazineethanesulfonic acid (HEPES), 150 μ M Na Cl) were studied by UV–vis spectrometry at wavelength range 200 to 500 nm for ligands concentration 25 μ M at different concentration of the metal salts [CuCl₂ or ZnCl₂] ; (0, 25, 50, 100, 150, 200, 250 and 500) μ M which was recorded after 5 min at room temperature.

4.3 Results and discussion

The obtained results are shown in Figures 43- 90.

The ligand showed spectral changes upon addition of Cu(II) and Zn(II) solutions.

The UV-Vis spectra of compounds ST01-ST24 at increasing Cu^{+2} concentrations given as an example. The increase in the absorbance could be better value by inspection of differential spectra as shown in (Fig 43-90) The obtained spectra indicated that there is a strong interaction between Cu^{+2} and the phen-5,6-dione derivatives.

Similar behaviour or trend was observed when using Zn^{+2} . The obtained results showed that the studied compounds could effectively form chelates with Cu^{+2} and Zn^{+2} , and could serve as metal chelators in treating AD.

The ratio of ligand/metal ion in the complex was investigated by mixing the fix amount of metal ion solutions with increasing ligand concentration; it was possible to observe that the maximum intensity of difference spectra was reached at about 1:1 ratio, which was taken as an indication of the stoichiometry of the complex.

As shown in the spectra the absorption peaks of the ligands where shifted to higher wave length which are related to the absorption of the complex, this indicate clearly the capability of all the ligands investigated in this study are capable of forming complexes with the two studied ions Cu^{+2} and Zn^{+2} which means these new phen-5,6-dione derivatives could be possible “like drugs “for AD based on the hypothesis of bio- metal complexes explained in paragraph 4.1 .The obtained results estimated from the spectra shown in Figures 43-90 are listed in Table 7.

From the analysis of the obtained UV-Vis spectrum Figure 43 for the ST01 ligand,

the peak at 256 nm of the ligand ST01 was shifted to 307 nm in the Cu^{+2} complex due to the attributed $\pi-\pi^*$ intra ligand transitions while the peak at 318 nm in the Cu^{+2} complex is assigned to the metal –ligand charge transfer (MLCT). Accordingly the obtained results indicate that the compound ST01 could interact with the Cu^{+2} ion effectively.

With zinc complexes the peak at 256 nm of the ligand ST01 had been shifted to 303 nm due to the attributed $\pi-\pi^*$ intra ligand transitions while the peak 312 nm in complex is assigned to metal –ligand charge transfer (MLCT). These results indicated that the compound ST01 could interact with the Zn^{+2} ion effectively as shown in Figure 44.

For the ST02 ligand the peak at 259 nm was shifted to 304 nm in Cu^{+2} complex and the peak related to the ligand at 301 nm had been shifted to 318 nm in Cu^{+2} complex due to attributed the $\pi-\pi^*$ intra ligand transitions indication that ST02 could interact with Cu^{+2} as shown in Figure 45.

For the Zn^{+2} complex the peak at 259 nm of the ligand ST02 had been shifted to 300 nm in the complex and the peak at 301 nm related to ligand had been shifted to 313 nm in the Zn^{+2} complex due to attributed the $\pi-\pi^*$ intra ligand transitions indicated that ST02 could interact with Zn^{+2} as shown in Figure 46.

For the ST03 ligand the peak at 208 nm of the ligand ST03 had been shifted to 316 nm in Cu^{+2} complex due to attributed the $\pi-\pi^*$ intra ligand transitions indicated that ST03 could interact with Cu^{+2} as shown in Figure 47.

For the Zn^{+2} complex the peak at 208 nm of ligand ST03 had been shifted to 314 nm in Zn^{+2} complex due to attributed the $\pi-\pi^*$ intra ligand transitions indicated that ST03 could interact with Zn^{+2} as shown in Figure 48.

For the ST04 ligand the peak at 251 nm of the ligand ST04 had been shifted to 282 nm in the Cu^{+2} complex due to attributed the $\pi-\pi^*$ intra ligand transitions and the peak at 301 nm related to ligand had been shifted to 346 nm in Cu^{+2} complex assigned to metal –ligand charge transfer (MLCT) indicated that ST04 could interact with Cu^{+2} as shown in Figure 49.

Whereas the peak at 251 nm of ligand ST04 has been shifted to 279 nm in complex with Zn^{+2} due to attributed the $\pi-\pi^*$ intra ligand transitions and the peak at 301 nm related to ligand had been shifted to 404 nm in complex with Zn^{+2} assigned to metal –ligand charge transfer (MLCT) indicate formation of ST04- Zn^{+2} complex as shown in Figure 50.

The peak at 254 nm of ligand ST05 has been shifted to 275 nm in complex with Cu^{+2} due to attributed the $\pi-\pi^*$ intra ligand transitions and the peak at 314 nm related to ligand had been shifted to 359 nm in complex with Cu^{+} assigned to metal –ligand charge transfer (MLCT)

indicated that ST05 could interact with Cu^{+2} as shown in Figure 51. Whereas the peak at 254 nm of ligand ST05 has been shifted to 278 nm in complex with Zn^{+2} due to attributed the $\pi-\pi^*$ intra ligand transitions and the peak at 314 nm related to ligand had

been shifted to 340 nm in complex with Zn^{+2} assigned to metal –ligand charge transfer (MLCT) indicated that ST05 could interact with Zn^{+2} as shown in Figure 52.

The peak at 246 nm of ligand ST06 had been shifted to 290 nm in complex with Cu^{+2} and the peak 312 nm related to ligand had been shifted 346 nm in complex with Cu^{+2} and the peak 344 related to ligand had been shifted to 453 nm in complex with Cu^{+2} due to attributed the $\pi-\pi^*$ intra ligand transitions while the peak 478 nm in complex with Cu^{+2} assigned to metal –ligand charge transfer (MLCT) indicated at ST06 could interact with Cu^{+2} as shown in Figure 53.

The peak at 246 nm of ligand ST06 had been shifted to 289 nm in complex with Zn^{+2} and the peak 312 nm related to ligand had been shifted 327 nm in complex with Zn^{+2} and the peak 344 related to ligand had been shifted to 386 nm in complex with Zn^{+2} due to attributed the $\pi-\pi^*$ intra ligand transitions indicated at ST06 could interact with Zn^{+2} as shown in Figure 54.

The peak at 259 nm of ligand ST07 had been shifted to 279 nm in complex with Cu^{+2} and the peak 282 nm related to ligand had been shifted to 313 nm in complex with Cu^{+2} due to attributed the $\pi-\pi^*$ intra ligand transitions indicated at ST07 could interact with Cu^{+2} as shown in Figure 55.

Whereas the peak at 259 nm of ligand ST07 had been shifted to 274 in complex with Zn^{+2} and the peak 282 nm related to ligand had been shifted to 309 nm in complex with Zn^{+2} due to attributed the $\pi-\pi^*$ intra ligand transitions while the peak 384 nm in complex with Zn^{+2} assigned to metal –ligand charge transfer (MLCT) indicated that ST07 could interact with Zn^{+2} as shown in Figure 56.

The peak at 256 nm of ligand ST08 had been shifted to 290 nm in complex with Cu^{+2} and the peak 341 related to ligand had been shifted to 386 nm due to attributed the $\pi-\pi^*$ intra ligand transitions while the peak 480 nm in complex with Cu^{+2} assigned to metal –ligand charge transfer (MLCT) indicated that ST08 could interact with Cu^{+2} as shown in Figure 57.

Whereas the peak at 256 nm of ligand ST08 had been shifted to 297 nm in complex with Zn^{+2} and the peak 341 nm related to ligand had been shifted to 381 nm in complex with Zn^{+2} assigned to metal –ligand charge transfer (MLCT) indicated that ST08 could interact with Zn^{+2} as shown in Figure 58.

The peak at 266 nm of ligand ST09 had been shifted to 292 nm in complex with Cu^{+2} and the peak at 303 nm related to ligand had been shifted to 318 nm in complex with Cu^{+2} and the peak at 390 nm related to ligand had been shifted to 470 nm in complex with Cu^{+2} due to attributed the $\pi-\pi^*$ intra ligand transitions while the peak 497 nm in complex with Cu^{+2} assigned to metal –ligand charge transfer (MLCT) indicated that ST09 could interact with Cu^{+2} as shown in Figure 59.

The peak at 266 nm of ligand ST09 had been shifted 286 nm in complex with Zn^{+2} and the peak at 303 nm related to ligand had been shifted to 316 nm in complex with Zn^{+2} while the peak 390 nm related to ligand had been shifted to 446 nm in complex with Zn^{+2} due to attributed the $\pi-\pi^*$ intra ligand transitions indicated that ST09 could interact with Zn^{+2} as shown in Figure 60.

The peak at 264 nm of ligand ST10 had been shifted to 278 nm in complex with Cu^{+2} and the peak at 301 nm related to ligand had been shifted to 311 nm in complex with Cu^{+2} due to attributed the $\pi-\pi^*$ intra ligand transitions while the peak 388 nm in complex with Cu^{+2} assigned to metal –ligand charge transfer (MLCT) indicated that ST10 could interact with Cu^{+2} as shown in Figure 61.

The peak at 264 nm of ligand ST10 had been shifted to 274 nm in complex with Zn^{+2} and the peak at 301 nm related to ligand had been shifted to 309 nm in complex with Zn^{+2} due to attributed the $\pi-\pi^*$ intra ligand transitions while the peak 390 nm in complex with Zn^{+2} assigned to metal –ligand charge transfer (MLCT) indicated that ST10 could interact with Zn^{+2} as shown in Figure 62.

The peak at 257 nm of ligand ST11 had been shifted to 300 nm in complex with Cu^{+2} due to attributed the $\pi-\pi^*$ intra ligand transitions and the peak at 305 nm related to ligand had been shifted to 317 nm in complex with Cu^{+2} assigned to metal –ligand charge transfer (MLCT) indicated that ST11 could interact with Cu^{+2} as shown in Figure 63.

The peak at 257 nm of ligand ST11 had been shifted to 302 nm in the complex with Zn^{+2} due to attributed the $\pi-\pi^*$ intra ligand transitions and the peak 305 nm related to ligand had been shifted to 314 nm in the complex with Zn^{+2} assigned to metal –ligand charge transfer (MLCT) indicated that ST11 could interact with Zn^{+2} as shown in Figure 64.

The peak at 258 nm of ligand ST12 had been shifted to 305 nm in complex with Cu^{+2} due to attributed the $\pi-\pi^*$ intra ligand transitions and the peak 304 nm related to ligand had been shifted to 321 nm in complex with Cu^{+2} assigned to metal –ligand charge transfer (MLCT) indicated that ST12 could interact with Cu^{+2} as shown in Figure 65.

Whereas the peak at 258 nm of ligand ST12 had been shifted to 302 nm in complex with Zn^{+2} and the peak 304 nm related to ligand had been shifted to 317 nm in complex with Zn^{+2} assigned to metal –ligand charge transfer (MLCT) indicated that ST12 could interact with Zn^{+2} as shown in Figure 66.

The peak at 244 nm of ligand ST13 had been shifted to 302 nm in complex with Cu^{+2} due to attributed the $\pi-\pi^*$ intra ligand transitions and the peak 308 nm related to ligand had been shifted to 343 nm in complex with Cu^{+2} assigned to metal –ligand charge transfer (MLCT) indicated that ST13 could interact with Cu^{+2} as shown in Figure 67.

The peak at 244 nm in ligand ST13 had been shifted to 307 nm in complex with Zn^{+2} due to attributed the $\pi-\pi^*$ intra ligand transitions and the peak 308 related to ligand had been shifted to 340 nm in complex with Zn^{+2} assigned to metal –ligand charge transfer (MLCT) indicated that interact with Zn^{+2} as shown in Figure 68.

The peak at 258 nm in ligand ST14 had been shifted to 302 nm in complex with Cu^{+2} due to attributed the $\pi-\pi^*$ intra ligand transitions and the peak 318 nm in complex with Cu^{+2} assigned to metal –ligand charge transfer (MLCT) indicated that ST14 could interact with Cu^{+2} as shown in Figure 69.

Whereas the peak at 258 nm in ligand ST14 had been shifted to 269 nm in complex with Zn^{+2} due to attributed the $\pi-\pi^*$ intra ligand transitions and the peak 311 nm in complex with Zn^{+2} assigned to metal –ligand charge transfer (MLCT) indicated that ST14 could interact with Zn^{+2} as shown in Figure 70.

The peak at 257 nm in ligand ST15 had been shifted to 260 nm in complex with Cu^{+2} due to attributed the $\pi-\pi^*$ intra ligand transitions and the peak 319 nm in complex with Cu^{+2} assigned to metal –ligand charge transfer (MLCT) indicated that ST15 could interact with Cu^{+2} as shown in Figure 71.

Whereas the peak at 257 nm in ligand ST15 had been shifted to 258 nm in complex with Zn^{+2} due to attributed the $\pi-\pi^*$ intra ligand transitions and the peak 314 nm in complex with Zn^{+2} assigned to metal –ligand charge transfer (MLCT) indicated that ST15 could interact with Zn^{+2} as shown in Figure 72.

The peak at 260 nm in ligand ST16 had been shifted to 314 nm in complex with Cu^{+2} due to attributed the $\pi-\pi^*$ intra ligand transitions indicated that ST16 could interact with Cu^{+2} as shown in Figure 73.

Whereas the peak at 260 nm in ligand ST16 shift to 302 nm in complex with Zn^{+2} due to attributed the $\pi-\pi^*$ intra ligand transitions and the peak 312 nm in complex with Zn^{+2} assigned to metal –ligand charge transfer (MLCT) indicated that ST16 could interact with Zn^{+2} as shown in Figure 74.

The peak at 258 nm in ligand ST17 had been shifted to 304 nm in complex with Cu^{+2} due to attributed the $\pi-\pi^*$ intra ligand transitions and the peak at 317 nm in complex with Cu^{+2} assigned to metal –ligand charge transfer (MLCT) indicated that ST17 could interact with Cu^{+2} as shown in Figure 75.

Whereas the peak at 258 nm in ligand ST17 had been shifted to 296 nm in complex with Zn^{+2} due to attributed the $\pi-\pi^*$ intra ligand transitions and the peak at 311 nm in complex with Zn^{+2} assigned to metal –ligand charge transfer (MLCT) indicated that ST17 could interact with Zn^{+2} as shown in Figure 76.

The peak at 260 nm in ligand ST18 had been shifted to 305 in complex with Cu^{+2} due to attributed the $\pi-\pi^*$ intra ligand transitions and the peak at 315 nm in complex with Cu^{+2} assigned to metal –ligand charge transfer (MLCT) indicated that ST18 could interact with Cu^{+2} as shown in Figure 77.

Where as the peak at 260 nm in ligand ST18 had been shifted to 300 nm in complex with Zn^{+2} due to attributed the $\pi-\pi^*$ intra ligand transitions and the peak 313 nm in complex with Zn^{+2} assigned to metal –ligand charge transfer (MLCT) indicated that ST18 could interact with Zn^{+2} as shown in Figure 78.

The peak at 254 nm in ligand ST19 had been shifted to 276 nm in complex with Cu^{+2} due to attributed the $\pi-\pi^*$ intra ligand transitions and the peak 360 nm and 378 nm in complex with Cu^{+2} assigned to metal –ligand charge transfer (MLCT) indicated that ST19 could interact with Cu^{+2} as shown in Figure 79.

Where as the peak at 254 nm in ligand ST19 had been shifted to 274 nm in complex with Zn^{+2} due to attributed the $\pi-\pi^*$ intra ligand transitions and the peak 364 nm and 378 nm in complex with Zn^{+2} assigned to metal –ligand charge transfer (MLCT) indicated that ST19 could interact with Zn^{+2} as shown in Figure 80.

The peak at 259 nm in ligand ST20 had been shifted to 300 nm in complex with Cu^{+2} and the peak at 316 nm in complex with Cu^{+2} assigned to metal –ligand charge transfer (MLCT) indicated that ST20 could interact with Cu^{+2} as shown in Figure 81.

Whereas the peak at 259 nm in ligand ST20 had been shifted to 298 nm in complex with Zn^{+2} due to attributed the $\pi-\pi^*$ intra ligand transitions and the peak at 311 nm in complex with Zn^{+2} assigned to metal –ligand charge transfer (MLCT) indicated that ST20 could interact with Zn^{+2} as shown in Figure 82.

The peak at 261 nm in ligand ST21 had been shifted to 282 nm in complex with Cu^{+2} and the peak 305 nm related to ligand had been shifted to 316 nm in complex with Cu^{+2} due to attributed the $\pi-\pi^*$ intra ligand transitions related to ligand had been and the peak at 342 nm in complex with Cu^{+2} assigned to metal –ligand charge transfer (MLCT) indicated that ST21 could interact with Cu^{+2} as shown in Figure 83.

Whereas the peak at 261 nm in ligand ST21 had been shifted to 285 nm in complex with Zn^{+2} and the peak 305 nm related to ligand had been shifted to 315 nm in complex with Zn^{+2} due to attributed the $\pi-\pi^*$ intra ligand transitions and the peak at 345 nm in complex with Zn^{+2} assigned to metal –ligand charge transfer (MLCT) indicated that ST21 could interact with Zn^{+2} as shown in Figure 84.

The peak at 254 nm in ligand ST22 had been shifted to 303 nm in complex with Cu^{+2} due to attributed the $\pi-\pi^*$ intra ligand transitions and the peak at 305 related to ligand had been shifted to 317 nm in complex with Cu^{+2} assigned to metal –ligand charge transfer (MLCT) indicated that ST22 could interact with Cu^{+2} as shown in Figure 85.

Whereas the peak at 254 nm in ligand ST22 had been shifted to 299 nm in complex with Zn^{+2} due to attributed the $\pi-\pi^*$ intra ligand and the peak 305 nm related to ligand had been shifted to 312 nm in complex with Zn^{+2} assigned to metal –ligand charge transfer (MLCT) indicated that ST22 could interact with Zn^{+2} as shown in Figure 86.

The peak at 249 nm in ligand ST23 had been shifted to 283 nm in complex with Cu^{+2} and the peak at 271 nm related to ligand had been shifted to 305 nm in complex with Cu^{+2} due to attributed the $\pi-\pi^*$ intra ligand transitions while the peak at 347 nm in in complex with Cu^{+2} assigned to metal –ligand charge transfer (MLCT) indicated that ST23 could interact with Cu^{+2} as shown in Figure 87.

Whereas the peak at 249 nm in ligand ST23 had been shifted to 279 nm in complex with Zn^{+2} and the peak at 271 related to ligand had been shifted to 301 nm in complex with Zn^{+2} due to attributed the $\pi-\pi^*$ intra ligand transitions while the peak at 407 nm in complex with Zn^{+2} assigned to metal –ligand charge transfer (MLCT) indicated that ST23 could interact with Zn^{+2} as shown in Figure 88.

The peak at 252 nm in ligand ST24 had been shifted to 260 nm in complex with Cu^{+2} and the peak at 301 nm related to ligand had been shifted to 327 nm in complex with Cu^{+2} due to attributed the $\pi-\pi^*$ intra ligand transitions while the peak at 338 nm in complex with Cu^{+2} assigned to metal –ligand charge transfer (MLCT) indicated that ST24 could interact with Cu^{+2} as shown in Figure 89.

Whereas the peak at 252 nm in ligand ST24 had been shifted to 259 nm in complex with Zn^{+2} and the peak at 301 nm related to ligand had been shifted to 324 nm in complex with Zn^{+2} due to attributed the $\pi-\pi^*$ intra ligand transitions while the peak at 337 nm in complex with Zn^{+2} assigned to metal –ligand charge transfer (MLCT) indicated that ST24 could interact with Zn^{+2} as shown in Figure 90.

4.4 Conclusions

We have demonstrated in this chapter that phen-5,6-dione complexes with Cu^{+2} and Zn^{+2} have a similarities in absorption spectra including $\pi-\pi^*$ intra ligand transitions and a strong metal – ligand charge transfer (MLCT) in visible region. This hypothesis will support the idea that the phen-5,6-dione structure and electronic properties of this ligand incorporate features of both diamine and quinone ligands. May be beneficial in decreasing the rate of cognitive decline in moderate to server AD patients.

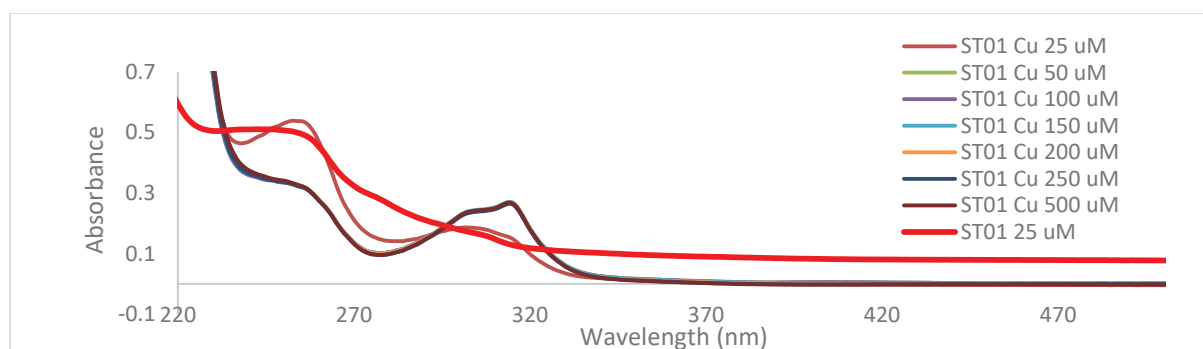


Figure 43: UV-Vis spectra of the ST01 at 25 uM at different concentration of Cu^{+2} in buffer at pH 7.4

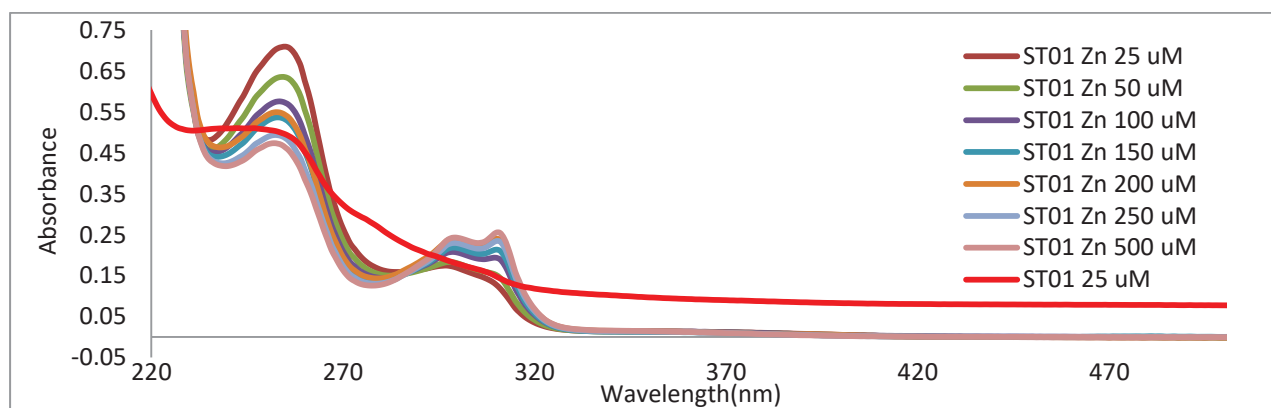


Figure 44: UV-Vis spectra of the ST01 at 25 uM at different concentration of Zn^{+2} in buffer pH 7.4

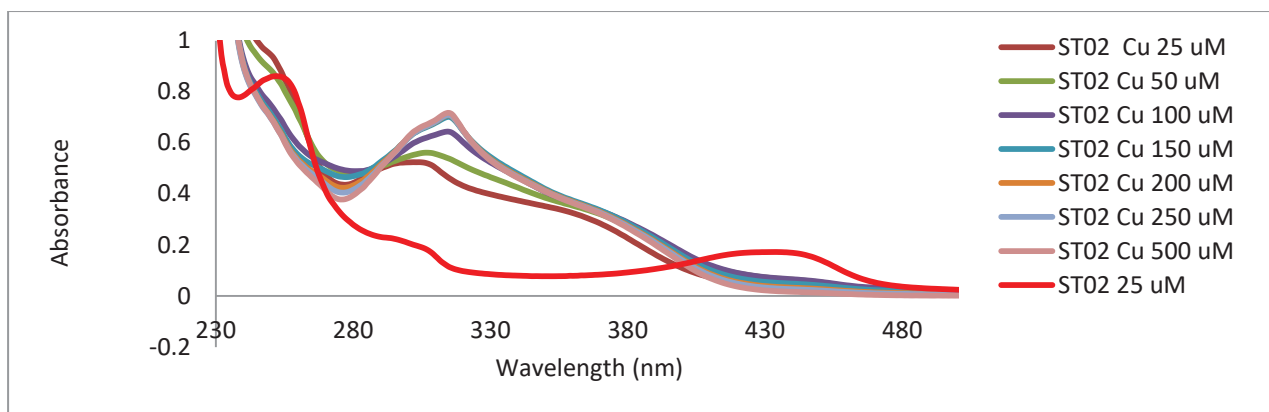


Figure 45: UV-Vis spectra of the ST02 at 25 uM at different concentration of Cu^{+2} in buffer pH 7.4

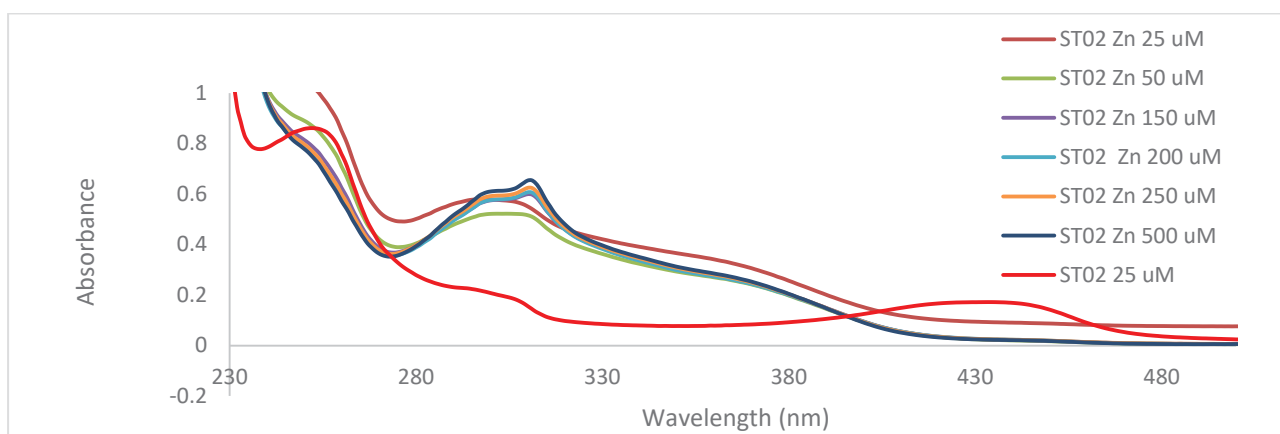


Figure 46: UV-Vis spectra of the ST02 at 25 uM at different concentration of Zn^{+2} in buffer pH 7.4

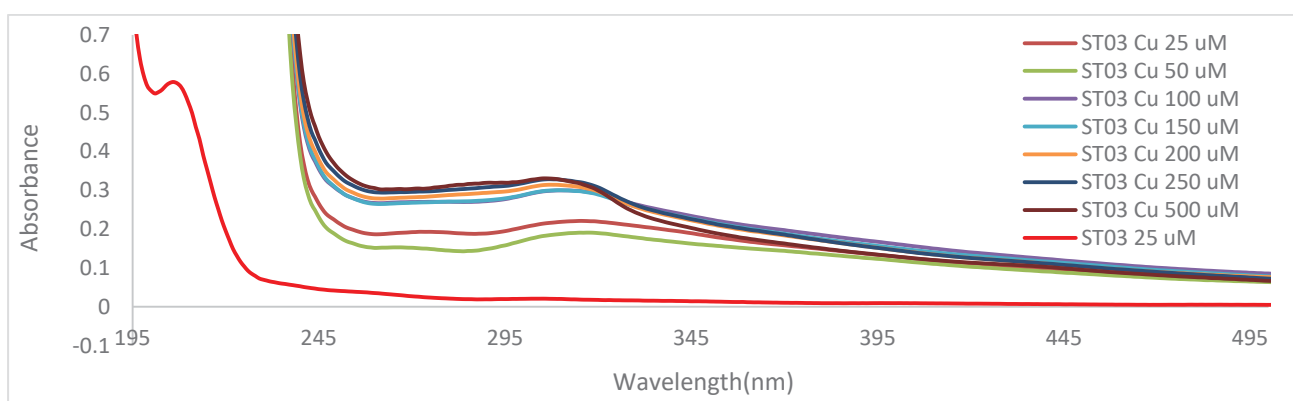


Figure 47: UV-Vis spectra of the ST03 at 25 uM at different concentration of Cu^{+2} in buffer at pH 7.4

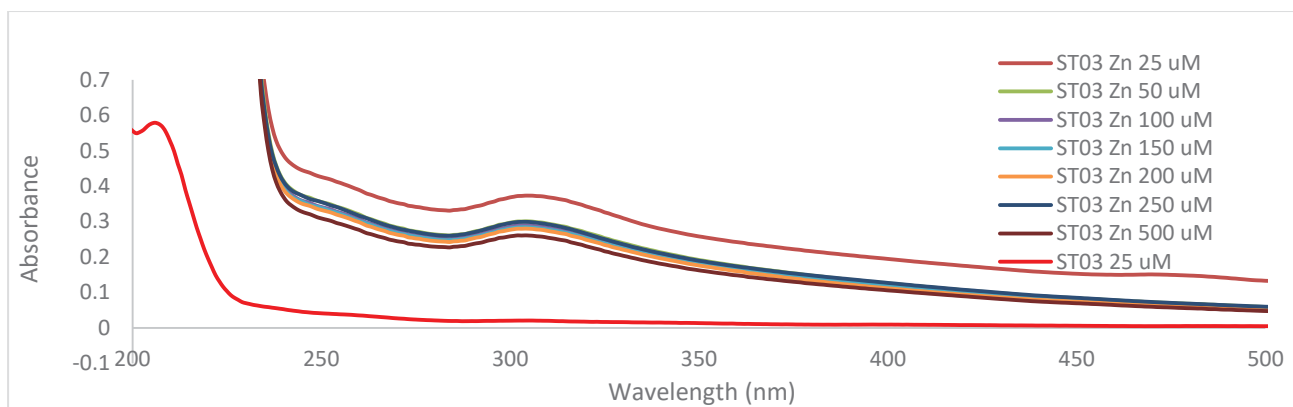


Figure 48: UV-Vis spectra of the ST03 at 25 uM at different concentration of Zn^{+2} in buffer pH 7.4

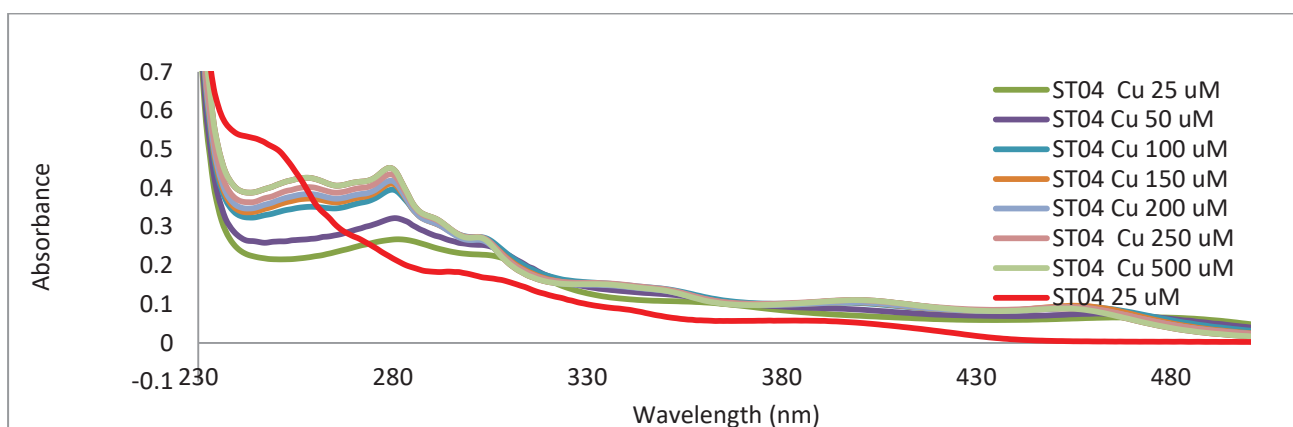


Figure 49: UV-Vis spectra of the ST04 at 25 uM at different concentration of Cu^{+2} in buffer at pH 7.4

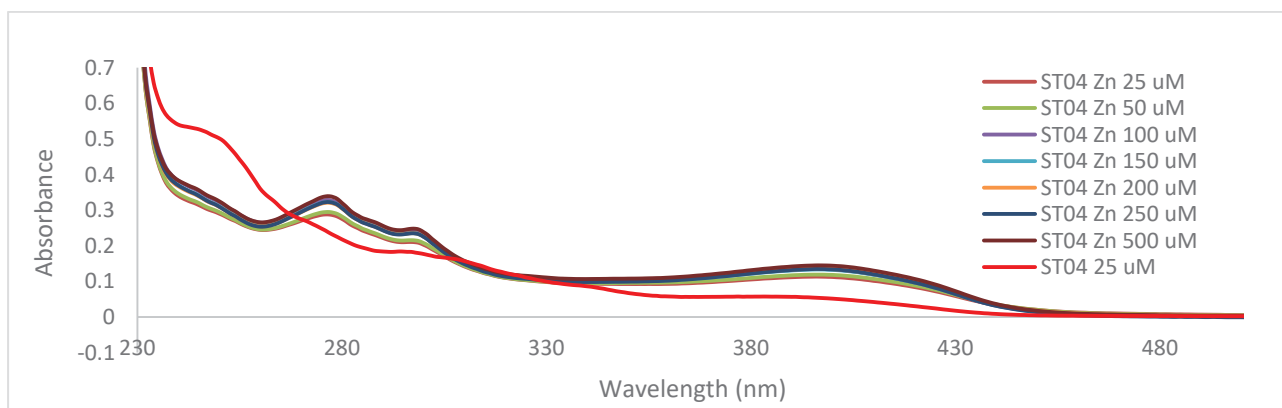


Figure 50: UV-Vis spectra of the ST04 at 25 uM at different concentration of Zn^{+2} in buffer pH 7.4

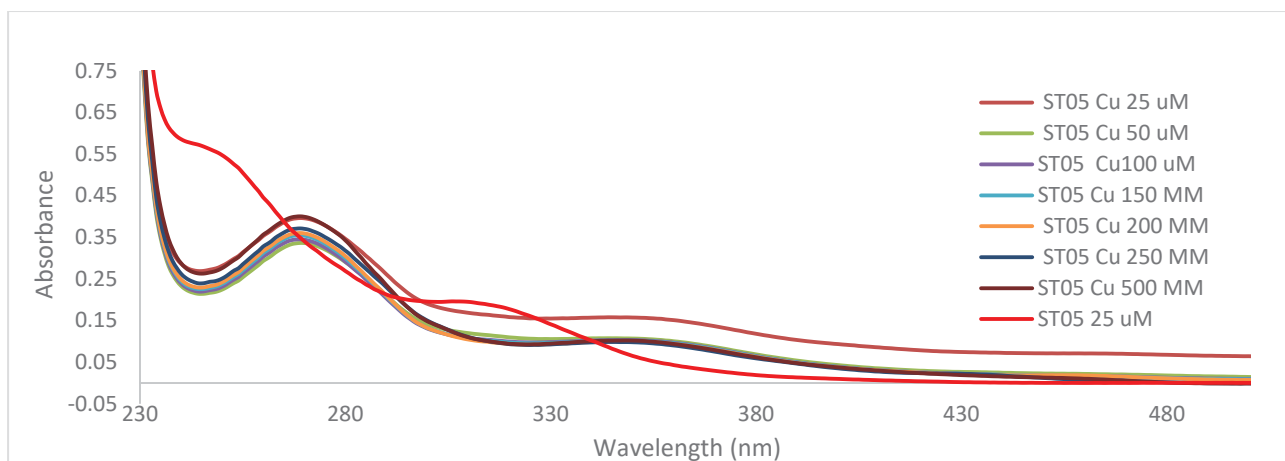


Figure 51: UV-Vis spectra of the ST05 at 25 uM at different concentration of Cu⁺² in buffer at pH 7.4

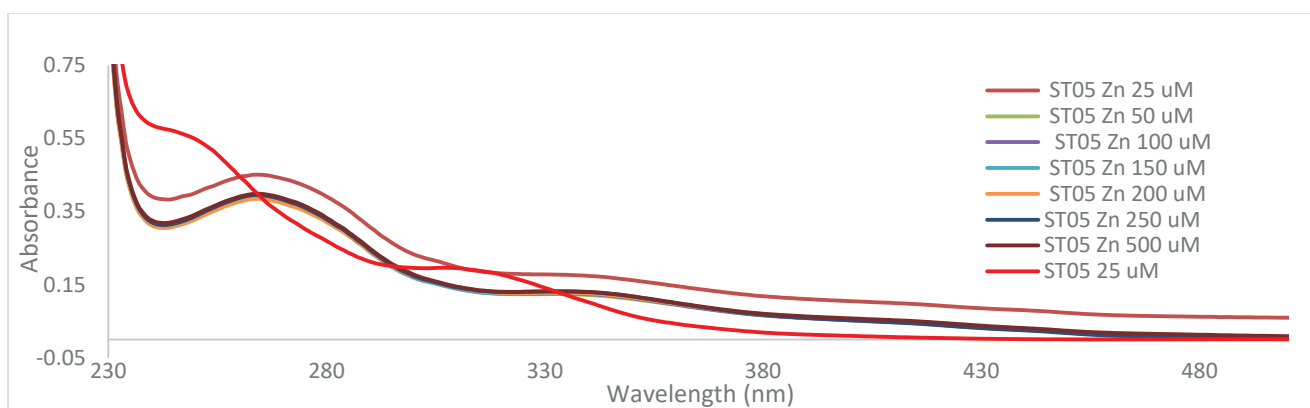


Figure 52: UV-Vis spectra of the ST05 at 25 uM at different concentration of Zn⁺² in buffer pH 7.4

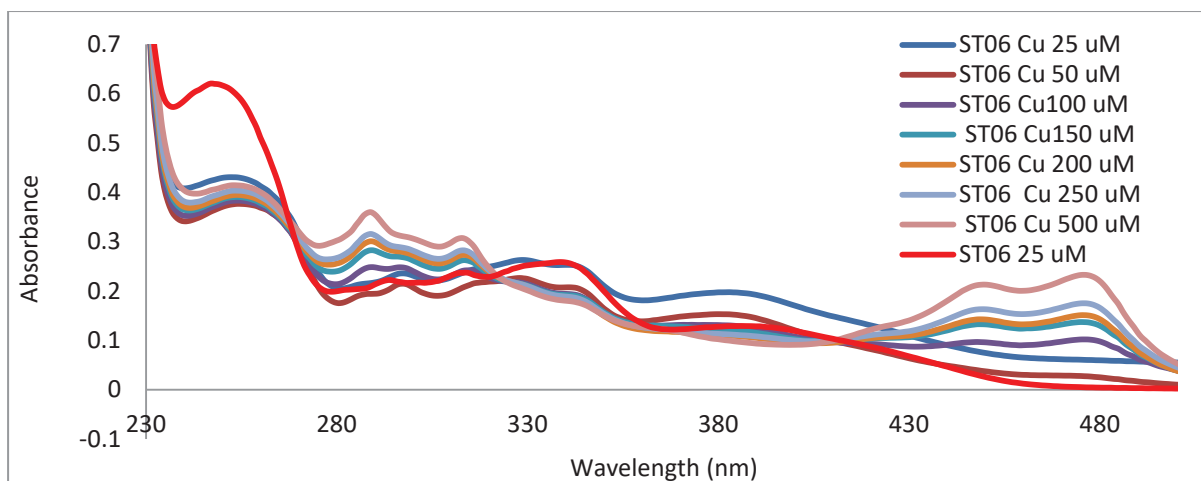


Figure 53: UV-Vis spectra of the ST06 at 25 uM at different concentration of Cu²⁺ in buffer at pH 7.4

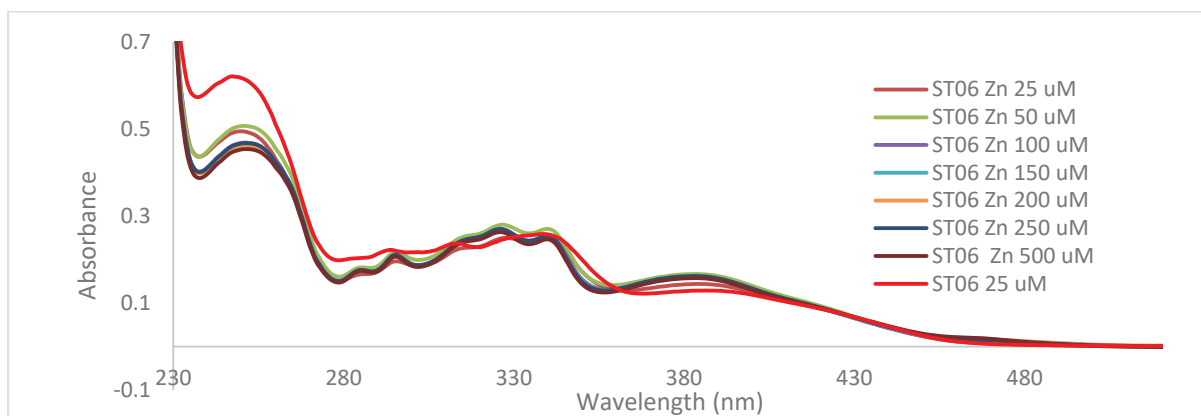


Figure 54: UV-Vis spectra of the ST06 at 25 uM at different concentration of Zn²⁺ in buffer pH 7.4

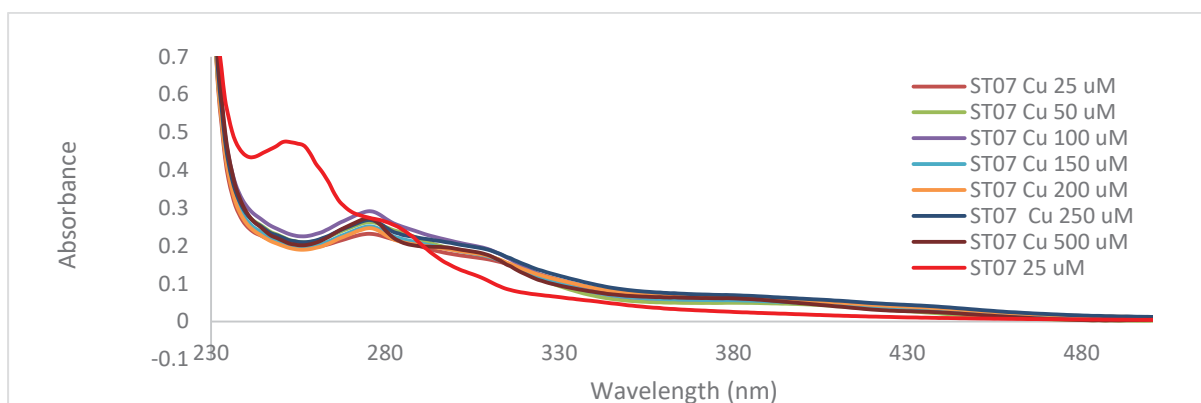


Figure 55: UV-Vis spectra of the ST07 at 25 uM at different concentration of Cu²⁺ in buffer at pH 7.4

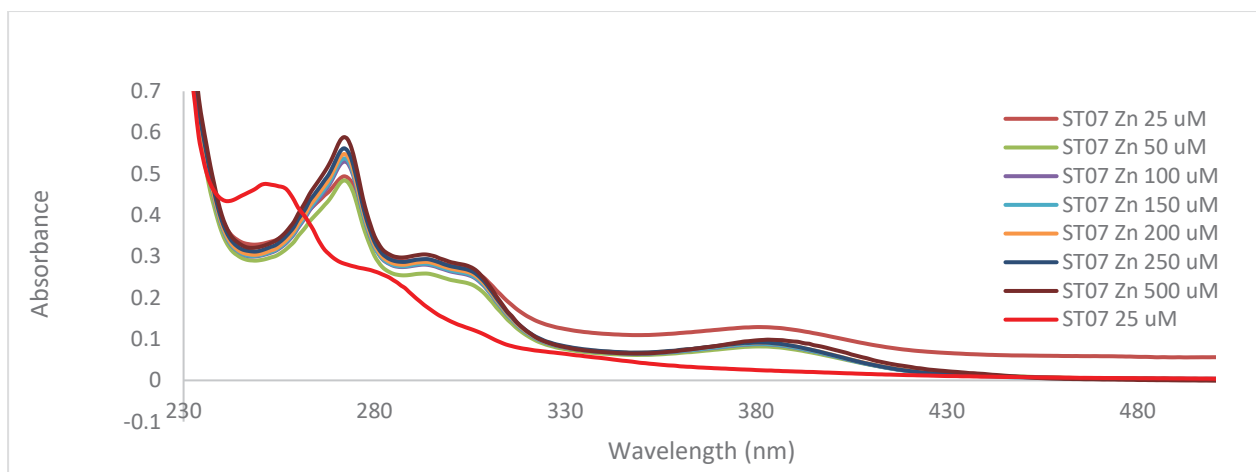


Figure 56: UV-Vis spectra of the ST07 at 25 uM at different concentration of Zn⁺² in buffer pH 7.4

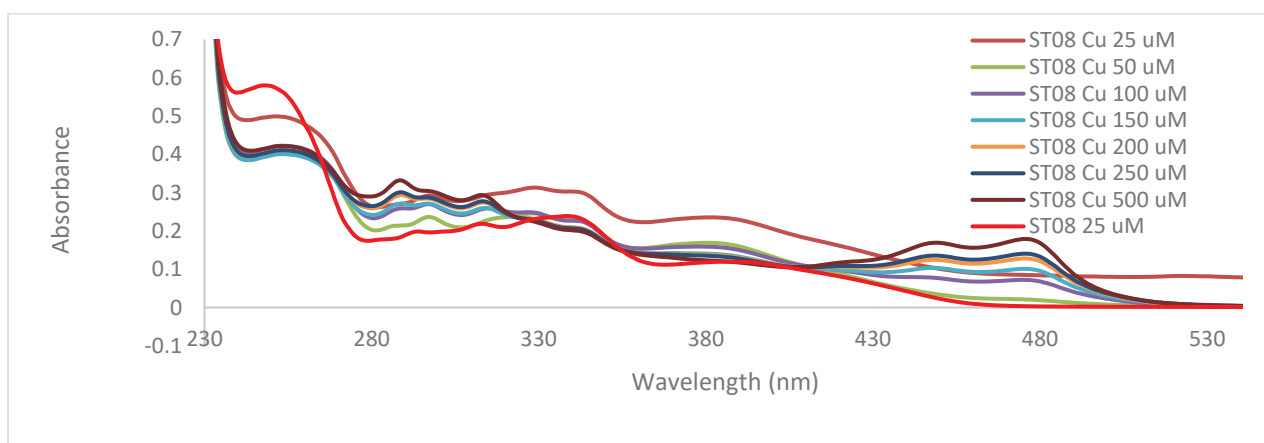


Figure 57: UV-Vis spectra of the ST08 at 25 uM at different concentration of Cu⁺² in buffer at pH 7.4

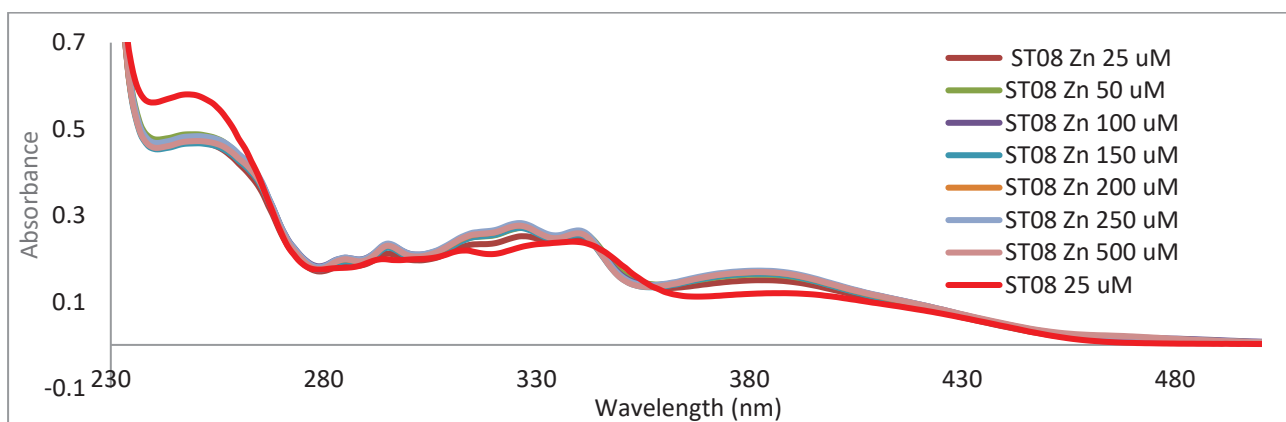


Figure 58: UV-Vis spectra of the ST08 at 25 uM at different concentration of Zn⁺² in buffer pH 7.4

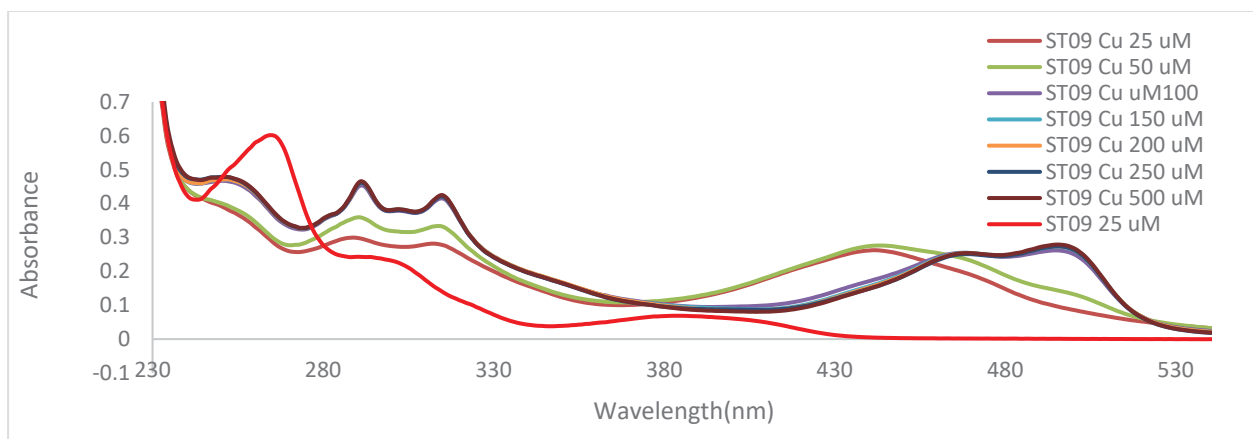


Figure 59: UV-Vis spectra of the ST09 at 25 uM at different concentration of Cu^{+2} in buffer at pH 7.4

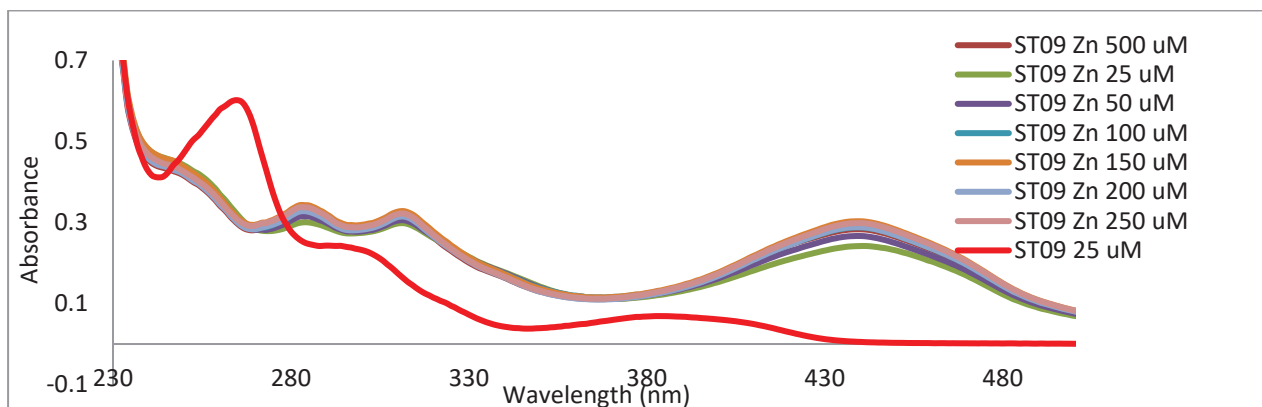


Figure 60: UV-Vis spectra of the ST09 at 25 uM at different concentration of Zn^{+2} in buffer pH 7.4

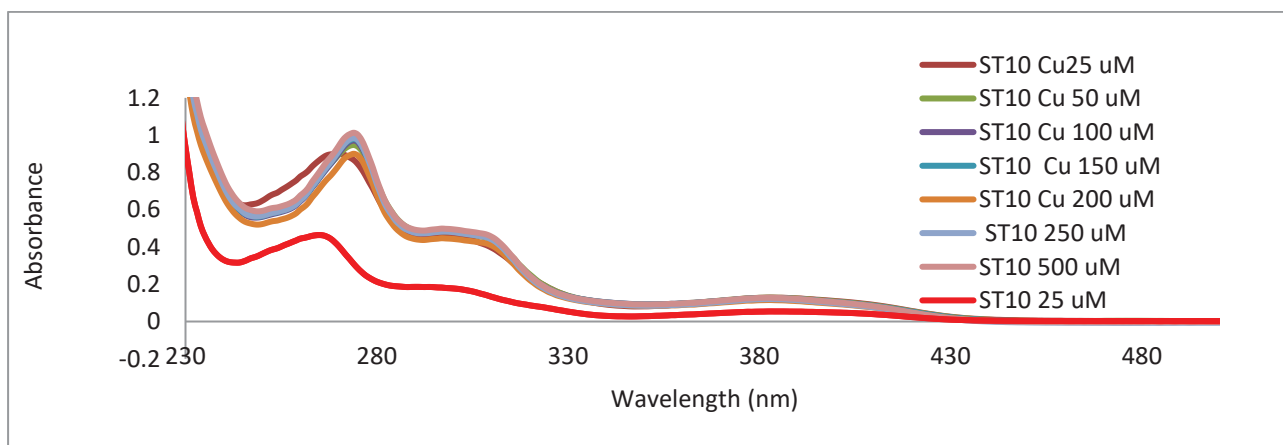


Figure 61: UV-Vis spectra of the ST10 at 25 uM at different concentration of Cu^{+2} in buffer at pH 7.4

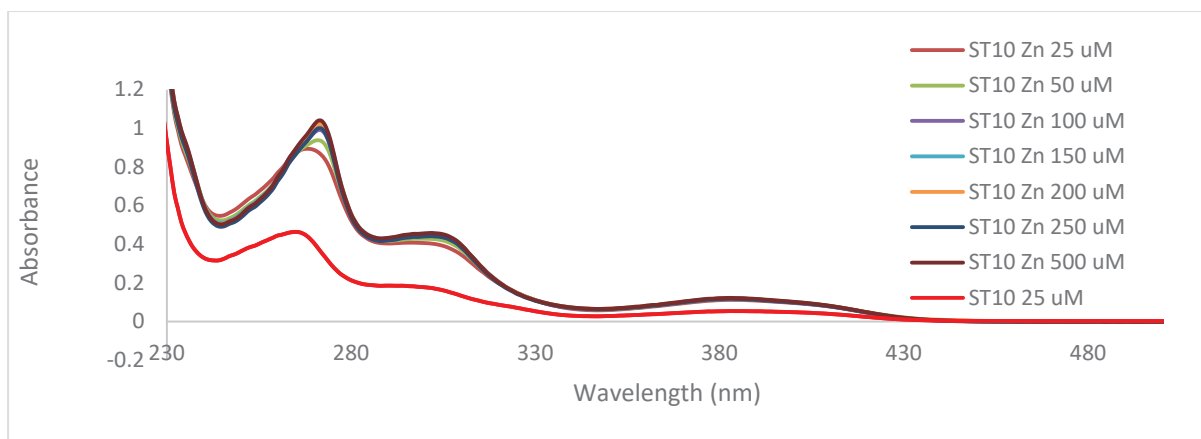


Figure 62: UV-Vis spectra of the ST10 at 25 uM at different concentration of Zn²⁺ in buffer pH 7.4

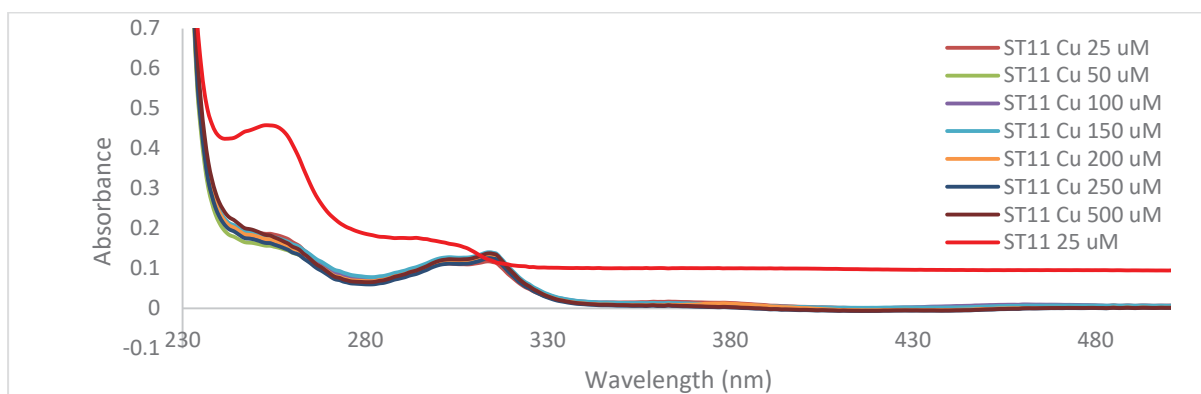


Figure 63: UV-Vis spectra of the ST11 at 25 uM at different concentration of Cu²⁺ in buffer at pH 7.4

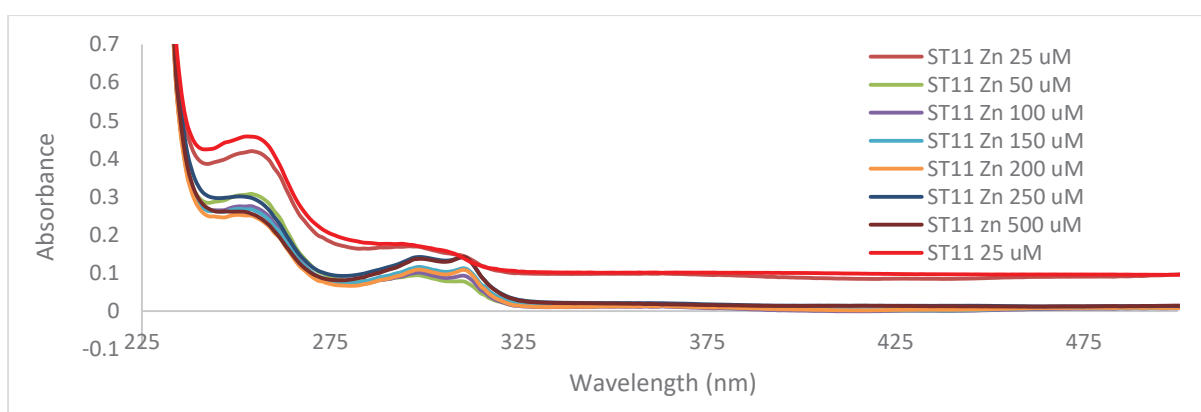


Figure 64: UV-Vis spectra of the ST11 at 25 uM at different concentration of Zn²⁺ in buffer pH 7.4

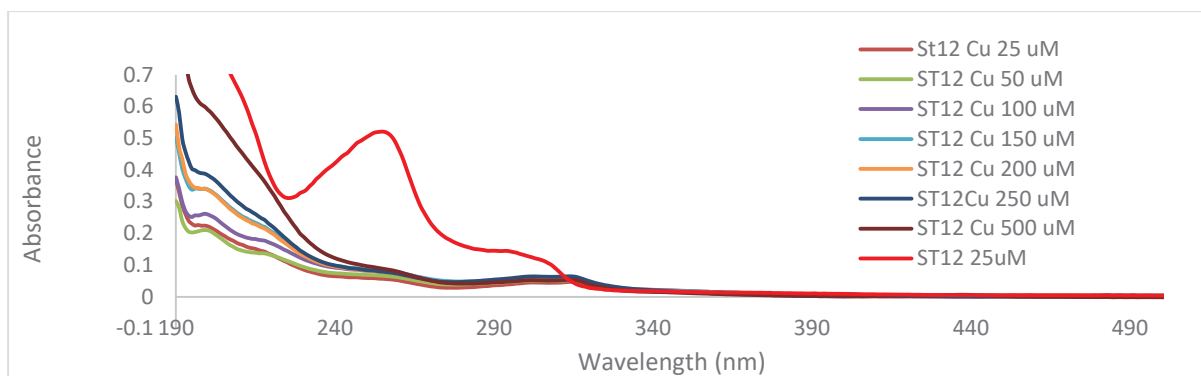


Figure 65: UV-Vis spectra of the ST012 at 25 uM at different concentration of Cu⁺² in buffer at pH 7.4

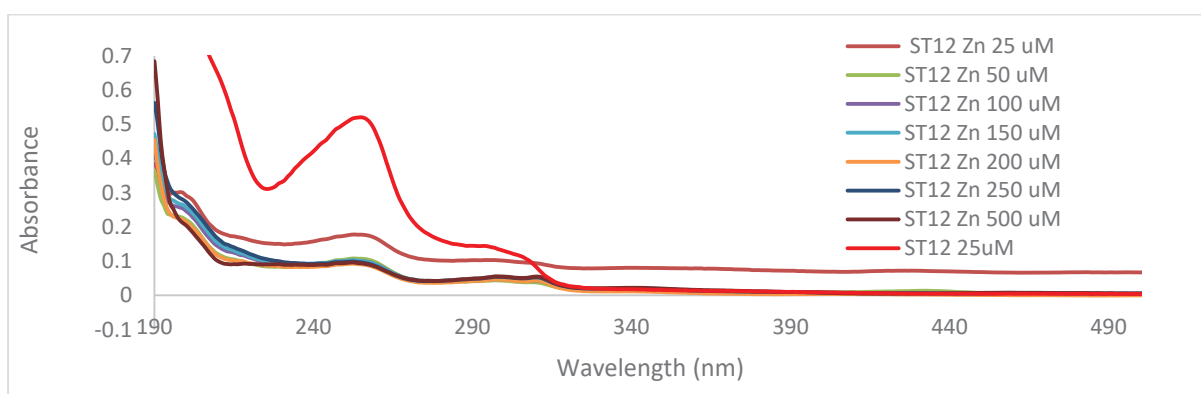


Figure 66: UV-Vis spectra of the ST12 at 25 uM at different concentration of Zn⁺² in buffer pH 7.4

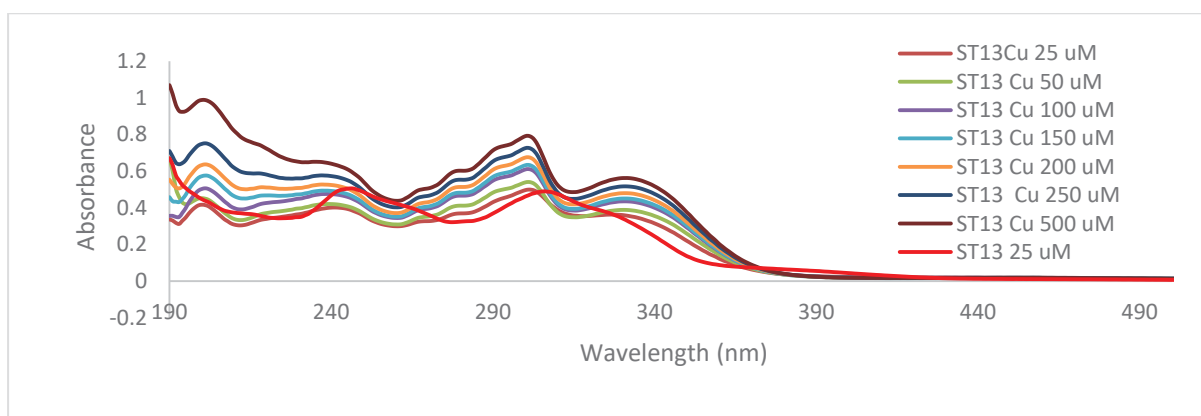


Figure 67: UV-Vis spectra of the ST13 at 25 uM at different concentration of Cu⁺² in buffer at pH 7.4

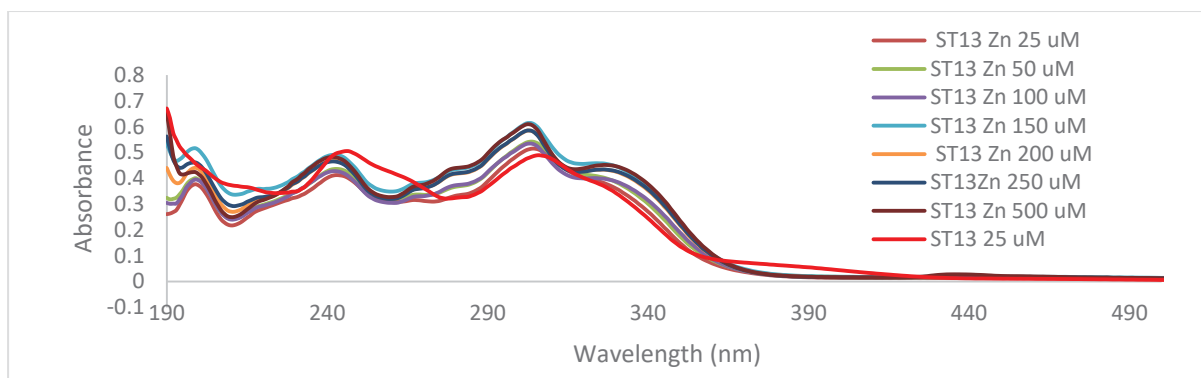


Figure 68: UV-Vis spectra of the ST13 at 25 uM at different concentration of Zn⁺² in buffer pH 7.4

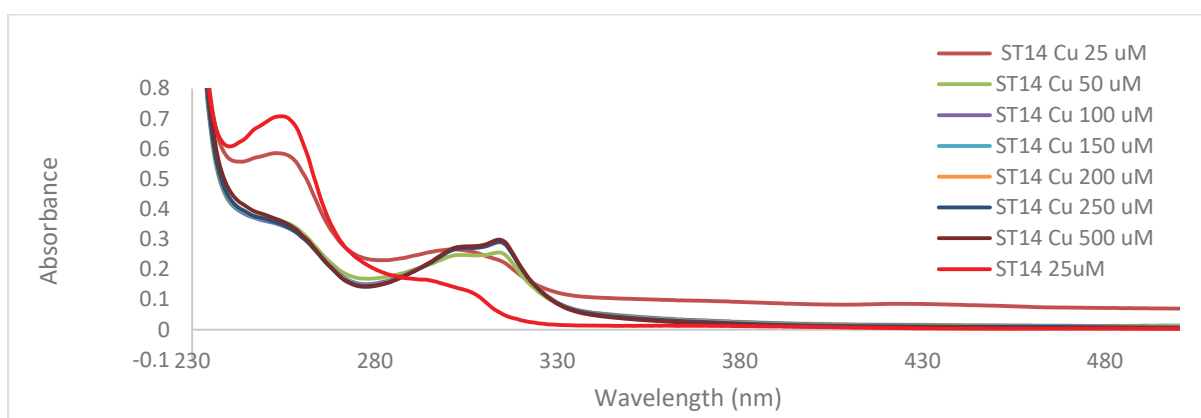


Figure 69: UV-Vis spectra of the ST14 at 25 uM at different concentration of Cu⁺² in buffer at pH 7.4

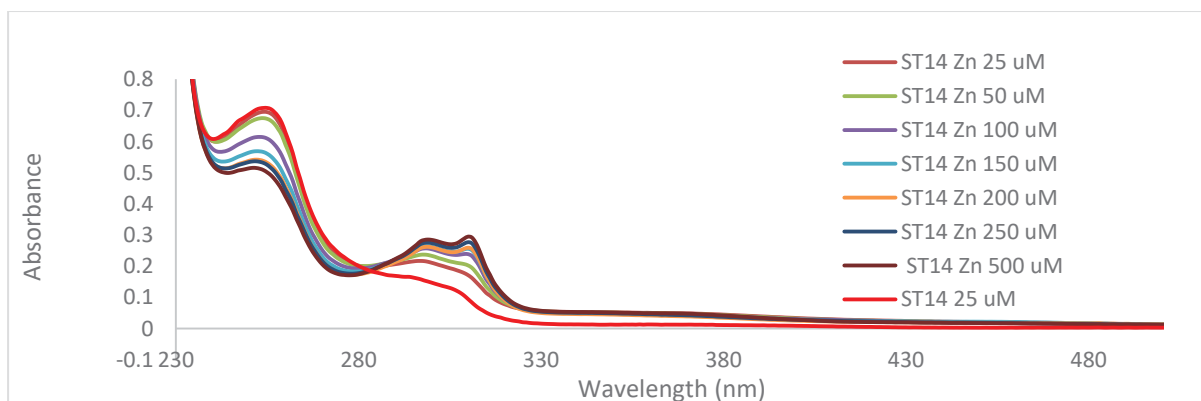


Figure 70: UV-Vis spectra of the ST14 at 25 uM at different concentration of Zn⁺² in buffer pH 7.4

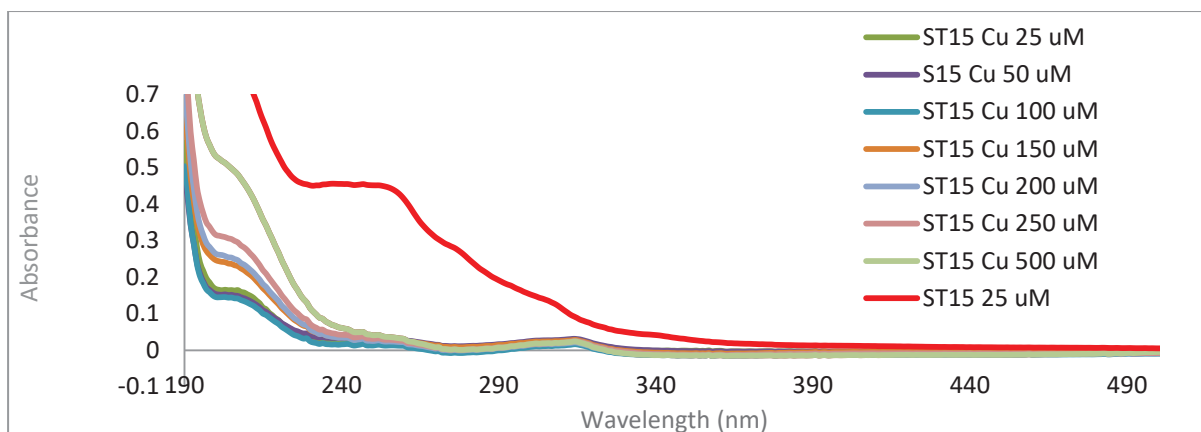


Figure 71: UV-Vis spectra of the ST15 at 25 uM at different concentration of Cu^{+2} in buffer at pH 7.4

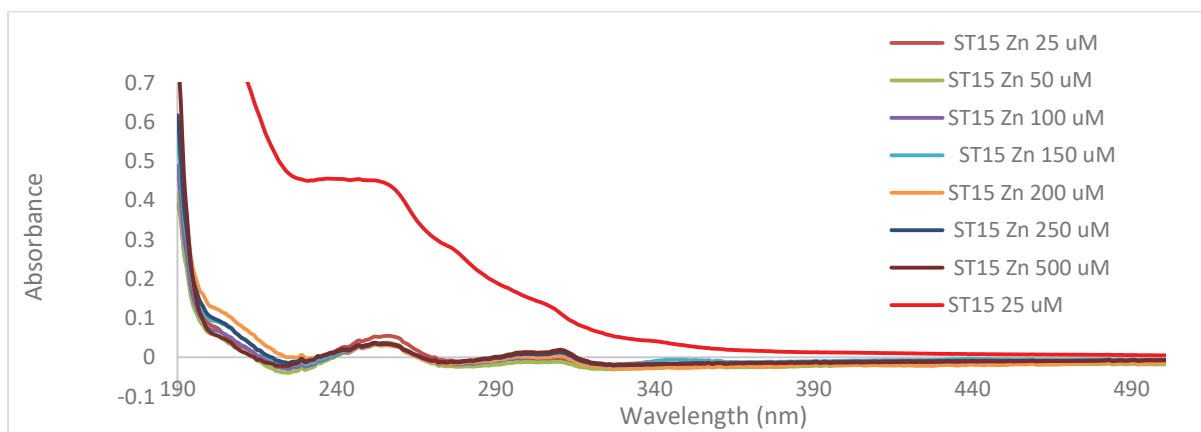


Figure 72: UV-Vis spectra of the ST15 at 25 uM at different concentration of Zn^{+2} in buffer pH 7.4

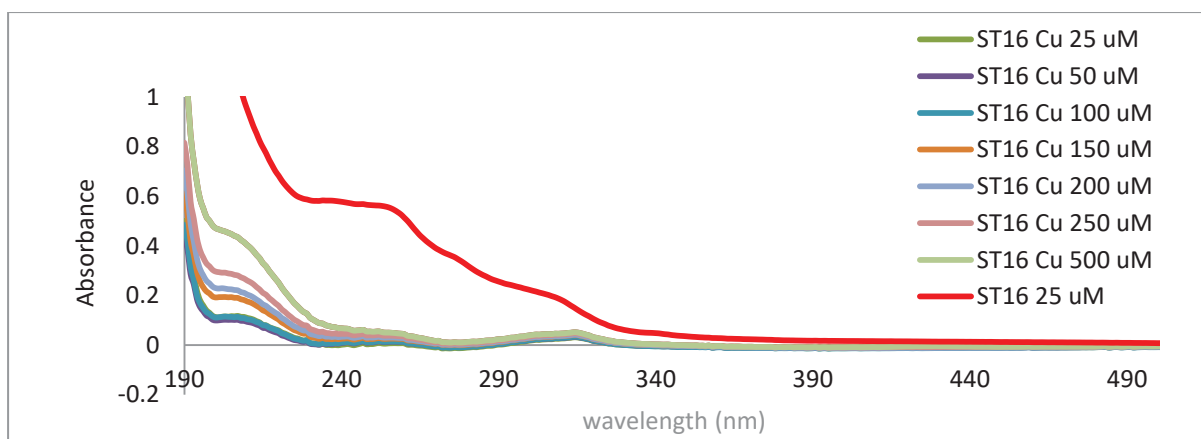


Figure 73: UV-Vis spectra of the ST16 at 25 uM at different concentration of Cu^{+2} in buffer at pH 7.4

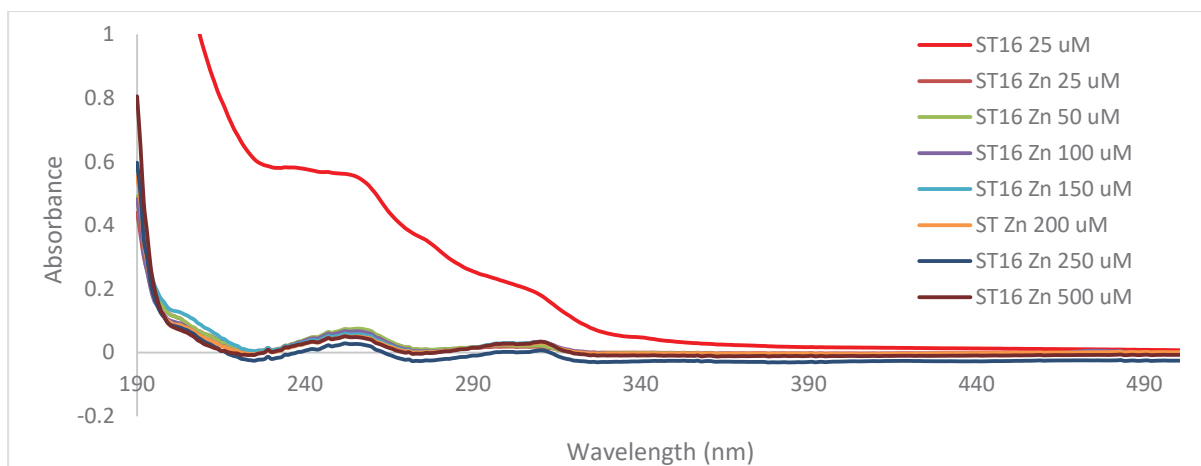


Figure 74: UV-Vis spectra of the ST016 at 25 uM at different concentration of Zn⁺² in buffer pH 7.4

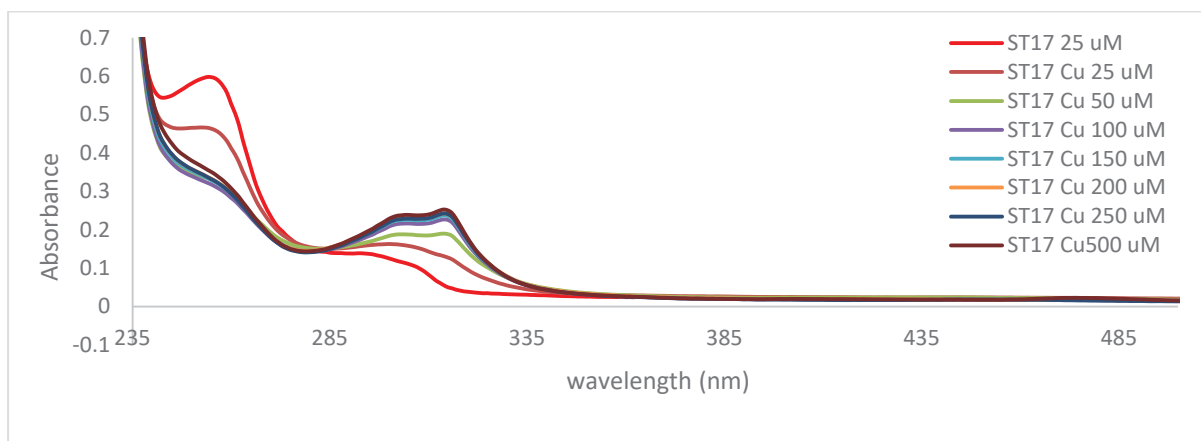


Figure 75: UV-Vis spectra of the ST17 at 25 uM at different concentration of Cu⁺² in buffer at pH 7.4

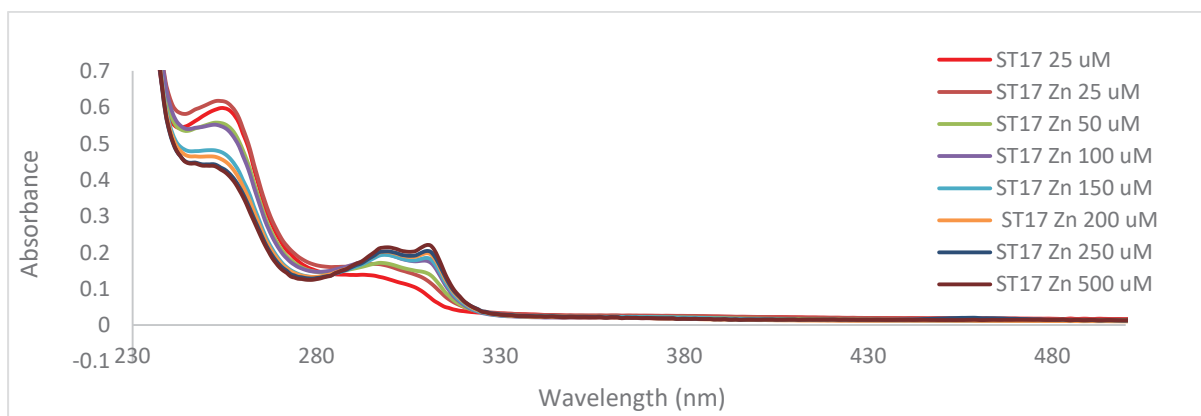


Figure 76: UV-Vis spectra of the ST017 at 25 uM at different concentration of Zn⁺² in buffer pH 7.4

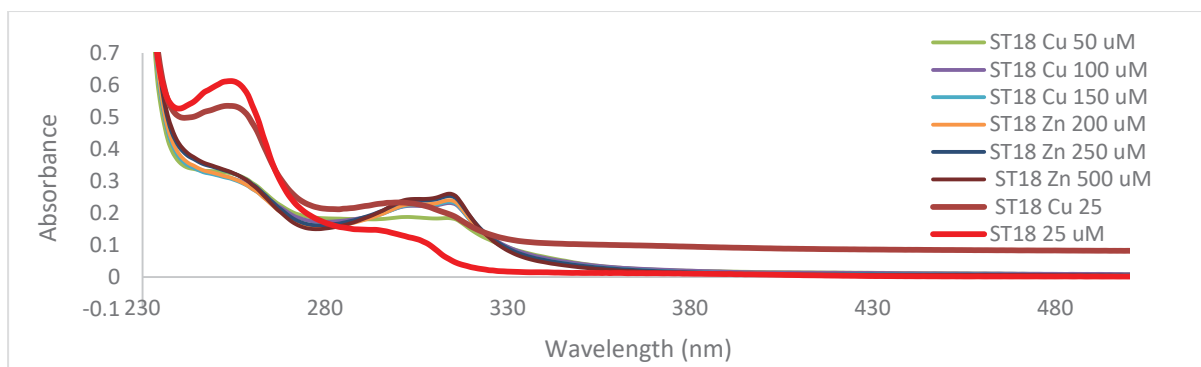


Figure 77: UV-Vis spectra of the ST18 at 25 uM at different concentration of Cu²⁺ in buffer at pH 7.4

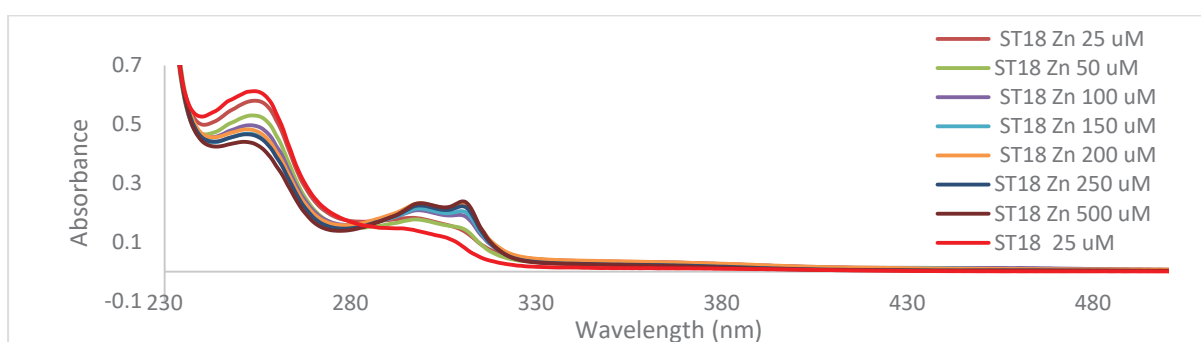


Figure 78: UV-Vis spectra of the ST18 at 25 uM at different concentration of Zn²⁺ in buffer pH 7.4

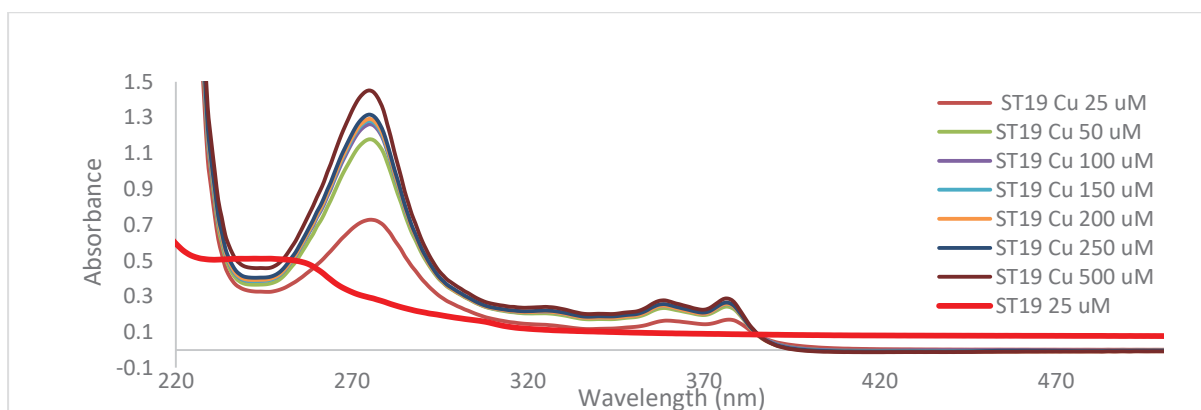


Figure 79: UV-Vis spectra of the ST19 at 25 uM at different concentration of Cu²⁺ in buffer at pH 7.4

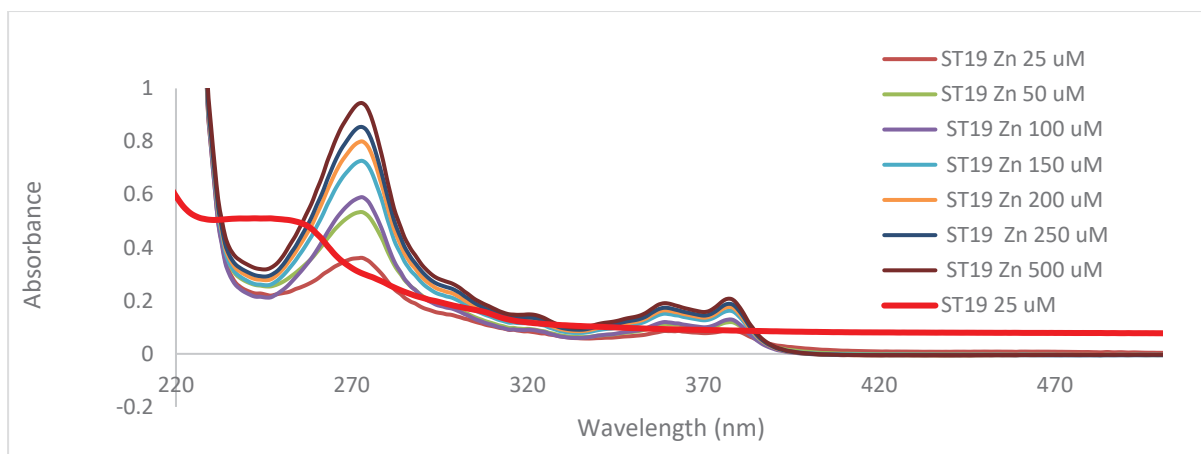


Figure 80: UV-Vis spectra of the ST19 at 25 uM at different concentration of Zn⁺² in buffer pH 7.4

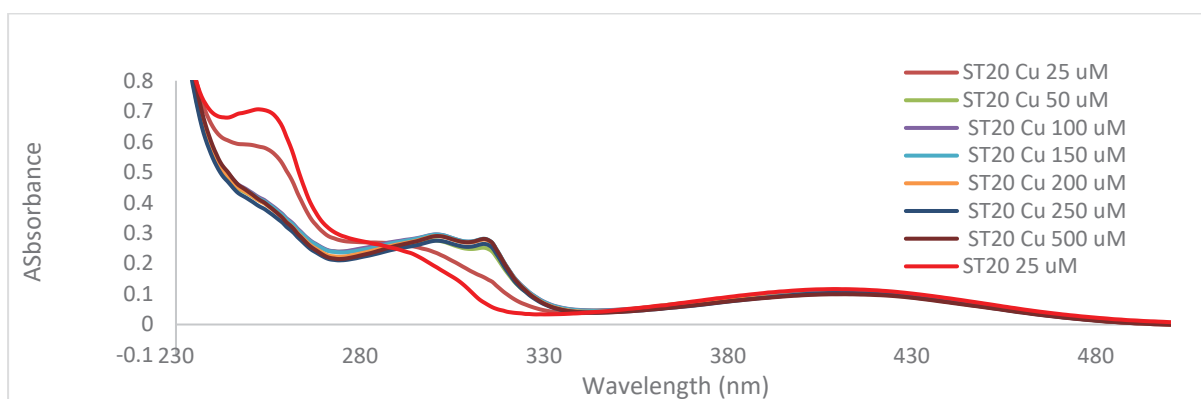


Figure 81: UV-Vis spectra of the ST 20 at 25 uM at different concentration of Cu⁺² in buffer at pH 7.4

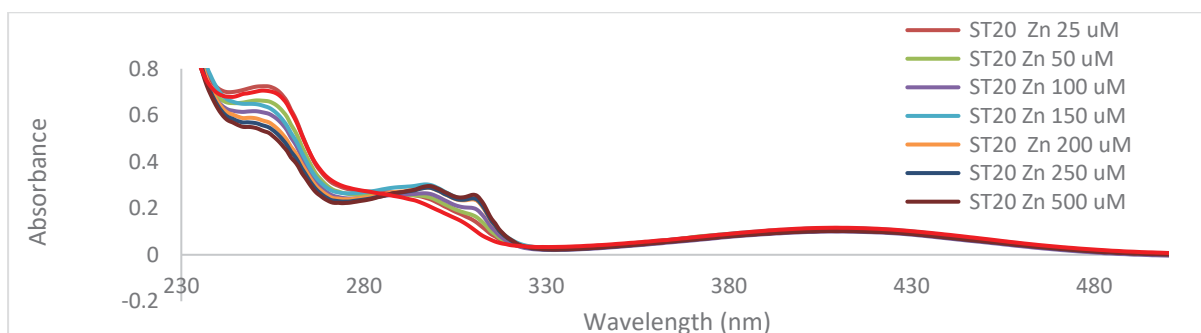


Figure 82: UV-Vis spectra of the ST20 at 25 uM at different concentration of Zn⁺² in buffer pH 7.4

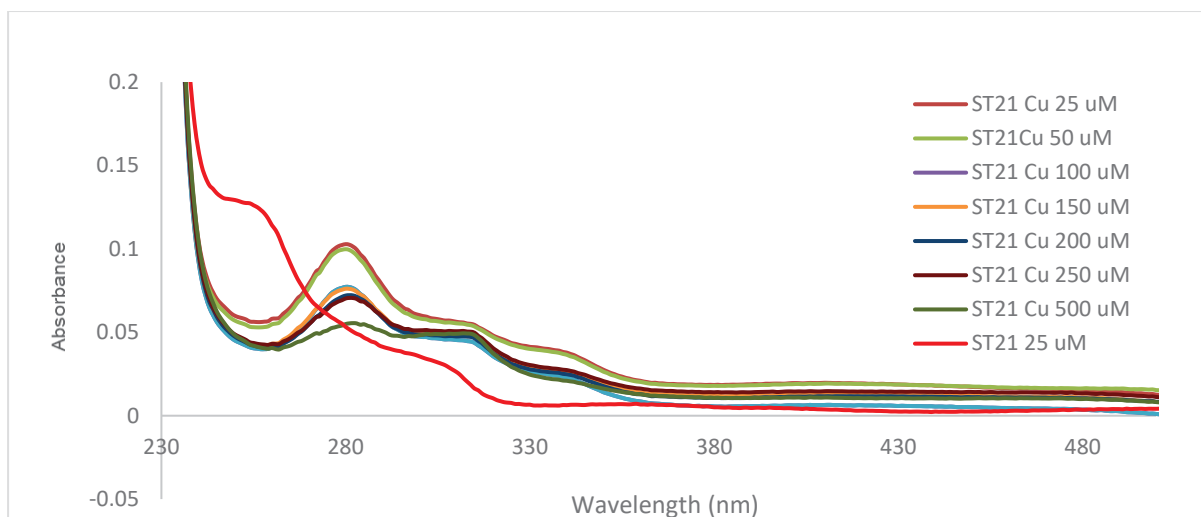


Figure 83: UV-Vis spectra of the ST21 at 25 uM at different concentration of Cu²⁺ in buffer at pH 7.4

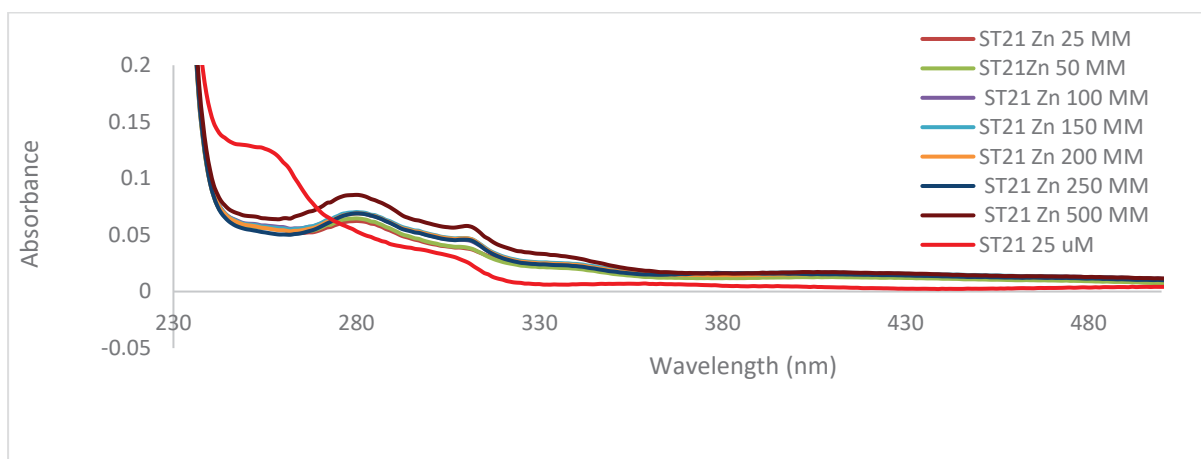


Figure 84: UV-Vis spectra of the ST21 at 25 uM at different concentration of Zn²⁺ in buffer pH 7.4

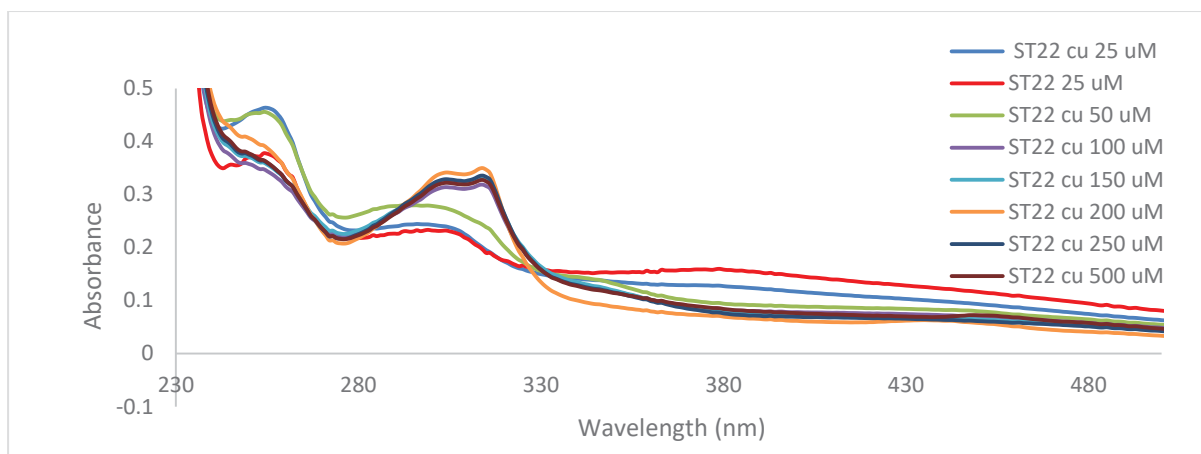


Figure 85: UV-Vis spectra of the ST22 at 25 uM at different concentration of Cu⁺² in buffer at pH 7.4

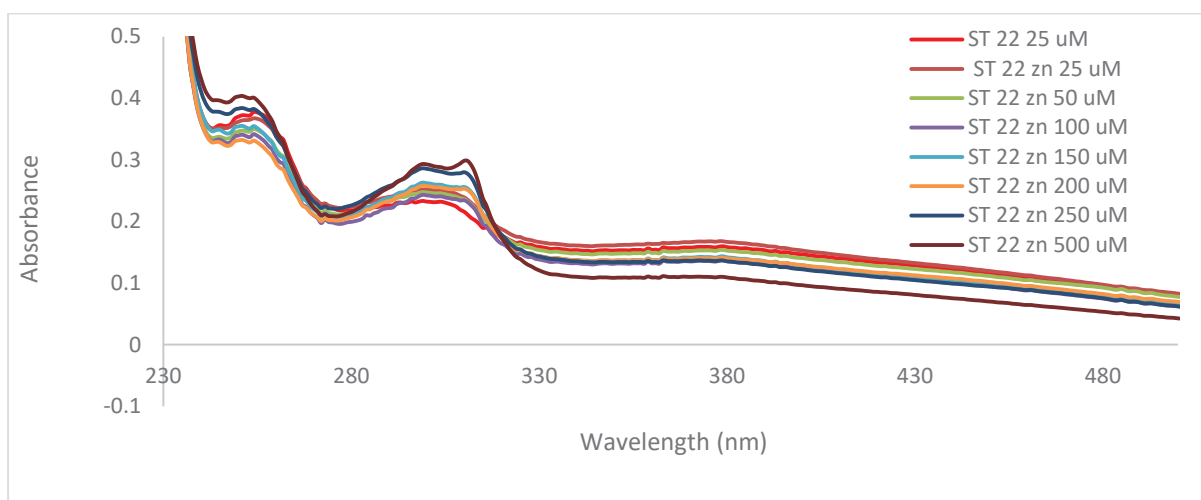


Figure 86: UV-Vis spectra of the ST22 at 25 uM at different concentration of Zn⁺² in buffer pH 7.4

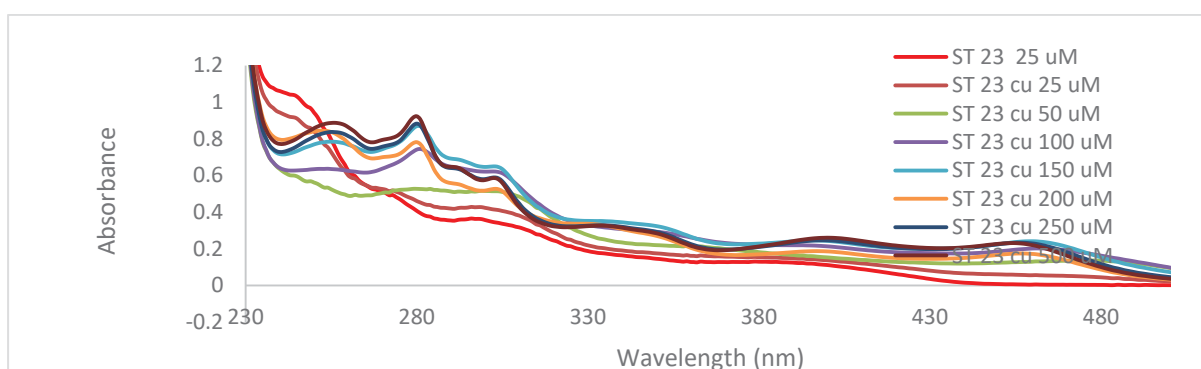


Figure 87: UV-Vis spectra of the ST23 at 25 uM at different concentration of Cu⁺² in buffer at pH 7.4

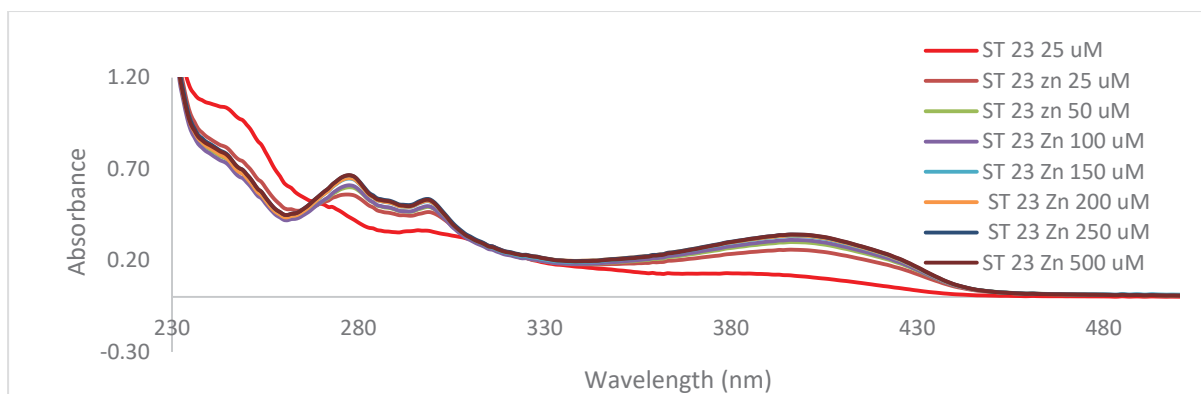


Figure 88: UV-Vis spectra of the ST23 at 25 uM at different concentration of Zn⁺² in buffer pH 7.4

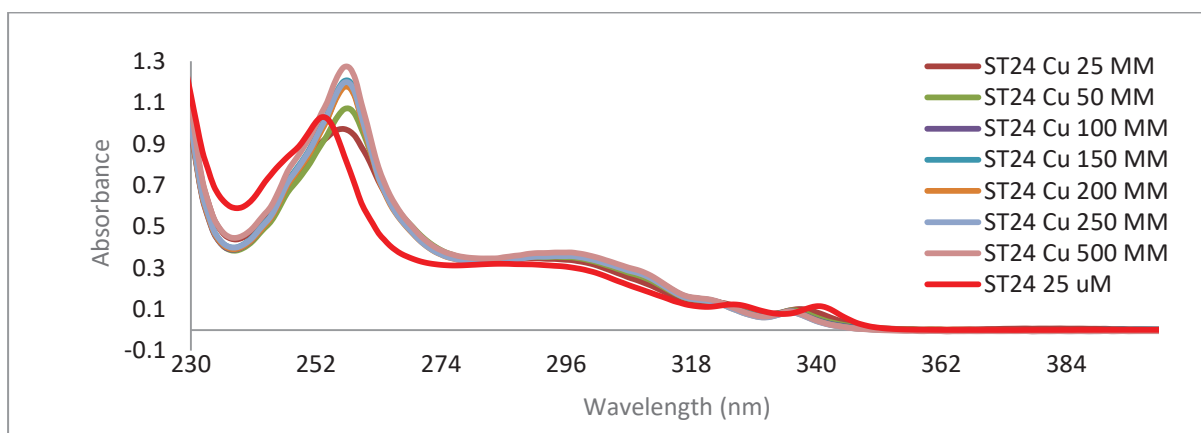


Figure 89: UV-Vis spectra of the ST24 at 25 uM at different concentration of Cu⁺² in buffer at pH 7.4

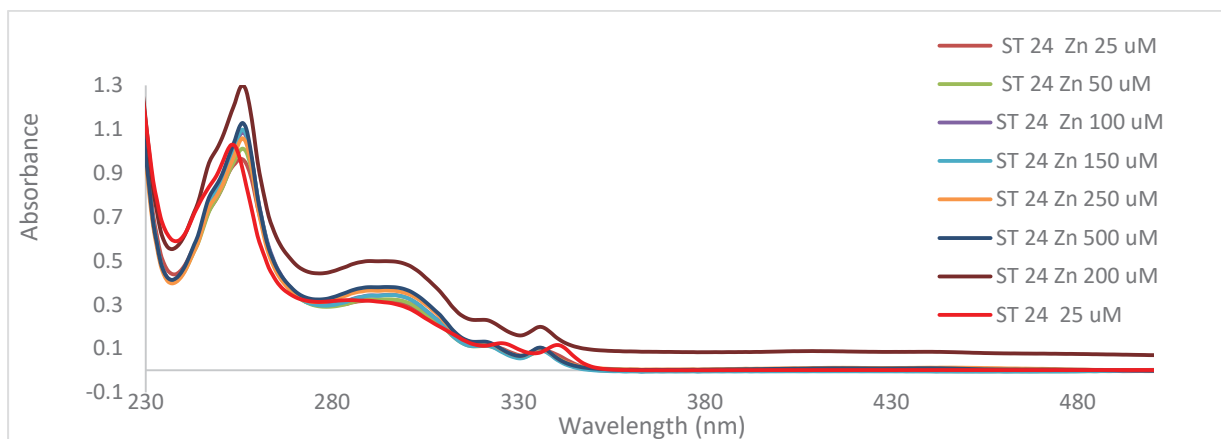


Figure 90: UV-Vis spectra of the ST24 at 25 uM at different concentration of Zn⁺² in buffer pH 7.4

Table 7: Typical UV-Vis spectral characteristic of phen-5,6-dione derivatives and there complexes with Cu^{+2} and Zn^{+2} extracted from Figures 43-90.

ligand	λ_{max} (nm) /ligand	λ_{max} (nm)/ Cu^{+2} complex	λ_{max} (nm)/ Zn^{+2} complex
ST01	256	307, 318	303, 312
ST02	259, 301	304, 318	300, 313
ST03	208	316	314
ST04	251, 301	282, 346	279, 404
ST05	254, 314	275, 359	278, 340
ST06	246, 312, 344	290, 346, 453, 478	289, 327, 386
ST07	259, 282	279, 313	274, 309, 384
ST08	256, 341	290, 386, 480	297, 381
ST09	266, 303, 390	292, 318, 470, 497	286, 316, 446
ST10	264, 301	278, 311, 388	274, 309, 390
ST11	257, 305	300, 317	302, 314
ST12	258,304	305,321	302, 317
ST13	244, 308	302, 343	307, 340
ST14	258	302, 318	269, 311
ST15	257	260, 319	258, 314
ST16	260	314	302, 312
ST17	258	304, 317	296, 311
ST18	260	305, 315	300, 313
ST19	254	276, 360, 378	274, 364, 378
ST20	259	300, 316	298, 311
ST21	261, 305	282, 316, 342	285, 315, 345
ST22	254, 305	303, 317	299, 312
ST23	249, 271	283, 305, 347	279, 301, 407
ST24	252, 301	260, 327, 338	259, 324, 337

4.5 References

- Adlard, P.A. & Bush, A.I. 2006, 'Metals and Alzheimer's disease', *Journal of Alzheimer's disease: JAD*, vol. 10, no. 2-3, pp. 145-63.
- Ali-Shtayeh, M.S., Jamous, R.M., Zaitoun, S.Y.A. & Qasem, I.B. 2014, 'In-vitro screening of acetylcholinesterase inhibitory activity of extracts from Palestinian indigenous flora in relation to the treatment of Alzheimer's disease', *Functional Foods in Health and Disease*, vol. 4, no. 9, pp. 381-400.
- Atwood, C.S., Perry, G., Zeng, H., Kato, Y., Jones, W.D., Ling, K.-Q., Huang, X., Moir, R.D., Wang, D. & Sayre, L.M. 2004, 'Copper mediates dityrosine cross-linking of Alzheimer's amyloid- β ', *Biochemistry*, vol. 43, no. 2, pp. 560-8.
- Bajda, M., Guzior, N., Ignasik, M. & Malawska, B. 2011, 'Multi-target-directed ligands in Alzheimer's disease treatment', *Current medicinal chemistry*, vol. 18, no. 32, pp. 4949-75.
- Bandyopadhyay, S., Huang, X., Lahiri, D.K. & Rogers, J.T. 2010, 'Novel drug targets based on metallobiology of Alzheimer's disease', *Expert Opinion on Therapeutic Targets*, vol. 14, no. 11, pp. 1177-97.
- Barnard, E.A. 1974, 'Neuromuscular transmission—enzymatic destruction of acetylcholine', *The peripheral nervous system*, Springer, pp. 201-24.
- Barnham, K.J. & Bush, A.I. 2008, 'Metals in Alzheimer's and Parkinson's diseases', *Current opinion in chemical biology*, vol. 12, no. 2, pp. 222-8.
- Barnham, K.J. & Bush, A.I. 2014, 'Biological metals and metal-targeting compounds in major neurodegenerative diseases', *Chemical Society Reviews*, vol. 43, no. 19, pp. 6727-49.
- Bartolucci, C., Haller, L.A., Jordis, U., Fels, G. & Lamba, D. 2009, 'Probing Torpedo californica acetylcholinesterase catalytic gorge with two novel bis-functional galanthamine derivatives', *Journal of medicinal chemistry*, vol. 53, no. 2, pp. 745-51.
- Bartus, R.T., Dean, R.L., Beer, B. & Lippa, A.S. 1982a, 'The cholinergic hypothesis of geriatric memory dysfunction', *Science*, vol. 217, no. 4558, pp. 408-14.
- Bartus, R.T., Dean, R.r., Beer, B. & Lippa, A.S. 1982b, 'The cholinergic hypothesis of geriatric memory dysfunction', *Science*, vol. 217, no. 4558, pp. 408-14.
- Berchtold, N., '8c Cotman, CW.(1998) Evolution in the conceptualization of dementia and Alzheimer's disease: Greco-Roman period to the 1960s', *Neurobiology of Ageing*, pp. 19,173-89.
- Berchtold, N.C. & Cotman, C.W. 1998, 'Evolution in the conceptualization of dementia and Alzheimer's disease: Greco-Roman period to the 1960s', *Neurobiology of aging*, vol. 19, no. 3, pp. 173-89.
- Binnemans, K., Lenaerts, P., Driesen, K. & Gorller-Walrand, C. 2004, 'A luminescent tris(2-thenoyltrifluoroacetato)europium(iii) complex covalently linked to a 1,10-phenanthroline-functionalised sol-gel glass', *Journal of Materials Chemistry*, vol. 14, no. 2, pp. 191-5.
- Birks, J. 2012, 'Cholinesterase inhibitors for Alzheimer's disease (Review)'.
Bizyaev, S.N., Gatilov, Y.V. & Tkachev, A.V. 2015, 'Syntheses of α -cyano substituted oximes from terpenic hydrocarbons via nitroso chlorides: X-ray structures of 3-cyanocaran-4-one oxime, 2-cyanopinan-3-one oxime and 1-cyano-p-menth-8-en-2-one oxime', *Mendeleev Communications*, vol. 25, no. 2, pp. 93-5.
- Bodick, N.C., Offen, W.W., Levey, A.I., Cutler, N.R., Gauthier, S.G., Satlin, A., Shannon, H.E., Tollefson, G.D., Rasmussen, K. & Bymaster, F.P. 1997, 'Effects of xanomeline, a selective muscarinic receptor agonist, on cognitive function and behavioral symptoms in Alzheimer disease', *Archives of neurology*, vol. 54, no. 4, pp. 465-73.
- Bodige, S. & MacDonnell, F.M. 1997a, 'Synthesis of Free and Ruthenium Coordinated 5,6-Diamino-1,10-phenanthroline', *Tetrahedron Letters*, vol. 38, no. 47, pp. 8159-60.
- Bodige, S. & MacDonnell, F.M. 1997b, 'Synthesis of free and ruthenium coordinated 5, 6-diamino-1, 10-phenanthroline', *Tetrahedron letters*, vol. 38, no. 47, pp. 8159-60.

- Boghaei, D.M. & Behzadian-Asl, F. 2007, 'Synthesis, characterization and fluorescence spectra of mononuclear Zn(II), Cd(II) and Hg(II) complexes with 1,10-phenanthroline-5,6-dione ligand', *Journal of Coordination Chemistry*, vol. 60, no. 3, pp. 347-53.
- Boghaei, D.M. & Behzadian Asl, F. 2007, 'Synthesis, characterization and fluorescence spectra of mixed ligand Zn(II), Cd(II) and Hg(II) complexes with 1,10-phenanthroline-5,6-dione ligand', *Journal of Coordination Chemistry*, vol. 60, no. 15, pp. 1629-35.
- Bolognesi, M.L., Andrisano, V., Bartolini, M., Banzi, R. & Melchiorre, C. 2005, 'Propidium-based polyamine ligands as potent inhibitors of acetylcholinesterase and acetylcholinesterase-induced amyloid- β aggregation', *Journal of medicinal chemistry*, vol. 48, no. 1, pp. 24-7.
- Bolognesi, M.L., Andrisano, V., Bartolini, M., Cavalli, A., Minarini, A., Recanatini, M., Rosini, M., Tumiatti, V. & Melchiorre, C. 2005, 'Heterocyclic inhibitors of AChE acylation and peripheral sites', *Il Farmaco*, vol. 60, no. 6, pp. 465-73.
- Bolognesi, M.L., Cavalli, A., Valgimigli, L., Bartolini, M., Rosini, M., Andrisano, V., Recanatini, M. & Melchiorre, C. 2007, 'Multi-target-directed drug design strategy: from a dual binding site acetylcholinesterase inhibitor to a trifunctional compound against Alzheimer's disease', *Journal of medicinal chemistry*, vol. 50, no. 26, pp. 6446-9.
- Bolognesi, M.L., Minarini, A., Budriesi, R., Cacciaguerra, S., Chiarini, A., Spampinato, S., Tumiatti, V. & Melchiorre, C. 1998, 'Universal template approach to drug design: polyamines as selective muscarinic receptor antagonists', *Journal of medicinal chemistry*, vol. 41, no. 21, pp. 4150-60.
- Bonda, D.J., Lee, H.-g., Blair, J.A., Zhu, X., Perry, G. & Smith, M.A. 2011, 'Role of metal dyshomeostasis in Alzheimer's disease', *Metallomics*, vol. 3, no. 3, pp. 267-70.
- Borra, N.K. & Kuna, Y. 2013, 'Evolution of toxic properties of anti alzheimer's drugs through Lipinski's rule of five', *Int. J. Pure App. Biosci*, vol. 1, no. 4, pp. 28-36.
- Bourne, Y., Taylor, P., Kanter, J., Bougis, P. & Marchot, P. 1998, 'Crystal Structure of Mouse Acetylcholinesterase', in B. Doctor, P. Taylor, D. Quinn, R. Rotundo & M. Gentry (eds), *Structure and Function of Cholinesterases and Related Proteins*, Springer US, pp. 315-22.
- Bourne, Y., Taylor, P., Radić, Z. & Marchot, P. 2003, 'Structural insights into ligand interactions at the acetylcholinesterase peripheral anionic site', *The EMBO journal*, vol. 22, no. 1, pp. 1-12.
- Braymer, J.J., DeToma, A.S., Choi, J.-S., Ko, K.S. & Lim, M.H. 2010, 'Recent development of bifunctional small molecules to study metal-amyloid- β species in Alzheimer's disease', *International Journal of Alzheimer's Disease*, vol. 2011.
- Busciglio, J., Lorenzo, A., Yeh, J. & Yankner, B.A. 1995, ' β -Amyloid fibrils induce tau phosphorylation and loss of microtubule binding', *Neuron*, vol. 14, no. 4, pp. 879-88.
- Bush, A. & Tanzi, R. 2008a, 'Therapeutics for Alzheimer's disease based on the metal hypothesis', *Neurotherapeutics*, vol. 5, no. 3, pp. 421-32.
- Bush, A.I. & Tanzi, R.E. 2008b, 'Therapeutics for Alzheimer's disease based on the metal hypothesis', *Neurotherapeutics*, vol. 5, no. 3, pp. 421-32.
- Calderazzo, F., Marchetti, F., Pampaloni, G. & Passarelli, V. 1999, 'Co-ordination properties of 1,10-phenanthroline-5,6-dione towards group 4 and 5 metals in low and high oxidation states [dagger]', *Journal of the Chemical Society, Dalton Transactions*, no. 24, pp. 4389-96.
- Carlson, D.L., Huchital, D.H., Mantilla, E.J., Sheardy, R.D. & Murphy Jr, W.R. 1993, 'A new class of DNA metallobinders showing spectator ligand size selectivity: binding of ligand-bridged bimetallic complexes of ruthenium (II) to calf thymus DNA', *Journal of the American Chemical Society*, vol. 115, no. 14, pp. 6424-5.
- Carolan, C.G., Dillon, G.P., Khan, D., Ryder, S.A., Gaynor, J.M., Reidy, S., Marquez, J.F., Jones, M., Holland, V. & Gilmer, J.F. 2010, 'Isosorbide-2-benzyl carbamate-5-salicylate, a peripheral anionic site binding subnanomolar selective butyrylcholinesterase inhibitor', *Journal of medicinal chemistry*, vol. 53, no. 3, pp. 1190-9.
- Carter, M., Simms, G. & Weaver, D. 2010, 'The development of new therapeutics for Alzheimer's disease', *Clinical Pharmacology & Therapeutics*, vol. 88, no. 4, pp. 475-86.

- Chen, Y., Sun, J., Fang, L., Liu, M., Peng, S., Liao, H., Lehmann, J. & Zhang, Y. 2012, 'Tacrine–ferulic acid–nitric oxide (NO) donor trihybrids as potent, multifunctional acetyl- and butyrylcholinesterase inhibitors', *Journal of medicinal chemistry*, vol. 55, no. 9, pp. 4309-21.
- Chitra, L., Kumar, C.R., Basha, H.M., Ponne, S. & Boopathy, R. 2013, 'Interaction of metal chelators with different molecular forms of acetylcholinesterase and its significance in Alzheimer's disease treatment', *Proteins: Structure, Function, and Bioinformatics*, vol. 81, no. 7, pp. 1179-91.
- Çokuğraş, A.N. 2003, 'Butyrylcholinesterase: structure and physiological importance', *Turk J Biochem*, vol. 28, no. 2, pp. 54-61.
- Congreve, M., Murray, C.W. & Blundell, T.L. 2005, 'Keynote review: Structural biology and drug discovery', *Drug discovery today*, vol. 10, no. 13, pp. 895-907.
- Constable, E.C. 1996, *Metals and ligand reactivity: An Introduction to the Organic Chemistry of Metal Complexes*, Verlagsgesellschaft mbH (VCH), Weinheim.
- Contestabile, A. 2011, 'The history of the cholinergic hypothesis', *Behavioural brain research*, vol. 221, no. 2, pp. 334-40.
- Coyle, B., Kavanagh, K., McCann, M., Devereux, M. & Geraghty, M. 2003, 'Mode of anti-fungal activity of 1, 10-phenanthroline and its Cu (II), Mn (II) and Ag (I) complexes', *Biomaterials*, vol. 16, no. 2, pp. 321-9.
- Csermely, P., Agoston, V. & Pongor, S. 2005, 'The efficiency of multi-target drugs: the network approach might help drug design', *Trends in pharmacological sciences*, vol. 26, no. 4, pp. 178-82.
- Cuajungco, M.P., Frederickson, C.J. & Bush, A.I. 2005, 'Amyloid- β metal interaction and metal chelation', *Alzheimer's disease*, Springer, pp. 235-54.
- Cummings, J.L. 2003, 'Treatment of Alzheimer's disease: current and future therapeutic approaches', *Reviews in neurological diseases*, vol. 1, no. 2, pp. 60-9.
- Cummings, J.L. & Back, C. 1998, 'The cholinergic hypothesis of neuropsychiatric symptoms in Alzheimer's disease', *The American Journal of Geriatric Psychiatry*, vol. 6, no. 2, pp. S64-S78.
- Danysz, W. & Parsons, C.G. 1998, 'Glycine and N-methyl-D-aspartate receptors: physiological significance and possible therapeutic applications', *Pharmacological reviews*, vol. 50, no. 4, pp. 597-664.
- Darvesh, S., Grantham, D. & Hopkins, D. 1998, 'Distribution of butyrylcholinesterase in the human amygdala and hippocampal formation', *Journal of Comparative Neurology*, vol. 393, no. 3, pp. 374-90.
- Darvesh, S., Hopkins, D.A. & Geula, C. 2003, 'Neurobiology of butyrylcholinesterase', *Nature reviews. Neuroscience*, vol. 4, no. 2, p. 131.
- Darvesh, S., McDonald, R.S., Darvesh, K.V., Mataija, D., Conrad, S., Gomez, G., Walsh, R. & Martin, E. 2007, 'Selective reversible inhibition of human butyrylcholinesterase by aryl amide derivatives of phenothiazine', *Bioorganic & medicinal chemistry*, vol. 15, no. 19, pp. 6367-78.
- Das, O., Chatterjee, S. & Paine, T. 2013, 'Functional models of α -keto acid dependent nonheme iron oxygenases: synthesis and reactivity of biomimetic iron(II) benzoylformate complexes supported by a 2,9-dimethyl-1,10-phenanthroline ligand', *JBIC Journal of Biological Inorganic Chemistry*, vol. 18, no. 3, pp. 401-10.
- Decker, M., Kraus, B. & Heilmann, J. 2008, 'Design, synthesis and pharmacological evaluation of hybrid molecules out of quinazolinimines and lipoic acid lead to highly potent and selective butyrylcholinesterase inhibitors with antioxidant properties', *Bioorganic & medicinal chemistry*, vol. 16, no. 8, pp. 4252-61.
- Deegan, C., Coyle, B., McCann, M., Devereux, M. & Egan, D.A. 2006, 'In vitro anti-tumour effect of 1,10-phenanthroline-5,6-dione (phendione), [Cu(phendione)₃](ClO₄)₂·4H₂O and [Ag(phendione)₂](ClO₄) using human epithelial cell lines', *Chemico-Biological Interactions*, vol. 164, no. 1-2, pp. 115-25.

- Demirhan, N., Avciata, U. & Gul, A. 2005, 'Synthesis and characterisation of 5, 6-bis (salicylideneimino)-1, 10-phenanthroline and its trinuclear complexes', *Indian Journal of Chemistry*, vol. 44, no. 4, pp. 729-32.
- DeToma, A.S., Salamekh, S., Ramamoorthy, A. & Lim, M.H. 2012, 'Misfolded proteins in Alzheimer's disease and type II diabetes', *Chemical Society Reviews*, vol. 41, no. 2, pp. 608-21.
- Dietrich-Buchecker, C., Sauvage, J.P. & Kern, J.M. 1989, 'Synthesis and electrochemical studies of catenates: Stabilization of low oxidation states by interlocked macrocyclic ligands', *Journal of the American Chemical Society*, vol. 111, no. 20, pp. 7791-800.
- Dillon, G.P., Gaynor, J.M., Khan, D., Carolan, C.G., Ryder, S.A., Marquez, J.F., Reidy, S. & Gilmer, J.F. 2010, 'Isosorbide-based cholinesterase inhibitors; replacement of 5-ester groups leading to increased stability', *Bioorganic & medicinal chemistry*, vol. 18, no. 3, pp. 1045-53.
- Doble, A. 1999, 'The role of excitotoxicity in neurodegenerative disease: implications for therapy', *Pharmacology & therapeutics*, vol. 81, no. 3, pp. 163-221.
- Dolmella, A., Bandoli, G. & Nicolini, M. 1994, 'Alzheimer's disease: a pharmacological challenge', *Advances in Drug Research*, vol. 25, pp. 203-94.
- Doraiswamy, P.M. & Finefrock, A.E. 2004, 'Metals in our minds: therapeutic implications for neurodegenerative disorders', *The Lancet Neurology*, vol. 3, no. 7, pp. 431-4.
- Dressman, J.B., Amidon, G.L., Reppas, C. & Shah, V.P. 1998, 'Dissolution testing as a prognostic tool for oral drug absorption: immediate release dosage forms', *Pharmaceutical research*, vol. 15, no. 1, pp. 11-22.
- Duce, J.A. & Bush, A.I. 2010, 'Biological metals and Alzheimer's disease: implications for therapeutics and diagnostics', *Progress in neurobiology*, vol. 92, no. 1, pp. 1-18.
- Dyachenko, V. & Rusanov, E. 2003, 'Synthesis and Crystal Structure of 5-Amino-4-cyano-8-isobutyl-7-isopropyl-6-thiocarbamoyl-2-azabicyclo [2.2. 2] oct-5-en-3-thione', *Chemistry of Heterocyclic Compounds*, vol. 39, no. 5, pp. 645-90.
- Egan, W.J. & Lauri, G. 2002, 'Prediction of intestinal permeability', *Advanced drug delivery reviews*, vol. 54, no. 3, pp. 273-89.
- Egan, W.J., Merz, K.M. & Baldwin, J.J. 2000, 'Prediction of drug absorption using multivariate statistics', *Journal of medicinal chemistry*, vol. 43, no. 21, pp. 3867-77.
- Ellman, G.L., Courtney, K.D., Andres, V. & Featherstone, R.M. 1961a, 'A new and rapid colorimetric determination of acetylcholinesterase activity', *Biochemical pharmacology*, vol. 7, no. 2, pp. 88-95.
- Ellman, G.L., Courtney, K.D., Andres, V. & Featherstone, R.M. 1961b, 'A new and rapid colorimetric determination of acetylcholinesterase activity', *Biochemical pharmacology*, vol. 7, no. 2, pp. 88-95.
- Elsinghorst, P.W., González Tanarro, C.M. & Gütschow, M. 2006, 'Novel heterobivalent tacrine derivatives as cholinesterase inhibitors with notable selectivity toward butyrylcholinesterase', *Journal of medicinal chemistry*, vol. 49, no. 25, pp. 7540-4.
- Espinoza-Fonseca, L.M. 2006, 'The benefits of the multi-target approach in drug design and discovery', *Bioorganic & medicinal chemistry*, vol. 14, no. 4, pp. 896-7.
- Falangola, M.F., Lee, S.-P., Nixon, R.A., Duff, K. & Helpner, J.A. 2005, 'Histological Co-Localization of Iron in A β Plaques of PS/APP Transgenic Mice', *Neurochemical research*, vol. 30, no. 2, pp. 201-5.
- Fernández-Bachiller, M.I., Pérez, C.n., Monjas, L., Rademann, J.r. & Rodríguez-Franco, M.I. 2012, 'New Tacrine-4-Oxo-4 H-chromene Hybrids as Multifunctional Agents for the Treatment of Alzheimer's Disease, with Cholinergic, Antioxidant, and β -Amyloid-Reducing Properties', *Journal of medicinal chemistry*, vol. 55, no. 3, pp. 1303-17.
- Fernandez, H.L., Moreno, R.D. & Inestrosa, N.C. 1996, 'Tetrameric (G4) acetylcholinesterase: structure, localization, and physiological regulation', *Journal of neurochemistry*, vol. 66, no. 4, pp. 1335-46.

- Fodero-Tavoletti, M.T., Villemagne, V.L., Paterson, B.M., White, A.R., Li, Q.-X., Camakaris, J., O'Keefe, G., Cappai, R., Barnham, K.J. & Donnelly, P.S. 2010, 'Bis (thiosemicarbazonato) Cu-64 Complexes for Positron Emission Tomography Imaging of Alzheimer's Disease', *Journal of Alzheimer's Disease*, vol. 20, no. 1, pp. 49-55.
- Forster, M.J. 2002, 'Molecular modelling in structural biology', *Micron*, vol. 33, no. 4, pp. 365-84.
- Foxon, S.P., Green, C., Walker, M.G., Wragg, A., Adams, H., Weinstein, J.A., Parker, S.C., Meijer, A.J. & Thomas, J.A. 2011, 'Synthesis, characterization, and DNA binding properties of ruthenium (II) complexes containing the redox active ligand benzo [i] dipyrido [3, 2-a: 2', 3'-c] phenazine-11, 16-quinone', *Inorganic chemistry*, vol. 51, no. 1, pp. 463-71.
- Francis, P.T., Nordberg, A. & Arnold, S.E. 2005, 'A preclinical view of cholinesterase inhibitors in neuroprotection: do they provide more than symptomatic benefits in Alzheimer's disease?', *Trends in pharmacological sciences*, vol. 26, no. 2, pp. 104-11.
- Francis, P.T., Palmer, A.M., Snape, M. & Wilcock, G.K. 1999, 'The cholinergic hypothesis of Alzheimer's disease: a review of progress', *Journal of Neurology, Neurosurgery & Psychiatry*, vol. 66, no. 2, pp. 137-47.
- Franco, L.L., de Almeida, M.V., Vieira, P.P.R., Pohlit, A.M. & Valle, M.S. 2012, 'Synthesis and antimalarial activity of dihydroperoxides and tetraoxanes conjugated with bis (benzyl) acetone derivatives', *Chemical biology & drug design*, vol. 79, no. 5, pp. 790-7.
- Frölich, L. 2002, 'The cholinergic pathology in Alzheimer's disease – discrepancies between clinical experience and pathophysiological findings', *Journal of Neural Transmission*, vol. 109, no. 7, pp. 1003-13.
- Fujii, T., Mori, Y., Tominaga, T., Hayasaka, I. & Kawashima, K. 1997, 'Maintenance of constant blood acetylcholine content before and after feeding in young chimpanzees', *Neuroscience letters*, vol. 227, no. 1, pp. 21-4.
- Fukuto, T.R. 1990, 'Mechanism of action of organophosphorus and carbamate insecticides', *Environmental health perspectives*, vol. 87, p. 245.
- Gaeta, A. & Hider, R.C. 2005, 'The crucial role of metal ions in neurodegeneration: the basis for a promising therapeutic strategy', *British journal of pharmacology*, vol. 146, no. 8, pp. 1041-59.
- Gaggelli, E., Kozlowski, H., Valensin, D. & Valensin, G. 2006, 'Copper homeostasis and neurodegenerative disorders (Alzheimer's, prion, and Parkinson's diseases and amyotrophic lateral sclerosis)', *Chemical reviews*, vol. 106, no. 6, pp. 1995-2044.
- Gandy, S. & Greengard, P. 1994, 'Processing of Alzheimer A β -Amyloid Precursor Protein: Cell Biology, Regulation, and Role in Alzheimer Disease', in J.B. Ronald & R.A. Harris (eds), *International Review of Neurobiology*, vol. Volume 36, Academic Press, pp. 29-50.
- Ganong, W.F. & Ganong, W. 1995, *Review of medical physiology*, Appleton & Lange Norwalk, CT.
- Gao, F., Chao, H., Wang, J.-Q., Yuan, Y.-X., Sun, B., Wei, Y.-F., Peng, B. & Ji, L.-N. 2007, 'Targeting topoisomerase II with the chiral DNA-intercalating ruthenium (II) polypyridyl complexes', *JBIC Journal of Biological Inorganic Chemistry*, vol. 12, no. 7, pp. 1015-27.
- Garzone, P.D. 1993, 'Treatment of Dementias. A New Generation of Progress', *Pharmaceutical Research*, vol. 10, no. 11, p. 1697.
- Gayathri, P. & Senthil Kumar, A. 2014, 'Electrochemical Behavior of the 1, 10-Phenanthroline Ligand on a Multiwalled Carbon Nanotube Surface and Its Relevant Electrochemistry for Selective Recognition of Copper Ion and Hydrogen Peroxide Sensing', *Langmuir*, vol. 30, no. 34, pp. 10513-21.
- Giacobini, E. 2004, 'Cholinesterase inhibitors: new roles and therapeutic alternatives', *Pharmacological research*, vol. 50, no. 4, pp. 433-40.
- Giacobini, E., Spiegel, R., Enz, A., Veroff, A. & Cutler, N. 2002, 'Inhibition of acetyl- and butyryl-cholinesterase in the cerebrospinal fluid of patients with Alzheimer's disease by rivastigmine: correlation with cognitive benefit', *Journal of Neural Transmission*, vol. 109, no. 7, pp. 1053-65.

- Gillard, R.D. & Hill, R.E.E. 1974, 'Optically active co-ordination compounds. Part XXXIV. Modification of reaction pathways in 1,10-phenanthroline and its derivatives by metal ions', *Journal of the Chemical Society, Dalton Transactions*, no. 11, pp. 1217-36.
- Gillard, R.D., Hill, R.E.E. & Maskill, R. 1970, 'Optically active co-ordination compounds. Part XX. Reactions of 1,10-phenanthroline co-ordinated to cobalt(III)', *Journal of the Chemical Society A: Inorganic, Physical, Theoretical*, no. 0, pp. 1447-51.
- Girgis, A.Y., Sohn, Y.S. & Balch, A.L. 1975, 'Preparation and oxidation of some quinone adducts of transition metal complexes', *Inorganic Chemistry*, vol. 14, no. 10, pp. 2327-31.
- Gomleksiz, M., Alkan, C. & Erdem, B. 2013, 'Synthesis, characterization and antibacterial activity of imidazole derivatives of 1,10-phenanthroline and their Cu(II), Co(II) and Ni(II) complexes : research article', vol. 66, pp. 107-12,
<http://reference.sabinet.co.za/webx/access/electronic_journals/chem/chem_v66_a17.pdf>.
- Goss, C.A. & Abruna, H.D. 1985, 'Spectral, electrochemical and electrocatalytic properties of 1,10-phenanthroline-5,6-dione complexes of transition metals', *Inorganic Chemistry*, vol. 24, no. 25, pp. 4263-7.
- Greenlee, W., Clader, J., Asberom, T., McCombie, S., Ford, J., Guzik, H., Kozlowski, J., Li, S., Liu, C. & Lowe, D. 2001, 'Muscarinic agonists and antagonists in the treatment of Alzheimer's disease', *Il Farmaco*, vol. 56, no. 4, pp. 247-50.
- Greig, N.H., Utsuki, T., Ingram, D.K., Wang, Y., Pepeu, G., Scali, C., Yu, Q.-S., Mamczarz, J., Holloway, H.W. & Giordano, T. 2005, 'Selective butyrylcholinesterase inhibition elevates brain acetylcholine, augments learning and lowers Alzheimer β -amyloid peptide in rodent', *Proceedings of the National Academy of Sciences of the United States of America*, vol. 102, no. 47, pp. 17213-8.
- Greig, N.H., Utsuki, T., Yu, Q.-s., Zhu, X., Holloway, H.W., Perry, T., Lee, B., Ingram, D.K. & Lahiri, D.K. 2001, 'A new therapeutic target in Alzheimer's disease treatment: attention to butyrylcholinesterase', *Current medical research and opinion*, vol. 17, no. 3, pp. 159-65.
- Gualtieri, F., Dei, S., Manetti, D., Romanelli, M., Scapecchi, S. & Teodori, E. 1995, 'The medicinal chemistry of Alzheimer's and Alzheimer-like diseases with emphasis on the cholinergic hypothesis', *Farmaco (Società chimica italiana: 1989)*, vol. 50, no. 7-8, p. 489.
- Guo, J., Hurley, M.M., Wright, J.B. & Lushington, G.H. 2004, 'A docking score function for estimating ligand-protein interactions: Application to acetylcholinesterase inhibition', *Journal of medicinal chemistry*, vol. 47, no. 22, pp. 5492-500.
- Gutiérrez, M., Matus, M.F., Poblete, T., Amigo, J., Vallejos, G. & Astudillo, L. 2013, 'Isoxazoles: synthesis, evaluation and bioinformatic design as acetylcholinesterase inhibitors', *Journal of Pharmacy and Pharmacology*, vol. 65, no. 12, pp. 1796-804.
- Haass, C., Schlossmacher, M.G., Hung, A.Y., Vigo-Pelfrey, C., Mellon, A., Ostaszewski, B.L., Lieberburg, I., Koo, E.H., Schenk, D. & Teplow, D.B. 1992, 'Amyloid β -peptide is produced by cultured cells during normal metabolism', *Nature*, vol. 359, no. 6393, pp. 322-5.
- Hardy, J. 2009, 'The amyloid hypothesis for Alzheimer's disease: a critical reappraisal', *Journal of neurochemistry*, vol. 110, no. 4, pp. 1129-34.
- Hardy, J. & Allsop, D. 1991, 'Amyloid deposition as the central event in the aetiology of Alzheimer's disease', *Trends in pharmacological sciences*, vol. 12, pp. 383-8.
- Hardy, J., Duff, K., Hardy, K.G., Perez-Tur, J. & Hutton, M. 1998, 'Genetic dissection of Alzheimer's disease and related dementias: amyloid and its relationship to tau', *Nature neuroscience*, vol. 1, no. 5, pp. 355-8.
- Hartmann, C., Antes, I. & Lengauer, T. 2009, 'Docking and scoring with alternative side-chain conformations', *Proteins: Structure, Function, and Bioinformatics*, vol. 74, no. 3, pp. 712-26.
- Hebert, L.E., Scherr, P.A., Bienias, J.L., Bennett, D.A. & Evans, D.A. 2003, 'Alzheimer disease in the US population: prevalence estimates using the 2000 census', *Archives of neurology*, vol. 60, no. 8, pp. 1119-22.

- Heinrich, M. & Teoh, H.L. 2004, 'Galanthamine from snowdrop—the development of a modern drug against Alzheimer's disease from local Caucasian knowledge', *Journal of ethnopharmacology*, vol. 92, no. 2, pp. 147-62.
- Hilt, G. & Steckhan, E. 1993, 'Transition metal complexes of 1,10-phenanthroline-5,6-dione as efficient mediators for the regeneration of NAD⁺ in enzymatic synthesis', *Journal of the Chemical Society, Chemical Communications*, no. 22, pp. 1706-7.
- Hiort, C., Lincoln, P. & Norden, B. 1993, 'DNA binding of .DELTA.- and .LAMBDA.-[Ru(phen)2DPPZ]2⁺', *Journal of the American Chemical Society*, vol. 115, no. 9, pp. 3448-54.
- Holmlin, R.E., Dandliker, P.J. & Barton, J.K. 1997, 'Charge transfer through the DNA base stack', *Angewandte Chemie International Edition in English*, vol. 36, no. 24, pp. 2714-30.
- Hopkins, A.L., Mason, J.S. & Overington, J.P. 2006, 'Can we rationally design promiscuous drugs?', *Current opinion in structural biology*, vol. 16, no. 1, pp. 127-36.
- Huang, S.-M., Mouri, A., Kokubo, H., Nakajima, R., Suemoto, T., Higuchi, M., Staufenbiel, M., Noda, Y., Yamaguchi, H. & Nabeshima, T. 2006, 'Nepriylsin-sensitive synapse-associated amyloid- β peptide oligomers impair neuronal plasticity and cognitive function', *Journal of Biological Chemistry*, vol. 281, no. 26, pp. 17941-51.
- Hunt, R. & De M. Taveau, R. 1906, 'On the physiological action of certain cholin derivatives and new methods for detecting cholin', *The British Medical Journal*, pp. 1788-91.
- Hureau, C., Sasaki, I., Gras, E. & Faller, P. 2010, 'Two Functions, One Molecule: A Metal-Binding and a Targeting Moiety to Combat Alzheimer's Disease', *ChemBioChem*, vol. 11, no. 7, pp. 950-3.
- Inestrosa, N.C., Sagal, J.P. & Colombres, M. 2005, 'Acetylcholinesterase interaction with Alzheimer amyloid β ', *Alzheimer's Disease*, pp. 299-317.
- Ingkaninan, K., Temkitthawon, P., Chuenchom, K., Yuyaem, T. & Thongnoi, W. 2003, 'Screening for acetylcholinesterase inhibitory activity in plants used in Thai traditional rejuvenating and neurotonic remedies', *Journal of Ethnopharmacology*, vol. 89, no. 2, pp. 261-4.
- Inglett, G.E. & Smith, G.F. 1950, 'The Formation of a New Nitrogen Heterocyclic Ring System by the Loss of Carbon Monoxide from 1, 10-Phenanthroline-5, 6-quinone¹', *Journal of the American Chemical Society*, vol. 72, no. 2, pp. 842-4.
- Iwata, N., Mizukami, H., Shirotani, K., Takaki, Y., Muramatsu, S.-i., Lu, B., Gerard, N.P., Gerard, C., Ozawa, K. & Saido, T.C. 2004, 'Presynaptic localization of neprilysin contributes to efficient clearance of amyloid- β peptide in mouse brain', *Journal of Neuroscience*, vol. 24, no. 4, pp. 991-8.
- JÄRV, J., KESVATERA, T. & AAVIKSAAR, A. 1976, 'Structure-Activity Relationships in Acetylcholinesterase Reactions', *The FEBS Journal*, vol. 67, no. 2, pp. 315-22.
- Jenkins, Y., Friedman, A.E., Turro, N.J. & Barton, J.K. 1992, 'Characterization of dipyridophenazine complexes of ruthenium (II): the light switch effect as a function of nucleic acid sequence and conformation', *Biochemistry*, vol. 31, no. 44, pp. 10809-16.
- Jomova, K., Vondrakova, D., Lawson, M. & Valko, M. 2010, 'Metals, oxidative stress and neurodegenerative disorders', *Molecular and cellular biochemistry*, vol. 345, no. 1-2, pp. 91-104.
- Kalidasu, S. & Kuna, Y. 2012, 'Validation of selected Anti-Alzheimer's drugs through Lipinski rule of five', *Journal of Pharmacy Research Vol*, vol. 5, no. 4, pp. 2174-7.
- Kelly, T.A., McNeil, D.W., Rose, J.M., David, E., Shih, C.-K. & Grob, P.M. 1997, 'Novel non-nucleoside inhibitors of human immunodeficiency virus type 1 reverse transcriptase. 6. 2-Indol-3-yl-and 2-azaindol-3-yl-dipyridodiazepinones', *Journal of Medicinal Chemistry*, vol. 40, no. 15, pp. 2430-3.
- Kern, J.-M., Sauvage, J.-P., Weidmann, J.-L., Armaroli, N., Flamigni, L., Ceroni, P. & Balzani, V. 1997, 'Complexes containing 2, 9-bis (p-biphenyl)-1, 10-phenanthroline units incorporated into a 56-membered ring. Synthesis, electrochemistry, and photophysical properties', *Inorganic Chemistry*, vol. 36, no. 23, pp. 5329-38.

- Khlistunova, I., Biernat, J., Wang, Y., Pickhardt, M., von Bergen, M., Gazova, Z., Mandelkow, E. & Mandelkow, E.-M. 2006, 'Inducible expression of Tau repeat domain in cell models of tauopathy aggregation is toxic to cells but can be reversed by inhibitor drugs', *Journal of Biological Chemistry*, vol. 281, no. 2, pp. 1205-14.
- Kim, M.-J., Konduri, R., Ye, H., MacDonnell, F.M., Puntoriero, F., Serroni, S., Campagna, S., Holder, T., Kinsel, G. & Rajeshwar, K. 2002, 'Dinuclear Ruthenium(II) Polypyridyl Complexes Containing Large, Redox-Active, Aromatic Bridging Ligands: Synthesis, Characterization, and Intramolecular Quenching of MLCT Excited States', *Inorganic Chemistry*, vol. 41, no. 9, pp. 2471-6.
- Kim, S., Cheon, H.-S., Kim, S.-Y., Juhn, Y.-S. & Kim, Y.-Y. 2013, 'Cadmium induces neuronal cell death through reactive oxygen species activated by GADD153', *BMC cell biology*, vol. 14, no. 1, p. 4.
- Kleineweischede, A. & Mattay, J. 2006, 'Synthesis of amino- and bis (bromomethyl)-substituted bi- and tetradentate N-Heteroaromatic ligands: building blocks for pyrazino-functionalized fullerene dyads', *European journal of organic chemistry*, vol. 2006, no. 4, pp. 947-57.
- Kobetić, R., Denžić, M., Zimmermann, B., Rončević, S. & Baranović, G. 2012, 'Preparation and separation of mixed-ligand Fe(II) complexes containing 1,10-phenanthroline-5,6-dione as ligand', *Journal of Coordination Chemistry*, vol. 65, no. 19, pp. 3433-48.
- Kochius, S., Magnusson, A., Hollmann, F., Schrader, J. & Holtmann, D. 2012, 'Immobilized redox mediators for electrochemical NAD(P)⁺ regeneration', *Applied Microbiology and Biotechnology*, vol. 93, no. 6, pp. 2251-64.
- KoSIK, K.S., Joachim, C.L. & Selkoe, D.J. 1986, 'Microtubule-associated protein tau (tau) is a major antigenic component of paired helical filaments in Alzheimer disease', *Proceedings of the National Academy of Sciences*, vol. 83, no. 11, pp. 4044-8.
- Kryger, G., Giles, K., Harel, M., Toker, L., Velan, B., Lazar, A., Kronman, C., Barak, D., Ariel, N., Shafferman, A., Silman, I. & Sussman, J. 1998, '3D Structure at 2.7 Å Resolution of Native and E202Q Mutant Human Acetylcholinesterase Complexed with Fasciculin-II', in B. Doctor, P. Taylor, D. Quinn, R. Rotundo & M. Gentry (eds), *Structure and Function of Cholinesterases and Related Proteins*, Springer US, pp. 323-6.
- Kryger, G., Silman, I. & Sussman, J.L. 1999, 'Structure of acetylcholinesterase complexed with E2020 (Aricept®): implications for the design of new anti-Alzheimer drugs', *Structure*, vol. 7, no. 3, pp. 297-307.
- Lage, J.M.M. 2006, '100 Years of Alzheimer's disease (1906–2006)', *Journal of Alzheimer's Disease*, vol. 9, no. s3, pp. 15-26.
- Lee, S., Zheng, X., Krishnamoorthy, J., Savelieff, M.G., Park, H.M., Brender, J.R., Kim, J.H., Derrick, J.S., Kochi, A. & Lee, H.J. 2013, 'Rational design of a structural framework with potential use to develop chemical reagents that target and modulate multiple facets of Alzheimer's disease', *Journal of the American Chemical Society*, vol. 136, no. 1, pp. 299-310.
- Lengauer, T. & Rarey, M. 1996, 'Computational methods for biomolecular docking', *Current opinion in structural biology*, vol. 6, no. 3, pp. 402-6.
- Leonard, B. 1998, 'Advances in the drug treatment of Alzheimer's disease', *Human Psychopharmacology: Clinical and Experimental*, vol. 13, no. 2, pp. 83-90.
- Li, B., Stribley, J.A., Ticu, A., Xie, W., Schopfer, L.M., Hammond, P., Brimijoin, S., Hinrichs, S.H. & Lockridge, O. 2000, 'Abundant tissue butyrylcholinesterase and its possible function in the acetylcholinesterase knockout mouse', *Journal of neurochemistry*, vol. 75, no. 3, pp. 1320-31.
- Li, S.-Y., Wang, X.-B. & Kong, L.-Y. 2014, 'Design, synthesis and biological evaluation of imine resveratrol derivatives as multi-targeted agents against Alzheimer's disease', *European journal of medicinal chemistry*, vol. 71, pp. 36-45.
- Lipinski, C.A. 2004, 'Lead- and drug-like compounds: the rule-of-five revolution', *Drug Discovery Today: Technologies*, vol. 1, no. 4, pp. 337-41.

- Lipinski, C.A., Lombardo, F., Dominy, B.W. & Feeney, P.J. 1997, 'Experimental and computational approaches to estimate solubility and permeability in drug discovery and development settings', *Advanced drug delivery reviews*, vol. 23, no. 1-3, pp. 3-25.
- Lipinski, C.A., Lombardo, F., Dominy, B.W. & Feeney, P.J. 2001, 'Experimental and computational approaches to estimate solubility and permeability in drug discovery and development settings', *Advanced drug delivery reviews*, vol. 46, no. 1-3, pp. 3-26.
- Liu, F., Wang, K., Bai, G., Zhang, Y. & Gao, L. 2004, 'The pH-Induced Emission Switching and Interesting DNA-Binding Properties of a Novel Dinuclear Ruthenium(II) Complex', *Inorganic Chemistry*, vol. 43, no. 5, pp. 1799-806.
- Liu, X., Xu, L. & Li, H. 2009, 'H. Chao, KC Zheng and LN Ji', *J. Mol. Struct*, vol. 920, pp. 163-71.
- Luo, W., Li, Y.-P., He, Y., Huang, S.-L., Tan, J.-H., Ou, T.-M., Li, D., Gu, L.-Q. & Huang, Z.-S. 2011, 'Design, synthesis and evaluation of novel tacrine-multialkoxybenzene hybrids as dual inhibitors for cholinesterases and amyloid beta aggregation', *Bioorganic & medicinal chemistry*, vol. 19, no. 2, pp. 763-70.
- Ma, X., Li, L., Zhu, T., Ba, M., Li, G., Gu, Q., Guo, Y. & Li, D. 2013, 'Phenylspirodrimanones with anti-HIV activity from the sponge-derived fungus *Stachybotrys chartarum* MXH-X73', *Journal of natural products*, vol. 76, no. 12, pp. 2298-306.
- Mabood, S. 1981, 'Kinetic alteration of Acetyl cholinesterase activity in diseases state', *Pak J Sci. Ind Res*, vol. 24, p. 27.
- Maelicke, A. & Albuquerque, E.X. 1996, 'New approach to drug therapy in Alzheimer's dementia Alfred Maelicke and Edson X. Albuquerque', *Drug Discovery Today*, vol. 1, no. 2, pp. 53-9.
- Manoharan, I., Boopathy, R., Darvesh, S. & Lockridge, O. 2007, 'A medical health report on individuals with silent butyrylcholinesterase in the Vysya community of India', *Clinica chimica acta*, vol. 378, no. 1, pp. 128-35.
- Markesbery, W.R. 1997, 'Oxidative stress hypothesis in Alzheimer's disease', *Free Radical Biology and Medicine*, vol. 23, no. 1, pp. 134-47.
- Marminon, C., Pierré, A., Pfeiffer, B., Pérez, V., Léonce, S., Joubert, A., Bailly, C., Renard, P., Hickman, J. & Prudhomme, M. 2003, 'Syntheses and antiproliferative activities of 7-azarebeccamycin analogues bearing one 7-azaindole moiety', *Journal of medicinal chemistry*, vol. 46, no. 4, pp. 609-22.
- Massoulié, J., Pezzementi, L., Bon, S., Krejci, E. & Vallette, F.-M. 1993, 'Molecular and cellular biology of cholinesterases', *Progress in neurobiology*, vol. 41, no. 1, pp. 31-91.
- Maurer, K., Volk, S. & Gerbaldo, H. 1997, 'Auguste D and Alzheimer's disease', *The Lancet*, vol. 349, no. 9064, pp. 1546-9.
- McCann, M., Coyle, B., McKay, S., McCormack, P., Kavanagh, K., Devereux, M., McKee, V., Kinsella, P., O'connor, R. & Clynes, M. 2004, 'Synthesis and X-ray crystal structure of [Ag (phendio) 2] ClO₄ (phendio= 1, 10-phenanthroline-5, 6-dione) and its effects on fungal and mammalian cells', *Biometals*, vol. 17, no. 6, pp. 635-45.
- McCann, M., Geraghty, M., Devereux, M., O'Shea, D., Mason, J. & O'Sullivan, L. 2000, 'Insights into the mode of action of the anti-Candida activity of 1, 10-phenanthroline and its metal chelates', *Metal-Based Drugs*, vol. 7, no. 4, p. 185.
- McCormick, D.A. 1989, 'Acetylcholine: distribution, receptors, and actions', *Semin Neurosci*, vol. 1, pp. 91-101.
- McGeer, P.L. 1984, 'The 12th J. A. F. Stevenson Memorial Lecture: Aging, Alzheimer's disease, and the cholinergic system', *Canadian Journal of Physiology and Pharmacology*, vol. 62, no. 7, pp. 741-54.
- McGleenon, B., Dynan, K. & Passmore, A. 1999, 'Acetylcholinesterase inhibitors in Alzheimer's disease', *British journal of clinical pharmacology*, vol. 48, no. 4, p. 471.

- McLaurin, J., Kierstead, M.E., Brown, M.E., Hawkes, C.A., Lambermon, M.H., Phinney, A.L., Darabie, A.A., Cousins, J.E., French, J.E. & Lan, M.F. 2006, 'Cyclohexanehexol inhibitors of A β aggregation prevent and reverse Alzheimer phenotype in a mouse model', *Nature medicine*, vol. 12, no. 7, pp. 801-8.
- Melchiorre, C., Andrisano, V., Bolognesi, M.L., Budriesi, R., Cavalli, A., Cavrini, V., Rosini, M., Tumiatti, V. & Recanatini, M. 1998, 'Acetylcholinesterase noncovalent inhibitors based on a polyamine backbone for potential use against Alzheimer's disease', *Journal of medicinal chemistry*, vol. 41, no. 22, pp. 4186-9.
- Melchiorre, C., Angeli, P., Brasili, L., Giardinà, D., Pignini, M. & Quaglia, W. 1988, 'Polyamines: a possible "passe-partout" for receptor characterization', *Actual. Chim. Ther.*, pp. 149-68.
- Mesulam, M.-M., Guillozet, A., Shaw, P., Levey, A., Duysen, E. & Lockridge, O. 2002, 'Acetylcholinesterase knockouts establish central cholinergic pathways and can use butyrylcholinesterase to hydrolyze acetylcholine', *neuroscience*, vol. 110, no. 4, pp. 627-39.
- Mesulam, M., Guillozet, A., Shaw, P. & Quinn, B. 2002, 'Widely spread butyrylcholinesterase can hydrolyze acetylcholine in the normal and Alzheimer brain', *Neurobiology of disease*, vol. 9, no. 1, pp. 88-93.
- Miao, Y., He, N. & Zhu, J.-J. 2010, 'History and new developments of assays for cholinesterase activity and inhibition', *Chemical reviews*, vol. 110, no. 9, pp. 5216-34.
- Mirífico, M.V., Svartman, E.L., Caram, J.A. & Vasini, E.J. 2004, 'Partial electrooxidation of nitrogenated heterocycles: novel synthesis of 1,10-phenanthroline-5,6-quinone by electrooxidation of 1,10-phenanthroline', *Journal of Electroanalytical Chemistry*, vol. 566, no. 1, pp. 7-13.
- Mitra, J., Guerrero, E.N., Hegde, P.M., Wang, H., Boldogh, I., Rao, K.S., Mitra, S. & Hegde, M.L. 2014, 'New perspectives on oxidized genome damage and repair inhibition by pro-oxidant metals in neurological diseases', *Biomolecules*, vol. 4, no. 3, pp. 678-703.
- Molina-Holgado, F., Hider, R.C., Gaeta, A., Williams, R. & Francis, P. 2007, 'Metals ions and neurodegeneration', *Biometals*, vol. 20, no. 3-4, pp. 639-54.
- Moody, C.J., Rees, C.W. & Thomas, R. 1992, 'The synthesis of ascididemin', *Tetrahedron*, vol. 48, no. 17, pp. 3589-602.
- Mount, C. & Downton, C. 2006, 'Alzheimer disease: progress or profit?', *Nature medicine*, vol. 12, no. 7, pp. 780-4.
- Mouritsen, O.G. & Jørgensen, K. 1998, 'A new look at lipid-membrane structure in relation to drug research', *Pharmaceutical research*, vol. 15, no. 10, pp. 1507-19.
- Murali, S., Sastri, C. & Maiya, B.G. 2002, 'New mixed ligand complexes of ruthenium (II) that incorporate a modified phenanthroline ligand: Synthesis, spectral characterization and DNA binding', *Journal of Chemical Sciences*, vol. 114, no. 4, pp. 403-15.
- Nayyar, A. & Jain, R. 2008, 'Synthesis and anti-tuberculosis activity of 2, 4-disubstituted quinolines', *Indian journal of chemistry. Section B, Organic including medicinal*, vol. 47, no. 1, p. 117.
- Noël, S., Cadet, S., Gras, E. & Hureau, C. 2013, 'The benzazole scaffold: a SWAT to combat Alzheimer's disease', *Chemical Society Reviews*, vol. 42, no. 19, pp. 7747-62.
- Nunomura, A., Perry, G., Aliev, G., Hirai, K., Takeda, A., Balraj, E.K., Jones, P.K., Ghanbari, H., Wataya, T. & Shimohama, S. 2001, 'Oxidative damage is the earliest event in Alzheimer disease', *Journal of Neuropathology & Experimental Neurology*, vol. 60, no. 8, pp. 759-67.
- Nunomura, A., Perry, G., Pappolla, M.A., Wade, R., Hirai, K., Chiba, S. & Smith, M.A. 1999, 'RNA oxidation is a prominent feature of vulnerable neurons in Alzheimer's disease', *Journal of Neuroscience*, vol. 19, no. 6, pp. 1959-64.
- Oztekin, Y. & Yazicigil, Z. 2009, 'Preparation and characterization of a 1, 10-phenanthroline-modified glassy carbon electrode', *Electrochimica Acta*, vol. 54, no. 28, pp. 7294-8.
- Pan, L.-F., Wang, X.-B., Xie, S.-S., Li, S.-Y. & Kong, L.-Y. 2014, 'Multitarget-directed resveratrol derivatives: anti-cholinesterases, anti- β -amyloid aggregation and monoamine oxidase inhibition properties against Alzheimer's disease', *MedChemComm*, vol. 5, no. 5, pp. 609-16.

- Pang, Y.-P., Quiram, P., Jelacic, T., Hong, F. & Brimijoin, S. 1996, 'Highly Potent, Selective, and Low Cost Bis-tetrahydroaminacrine Inhibitors of Acetylcholinesterase Steps toward Novel Drugs for Treating Alzheimer's Disease', *Journal of Biological Chemistry*, vol. 271, no. 39, pp. 23646-9.
- Pansuriya, P.B., Dhandhukia, P., Thakkar, V. & Patel, M.N. 2007, 'Synthesis, spectroscopic and biological aspects of iron (II) complexes', *Journal of enzyme inhibition and medicinal chemistry*, vol. 22, no. 4, pp. 477-87.
- Pardío, V.T., Ibarra, N., Rodríguez, M.A. & Waliszewski, K.N. 2001, 'Use of cholinesterase activity in monitoring organophosphate pesticide exposure of cattle produced in tropical areas', *Journal of agricultural and food chemistry*, vol. 49, no. 12, pp. 6057-62.
- Pardridge, W.M. 2009a, 'Alzheimer's disease drug development and the problem of the blood-brain barrier', *Alzheimer's & dementia*, vol. 5, no. 5, pp. 427-32.
- Pardridge, W.M. 2009b, 'Alzheimer's disease drug development and the problem of the blood-brain barrier', *Alzheimer's & dementia: the journal of the Alzheimer's Association*, vol. 5, no. 5, pp. 427-32.
- Pardridge, W.M. 2010, 'Biopharmaceutical drug targeting to the brain', *Journal of drug targeting*, vol. 18, no. 3, pp. 157-67.
- Park, S.-Y. 2010, 'Potential therapeutic agents against Alzheimer's disease from natural sources', *Archives of pharmacal research*, vol. 33, no. 10, pp. 1589-609.
- Patel, S.V. 1995, 'Pharmacotherapy of cognitive impairment in Alzheimer's disease: a review', *Journal of geriatric psychiatry and neurology*, vol. 8, no. 2, pp. 81-95.
- Paterson, B.M. & Donnelly, P.S. 2011, 'Copper complexes of bis (thiosemicarbazones): from chemotherapeutics to diagnostic and therapeutic radiopharmaceuticals', *Chemical Society Reviews*, vol. 40, no. 5, pp. 3005-18.
- Perez, L.R. & Franz, K.J. 2010, 'Minding metals: tailoring multifunctional chelating agents for neurodegenerative disease', *Dalton Transactions*, vol. 39, no. 9, pp. 2177-87.
- Petersen, C.A.H., Alikhani, N., Behbahani, H., Wiehager, B., Pavlov, P.F., Alafuzoff, I., Leinonen, V., Ito, A., Winblad, B. & Glaser, E. 2008, 'The amyloid β -peptide is imported into mitochondria via the TOM import machinery and localized to mitochondrial cristae', *Proceedings of the National Academy of Sciences*, vol. 105, no. 35, pp. 13145-50.
- Petrie, R.X., Reid, I.C. & Stewart, C.A. 2000, 'The N-methyl-D-aspartate receptor, synaptic plasticity, and depressive disorder: a critical review', *Pharmacology & therapeutics*, vol. 87, no. 1, pp. 11-25.
- Pohanka, M. 2012, 'Acetylcholinesterase inhibitors: a patent review (2008–present)', *Expert Opinion on Therapeutic Patents*, vol. 22, no. 8, pp. 871-86.
- Poteet, S.A., Majewski, M.B., Breitbach, Z.S., Griffith, C.A., Singh, S., Armstrong, D.W., Wolf, M.O. & MacDonnell, F.M. 2013, 'Cleavage of DNA by Proton-Coupled Electron Transfer to a Photoexcited, Hydrated Ru (II) 1, 10-Phenanthroline-5, 6-dione Complex', *Journal of the American Chemical Society*, vol. 135, no. 7, pp. 2419-22.
- Praticò, D. 2005, 'Peripheral biomarkers of oxidative damage in Alzheimer's disease: the road ahead', *Neurobiology of Aging*, vol. 26, no. 5, pp. 581-3.
- Priller, C., Bauer, T., Mitteregger, G., Krebs, B., Kretzschmar, H.A. & Herms, J. 2006, 'Synapse formation and function is modulated by the amyloid precursor protein', *Journal of Neuroscience*, vol. 26, no. 27, pp. 7212-21.
- Qizhuang, H., Jing, Y., Hui, M. & Hexing, L. 2006, 'Studies on the spectra and antibacterial properties of rare earth dinuclear complexes with L-phenylalanine and o-phenanthroline', *Materials Letters*, vol. 60, no. 3, pp. 317-20.
- Querfurth, H.W. & LaFerla, F.M. 2010, 'Mechanisms of disease', *N Engl J Med*, vol. 362, no. 4, pp. 329-44.

- Rahim, F., Javed, M.T., Ullah, H., Wadood, A., Taha, M., Ashraf, M., Khan, M.A., Khan, F., Mirza, S. & Khan, K.M. 2015, 'Synthesis, molecular docking, acetylcholinesterase and butyrylcholinesterase inhibitory potential of thiazole analogs as new inhibitors for Alzheimer disease', *Bioorganic chemistry*, vol. 62, pp. 106-16.
- Rajasree, P., Singh, R. & Sankar, C. 2012, 'Screening for acetylcholinesterase inhibitory activity of methanolic extract of *Cassia fistula* roots', *International Journal of Pharmacy & Life Sciences*, vol. 3, no. 9.
- Rao, G.N., Ney, E. & Herbert, R.A. 1999, 'Changes associated with delay of mammary cancer by retinoid analogues in transgenic mice bearing c-neu oncogene', *Breast cancer research and treatment*, vol. 58, no. 3, pp. 239-52.
- Rashid, U. & Ansari, F.L. 2014, 'Chapter 2 - Challenges in Designing Therapeutic Agents for Treating Alzheimer's Disease-from Serendipity to Rationality', *Drug Design and Discovery in Alzheimer's Disease*, Elsevier, pp. 40-141.
- Rashid, U. & Ansari, F.L. 2015, 'Challenges in Designing Therapeutic Agents for Treating Alzheimer's Disease-from Serendipity to Rationality', *Drug Design and Discovery in Alzheimer's Disease*, Elsevier, pp. 40-141.
- Raves, M.L., Harel, M., Pang, Y.-P., Silman, I., Kozikowski, A.P. & Sussman, J.L. 1997, 'Structure of acetylcholinesterase complexed with the nootropic alkaloid,(-)-huperzine A', *Nature Structural & Molecular Biology*, vol. 4, no. 1, pp. 57-63.
- Reddy, P.H. & Beal, M.F. 2008, 'Amyloid beta, mitochondrial dysfunction and synaptic damage: implications for cognitive decline in aging and Alzheimer's disease', *Trends in molecular medicine*, vol. 14, no. 2, pp. 45-53.
- Rishton, G.M., LaBonte, K., Williams, A.J., Kassam, K. & Kolovanov, E. 2006, 'Computational approaches to the prediction of blood-brain barrier permeability: A comparative analysis of central nervous system drugs versus secretase inhibitors for Alzheimer's disease', *Current opinion in drug discovery & development*, vol. 9, no. 3, pp. 303-13.
- Rizzo, S., Bartolini, M., Ceccarini, L., Piazzzi, L., Gobbi, S., Cavalli, A., Recanatini, M., Andrisano, V. & Rampa, A. 2010, 'Targeting Alzheimer's disease: Novel indanone hybrids bearing a pharmacophoric fragment of AP2238', *Bioorganic & medicinal chemistry*, vol. 18, no. 5, pp. 1749-60.
- Rizzo, S., Rivière, C.I., Piazzzi, L., Bisi, A., Gobbi, S., Bartolini, M., Andrisano, V., Morroni, F., Tarozzi, A. & Monti, J.-P. 2008, 'Benzofuran-based hybrid compounds for the inhibition of cholinesterase activity, β amyloid aggregation, and A β neurotoxicity', *Journal of medicinal chemistry*, vol. 51, no. 10, pp. 2883-6.
- Rodríguez-Rodríguez, C., Sánchez de Groot, N., Rimola, A., Alvarez-Larena, A., Lloveras, V., Vidal-Gancedo, J., Ventura, S., Vendrell, J., Sodupe, M. & González-Duarte, P. 2009, 'Design, selection, and characterization of thioflavin-based intercalation compounds with metal chelating properties for application in Alzheimer's disease', *Journal of the American Chemical Society*, vol. 131, no. 4, pp. 1436-51.
- Rosenberry, T.L. 1975, 'Catalysis by acetylcholinesterase: evidence that the rate-limiting step for acylation with certain substrates precedes general acid-base catalysis', *Proceedings of the National Academy of Sciences*, vol. 72, no. 10, pp. 3834-8.
- Rydberg, E.H., Brumshtein, B., Greenblatt, H.M., Wong, D.M., Shaya, D., Williams, L.D., Carlier, P.R., Pang, Y.-P., Silman, I. & Sussman, J.L. 2006, 'Complexes of Alkylene-Linked Tacrine Dimers with Torpedo c alifornica Acetylcholinesterase: Binding of Bis (5)-tacrine Produces a Dramatic Rearrangement in the Active-Site Gorge', *Journal of medicinal chemistry*, vol. 49, no. 18, pp. 5491-500.
- Samadi, N. & Salamati, M. 2014, 'Determination of complex stabilities with 1, 10-phenanthroline-5, 6-dione as ligand for the complexation of several transition metallic cations using chemometrics methods', *Bulletin of the Chemical Society of Ethiopia*, vol. 28, no. 3, pp. 373-82.

- Sameem, S., Kumar, N. & Pathak, D. 2012, 'Synthesis and anticonvulsant activity of some newer semicarbazone derivatives', *IJPSDR*, vol. 4, no. 3, pp. 195-8.
- Sammes, P.G. & Yahioğlu, G. 1994, '1, 10-Phenanthroline: a versatile ligand', *Chem. Soc. Rev.*, vol. 23, no. 5, pp. 327-34.
- Sauvage, J.P., Collin, J.P., Chambron, J.C., Guillerez, S., Coudret, C., Balzani, V., Barigelletti, F., De Cola, L. & Flamigni, L. 1994, 'Ruthenium (II) and osmium (II) bis (terpyridine) complexes in covalently-linked multicomponent systems: synthesis, electrochemical behavior, absorption spectra, and photochemical and photophysical properties', *Chemical Reviews*, vol. 94, no. 4, pp. 993-1019.
- Saxena, A., Redman, A.M., Jiang, X., Lockridge, O. & Doctor, B. 1997, 'Differences in active site gorge dimensions of cholinesterases revealed by binding of inhibitors to human butyrylcholinesterase', *Biochemistry*, vol. 36, no. 48, pp. 14642-51.
- Sayre, L.M., Moreira, P.I., Smith, M.A. & Perry, G. 2005, 'Metal ions and oxidative protein modification in neurological disease', *Annali dell'Istituto superiore di sanita*, vol. 41, no. 2, pp. 143-64.
- Sayre, L.M., Perry, G. & Smith, M.A. 1999, '[10] In situ methods for detection and localization of markers of oxidative stress: Application in neurodegenerative disorders', *Methods in enzymology*, vol. 309, pp. 133-52.
- Schrag, M., Mueller, C., Oyoyo, U., Smith, M.A. & Kirsch, W.M. 2011, 'Iron, zinc and copper in the Alzheimer's disease brain: a quantitative meta-analysis. Some insight on the influence of citation bias on scientific opinion', *Progress in neurobiology*, vol. 94, no. 3, pp. 296-306.
- Scott, L.E. & Orvig, C. 2009, 'Medicinal inorganic chemistry approaches to passivation and removal of aberrant metal ions in disease', *Chemical reviews*, vol. 109, no. 10, pp. 4885-910.
- Šekutor, M., Mlinarić-Majerski, K., Hrenar, T., Tomić, S. & Primožič, I. 2012, 'Adamantane-substituted guanylhydrazones: novel inhibitors of butyrylcholinesterase', *Bioorganic chemistry*, vol. 41, pp. 28-34.
- Selkoe, D.J. 2001, 'Alzheimer's Disease: Genes, Proteins, and Therapy', *Physiological reviews*, vol. 81, no. 2, pp. 741-66.
- Seubert, P., Vigo-Pelfrey, C., Esch, F., Lee, M., Dovey, H., Davis, D., Sinha, S., Schiossmacher, M., Whaley, J. & Swindlehurst, C. 1992, 'Isolation and quantification of soluble Alzheimer's β -peptide from biological fluids', *Nature*, vol. 359, no. 6393, pp. 325-7.
- Shaik, K.A. & Ahmed, A. 2014, 'An Environmentally Benign Solvent Free Novel Methods for the Synthesis of Metal Complexes Using Imidazo [4, 5-F] 1, 10-Phenanthroline and their Derivatives and Biological Activities', *International Journal of Advanced Research in Chemical Science*, vol. 1, no. 4, pp. 29-34.
- Shoji, M., Golde, T.E., Ghiso, J., Cheung, T.T., Estus, S., Shaffer, L.M., Cai, X.-D., McKay, D.M., Tintner, R. & Frangione, B. 1992, 'Production of the Alzheimer amyloid β protein by normal proteolytic processing', *Science*, pp. 126-9.
- Shreevidhya Suresh, V., Sathya, S., Akila, A., Ponnuswamy, S. & Usha, G. 2014, 'Crystal structure of 1-[2, 4-bis (4-methoxyphenyl)-3-azabicyclo [3.3. 1] nonan-3-yl] ethanone', *Acta Crystallographica Section E: Structure Reports Online*, vol. 70, no. 11, pp. o1171-o2.
- Silman, I. & Sussman, J.L. 2005, 'Acetylcholinesterase: 'classical' and 'non-classical' functions and pharmacology', *Current opinion in pharmacology*, vol. 5, no. 3, pp. 293-302.
- Sinha, S.K. & Shrivastava, S.K. 2013, 'Synthesis, evaluation and molecular dynamics study of some new 4-aminopyridine semicarbazones as an anti-amnesic and cognition enhancing agents', *Bioorganic & medicinal chemistry*, vol. 21, no. 17, pp. 5451-60.
- Smith, M.A., Harris, P.L.R., Sayre, L.M. & Perry, G. 1997, 'Iron accumulation in Alzheimer disease is a source of redox-generated free radicals', *Proceedings of the National Academy of Sciences*, vol. 94, no. 18, pp. 9866-8.
- Soreq, H. & Seidman, S. 2001, 'Acetylcholinesterase—new roles for an old actor', *Nature Reviews Neuroscience*, vol. 2, no. 4, pp. 294-302.

- Spencer, B., Marr, R.A., Rockenstein, E., Crews, L., Adame, A., Potkar, R., Patrick, C., Gage, F.H., Verma, I.M. & Masliah, E. 2008, 'Long-term neprilysin gene transfer is associated with reduced levels of intracellular Abeta and behavioral improvement in APP transgenic mice', *BMC neuroscience*, vol. 9, no. 1, p. 109.
- Squadrone, S., Brizio, P., Mancini, C., Pozzi, E., Cavalieri, S., Abete, M.C. & Brusco, A. 2015, 'Blood metal levels and related antioxidant enzyme activities in patients with ataxia telangiectasia', *Neurobiology of disease*.
- Struble, R.G., Cork, L.C., Whitehouse, P.J. & Price, D.L. 1982, 'Cholinergic innervation in neuritic plaques', *Science*, vol. 216, no. 4544, pp. 413-5.
- Su, W., Qian, Q., Li, P., Lei, X., Xiao, Q., Huang, S., Huang, C. & Cui, J. 2013, 'Synthesis, Characterization, and Anticancer Activity of a Series of Ketone-N4-Substituted Thiosemicarbazones and Their Ruthenium(II) Arene Complexes', *Inorganic Chemistry*, vol. 52, no. 21, pp. 12440-9.
- Sugimoto, H., Yamanish, Y., Iimura, Y. & Kawakami, Y. 2000, 'Donepezil hydrochloride (E2020) and other acetylcholinesterase inhibitors', *Current medicinal chemistry*, vol. 7, no. 3, pp. 303-39.
- Sussman, J.L. & Harel, M. 1991, 'Atomic structure of acetylcholinesterase from *Torpedo californica*: a prototypic acetylcholine-binding protein', *Science*, vol. 253, no. 5022, p. 872.
- Sussman, J.L., Harel, M., Frolow, F., Oefner, C., Goldman, A., Toker, L. & Silman, I. 1991, 'Atomic structure of acetylcholinesterase from *Torpedo californica*: a prototypic acetylcholine-binding protein', *Science*, vol. 253, no. 5022, pp. 872-9.
- Tamano, H. & Takeda, A. 2011, 'Dynamic action of neurometals at the synapse', *Metallomics*, vol. 3, no. 7, pp. 656-61.
- Tariot, P.N., Solomon, P., Morris, J., Kershaw, P., Lilienfeld, S., Ding, C. & Group, G.U.-S. 2000, 'A 5-month, randomized, placebo-controlled trial of galantamine in AD', *Neurology*, vol. 54, no. 12, pp. 2269-76.
- Teh, L.K. & Bertilsson, L. 2012, 'Pharmacogenomics of CYP2D6: molecular genetics, interethnic differences and clinical importance', *Drug metabolism and pharmacokinetics*, vol. 27, no. 1, pp. 55-67.
- Teri, L., Rabins, P., Whitehouse, P., Berg, L., Reisberg, B., Sunderland, T., Eichelman, B. & Phelps, C. 1992, 'Management of behavior disturbance in Alzheimer disease: current knowledge and future directions', *Alzheimer Disease & Associated Disorders*, vol. 6, no. 2, pp. 77-88.
- Thal, L., Rosen, W., Sharpless, N. & Crystal, H. 1981, 'Choline chloride fails to improve cognition in Alzheimer's disease', *Neurobiology of aging*, vol. 2, no. 3, pp. 205-8.
- Thirumurugan, P., Mahalaxmi, S. & Perumal, P.T. 2010, 'Synthesis and anti-inflammatory activity of 3-indolyl pyridine derivatives through one-pot multi component reaction', *Journal of chemical sciences*, vol. 122, no. 6, pp. 819-32.
- Tougu, V. 2001, 'Acetylcholinesterase: mechanism of catalysis and inhibition', *Current Medicinal Chemistry-Central Nervous System Agents*, vol. 1, no. 2, pp. 155-70.
- Travis, W., Knapp, C.E., Savory, C.N., Ganose, A.M., Kafourou, P., Song, X., Sharif, Z., Cockcroft, J.K., Scanlon, D.O. & Bronstein, H. 2016, 'Hybrid Organic-Inorganic Coordination Complexes as Tunable Optical Response Materials', *Inorganic chemistry*, vol. 55, no. 7, pp. 3393-400.
- Tumiatti, V., Minarini, A., Bolognesi, M., Milelli, A., Rosini, M. & Melchiorre, C. 2010, 'Tacrine derivatives and Alzheimer's disease', *Current medicinal chemistry*, vol. 17, no. 17, pp. 1825-38.
- Tyson, D.S. & Castellano, F.N. 1999, 'Light-harvesting arrays with coumarin donors and MLCT acceptors', *Inorganic chemistry*, vol. 38, no. 20, pp. 4382-3.
- Vans, D.H. & Griffith, D.A. 1982, 'Effect of pH on the electrochemical reduction of some heterocyclic quinones', *Journal of Electroanalytical Chemistry and Interfacial Electrochemistry*, vol. 134, no. 2, pp. 301-10.

- Wallin, Å., Blennow, K., Andreasen, N. & Minthon, L. 2006a, 'CSF biomarkers for Alzheimer's Disease: levels of β -amyloid, tau, phosphorylated tau relate to clinical symptoms and survival', *Dementia and geriatric cognitive disorders*, vol. 21, no. 3, pp. 131-8.
- Wallin, A.K., Blennow, K., Andreasen, N. & Minthon, L. 2006b, 'CSF biomarkers for Alzheimer's Disease: levels of beta-amyloid, tau, phosphorylated tau relate to clinical symptoms and survival', *Dementia and Geriatric Cognitive Disorders*, vol. 21, no. 3, pp. 131-8.
- Wang, B., Yang, L.-P., Zhang, X.-Z., Huang, S.-Q., Bartlam, M. & Zhou, S.-F. 2009, 'New insights into the structural characteristics and functional relevance of the human cytochrome P450 2D6 enzyme', *Drug metabolism reviews*, vol. 41, no. 4, pp. 573-643.
- Wang, H., Carlier, P.R., Ho, W.L., Wu, D.C., Lee, N.T.K., Li, C.P., Pang, Y.P. & Han, Y.F. 1999, 'Effects of bis (7)-tacrine, a novel anti-Alzheimer's agent, on rat brain AChE', *Neuroreport*, vol. 10, no. 4, pp. 789-93.
- Wang, J., Timchalk, C. & Lin, Y. 2008, 'Carbon nanotube-based electrochemical sensor for assay of salivary cholinesterase enzyme activity: an exposure biomarker of organophosphate pesticides and nerve agents', *Environmental science & technology*, vol. 42, no. 7, pp. 2688-93.
- Wang, P. & Zhu, G.-Y. 2002, 'Sol-Gel Derived Carbon Ceramic Electrode Bulk-Modified with Tris (1, 10-phenanthroline-5, 6-dione) iron (II) Hexafluorophosphate and Its Use as an Amperometric Iodate Sensor', *Chinese Journal of Chemistry*, vol. 20, no. 2, pp. 153-9.
- Wang, X., Wang, X., Zhang, C., Jiao, Y. & Guo, Z. 2012, 'Inhibitory action of macrocyclic platiniferous chelators on metal-induced A β aggregation', *Chemical Science*, vol. 3, no. 4, pp. 1304-12.
- Watkins, P.B., Zimmerman, H.J., Knapp, M.J., Gracon, S.I. & Lewis, K.W. 1994, 'Hepatotoxic effects of tacrine administration in patients with Alzheimer's disease', *Jama*, vol. 271, no. 13, pp. 992-8.
- Weinstock, M. & Groner, E. 2008, 'Rational design of a drug for Alzheimer's disease with cholinesterase inhibitory and neuroprotective activity', *Chemico-biological interactions*, vol. 175, no. 1, pp. 216-21.
- Wendlandt, A.E. & Stahl, S.S. 2014, 'Bioinspired Aerobic Oxidation of Secondary Amines and Nitrogen Heterocycles with a Bifunctional Quinone Catalyst', *Journal of the American Chemical Society*, vol. 136, no. 1, pp. 506-12.
- Wiesner, J., Kříž, Z., Kuča, K., Jun, D. & Koča, J. 2007, 'Acetylcholinesterases—the structural similarities and differences', *Journal of enzyme inhibition and medicinal chemistry*, vol. 22, no. 4, pp. 417-24.
- Wilcock, D.M. 2012, 'A changing perspective on the role of neuroinflammation in Alzheimer's disease', *International journal of Alzheimer's disease*, vol. 2012.
- Wimo, A., Winblad, B., Aguero-Torres, H. & von Strauss, E. 2003, 'The magnitude of dementia occurrence in the world', *Alzheimer Disease & Associated Disorders*, vol. 17, no. 2, pp. 63-7.
- Wright, C.I., Geula, C. & Mesulam, M. 1993, 'Neuroglial cholinesterases in the normal brain and in Alzheimer's disease: relationship to plaques, tangles, and patterns of selective vulnerability', *Annals of neurology*, vol. 34, no. 3, pp. 373-84.
- Wu, G., Robertson, D.H., Brooks, C.L. & Vieth, M. 2003, 'Detailed analysis of grid-based molecular docking: A case study of CDOCKER—A CHARMM-based MD docking algorithm', *Journal of computational chemistry*, vol. 24, no. 13, pp. 1549-62.
- Wu, J.-Z., Li, H., Zhang, J.-G. & Xu, J.-H. 2002, 'Synthesis and DNA binding behavior of a dipyrrocatechol bridged dicopper (II) complex', *Inorganic Chemistry Communications*, vol. 5, no. 1, pp. 71-5.
- Xie, S.-S., Wang, X.-B., Li, J.-Y., Yang, L. & Kong, L.-Y. 2013, 'Design, synthesis and evaluation of novel tacrine-coumarin hybrids as multifunctional cholinesterase inhibitors against Alzheimer's disease', *European journal of medicinal chemistry*, vol. 64, pp. 540-53.

- Xu, H.-H., Tao, X., Li, Y.-Q., Shen, Y.-Z. & Wei, Y.-H. 2012, 'Synthesis and characterization of a series of transition metal polypyridyl complexes and the pH-induced luminescence switch of Zn(II) and Ru(II) complexes', *Polyhedron*, vol. 33, no. 1, pp. 347-52.
- Xu, S., Wang, J., Zhao, F., Xia, H. & Wang, Y. 2015, 'Photophysical properties of copper (I) complexes containing pyrazine-fused phenanthroline ligands: a joint experimental and theoretical investigation', *Journal of molecular modeling*, vol. 21, no. 12, p. 313.
- Yamada, M., Tanaka, Y., Yoshimoto, Y., Kuroda, S. & Shimao, I. 1992, 'Synthesis and Properties of Diamino-Substituted Dipyrido (3, 2-a: 2', 3'-c) phenazine', *Bulletin of the Chemical Society of Japan*, vol. 65, no. 4, pp. 1006-11.
- Yamada, Y., Sakurai, H., Miyashita, Y., Fujisawa, K. & Okamoto, K.-i. 2002, 'Crystal structures, electronic absorption and reflectance spectral behaviors, and electrochemical properties of five-coordinated chlorocopper (II) complexes with 5, 6-disubstituted-1, 10-phenanthroline', *Polyhedron*, vol. 21, no. 21, pp. 2143-7.
- Yang, F., Nickols, N.G., Li, B.C., Marinov, G.K., Said, J.W. & Dervan, P.B. 2013, 'Antitumor activity of a pyrrole-imidazole polyamide', *Proceedings of the National Academy of Sciences*, vol. 110, no. 5, pp. 1863-8.
- Yar, S.M., Siddiqui, A.A. & Ali, A.M. 2007, 'Synthesis and antimycobacterial activity of novel heterocycles', *Journal of the Serbian Chemical Society*, vol. 72, no. 1, pp. 5-11.
- Ying, P., Tian, X., Zeng, P., Lu, J. & Chen, H. 2014, 'Synthesis, DNA-binding, Photocleavage and in vitro Cytotoxicity of Novel Imidazole [4, 5-f][1, 10] phenanthroline-based Oxovanadium Complexes', *Med chem*, vol. 4, pp. 549-57.
- Youdim, M. & Buccafusco, J. 2005a, 'CNS Targets for multi-functional drugs in the treatment of Alzheimer's and Parkinson's diseases', *Journal of neural transmission*, vol. 112, no. 4, pp. 519-37.
- Youdim, M.B. & Buccafusco, J.J. 2005b, 'Multi-functional drugs for various CNS targets in the treatment of neurodegenerative disorders', *Trends in Pharmacological Sciences*, vol. 26, no. 1, pp. 27-35.
- Zecca, L., Youdim, M.B., Riederer, P., Connor, J.R. & Crichton, R.R. 2004, 'Iron, brain ageing and neurodegenerative disorders', *Nature Reviews Neuroscience*, vol. 5, no. 11, pp. 863-73.
- Zhang, Q.-L., Liu, J.-H., Liu, J.-Z., Zhang, P.-X., Ren, X.-Z., Liu, Y., Huang, Y. & Ji, L.-N. 2004, 'DNA-binding and photoactivated enantiospecific cleavage of chiral polypyridyl ruthenium (II) complexes', *Journal of inorganic biochemistry*, vol. 98, no. 8, pp. 1405-12.
- Zheng, H., Youdim, M.B. & Fridkin, M. 2009, 'Site-Activated Multifunctional Chelator with Acetylcholinesterase and Neuroprotective- Neurorestorative Moieties for Alzheimer's Therapy', *Journal of medicinal chemistry*, vol. 52, no. 14, pp. 4095-8.
- Zhong, K.-L. 2012, 'Tris (1, 10-phenanthroline-κ2N, N') iron (II) bis (2, 4, 5-tricarboxybenzoate) monohydrate and tris (2, 2'-bipyridine-κ2N, N') iron (II) 2, 5-dicarboxybenzene-1, 4-dicarboxylate-benzene-1, 2, 4, 5-tetracarboxylic acid-water (1/1/2)', *Acta Crystallographica Section C: Crystal Structure Communications*, vol. 68, no. 9, pp. 259-64.
- Ziessel, R. 1991, 'Photocatalysis of the Homogeneous Water-Gas Shift Reaction under Ambient Conditions by Cationic Iridium (III) Complexes', *Angewandte Chemie International Edition in English*, vol. 30, no. 7, pp. 844-7.
- Zilka, N. & Novak, M. 2006, 'The tangled story of Alois Alzheimer', *Bratislavske lekarske listy*, vol. 107, no. 9/10, p. 343.
- Zotova, E., Nicoll, J.A., Kalaria, R., Holmes, C. & Boche, D. 2010, 'Inflammation in Alzheimer's disease: relevance to pathogenesis and therapy', *Alzheimers Res Ther*, vol. 2, no. 1, p. 1.

4.6 Future research outlines

- 1- Preparation of new derivatives of 1,10-phenanthroline-5,6-dione such as bipyridine dicarbonyl and other reactive substituent groups with multi hetero atoms and study their biological characteristics as pro drugs for AD and other diseases also the synthesis of phenanthroline-5,6-dione derivatives were attempted and the yield was either low or produce and desired product. If a permitted time was available, the reaction condition and the catalyst used should be modified in future toward the reaction completion.
- 2- The biological study should be expanded in future to include the investigation of AB aggregation in vitro, and the attempt to study the effect of these compounds in Vivo on animals as an important stage in prodrug studies.
- 3- Based on the encouraging positive antimicrobial screening for bacterial and fungal results on synthesised of twenty four derivatives of 1,10-phenanthroline-5,6-dione examined by the service of community for open antimicrobial drug discovery program. The accomplishment of other suggested requirements will be one of our goals in future studies such as evaluation their toxicity plus in vitro and in vivo studies on animals postponed for the potential future work.
- 4- The docking was attempted on a selected protein, however more work need to be done in future of docking study of different protein, to proof the concept of this study.
- 5- Based on the positive results of docking studies for some of the prepared compounds. The evaluation studies of these active ingredients as pro drugs for other diseases will be considered
- 6- Attempt to study the biological activity of phenanthroline-5,6-dione derivatives with other disease such as cancer disease.

APPENDIX1

Primary Antimicrobial Screening Bacterial and Fungal Procedure and Materials

Content

1.0 Summary	3
1.1 Study	3
1.2 Assay Parameters.....	3
1.3 Outcomes.....	3
1.4 Comments.....	4
1.5 Publishing CO-ADD data	4
2.0 Methods	5
2.1 Sample preparation.....	5
2.2 Antimicrobial Assay.....	5
2.2.1 Procedure	5
2.2.2 Analysis	5
2.3 Antifungal Assay	5
2.3.1 Procedure	5
2.3.2 Analysis	6
2.4 Antibiotic standards preparation and Quality control	6
3.0 Materials	7
3.1 Assay materials.....	7
3.2 Standards.....	7
3.3 Microbial Strains.....	7
4.0 Controls	8

1.0 Summary

1.1 Study

Primary antimicrobial screening study by whole cell growth inhibition assays, using the provided samples at a single concentration, in duplicate (n=2). The inhibition of growth is measured against 5 bacteria: *Escherichia coli*, *Klebsiella pneumoniae*, *Acinetobacter baumannii*, *Pseudomonas aeruginosa* and *Staphylococcus aureus*, and 2 fungi: *Candida albicans* and *Cryptococcus neoformans*.

1.2 Assay Parameters

Test concentration	32 µg/mL or 20 µM ≤1% DMSO
QC	Duplicate (n=2) Control MIC: Pass
Plates	Non-Binding Surface, 384 well plate
Media <i>Bacteria</i> <i>Fungi</i>	Cation-adjusted Mueller Hinton broth Yeast Nitrogen Base
Read Out <i>Bacteria</i> <i>C. albicans</i> <i>C. neoformans</i>	OD ₆₀₀ OD ₅₃₀ Resazurin OD ₆₀₀₋₅₇₀

1.3 Outcomes

Primary Screening outcomes are detailed in individual Project reports, personalised for each Project Submission for each CO-ADD user.

Please see your data sheet with file extension **P0XXX_PS_data.xlsx**, for example CO-ADD Project **P0100**, **P0100_PS_data.xlsx**

1.4 Comments

To confirm the inhibitory activity, the hit compound/s will be re-tested against the strains in a dose response assay to determine the minimum inhibitory concentration (MIC) of the compounds. Furthermore, to further evaluate the antimicrobial potential of the compounds they will be assayed against a mammalian cell line to determine general cell toxicity.

In order to continue with Hit Confirmation assays, CO-ADD requests (as per the standard T&C's) that chemical structures of the compound/s (both active and inactive) be supplied after receipt of the primary screening report. All structural information will be kept confidential and only used internally by CO-ADD for the purpose of evaluating novelty of the chemistry to choose compounds for further validation. No publication will result without your written consent.

If possible, please provide structures as **smiles**, **sdf/sd** or **cdx** files. If you do not have this means, images may also be accepted. Once we have received your structures, we will schedule the dose response assay of the active compound.

If you have not already provided structures to CO-ADD for your full compound set, please do so within a reasonable timeframe after receiving this report, so as not to delay Hit Confirmation.

1.5 Publishing CO-ADD data

If you wish to publish data provided by CO-ADD, we kindly ask that you acknowledge CO-ADD appropriately with the following text:

"Antimicrobial screening was performed by CO-ADD (The Community for Antimicrobial Drug Discovery), funded by the Wellcome Trust (UK) and The University of Queensland (Australia)."

Please advise us at your earliest convenience that you have used provided data for publication purposes. This information is extremely helpful in keeping track of the outputs from the CO-ADD initiative and supports the program in renewed funding possibilities to continue CO-ADD as a free screening service available to the academic community.

CO-ADD also asks, that where possible you publish your data in an openly accessible journal.

2.0 Methods

2.1 Sample preparation

Samples were provided by the collaborator and stored frozen at -20 °C. Samples were prepared in DMSO and water to a final testing concentration of 32 µg/mL or 20 µM (unless otherwise indicated in the data sheet), in 384-well, non-binding surface plate (NBS) for each bacterial/fungal strain, and in duplicate (n=2), and keeping the final DMSO concentration to a maximum of 1% DMSO. All the sample-preparation were done using liquid handling robots.

Compounds that showed solubility issues during stock solution preparation are detailed in the data sheet.

2.2 Antimicrobial Assay

2.2.1 Procedure

All bacteria were cultured in Cation-adjusted Mueller Hinton broth (**CAMHB**) at 37 °C overnight. A sample of each culture was then diluted 40-fold in fresh broth and incubated at 37 °C for 1.5-3 h. The resultant mid-log phase cultures were diluted (CFU/mL measured by OD₆₀₀), then added to each well of the compound containing plates, giving a cell density of 5×10⁵ CFU/mL and a total volume of 50 µL. All the plates were covered and incubated at 37 °C for 18 h without shaking.

2.2.2 Analysis

Inhibition of bacterial growth was determined measuring absorbance at 600 nm (OD₆₀₀), using a Tecan M1000 Pro monochromator plate reader. The percentage of growth inhibition was calculated for each well, using the negative control (media only) and positive control (bacteria without inhibitors) on the same plate as references. The significance of the inhibition values was determined by modified Z-scores, calculated using the median and MAD of the samples (no controls) on the same plate. Samples with inhibition value above 80% and Z-Score above 2.5 for either replicate (n=2 on different plates) were classed as actives. Samples with inhibition values between 50 - 80% and Z-Score above 2.5 for either replicate (n=2 on different plates) were classed as partial actives. Samples with inhibition values between 50 - 80% and Z-Score above 2.5 for either replicate (n=2 on different plates) were classed as partial actives.

2.3 Antifungal Assay

2.3.1 Procedure

Fungi strains were cultured for 3 days on Yeast Extract-Peptone Dextrose (**YPD**) agar at 30 °C. A yeast suspension of 1 x 10⁶ to 5 x 10⁶ CFU/mL (as determined by OD₅₃₀) was prepared from five colonies. The suspension was subsequently diluted and added to each well of the compound-containing plates giving a final cell density of fungi suspension of 2.5 ×10³ CFU/mL and a total volume of 50 µL. All plates were covered and incubated at 35 °C for 24 h without shaking.

2.3.2 Analysis

Growth inhibition of *C. albicans* was determined measuring absorbance at 530 nm (OD₅₃₀), while the growth inhibition of *C. neoformans* was determined measuring the difference in absorbance between 600 and 570 nm (OD₆₀₀₋₅₇₀), after the addition of resazurin (0.001% final concentration) and incubation at 35 °C for additional 2 h. The absorbance was measured using a Biotek Synergy HTX plate reader. The percentage of growth inhibition was calculated for each well, using the negative control (media only) and positive control (fungi without inhibitors) on the same plate. The significance of the inhibition values was determined by modified Z-scores, calculated using the median and MAD of the samples (no controls) on the same plate. Samples with inhibition value above 80% and Z-Score above 2.5 for either replicate (n=2 on different plates) were classed as actives. Samples with inhibition values between 50 - 80% and Z-Score above 2.5 for either replicate (n=2 on different plates) were classed as partial actives.

2.4 Antibiotic standards preparation and Quality control

Colistin and Vancomycin were used as positive bacterial inhibitor standards for Gram-negative and Gram-positive bacteria, respectively. Fluconazole was used as a positive fungal inhibitor standard for *C. albicans* and *C. neoformans*.

The antibiotics were provided in 4 concentrations, with 2 above and 2 below its MIC value, and plated into the first 8 wells of column 23 of the 384-well NBS plates.

The quality control (QC) of the assays was determined by the antimicrobial controls and the Z'-factor (using positive and negative controls). Each plate was deemed to fulfil the quality criteria (pass QC), if the Z'-factor was above 0.4, and the antimicrobial standards showed full range of activity, with full growth inhibition at their highest concentration, and no growth inhibition at their lowest concentration.

3.0 Materials

3.1 Assay materials

Material	Code	Brand	Cat No.
Compound preparation plate [Polypropylene]	PP	Corning	3364
Assay Plates [Non-binding surface]	NBS 384w	Corning	3640
Growth media - bacteria	CAMHB	Bacto Laboratories	212322
Culture agar - fungi	YPD	Becton Dickinson	242720
Growth media - fungi	YNB	Becton Dickinson	233520
Resazurin		Sigma-Aldrich	R7017

3.2 Standards

Sample Name	Sample ID	Full MW	Stock Conc. (mg/mL)	Solvent	Source
Colistin - Sulfate	MCC_000094:02	1400.63	10.0	DMSO	Sigma; C4461
Vancomycin - HCL	MCC_000095:02	1485.71	10.0	DMSO	Sigma; 861987
Fluconazole	MCC_008383:01	306.27	2.56	DMSO	Sigma; F8929

3.3 Microbial Strains

ID	Batch	Organism	Strain	Description
GN_001	02	<i>Escherichia coli</i>	ATCC 25922	FDA control strain
GN_003	02	<i>Klebsiella pneumoniae</i>	ATCC 700603	MDR
GN_034	02	<i>Acinetobacter baumannii</i>	ATCC 19606	Type strain
GN_042	02	<i>Pseudomonas aeruginosa</i>	ATCC 27853	Quality control strain
GP_020	02	<i>Staphylococcus aureus</i>	ATCC 43300	MRSA
FG_001	01	<i>Candida albicans</i>	ATCC 90028	CLSI reference
FG_002	01	<i>Cryptococcus neoformans</i>	ATCC 208821	H99 - Type strain

4.0 Controls

All antibiotic and antifungal controls displayed inhibitory values within the expected range. For inhibitory results for controls please contact the CO-ADD at support@co-add.org.

Strain ID	Species	Antibiotic	Pass/Fail
GN_001:02	<i>E. coli</i>	Colistin	Pass
GN_003:02	<i>K. pneumoniae</i> (MDR)	Colistin	Pass
GN_034:02	<i>A. baumannii</i>	Colistin	Pass
GN_042:02	<i>P. aeruginosa</i>	Colistin	Pass
GP_020:02	<i>S. aureus</i> (MRSA)	Vancomycin	Pass
FG_001:01	<i>C. albicans</i>	Fluconazole	Pass
FG_002:01	<i>C. neoformans</i> (H99)	Fluconazole	Pass

Summary

CompoundID	Compo	ProjectID	RunID	Sel	Act	Sa	Ec	Kp	Pa	Ab	Ca	Cn	Conc
C0334780	ST11	P0529	PSR00152	3	2	85.75	77.36	37.1	18.32	73.37	73.6	109.9	32 ug/mL
C0334791	ST22	P0529	PSR00152	3	3	97.29	96.52	94.43	42.31	96.26	94.09	108.2	32 ug/mL
C0334770	ST01	P0529	PSR00152	3	3	94.52	95.79	96.14	97.79	96.24	100.4	113.1	32 ug/mL
C0334781	ST12	P0529	PSR00152	3	3	86.34	92.15	38.37	9.28	91.73	9.57	111.5	32 ug/mL
C0334792	ST23	P0529	PSR00152	3	3	92.01	96.06	94.49	83.2	95.53	99.61	116.4	32 ug/mL
C0334771	ST02	P0529	PSR00152	3	3	95.28	96.23	49.55	13.43	94	96.55	113.4	32 ug/mL
C0334782	ST13	P0529	PSR00152	2	2	87.31	90.94	35.61	9.36	90.31	7.02	-22.29	32 ug/mL
C0334793	ST24	P0529	PSR00152	3	3	84.47	71.86	84.44	91.69	85.94	52.35	111.7	32 ug/mL
C0334772	ST03	P0529	PSR00152	0	0	9.67	-6.96	9.18	8.78	-11.15	9.13	-18.35	32 ug/mL
C0334783	ST14	P0529	PSR00152	3	3	86.05	92.46	32.4	7.86	92.68	5.12	108.9	32 ug/mL
C0334773	ST04	P0529	PSR00152	3	3	90.34	91.83	88.03	94.34	90.13	101.2	92.85	32 ug/mL
C0334784	ST15	P0529	PSR00152	3	3	98.81	97.91	97.64	98.69	97.82	101.2	106.1	32 ug/mL
C0334774	ST05	P0529	PSR00152	2	2	79.01	87.17	61.96	46.35	86.61	8.44	88.5	32 ug/mL
C0334785	ST16	P0529	PSR00152	3	3	96.26	97.02	97.04	98.38	96.27	101.7	106.4	32 ug/mL
C0334775	ST06	P0529	PSR00152	2	2	84.79	89.13	77.19	82	88.97	10.47	1.2	32 ug/mL
C0334786	ST17	P0529	PSR00152	2	2	26.14	87.45	34.64	25.87	15.91	96.78	92.68	32 ug/mL
C0334776	ST07	P0529	PSR00152	0	0	12.8	6.46	19.09	8.02	10.9	10.56	-0.9	32 ug/mL
C0334787	ST18	P0529	PSR00152	3	3	95.19	97.45	39.66	10.66	97.48	7.38	107.7	32 ug/mL
C0334790	ST21	P0529	PSR00152	1	1	56.99	70.67	34.08	31.96	98.13	5.27	41.83	32 ug/mL
C0334777	ST08	P0529	PSR00152	2	2	88.82	92.3	67.67	83.07	90.52	6.46	-14.14	32 ug/mL
C0334788	ST19	P0529	PSR00152	1	1	21.66	16.09	18.3	18.68	34.32	9.57	105.5	32 ug/mL
C0334778	ST09	P0529	PSR00152	2	2	85.84	92.57	34.78	16.64	91.06	7.3	-14.14	32 ug/mL
C0334789	ST20	P0529	PSR00152	3	3	95.81	94.46	95.4	97.84	94.31	100.1	109.9	32 ug/mL
C0334779	ST10	P0529	PSR00152	0	0	47.39	-50.89	-25.91	9.86	-11.37	9.08	33.25	32 ug/mL

Details

CompoundID	CompoundName	ProjectID	RunID	Sel	Act	Act_GP	Act_ON	Act_FS	Kp_Inhibition	Kp_ZScore	Kp_Act	Pa_Inhibition	Pa_ZScore	Pa_Ab_Act	Ca_Inhibition	Ca_ZScore	Ca_Act	Cn_Inhibition	Cn_ZScore	Cn_Act
C0334780	ST11	P0529	PSR00152	3	2	1	0	1	21.8 97.1 PCT;	-10.49	I 183.95 PCT;	-02.16	P P	30.1; 79.6; PCT;	-15.7; -6.9	I P	102.8; 109.9; PCT;	-13.3; -7.6	A A	
C0334791	ST22	P0529	PSR00152	3	3	1	3	2	51.0 94.4 PCT;	-13.4 -3.6	A P 380.423 PCT;	-51. -53	A A	90.6; 94.1; PCT;	-19.5; -23.1	A A	102.6; 108.2; PCT;	-13.2; -7.6	A A	
C0334770	ST01	P0529	PSR00152	3	3	1	4	2	91.6 96.1 PCT;	-13.2 -7.6	A A 97.1 97.8 PCT;	-137. -154	A A	100.4; 99.7; PCT;	-21.7; -24.5	A A	105.5; 113.1; PCT;	-13.6; -7.8	A A	
C0334781	ST12	P0529	PSR00152	3	3	1	2	1	34.6 38.4 PCT;	-10. -51	I 1 2.9 93 PCT;	-02.10	A A	2.7; 9.6; PCT;	-1.3; 0.0	I I	106.7; 111.5; PCT;	-13.5; -7.9	A A	
C0334792	ST23	P0529	PSR00152	3	3	1	4	2	94.2 94.5 PCT;	-13.4 -7.4	A A 81.2 83.2 PCT;	-115. -126	A A	98.8; 99.6; PCT;	-21.5; -24.2	A A	108.5; 116.4; PCT;	-13.9; -8.0	A A	
C0334771	ST02	P0529	PSR00152	3	3	1	2	2	41.9 49.6 PCT;	-27. -68	I 127.134 PCT;	-07. -09	A A	86.7; 96.6; PCT;	-18.6; -23.7	A A	105.3; 113.4; PCT;	-13.7; -7.8	A A	
C0334782	ST13	P0529	PSR00152	2	2	1	2	0	31.3 35.6 PCT;	-17. -47	I 30.9 34 PCT;	-02.09	A A	3.9; 7.0; PCT;	-0.0; -1.1	I I	-22.3; -25.7; PCT;	-0.8; 0.9	I I	
C0334793	ST24	P0529	PSR00152	3	3	1	3	1	82.9 84.4 PCT;	-11.9 -6.4	A A 78.9 91.7 PCT;	-122. -128	A P	35.7; 52.4; PCT;	-12.5; -7.2	I P	102.6; 111.7; PCT;	-13.5; -7.6	A A	
C0334772	ST03	P0529	PSR00152	0	0	0	0	0	-0.3 92 PCT;	0.3 0.6	I 23.8 88 PCT;	-01.08	I I	3.6; 9.1; PCT;	-1.6; 0.0	I I	-18.4; -31.7; PCT;	0.0; 0.4	I I	
C0334783	ST14	P0529	PSR00152	3	3	1	2	1	26.7 32.4 PCT;	-1.3; -42	I 53.7 9 PCT;	0.0 0.5	A A	3.9; 5.1; PCT;	-0.3; -0.3	I I	105.2; 108.9; PCT;	-13.2; -7.8	A A	
C0334773	ST04	P0529	PSR00152	3	3	1	4	2	87.4 88.0 PCT;	-12.3; -6.8	A A 94.2 94.3 PCT;	-132. -149	A A	100.2; 101.2; PCT;	-21.9; -24.6	A A	91.6; 92.9; PCT;	-11.6; -6.9	A A	
C0334784	ST15	P0529	PSR00152	3	3	1	4	2	97.6 97.6 PCT;	-13.8; -7.7	A A 98.4 98.7 PCT;	-13.9 -15.6	A A	100.0; 101.2; PCT;	-21.9; -24.5	A A	100.2; 106.1; PCT;	-13.0; -7.4	A A	
C0334774	ST05	P0529	PSR00152	2	2	0	2	1	56.1 62.0 PCT;	-3.9; -8.6	P P 44.0 46.4 PCT;	-5.9; -62	A A	4.1; 8.4; PCT;	-0.3; -1.1	I I	84.6; 88.5; PCT;	-11.3; -6.4	A A	
C0334785	ST16	P0529	PSR00152	3	3	1	4	2	95.6 97.0 PCT;	-13.5; -7.6	A A 98.1 98.4 PCT;	-13.8 -15.6	A A	100.5; 101.7; PCT;	-22.0; -24.7	A A	101.9; 106.4; PCT;	-13.0; -7.5	A A	
C0334775	ST06	P0529	PSR00152	2	2	1	3	0	66.6 77.2 PCT;	-10.8; -4.9	P P 80.1 82.0 PCT;	-11.3 -12.4	A A	10.5; 6.3; PCT;	-0.6; -1.9	I I	-31.4; 1.2; PCT;	-0.8; 0.0	I I	
C0334786	ST17	P0529	PSR00152	2	2	0	1	2	14.1 34.6 PCT;	-1.6; -2.0	I 23.8 25.9 PCT;	-2.4 -3.0	I I	96.1; 96.8; PCT;	-20.9; -23.6	A A	88.0; 92.7; PCT;	-11.7; -6.6	A A	
C0334776	ST07	P0529	PSR00152	0	0	0	0	0	19.1 5.8 PCT;	-0.3; -0.6	I 7.5 8.0 PCT;	-0.0 0.2	I I	0.0; 10.6; PCT;	-1.5; 0.7	I I	-0.9; -35.7; PCT;	-0.7; 0.4	I I	
C0334787	ST18	P0529	PSR00152	3	3	1	2	1	32.6 39.7 PCT;	-1.8; -5.3	I 107.2 17 PCT;	-0.4 1.0	A A	6.4; 7.4; PCT;	-0.8; -0.9	I I	103.2; 107.7; PCT;	-13.1; -7.6	A A	
C0334790	ST21	P0529	PSR00152	1	1	0	1	0	25.3 34.1 PCT;	-2.0; -3.2	I 28.3 32.0 PCT;	-3.3; -3.7	A A	-0.2; 5.3; PCT;	-0.6; 0.9	I I	17.9; 41.8; PCT;	-3.5; -4.6	I I	
C0334777	ST08	P0529	PSR00152	2	2	1	3	0	56.5 67.7 PCT;	-4.0; -9.4	P P 45.3 83.1 PCT;	-12.9 -5.7	A A	4.9; 6.5; PCT;	-0.5; -0.6	I I	-14.1; -40.1; PCT;	0.2; 0.8	I I	
C0334788	ST19	P0529	PSR00152	1	1	0	0	1	18.1 18.3 PCT;	-0.5; -2.2	I 15.9 18.7 PCT;	-12. -18	I I	6.0; 9.6; PCT;	-0.8; -1.3	I I	-35.5; 105.5; PCT;	-7.8; 0.4	A I	
C0334778	ST09	P0529	PSR00152	2	2	1	2	0	31.7 34.8 PCT;	-2.0; -4.1	I 13.2 16.6 PCT;	-0.8 -1.3	A A	4.3; 7.3; PCT;	-0.1; -1.1	I I	-14.1; -34.8; PCT;	0.2; 0.3	I I	
C0334789	ST20	P0529	PSR00152	3	3	1	4	2	94.9 95.4 PCT;	-13.4 -7.5	A A 96.2 97.8 PCT;	-13.5 -15.5	A A	100.1; 100.1; PCT;	-21.6; -24.6	A A	105.0; 109.9; PCT;	-13.3; -7.7	A A	
C0334779	ST10	P0529	PSR00152	0	0	0	0	0	-25.9 -32.2 PCT;	3.4 5.4	I 0.7 9.9 PCT;	-0.2 1.1	I I	5.7; 9.1; PCT;	-0.7; -1.2	I I	1.9; 33.3; PCT;	-3.0; -3.1	I I	

Inhibition

CompoundID	Compc	Project	OrgID	Organism	Strain	PSRunID	TestPlateID	TestIbition	Zscore	Conc	ConcUni
C0334791	ST22	P0529	GN_042	Pseudomonas aeruginosa	ATCC 27853	PSR00152	TP00476-08C	O15	42.31	-5.27	32.00 ug/mL
C0334791	ST22	P0529	FG_001	Candida albicans	ATCC 90028	PSR00152	TP00476-20F	O15	90.56	-19.50	32.00 ug/mL
C0334791	ST22	P0529	GN_042	Pseudomonas aeruginosa	ATCC 27853	PSR00152	TP00476-07C	O15	38.01	-5.12	32.00 ug/mL
C0334791	ST22	P0529	FG_001	Candida albicans	ATCC 90028	PSR00152	TP00476-19F	O15	94.09	-23.05	32.00 ug/mL
C0334791	ST22	P0529	GN_034	Acinetobacter baumannii	ATCC 19606	PSR00152	TP00476-05C	O15	94.92	-8.35	32.00 ug/mL
C0334791	ST22	P0529	GN_034	Acinetobacter baumannii	ATCC 19606	PSR00152	TP00476-06C	O15	96.26	-10.80	32.00 ug/mL
C0334791	ST22	P0529	GN_001	Escherichia coli	ATCC 25922	PSR00152	TP00476-01C	O15	96.52	-18.94	32.00 ug/mL
C0334791	ST22	P0529	GN_001	Escherichia coli	ATCC 25922	PSR00152	TP00476-02C	O15	90.67	-16.96	32.00 ug/mL
C0334791	ST22	P0529	GN_003	Klebsiella pneumoniae	MDR; ATCC 700603	PSR00152	TP00476-03C	O15	94.43	-13.36	32.00 ug/mL
C0334791	ST22	P0529	FG_002	Cryptococcus neoformans	H99; ATCC 208821	PSR00152	TP00476-17F	O15	108.18	-13.16	32.00 ug/mL
C0334791	ST22	P0529	FG_002	Cryptococcus neoformans	H99; ATCC 208821	PSR00152	TP00476-18F	O15	102.63	-7.58	32.00 ug/mL
C0334791	ST22	P0529	GP_020	Staphylococcus aureus	MRSA; ATCC 43300	PSR00152	TP00476-16V	O15	95.87	-10.85	32.00 ug/mL
C0334791	ST22	P0529	GP_020	Staphylococcus aureus	MRSA; ATCC 43300	PSR00152	TP00476-15V	O15	97.29	-8.03	32.00 ug/mL
C0334791	ST22	P0529	GN_003	Klebsiella pneumoniae	MDR; ATCC 700603	PSR00152	TP00476-04C	O15	52.01	-3.58	32.00 ug/mL
C0334780	ST11	P0529	GN_042	Pseudomonas aeruginosa	ATCC 27853	PSR00152	TP00476-08C	M15	18.32	-1.60	32.00 ug/mL
C0334780	ST11	P0529	FG_001	Candida albicans	ATCC 90028	PSR00152	TP00476-20F	M15	73.60	-15.69	32.00 ug/mL
C0334780	ST11	P0529	GN_042	Pseudomonas aeruginosa	ATCC 27853	PSR00152	TP00476-07C	M15	9.50	-0.18	32.00 ug/mL
C0334780	ST11	P0529	FG_001	Candida albicans	ATCC 90028	PSR00152	TP00476-19F	M15	30.07	-6.88	32.00 ug/mL
C0334780	ST11	P0529	GN_034	Acinetobacter baumannii	ATCC 19606	PSR00152	TP00476-05C	M15	71.88	-6.27	32.00 ug/mL
C0334780	ST11	P0529	GN_034	Acinetobacter baumannii	ATCC 19606	PSR00152	TP00476-06C	M15	73.37	-8.25	32.00 ug/mL
C0334780	ST11	P0529	GN_001	Escherichia coli	ATCC 25922	PSR00152	TP00476-01C	M15	49.60	-9.80	32.00 ug/mL
C0334780	ST11	P0529	GN_001	Escherichia coli	ATCC 25922	PSR00152	TP00476-02C	M15	77.36	-14.45	32.00 ug/mL
C0334780	ST11	P0529	GN_003	Klebsiella pneumoniae	MDR; ATCC 700603	PSR00152	TP00476-03C	M15	37.10	-4.93	32.00 ug/mL
C0334780	ST11	P0529	FG_002	Cryptococcus neoformans	H99; ATCC 208821	PSR00152	TP00476-17F	M15	109.93	-13.32	32.00 ug/mL
C0334780	ST11	P0529	FG_002	Cryptococcus neoformans	H99; ATCC 208821	PSR00152	TP00476-18F	M15	102.78	-7.59	32.00 ug/mL
C0334780	ST11	P0529	GP_020	Staphylococcus aureus	MRSA; ATCC 43300	PSR00152	TP00476-16V	M15	82.17	-9.07	32.00 ug/mL
C0334780	ST11	P0529	GP_020	Staphylococcus aureus	MRSA; ATCC 43300	PSR00152	TP00476-15V	M15	85.75	-6.99	32.00 ug/mL
C0334780	ST11	P0529	GN_003	Klebsiella pneumoniae	MDR; ATCC 700603	PSR00152	TP00476-04C	M15	22.79	-0.95	32.00 ug/mL
C0334792	ST23	P0529	GN_042	Pseudomonas aeruginosa	ATCC 27853	PSR00152	TP00476-08C	O17	83.20	-11.51	32.00 ug/mL
C0334792	ST23	P0529	FG_001	Candida albicans	ATCC 90028	PSR00152	TP00476-20F	O17	99.61	-21.53	32.00 ug/mL
C0334792	ST23	P0529	GN_042	Pseudomonas aeruginosa	ATCC 27853	PSR00152	TP00476-07C	O17	81.24	-12.62	32.00 ug/mL
C0334792	ST23	P0529	FG_001	Candida albicans	ATCC 90028	PSR00152	TP00476-19F	O17	98.80	-24.24	32.00 ug/mL
C0334792	ST23	P0529	GN_034	Acinetobacter baumannii	ATCC 19606	PSR00152	TP00476-05C	O17	93.31	-8.20	32.00 ug/mL
C0334792	ST23	P0529	GN_034	Acinetobacter baumannii	ATCC 19606	PSR00152	TP00476-06C	O17	95.53	-10.72	32.00 ug/mL
C0334792	ST23	P0529	GN_001	Escherichia coli	ATCC 25922	PSR00152	TP00476-01C	O17	96.06	-18.85	32.00 ug/mL
C0334792	ST23	P0529	GN_001	Escherichia coli	ATCC 25922	PSR00152	TP00476-02C	O17	95.14	-17.80	32.00 ug/mL
C0334792	ST23	P0529	GN_003	Klebsiella pneumoniae	MDR; ATCC 700603	PSR00152	TP00476-03C	O17	94.49	-13.37	32.00 ug/mL
C0334792	ST23	P0529	FG_002	Cryptococcus neoformans	H99; ATCC 208821	PSR00152	TP00476-17F	O17	116.37	-13.93	32.00 ug/mL
C0334792	ST23	P0529	FG_002	Cryptococcus neoformans	H99; ATCC 208821	PSR00152	TP00476-18F	O17	108.50	-7.97	32.00 ug/mL
C0334792	ST23	P0529	GP_020	Staphylococcus aureus	MRSA; ATCC 43300	PSR00152	TP00476-16V	O17	92.01	-10.35	32.00 ug/mL
C0334792	ST23	P0529	GP_020	Staphylococcus aureus	MRSA; ATCC 43300	PSR00152	TP00476-15V	O17	90.48	-7.42	32.00 ug/mL
C0334792	ST23	P0529	GN_003	Klebsiella pneumoniae	MDR; ATCC 700603	PSR00152	TP00476-04C	O17	94.19	-7.38	32.00 ug/mL
C0334781	ST12	P0529	GN_042	Pseudomonas aeruginosa	ATCC 27853	PSR00152	TP00476-08C	M17	9.28	-0.22	32.00 ug/mL
C0334781	ST12	P0529	FG_001	Candida albicans	ATCC 90028	PSR00152	TP00476-20F	M17	9.57	-1.31	32.00 ug/mL
C0334781	ST12	P0529	FG_001	Candida albicans	ATCC 90028	PSR00152	TP00476-20F	M17	9.57	-1.31	32.00 ug/mL

CompoundID	Compc	Project	OrgID	Organism	Strain	PSRunID	TestPlateID	TestIbibition	Zscore	Conc	ConcUn
C0334781	ST12	P0529	GN_042	Pseudomonas aeruginosa	ATCC 27853	PSR00152	TP00476-07C	M17	2.93	0.95	32.00 ug/mL
C0334781	ST12	P0529	FG_001	Candida albicans	ATCC 90028	PSR00152	TP00476-19F	M17	2.67	0.03	32.00 ug/mL
C0334781	ST12	P0529	GN_034	Acinetobacter baumannii	ATCC 19606	PSR00152	TP00476-05C	M17	89.46	-7.86	32.00 ug/mL
C0334781	ST12	P0529	GN_034	Acinetobacter baumannii	ATCC 19606	PSR00152	TP00476-06C	M17	91.73	-10.29	32.00 ug/mL
C0334781	ST12	P0529	GN_001	Escherichia coli	ATCC 25922	PSR00152	TP00476-01C	M17	91.94	-18.05	32.00 ug/mL
C0334781	ST12	P0529	GN_001	Escherichia coli	ATCC 25922	PSR00152	TP00476-02C	M17	92.15	-17.24	32.00 ug/mL
C0334781	ST12	P0529	GN_003	Klebsiella pneumoniae	MDR; ATCC 700603	PSR00152	TP00476-03C	M17	38.37	-5.12	32.00 ug/mL
C0334781	ST12	P0529	FG_002	Cryptococcus neoformans	H99; ATCC 208821	PSR00152	TP00476-17F	M17	111.49	-13.47	32.00 ug/mL
C0334781	ST12	P0529	FG_002	Cryptococcus neoformans	H99; ATCC 208821	PSR00152	TP00476-18F	M17	106.69	-7.85	32.00 ug/mL
C0334781	ST12	P0529	GP_020	Staphylococcus aureus	MRSA; ATCC 43300	PSR00152	TP00476-16V	M17	86.34	-9.61	32.00 ug/mL
C0334781	ST12	P0529	GP_020	Staphylococcus aureus	MRSA; ATCC 43300	PSR00152	TP00476-15V	M17	85.68	-6.99	32.00 ug/mL
C0334781	ST12	P0529	GN_003	Klebsiella pneumoniae	MDR; ATCC 700603	PSR00152	TP00476-04C	M17	34.59	-2.01	32.00 ug/mL
C0334770	ST01	P0529	GN_042	Pseudomonas aeruginosa	ATCC 27853	PSR00152	TP00476-08C	K17	97.79	-13.74	32.00 ug/mL
C0334770	ST01	P0529	FG_001	Candida albicans	ATCC 90028	PSR00152	TP00476-20F	K17	100.38	-21.71	32.00 ug/mL
C0334770	ST01	P0529	GN_042	Pseudomonas aeruginosa	ATCC 27853	PSR00152	TP00476-07C	K17	97.23	-15.39	32.00 ug/mL
C0334770	ST01	P0529	FG_001	Candida albicans	ATCC 90028	PSR00152	TP00476-19F	K17	99.71	-24.47	32.00 ug/mL
C0334770	ST01	P0529	GN_034	Acinetobacter baumannii	ATCC 19606	PSR00152	TP00476-05C	K17	92.16	-8.10	32.00 ug/mL
C0334770	ST01	P0529	GN_034	Acinetobacter baumannii	ATCC 19606	PSR00152	TP00476-06C	K17	96.24	-10.79	32.00 ug/mL
C0334770	ST01	P0529	GN_001	Escherichia coli	ATCC 25922	PSR00152	TP00476-01C	K17	95.79	-18.80	32.00 ug/mL
C0334770	ST01	P0529	GN_001	Escherichia coli	ATCC 25922	PSR00152	TP00476-02C	K17	95.25	-17.82	32.00 ug/mL
C0334770	ST01	P0529	GN_003	Klebsiella pneumoniae	MDR; ATCC 700603	PSR00152	TP00476-03C	K17	93.63	-13.24	32.00 ug/mL
C0334770	ST01	P0529	FG_002	Cryptococcus neoformans	H99; ATCC 208821	PSR00152	TP00476-17F	K17	113.06	-13.62	32.00 ug/mL
C0334770	ST01	P0529	FG_002	Cryptococcus neoformans	H99; ATCC 208821	PSR00152	TP00476-18F	K17	105.49	-7.77	32.00 ug/mL
C0334770	ST01	P0529	GP_020	Staphylococcus aureus	MRSA; ATCC 43300	PSR00152	TP00476-16V	K17	94.52	-10.67	32.00 ug/mL
C0334770	ST01	P0529	GP_020	Staphylococcus aureus	MRSA; ATCC 43300	PSR00152	TP00476-15V	K17	94.07	-7.74	32.00 ug/mL
C0334770	ST01	P0529	GN_003	Klebsiella pneumoniae	MDR; ATCC 700603	PSR00152	TP00476-04C	K17	96.14	-7.55	32.00 ug/mL
C0334793	ST24	P0529	GN_042	Pseudomonas aeruginosa	ATCC 27853	PSR00152	TP00476-08C	O19	91.69	-12.81	32.00 ug/mL
C0334793	ST24	P0529	FG_001	Candida albicans	ATCC 90028	PSR00152	TP00476-20F	O19	35.72	-7.18	32.00 ug/mL
C0334793	ST24	P0529	GN_042	Pseudomonas aeruginosa	ATCC 27853	PSR00152	TP00476-07C	O19	78.94	-12.22	32.00 ug/mL
C0334793	ST24	P0529	FG_001	Candida albicans	ATCC 90028	PSR00152	TP00476-19F	O19	52.35	-12.51	32.00 ug/mL
C0334793	ST24	P0529	GN_034	Acinetobacter baumannii	ATCC 19606	PSR00152	TP00476-05C	O19	79.16	-6.93	32.00 ug/mL
C0334793	ST24	P0529	GN_034	Acinetobacter baumannii	ATCC 19606	PSR00152	TP00476-06C	O19	85.94	-9.65	32.00 ug/mL
C0334793	ST24	P0529	GN_001	Escherichia coli	ATCC 25922	PSR00152	TP00476-01C	O19	28.77	-5.75	32.00 ug/mL
C0334793	ST24	P0529	GN_001	Escherichia coli	ATCC 25922	PSR00152	TP00476-02C	O19	71.86	-13.42	32.00 ug/mL
C0334793	ST24	P0529	GN_003	Klebsiella pneumoniae	MDR; ATCC 700603	PSR00152	TP00476-03C	O19	84.44	-11.89	32.00 ug/mL
C0334793	ST24	P0529	FG_002	Cryptococcus neoformans	H99; ATCC 208821	PSR00152	TP00476-17F	O19	111.67	-13.49	32.00 ug/mL
C0334793	ST24	P0529	FG_002	Cryptococcus neoformans	H99; ATCC 208821	PSR00152	TP00476-18F	O19	102.63	-7.58	32.00 ug/mL
C0334793	ST24	P0529	GP_020	Staphylococcus aureus	MRSA; ATCC 43300	PSR00152	TP00476-16V	O19	84.47	-9.37	32.00 ug/mL
C0334793	ST24	P0529	GP_020	Staphylococcus aureus	MRSA; ATCC 43300	PSR00152	TP00476-15V	O19	54.38	-4.17	32.00 ug/mL
C0334793	ST24	P0529	GN_003	Klebsiella pneumoniae	MDR; ATCC 700603	PSR00152	TP00476-04C	O19	82.89	-6.36	32.00 ug/mL
C0334782	ST13	P0529	GN_042	Pseudomonas aeruginosa	ATCC 27853	PSR00152	TP00476-08C	M19	9.36	-0.23	32.00 ug/mL
C0334782	ST13	P0529	FG_001	Candida albicans	ATCC 90028	PSR00152	TP00476-20F	M19	3.92	-0.04	32.00 ug/mL
C0334782	ST13	P0529	GN_042	Pseudomonas aeruginosa	ATCC 27853	PSR00152	TP00476-07C	M19	3.04	0.93	32.00 ug/mL
C0334782	ST13	P0529	FG_001	Candida albicans	ATCC 90028	PSR00152	TP00476-19F	M19	7.02	-1.06	32.00 ug/mL

CompoundID	Compc	Project	OrgID	Organism	Strain	PSRunID	TestPlateID	TestIbition	Zscore	Conc	ConcUn
C0334782	ST13	P0529	GN_034	Acinetobacter baumannii	ATCC 19606	PSR00152	TP00476-05C	M19	88.08	-7.73	32.00 ug/mL
C0334782	ST13	P0529	GN_034	Acinetobacter baumannii	ATCC 19606	PSR00152	TP00476-06C	M19	90.31	-10.13	32.00 ug/mL
C0334782	ST13	P0529	GN_001	Escherichia coli	ATCC 25922	PSR00152	TP00476-01C	M19	90.87	-17.84	32.00 ug/mL
C0334782	ST13	P0529	GN_001	Escherichia coli	ATCC 25922	PSR00152	TP00476-02C	M19	90.94	-17.01	32.00 ug/mL
C0334782	ST13	P0529	GN_003	Klebsiella pneumoniae	MDR; ATCC 700603	PSR00152	TP00476-03C	M19	35.61	-4.71	32.00 ug/mL
C0334782	ST13	P0529	FG_002	Cryptococcus neoformans	H99; ATCC 208821	PSR00152	TP00476-17F	M19	-22.29	-0.83	32.00 ug/mL
C0334782	ST13	P0529	FG_002	Cryptococcus neoformans	H99; ATCC 208821	PSR00152	TP00476-18F	M19	-25.73	0.93	32.00 ug/mL
C0334782	ST13	P0529	GP_020	Staphylococcus aureus	MRSA; ATCC 43300	PSR00152	TP00476-16V	M19	86.34	-9.61	32.00 ug/mL
C0334782	ST13	P0529	GP_020	Staphylococcus aureus	MRSA; ATCC 43300	PSR00152	TP00476-15V	M19	87.31	-7.13	32.00 ug/mL
C0334782	ST13	P0529	GN_003	Klebsiella pneumoniae	MDR; ATCC 700603	PSR00152	TP00476-04C	M19	31.45	-1.73	32.00 ug/mL
C0334771	ST02	P0529	GN_042	Pseudomonas aeruginosa	ATCC 27853	PSR00152	TP00476-08C	K19	12.68	-0.74	32.00 ug/mL
C0334771	ST02	P0529	FG_001	Candida albicans	ATCC 90028	PSR00152	TP00476-20F	K19	86.74	-18.64	32.00 ug/mL
C0334771	ST02	P0529	GN_042	Pseudomonas aeruginosa	ATCC 27853	PSR00152	TP00476-07C	K19	13.43	-0.86	32.00 ug/mL
C0334771	ST02	P0529	FG_001	Candida albicans	ATCC 90028	PSR00152	TP00476-19F	K19	96.55	-23.67	32.00 ug/mL
C0334771	ST02	P0529	GN_034	Acinetobacter baumannii	ATCC 19606	PSR00152	TP00476-05C	K19	94.00	-8.27	32.00 ug/mL
C0334771	ST02	P0529	GN_034	Acinetobacter baumannii	ATCC 19606	PSR00152	TP00476-06C	K19	93.81	-10.52	32.00 ug/mL
C0334771	ST02	P0529	GN_001	Escherichia coli	ATCC 25922	PSR00152	TP00476-01C	K19	96.23	-18.88	32.00 ug/mL
C0334771	ST02	P0529	GN_001	Escherichia coli	ATCC 25922	PSR00152	TP00476-02C	K19	96.23	-18.01	32.00 ug/mL
C0334771	ST02	P0529	GN_003	Klebsiella pneumoniae	MDR; ATCC 700603	PSR00152	TP00476-03C	K19	49.55	-6.76	32.00 ug/mL
C0334771	ST02	P0529	FG_002	Cryptococcus neoformans	H99; ATCC 208821	PSR00152	TP00476-17F	K19	113.41	-13.65	32.00 ug/mL
C0334771	ST02	P0529	FG_002	Cryptococcus neoformans	H99; ATCC 208821	PSR00152	TP00476-18F	K19	105.34	-7.76	32.00 ug/mL
C0334771	ST02	P0529	GP_020	Staphylococcus aureus	MRSA; ATCC 43300	PSR00152	TP00476-16V	K19	94.07	-10.61	32.00 ug/mL
C0334771	ST02	P0529	GP_020	Staphylococcus aureus	MRSA; ATCC 43300	PSR00152	TP00476-15V	K19	95.28	-7.85	32.00 ug/mL
C0334771	ST02	P0529	GN_003	Klebsiella pneumoniae	MDR; ATCC 700603	PSR00152	TP00476-04C	K19	41.89	-2.67	32.00 ug/mL
C0334783	ST14	P0529	GN_042	Pseudomonas aeruginosa	ATCC 27853	PSR00152	TP00476-08C	M21	7.86	0.00	32.00 ug/mL
C0334783	ST14	P0529	FG_001	Candida albicans	ATCC 90028	PSR00152	TP00476-20F	M21	5.12	-0.31	32.00 ug/mL
C0334783	ST14	P0529	GN_042	Pseudomonas aeruginosa	ATCC 27853	PSR00152	TP00476-07C	M21	5.51	0.50	32.00 ug/mL
C0334783	ST14	P0529	FG_001	Candida albicans	ATCC 90028	PSR00152	TP00476-19F	M21	3.93	-0.28	32.00 ug/mL
C0334783	ST14	P0529	GN_034	Acinetobacter baumannii	ATCC 19606	PSR00152	TP00476-05C	M21	89.36	-7.85	32.00 ug/mL
C0334783	ST14	P0529	GN_034	Acinetobacter baumannii	ATCC 19606	PSR00152	TP00476-06C	M21	92.68	-10.40	32.00 ug/mL
C0334783	ST14	P0529	GN_001	Escherichia coli	ATCC 25922	PSR00152	TP00476-01C	M21	92.46	-18.15	32.00 ug/mL
C0334783	ST14	P0529	GN_001	Escherichia coli	ATCC 25922	PSR00152	TP00476-02C	M21	91.79	-17.17	32.00 ug/mL
C0334783	ST14	P0529	GN_003	Klebsiella pneumoniae	MDR; ATCC 700603	PSR00152	TP00476-03C	M21	32.40	-4.24	32.00 ug/mL
C0334783	ST14	P0529	FG_002	Cryptococcus neoformans	H99; ATCC 208821	PSR00152	TP00476-17F	M21	108.88	-13.22	32.00 ug/mL
C0334783	ST14	P0529	FG_002	Cryptococcus neoformans	H99; ATCC 208821	PSR00152	TP00476-18F	M21	105.19	-7.75	32.00 ug/mL
C0334783	ST14	P0529	GP_020	Staphylococcus aureus	MRSA; ATCC 43300	PSR00152	TP00476-16V	M21	85.85	-9.55	32.00 ug/mL
C0334783	ST14	P0529	GP_020	Staphylococcus aureus	MRSA; ATCC 43300	PSR00152	TP00476-15V	M21	86.05	-7.02	32.00 ug/mL
C0334783	ST14	P0529	GN_003	Klebsiella pneumoniae	MDR; ATCC 700603	PSR00152	TP00476-04C	M21	26.66	-1.30	32.00 ug/mL
C0334772	ST03	P0529	GN_042	Pseudomonas aeruginosa	ATCC 27853	PSR00152	TP00476-08C	K21	2.33	0.83	32.00 ug/mL
C0334772	ST03	P0529	FG_001	Candida albicans	ATCC 90028	PSR00152	TP00476-20F	K21	3.56	0.03	32.00 ug/mL
C0334772	ST03	P0529	GN_042	Pseudomonas aeruginosa	ATCC 27853	PSR00152	TP00476-07C	K21	8.78	-0.06	32.00 ug/mL
C0334772	ST03	P0529	FG_001	Candida albicans	ATCC 90028	PSR00152	TP00476-19F	K21	9.13	-1.59	32.00 ug/mL
C0334772	ST03	P0529	GN_034	Acinetobacter baumannii	ATCC 19606	PSR00152	TP00476-05C	K21	-11.15	1.20	32.00 ug/mL
C0334772	ST03	P0529	GN_034	Acinetobacter baumannii	ATCC 19606	PSR00152	TP00476-06C	K21	-11.54	1.21	32.00 ug/mL

CompoundID	Compc	Project	OrgID	Organism	Strain	PSRunID	TestPlateID	TestIbibition	Zscore	Conc	ConcUni
C0334772	ST03	P0529	GN_001	Escherichia coli	ATCC 25922	PSR00152	TP00476-01C	K21	-7.78	1.36	32.00 ug/mL
C0334772	ST03	P0529	GN_001	Escherichia coli	ATCC 25922	PSR00152	TP00476-02C	K21	-6.96	1.42	32.00 ug/mL
C0334772	ST03	P0529	GN_003	Klebsiella pneumoniae	MDR; ATCC 700603	PSR00152	TP00476-03C	K21	-0.31	0.56	32.00 ug/mL
C0334772	ST03	P0529	FG_002	Cryptococcus neoformans	H99; ATCC 208821	PSR00152	TP00476-17F	K21	-31.70	0.04	32.00 ug/mL
C0334772	ST03	P0529	FG_002	Cryptococcus neoformans	H99; ATCC 208821	PSR00152	TP00476-18F	K21	-18.35	0.44	32.00 ug/mL
C0334772	ST03	P0529	GP_020	Staphylococcus aureus	MRSA; ATCC 43300	PSR00152	TP00476-16V	K21	9.67	0.29	32.00 ug/mL
C0334772	ST03	P0529	GP_020	Staphylococcus aureus	MRSA; ATCC 43300	PSR00152	TP00476-15V	K21	6.69	0.11	32.00 ug/mL
C0334772	ST03	P0529	GN_003	Klebsiella pneumoniae	MDR; ATCC 700603	PSR00152	TP00476-04C	K21	9.18	0.26	32.00 ug/mL
C0334784	ST15	P0529	GN_042	Pseudomonas aeruginosa	ATCC 27853	PSR00152	TP00476-08C	O01	98.69	-13.88	32.00 ug/mL
C0334784	ST15	P0529	FG_001	Candida albicans	ATCC 90028	PSR00152	TP00476-20F	O01	101.16	-21.88	32.00 ug/mL
C0334784	ST15	P0529	GN_042	Pseudomonas aeruginosa	ATCC 27853	PSR00152	TP00476-07C	O01	98.38	-15.59	32.00 ug/mL
C0334784	ST15	P0529	FG_001	Candida albicans	ATCC 90028	PSR00152	TP00476-19F	O01	100.00	-24.54	32.00 ug/mL
C0334784	ST15	P0529	GN_034	Acinetobacter baumannii	ATCC 19606	PSR00152	TP00476-05C	O01	97.82	-8.61	32.00 ug/mL
C0334784	ST15	P0529	GN_034	Acinetobacter baumannii	ATCC 19606	PSR00152	TP00476-06C	O01	97.80	-10.97	32.00 ug/mL
C0334784	ST15	P0529	GN_001	Escherichia coli	ATCC 25922	PSR00152	TP00476-01C	O01	97.45	-19.12	32.00 ug/mL
C0334784	ST15	P0529	GN_001	Escherichia coli	ATCC 25922	PSR00152	TP00476-02C	O01	97.91	-18.32	32.00 ug/mL
C0334784	ST15	P0529	GN_003	Klebsiella pneumoniae	MDR; ATCC 700603	PSR00152	TP00476-03C	O01	97.57	-13.82	32.00 ug/mL
C0334784	ST15	P0529	FG_002	Cryptococcus neoformans	H99; ATCC 208821	PSR00152	TP00476-17F	O01	106.09	-12.96	32.00 ug/mL
C0334784	ST15	P0529	FG_002	Cryptococcus neoformans	H99; ATCC 208821	PSR00152	TP00476-18F	O01	100.22	-7.42	32.00 ug/mL
C0334784	ST15	P0529	GP_020	Staphylococcus aureus	MRSA; ATCC 43300	PSR00152	TP00476-16V	O01	95.29	-10.77	32.00 ug/mL
C0334784	ST15	P0529	GP_020	Staphylococcus aureus	MRSA; ATCC 43300	PSR00152	TP00476-15V	O01	98.81	-8.17	32.00 ug/mL
C0334784	ST15	P0529	GN_003	Klebsiella pneumoniae	MDR; ATCC 700603	PSR00152	TP00476-04C	O01	97.64	-7.69	32.00 ug/mL
C0334773	ST04	P0529	GN_042	Pseudomonas aeruginosa	ATCC 27853	PSR00152	TP00476-08C	M01	94.34	-13.22	32.00 ug/mL
C0334773	ST04	P0529	FG_001	Candida albicans	ATCC 90028	PSR00152	TP00476-20F	M01	101.23	-21.90	32.00 ug/mL
C0334773	ST04	P0529	GN_042	Pseudomonas aeruginosa	ATCC 27853	PSR00152	TP00476-07C	M01	94.17	-14.86	32.00 ug/mL
C0334773	ST04	P0529	FG_001	Candida albicans	ATCC 90028	PSR00152	TP00476-19F	M01	100.21	-24.60	32.00 ug/mL
C0334773	ST04	P0529	GN_034	Acinetobacter baumannii	ATCC 19606	PSR00152	TP00476-05C	M01	90.13	-7.92	32.00 ug/mL
C0334773	ST04	P0529	GN_034	Acinetobacter baumannii	ATCC 19606	PSR00152	TP00476-06C	M01	89.45	-10.04	32.00 ug/mL
C0334773	ST04	P0529	GN_001	Escherichia coli	ATCC 25922	PSR00152	TP00476-01C	M01	89.95	-17.66	32.00 ug/mL
C0334773	ST04	P0529	GN_001	Escherichia coli	ATCC 25922	PSR00152	TP00476-02C	M01	91.83	-17.18	32.00 ug/mL
C0334773	ST04	P0529	GN_003	Klebsiella pneumoniae	MDR; ATCC 700603	PSR00152	TP00476-03C	M01	87.36	-12.32	32.00 ug/mL
C0334773	ST04	P0529	FG_002	Cryptococcus neoformans	H99; ATCC 208821	PSR00152	TP00476-17F	M01	91.63	-11.59	32.00 ug/mL
C0334773	ST04	P0529	FG_002	Cryptococcus neoformans	H99; ATCC 208821	PSR00152	TP00476-18F	M01	92.85	-6.93	32.00 ug/mL
C0334773	ST04	P0529	GP_020	Staphylococcus aureus	MRSA; ATCC 43300	PSR00152	TP00476-16V	M01	88.96	-9.95	32.00 ug/mL
C0334773	ST04	P0529	GP_020	Staphylococcus aureus	MRSA; ATCC 43300	PSR00152	TP00476-15V	M01	90.34	-7.41	32.00 ug/mL
C0334773	ST04	P0529	GN_003	Klebsiella pneumoniae	MDR; ATCC 700603	PSR00152	TP00476-04C	M01	88.03	-6.82	32.00 ug/mL
C0334785	ST16	P0529	GN_042	Pseudomonas aeruginosa	ATCC 27853	PSR00152	TP00476-08C	O03	98.38	-13.83	32.00 ug/mL
C0334785	ST16	P0529	FG_001	Candida albicans	ATCC 90028	PSR00152	TP00476-20F	O03	101.73	-22.01	32.00 ug/mL
C0334785	ST16	P0529	GN_042	Pseudomonas aeruginosa	ATCC 27853	PSR00152	TP00476-07C	O03	98.13	-15.55	32.00 ug/mL
C0334785	ST16	P0529	FG_001	Candida albicans	ATCC 90028	PSR00152	TP00476-19F	O03	100.49	-24.67	32.00 ug/mL
C0334785	ST16	P0529	GN_034	Acinetobacter baumannii	ATCC 19606	PSR00152	TP00476-05C	O03	95.52	-8.40	32.00 ug/mL
C0334785	ST16	P0529	GN_034	Acinetobacter baumannii	ATCC 19606	PSR00152	TP00476-06C	O03	96.27	-10.80	32.00 ug/mL
C0334785	ST16	P0529	GN_001	Escherichia coli	ATCC 25922	PSR00152	TP00476-01C	O03	94.91	-18.62	32.00 ug/mL
C0334785	ST16	P0529	GN_001	Escherichia coli	ATCC 25922	PSR00152	TP00476-02C	O03	97.02	-18.15	32.00 ug/mL

CompoundID	Compc	Project	OrgID	Organism	Strain	PSRunID	TestPlateID	TestIbition	Zscore	Conc	ConcUni
C0334785	ST16	P0529	GN_003	Klebsiella pneumoniae	MDR; ATCC 700603	PSR00152	TP00476-03C	O03	95.61	-13.53	32.00 ug/mL
C0334785	ST16	P0529	FG_002	Cryptococcus neoformans	H99; ATCC 208821	PSR00152	TP00476-17F	O03	106.44	-12.99	32.00 ug/mL
C0334785	ST16	P0529	FG_002	Cryptococcus neoformans	H99; ATCC 208821	PSR00152	TP00476-18F	O03	101.88	-7.53	32.00 ug/mL
C0334785	ST16	P0529	GP_020	Staphylococcus aureus	MRSA; ATCC 43300	PSR00152	TP00476-16V	O03	95.22	-10.76	32.00 ug/mL
C0334785	ST16	P0529	GP_020	Staphylococcus aureus	MRSA; ATCC 43300	PSR00152	TP00476-15V	O03	96.26	-7.94	32.00 ug/mL
C0334785	ST16	P0529	GN_003	Klebsiella pneumoniae	MDR; ATCC 700603	PSR00152	TP00476-04C	O03	97.04	-7.63	32.00 ug/mL
C0334774	ST05	P0529	GN_042	Pseudomonas aeruginosa	ATCC 27853	PSR00152	TP00476-08C	M03	46.35	-5.88	32.00 ug/mL
C0334774	ST05	P0529	FG_001	Candida albicans	ATCC 90028	PSR00152	TP00476-20F	M03	8.44	-1.06	32.00 ug/mL
C0334774	ST05	P0529	GN_042	Pseudomonas aeruginosa	ATCC 27853	PSR00152	TP00476-07C	M03	44.04	-6.17	32.00 ug/mL
C0334774	ST05	P0529	FG_001	Candida albicans	ATCC 90028	PSR00152	TP00476-19F	M03	4.14	-0.33	32.00 ug/mL
C0334774	ST05	P0529	GN_034	Acinetobacter baumannii	ATCC 19606	PSR00152	TP00476-05C	M03	84.33	-7.40	32.00 ug/mL
C0334774	ST05	P0529	GN_034	Acinetobacter baumannii	ATCC 19606	PSR00152	TP00476-06C	M03	86.61	-9.72	32.00 ug/mL
C0334774	ST05	P0529	GN_001	Escherichia coli	ATCC 25922	PSR00152	TP00476-01C	M03	85.71	-16.83	32.00 ug/mL
C0334774	ST05	P0529	GN_001	Escherichia coli	ATCC 25922	PSR00152	TP00476-02C	M03	87.17	-16.30	32.00 ug/mL
C0334774	ST05	P0529	GN_003	Klebsiella pneumoniae	MDR; ATCC 700603	PSR00152	TP00476-03C	M03	61.96	-8.58	32.00 ug/mL
C0334774	ST05	P0529	FG_002	Cryptococcus neoformans	H99; ATCC 208821	PSR00152	TP00476-17F	M03	88.50	-11.30	32.00 ug/mL
C0334774	ST05	P0529	FG_002	Cryptococcus neoformans	H99; ATCC 208821	PSR00152	TP00476-18F	M03	84.57	-6.38	32.00 ug/mL
C0334774	ST05	P0529	GP_020	Staphylococcus aureus	MRSA; ATCC 43300	PSR00152	TP00476-16V	M03	75.57	-8.22	32.00 ug/mL
C0334774	ST05	P0529	GP_020	Staphylococcus aureus	MRSA; ATCC 43300	PSR00152	TP00476-15V	M03	79.01	-6.39	32.00 ug/mL
C0334774	ST05	P0529	GN_003	Klebsiella pneumoniae	MDR; ATCC 700603	PSR00152	TP00476-04C	M03	56.06	-3.94	32.00 ug/mL
C0334786	ST17	P0529	GN_042	Pseudomonas aeruginosa	ATCC 27853	PSR00152	TP00476-08C	O05	23.83	-2.44	32.00 ug/mL
C0334786	ST17	P0529	FG_001	Candida albicans	ATCC 90028	PSR00152	TP00476-20F	O05	96.78	-20.90	32.00 ug/mL
C0334786	ST17	P0529	GN_042	Pseudomonas aeruginosa	ATCC 27853	PSR00152	TP00476-07C	O05	25.87	-3.02	32.00 ug/mL
C0334786	ST17	P0529	FG_001	Candida albicans	ATCC 90028	PSR00152	TP00476-19F	O05	96.06	-23.55	32.00 ug/mL
C0334786	ST17	P0529	GN_034	Acinetobacter baumannii	ATCC 19606	PSR00152	TP00476-05C	O05	12.71	-0.94	32.00 ug/mL
C0334786	ST17	P0529	GN_034	Acinetobacter baumannii	ATCC 19606	PSR00152	TP00476-06C	O05	15.91	-1.84	32.00 ug/mL
C0334786	ST17	P0529	GN_001	Escherichia coli	ATCC 25922	PSR00152	TP00476-01C	O05	85.75	-16.84	32.00 ug/mL
C0334786	ST17	P0529	GN_001	Escherichia coli	ATCC 25922	PSR00152	TP00476-02C	O05	87.45	-16.35	32.00 ug/mL
C0334786	ST17	P0529	GN_003	Klebsiella pneumoniae	MDR; ATCC 700603	PSR00152	TP00476-03C	O05	14.09	-1.55	32.00 ug/mL
C0334786	ST17	P0529	FG_002	Cryptococcus neoformans	H99; ATCC 208821	PSR00152	TP00476-17F	O05	92.68	-11.69	32.00 ug/mL
C0334786	ST17	P0529	FG_002	Cryptococcus neoformans	H99; ATCC 208821	PSR00152	TP00476-18F	O05	88.03	-6.61	32.00 ug/mL
C0334786	ST17	P0529	GP_020	Staphylococcus aureus	MRSA; ATCC 43300	PSR00152	TP00476-16V	O05	26.14	-1.83	32.00 ug/mL
C0334786	ST17	P0529	GP_020	Staphylococcus aureus	MRSA; ATCC 43300	PSR00152	TP00476-15V	O05	19.79	-1.06	32.00 ug/mL
C0334786	ST17	P0529	GN_003	Klebsiella pneumoniae	MDR; ATCC 700603	PSR00152	TP00476-04C	O05	34.64	-2.02	32.00 ug/mL
C0334775	ST06	P0529	GN_042	Pseudomonas aeruginosa	ATCC 27853	PSR00152	TP00476-08C	M05	82.00	-11.33	32.00 ug/mL
C0334775	ST06	P0529	FG_001	Candida albicans	ATCC 90028	PSR00152	TP00476-20F	M05	6.32	-0.58	32.00 ug/mL
C0334775	ST06	P0529	GN_042	Pseudomonas aeruginosa	ATCC 27853	PSR00152	TP00476-07C	M05	80.09	-12.42	32.00 ug/mL
C0334775	ST06	P0529	FG_001	Candida albicans	ATCC 90028	PSR00152	TP00476-19F	M05	10.47	-1.93	32.00 ug/mL
C0334775	ST06	P0529	GN_034	Acinetobacter baumannii	ATCC 19606	PSR00152	TP00476-05C	M05	85.32	-7.48	32.00 ug/mL
C0334775	ST06	P0529	GN_034	Acinetobacter baumannii	ATCC 19606	PSR00152	TP00476-06C	M05	88.97	-9.98	32.00 ug/mL
C0334775	ST06	P0529	GN_001	Escherichia coli	ATCC 25922	PSR00152	TP00476-01C	M05	88.07	-17.29	32.00 ug/mL
C0334775	ST06	P0529	GN_001	Escherichia coli	ATCC 25922	PSR00152	TP00476-02C	M05	89.13	-16.67	32.00 ug/mL
C0334775	ST06	P0529	GN_003	Klebsiella pneumoniae	MDR; ATCC 700603	PSR00152	TP00476-03C	M05	77.19	-10.82	32.00 ug/mL
C0334775	ST06	P0529	FG_002	Cryptococcus neoformans	H99; ATCC 208821	PSR00152	TP00476-17F	M05	-31.35	0.01	32.00 ug/mL

CompoundID	Compc	Project	OrgID	Organism	Strain	PSRunID	TestPlateID	TestVibition	Zscore	Conc	ConcUni
C0334775	ST06	P0529	FG_002	Cryptococcus neoformans	H99; ATCC 208821	PSR00152	TP00476-18F	M05	1.20	-0.84	32.00 ug/mL
C0334775	ST06	P0529	GP_020	Staphylococcus aureus	MRSA; ATCC 43300	PSR00152	TP00476-16V	M05	82.48	-9.11	32.00 ug/mL
C0334775	ST06	P0529	GP_020	Staphylococcus aureus	MRSA; ATCC 43300	PSR00152	TP00476-15V	M05	84.79	-6.91	32.00 ug/mL
C0334775	ST06	P0529	GN_003	Klebsiella pneumoniae	MDR; ATCC 700603	PSR00152	TP00476-04C	M05	66.60	-4.89	32.00 ug/mL
C0334787	ST18	P0529	GN_042	Pseudomonas aeruginosa	ATCC 27853	PSR00152	TP00476-08C	O07	10.66	-0.43	32.00 ug/mL
C0334787	ST18	P0529	FG_001	Candida albicans	ATCC 90028	PSR00152	TP00476-20F	O07	7.38	-0.82	32.00 ug/mL
C0334787	ST18	P0529	GN_042	Pseudomonas aeruginosa	ATCC 27853	PSR00152	TP00476-07C	O07	2.66	0.99	32.00 ug/mL
C0334787	ST18	P0529	FG_001	Candida albicans	ATCC 90028	PSR00152	TP00476-19F	O07	6.39	-0.90	32.00 ug/mL
C0334787	ST18	P0529	GN_034	Acinetobacter baumannii	ATCC 19606	PSR00152	TP00476-05C	O07	95.60	-8.41	32.00 ug/mL
C0334787	ST18	P0529	GN_034	Acinetobacter baumannii	ATCC 19606	PSR00152	TP00476-06C	O07	97.48	-10.93	32.00 ug/mL
C0334787	ST18	P0529	GN_001	Escherichia coli	ATCC 25922	PSR00152	TP00476-01C	O07	97.45	-19.12	32.00 ug/mL
C0334787	ST18	P0529	GN_001	Escherichia coli	ATCC 25922	PSR00152	TP00476-02C	O07	96.22	-18.00	32.00 ug/mL
C0334787	ST18	P0529	GN_003	Klebsiella pneumoniae	MDR; ATCC 700603	PSR00152	TP00476-03C	O07	39.66	-5.31	32.00 ug/mL
C0334787	ST18	P0529	FG_002	Cryptococcus neoformans	H99; ATCC 208821	PSR00152	TP00476-17F	O07	107.66	-13.11	32.00 ug/mL
C0334787	ST18	P0529	FG_002	Cryptococcus neoformans	H99; ATCC 208821	PSR00152	TP00476-18F	O07	103.23	-7.62	32.00 ug/mL
C0334787	ST18	P0529	GP_020	Staphylococcus aureus	MRSA; ATCC 43300	PSR00152	TP00476-16V	O07	94.52	-10.67	32.00 ug/mL
C0334787	ST18	P0529	GP_020	Staphylococcus aureus	MRSA; ATCC 43300	PSR00152	TP00476-15V	O07	95.19	-7.84	32.00 ug/mL
C0334787	ST18	P0529	GN_003	Klebsiella pneumoniae	MDR; ATCC 700603	PSR00152	TP00476-04C	O07	32.57	-1.83	32.00 ug/mL
C0334776	ST07	P0529	GN_042	Pseudomonas aeruginosa	ATCC 27853	PSR00152	TP00476-08C	M07	8.02	-0.03	32.00 ug/mL
C0334776	ST07	P0529	FG_001	Candida albicans	ATCC 90028	PSR00152	TP00476-20F	M07	10.56	-1.53	32.00 ug/mL
C0334776	ST07	P0529	GN_042	Pseudomonas aeruginosa	ATCC 27853	PSR00152	TP00476-07C	M07	7.53	0.15	32.00 ug/mL
C0334776	ST07	P0529	FG_001	Candida albicans	ATCC 90028	PSR00152	TP00476-19F	M07	0.00	0.71	32.00 ug/mL
C0334776	ST07	P0529	GN_034	Acinetobacter baumannii	ATCC 19606	PSR00152	TP00476-05C	M07	10.90	-0.78	32.00 ug/mL
C0334776	ST07	P0529	GN_034	Acinetobacter baumannii	ATCC 19606	PSR00152	TP00476-06C	M07	2.22	-0.31	32.00 ug/mL
C0334776	ST07	P0529	GN_001	Escherichia coli	ATCC 25922	PSR00152	TP00476-01C	M07	1.06	-0.35	32.00 ug/mL
C0334776	ST07	P0529	GN_001	Escherichia coli	ATCC 25922	PSR00152	TP00476-02C	M07	6.46	-1.10	32.00 ug/mL
C0334776	ST07	P0529	GN_003	Klebsiella pneumoniae	MDR; ATCC 700603	PSR00152	TP00476-03C	M07	5.84	-0.34	32.00 ug/mL
C0334776	ST07	P0529	FG_002	Cryptococcus neoformans	H99; ATCC 208821	PSR00152	TP00476-17F	M07	-35.71	0.42	32.00 ug/mL
C0334776	ST07	P0529	FG_002	Cryptococcus neoformans	H99; ATCC 208821	PSR00152	TP00476-18F	M07	-0.90	-0.70	32.00 ug/mL
C0334776	ST07	P0529	GP_020	Staphylococcus aureus	MRSA; ATCC 43300	PSR00152	TP00476-16V	M07	12.68	-0.09	32.00 ug/mL
C0334776	ST07	P0529	GP_020	Staphylococcus aureus	MRSA; ATCC 43300	PSR00152	TP00476-15V	M07	12.80	-0.43	32.00 ug/mL
C0334776	ST07	P0529	GN_003	Klebsiella pneumoniae	MDR; ATCC 700603	PSR00152	TP00476-04C	M07	19.09	-0.62	32.00 ug/mL
C0334790	ST21	P0529	GN_042	Pseudomonas aeruginosa	ATCC 27853	PSR00152	TP00476-08C	O13	31.96	-3.68	32.00 ug/mL
C0334790	ST21	P0529	FG_001	Candida albicans	ATCC 90028	PSR00152	TP00476-20F	O13	-0.17	0.87	32.00 ug/mL
C0334790	ST21	P0529	GN_042	Pseudomonas aeruginosa	ATCC 27853	PSR00152	TP00476-07C	O13	28.46	-3.47	32.00 ug/mL
C0334790	ST21	P0529	FG_001	Candida albicans	ATCC 90028	PSR00152	TP00476-19F	O13	5.27	-0.62	32.00 ug/mL
C0334790	ST21	P0529	GN_034	Acinetobacter baumannii	ATCC 19606	PSR00152	TP00476-05C	O13	96.44	-8.49	32.00 ug/mL
C0334790	ST21	P0529	GN_034	Acinetobacter baumannii	ATCC 19606	PSR00152	TP00476-06C	O13	98.13	-11.00	32.00 ug/mL
C0334790	ST21	P0529	GN_001	Escherichia coli	ATCC 25922	PSR00152	TP00476-01C	O13	68.78	-13.54	32.00 ug/mL
C0334790	ST21	P0529	GN_001	Escherichia coli	ATCC 25922	PSR00152	TP00476-02C	O13	70.67	-13.19	32.00 ug/mL
C0334790	ST21	P0529	GN_003	Klebsiella pneumoniae	MDR; ATCC 700603	PSR00152	TP00476-03C	O13	25.53	-3.23	32.00 ug/mL
C0334790	ST21	P0529	FG_002	Cryptococcus neoformans	H99; ATCC 208821	PSR00152	TP00476-17F	O13	17.94	-4.63	32.00 ug/mL
C0334790	ST21	P0529	FG_002	Cryptococcus neoformans	H99; ATCC 208821	PSR00152	TP00476-18F	O13	41.83	-3.54	32.00 ug/mL
C0334790	ST21	P0529	GP_020	Staphylococcus aureus	MRSA; ATCC 43300	PSR00152	TP00476-16V	O13	56.33	-5.73	32.00 ug/mL

CompoundID	Compc	Project	OrgID	Organism	Strain	PSRunID	TestPlateID	TestIbibition	Zscore	Conc	ConcUni
C0334790	ST21	P0529	GP_020	Staphylococcus aureus	MRSA; ATCC 43300	PSR00152	TP00476-15V	O13	56.99	-4.41	32.00 ug/mL
C0334790	ST21	P0529	GN_003	Klebsiella pneumoniae	MDR; ATCC 700603	PSR00152	TP00476-04C	O13	34.08	-1.97	32.00 ug/mL
C0334788	ST19	P0529	GN_042	Pseudomonas aeruginosa	ATCC 27853	PSR00152	TP00476-08C	O09	15.87	-1.23	32.00 ug/mL
C0334788	ST19	P0529	FG_001	Candida albicans	ATCC 90028	PSR00152	TP00476-20F	O09	9.57	-1.31	32.00 ug/mL
C0334788	ST19	P0529	GN_042	Pseudomonas aeruginosa	ATCC 27853	PSR00152	TP00476-07C	O09	18.68	-1.77	32.00 ug/mL
C0334788	ST19	P0529	FG_001	Candida albicans	ATCC 90028	PSR00152	TP00476-19F	O09	6.04	-0.81	32.00 ug/mL
C0334788	ST19	P0529	GN_034	Acinetobacter baumannii	ATCC 19606	PSR00152	TP00476-05C	O09	29.05	-2.42	32.00 ug/mL
C0334788	ST19	P0529	GN_034	Acinetobacter baumannii	ATCC 19606	PSR00152	TP00476-06C	O09	34.32	-3.89	32.00 ug/mL
C0334788	ST19	P0529	GN_001	Escherichia coli	ATCC 25922	PSR00152	TP00476-01C	O09	12.38	-2.55	32.00 ug/mL
C0334788	ST19	P0529	GN_001	Escherichia coli	ATCC 25922	PSR00152	TP00476-02C	O09	16.09	-2.91	32.00 ug/mL
C0334788	ST19	P0529	GN_003	Klebsiella pneumoniae	MDR; ATCC 700603	PSR00152	TP00476-03C	O09	18.30	-2.17	32.00 ug/mL
C0334788	ST19	P0529	FG_002	Cryptococcus neoformans	H99; ATCC 208821	PSR00152	TP00476-17F	O09	-35.54	0.41	32.00 ug/mL
C0334788	ST19	P0529	FG_002	Cryptococcus neoformans	H99; ATCC 208821	PSR00152	TP00476-18F	O09	105.49	-7.77	32.00 ug/mL
C0334788	ST19	P0529	GP_020	Staphylococcus aureus	MRSA; ATCC 43300	PSR00152	TP00476-16V	O09	18.43	-0.83	32.00 ug/mL
C0334788	ST19	P0529	GP_020	Staphylococcus aureus	MRSA; ATCC 43300	PSR00152	TP00476-15V	O09	21.66	-1.23	32.00 ug/mL
C0334788	ST19	P0529	GN_003	Klebsiella pneumoniae	MDR; ATCC 700603	PSR00152	TP00476-04C	O09	18.05	-0.52	32.00 ug/mL
C0334777	ST08	P0529	GN_042	Pseudomonas aeruginosa	ATCC 27853	PSR00152	TP00476-08C	M09	45.26	-5.72	32.00 ug/mL
C0334777	ST08	P0529	FG_001	Candida albicans	ATCC 90028	PSR00152	TP00476-20F	M09	6.46	-0.61	32.00 ug/mL
C0334777	ST08	P0529	GN_042	Pseudomonas aeruginosa	ATCC 27853	PSR00152	TP00476-07C	M09	83.07	-12.94	32.00 ug/mL
C0334777	ST08	P0529	FG_001	Candida albicans	ATCC 90028	PSR00152	TP00476-19F	M09	4.91	-0.53	32.00 ug/mL
C0334777	ST08	P0529	GN_034	Acinetobacter baumannii	ATCC 19606	PSR00152	TP00476-05C	M09	90.52	-7.95	32.00 ug/mL
C0334777	ST08	P0529	GN_034	Acinetobacter baumannii	ATCC 19606	PSR00152	TP00476-06C	M09	89.86	-10.08	32.00 ug/mL
C0334777	ST08	P0529	GN_001	Escherichia coli	ATCC 25922	PSR00152	TP00476-01C	M09	90.27	-17.72	32.00 ug/mL
C0334777	ST08	P0529	GN_001	Escherichia coli	ATCC 25922	PSR00152	TP00476-02C	M09	92.30	-17.27	32.00 ug/mL
C0334777	ST08	P0529	GN_003	Klebsiella pneumoniae	MDR; ATCC 700603	PSR00152	TP00476-03C	M09	67.67	-9.42	32.00 ug/mL
C0334777	ST08	P0529	FG_002	Cryptococcus neoformans	H99; ATCC 208821	PSR00152	TP00476-17F	M09	-40.06	0.83	32.00 ug/mL
C0334777	ST08	P0529	FG_002	Cryptococcus neoformans	H99; ATCC 208821	PSR00152	TP00476-18F	M09	-14.14	0.16	32.00 ug/mL
C0334777	ST08	P0529	GP_020	Staphylococcus aureus	MRSA; ATCC 43300	PSR00152	TP00476-16V	M09	86.55	-9.64	32.00 ug/mL
C0334777	ST08	P0529	GP_020	Staphylococcus aureus	MRSA; ATCC 43300	PSR00152	TP00476-15V	M09	88.82	-7.27	32.00 ug/mL
C0334777	ST08	P0529	GN_003	Klebsiella pneumoniae	MDR; ATCC 700603	PSR00152	TP00476-04C	M09	56.48	-3.98	32.00 ug/mL
C0334789	ST20	P0529	GN_042	Pseudomonas aeruginosa	ATCC 27853	PSR00152	TP00476-08C	O11	96.21	-13.50	32.00 ug/mL
C0334789	ST20	P0529	FG_001	Candida albicans	ATCC 90028	PSR00152	TP00476-20F	O11	100.10	-21.64	32.00 ug/mL
C0334789	ST20	P0529	GN_042	Pseudomonas aeruginosa	ATCC 27853	PSR00152	TP00476-07C	O11	97.84	-15.50	32.00 ug/mL
C0334789	ST20	P0529	FG_001	Candida albicans	ATCC 90028	PSR00152	TP00476-19F	O11	100.14	-24.58	32.00 ug/mL
C0334789	ST20	P0529	GN_034	Acinetobacter baumannii	ATCC 19606	PSR00152	TP00476-05C	O11	91.43	-8.04	32.00 ug/mL
C0334789	ST20	P0529	GN_034	Acinetobacter baumannii	ATCC 19606	PSR00152	TP00476-06C	O11	94.31	-10.58	32.00 ug/mL
C0334789	ST20	P0529	GN_001	Escherichia coli	ATCC 25922	PSR00152	TP00476-01C	O11	94.46	-18.54	32.00 ug/mL
C0334789	ST20	P0529	GN_001	Escherichia coli	ATCC 25922	PSR00152	TP00476-02C	O11	88.58	-16.56	32.00 ug/mL
C0334789	ST20	P0529	GN_003	Klebsiella pneumoniae	MDR; ATCC 700603	PSR00152	TP00476-03C	O11	94.86	-13.42	32.00 ug/mL
C0334789	ST20	P0529	FG_002	Cryptococcus neoformans	H99; ATCC 208821	PSR00152	TP00476-17F	O11	109.93	-13.32	32.00 ug/mL
C0334789	ST20	P0529	FG_002	Cryptococcus neoformans	H99; ATCC 208821	PSR00152	TP00476-18F	O11	105.04	-7.74	32.00 ug/mL
C0334789	ST20	P0529	GP_020	Staphylococcus aureus	MRSA; ATCC 43300	PSR00152	TP00476-16V	O11	95.81	-10.84	32.00 ug/mL
C0334789	ST20	P0529	GP_020	Staphylococcus aureus	MRSA; ATCC 43300	PSR00152	TP00476-15V	O11	92.49	-7.60	32.00 ug/mL
C0334789	ST20	P0529	GN_003	Klebsiella pneumoniae	MDR; ATCC 700603	PSR00152	TP00476-04C	O11	95.40	-7.48	32.00 ug/mL

CompoundID	Compc	Project	OrgID	Organism	Strain	PSRunID	TestPlateID	Test	vibition	Zscore	Conc	ConcUni
C0334778	ST09	P0529	GN_042	<i>Pseudomonas aeruginosa</i>	ATCC 27853	PSR00152	TP00476-08C	M11	16.64	-1.34	32.00	ug/mL
C0334778	ST09	P0529	FG_001	<i>Candida albicans</i>	ATCC 90028	PSR00152	TP00476-20F	M11	4.27	-0.12	32.00	ug/mL
C0334778	ST09	P0529	GN_042	<i>Pseudomonas aeruginosa</i>	ATCC 27853	PSR00152	TP00476-07C	M11	13.19	-0.82	32.00	ug/mL
C0334778	ST09	P0529	FG_001	<i>Candida albicans</i>	ATCC 90028	PSR00152	TP00476-19F	M11	7.30	-1.13	32.00	ug/mL
C0334778	ST09	P0529	GN_034	<i>Acinetobacter baumannii</i>	ATCC 19606	PSR00152	TP00476-05C	M11	88.12	-7.74	32.00	ug/mL
C0334778	ST09	P0529	GN_034	<i>Acinetobacter baumannii</i>	ATCC 19606	PSR00152	TP00476-06C	M11	91.06	-10.22	32.00	ug/mL
C0334778	ST09	P0529	GN_001	<i>Escherichia coli</i>	ATCC 25922	PSR00152	TP00476-01C	M11	90.35	-17.74	32.00	ug/mL
C0334778	ST09	P0529	GN_001	<i>Escherichia coli</i>	ATCC 25922	PSR00152	TP00476-02C	M11	92.57	-17.32	32.00	ug/mL
C0334778	ST09	P0529	GN_003	<i>Klebsiella pneumoniae</i>	MDR; ATCC 700603	PSR00152	TP00476-03C	M11	31.71	-4.14	32.00	ug/mL
C0334778	ST09	P0529	FG_002	<i>Cryptococcus neoformans</i>	H99; ATCC 208821	PSR00152	TP00476-17F	M11	-34.84	0.34	32.00	ug/mL
C0334778	ST09	P0529	FG_002	<i>Cryptococcus neoformans</i>	H99; ATCC 208821	PSR00152	TP00476-18F	M11	-14.14	0.16	32.00	ug/mL
C0334778	ST09	P0529	GP_020	<i>Staphylococcus aureus</i>	MRSA; ATCC 43300	PSR00152	TP00476-16V	M11	83.99	-9.31	32.00	ug/mL
C0334778	ST09	P0529	GP_020	<i>Staphylococcus aureus</i>	MRSA; ATCC 43300	PSR00152	TP00476-15V	M11	85.84	-7.00	32.00	ug/mL
C0334778	ST09	P0529	GN_003	<i>Klebsiella pneumoniae</i>	MDR; ATCC 700603	PSR00152	TP00476-04C	M11	34.78	-2.03	32.00	ug/mL
C0334779	ST10	P0529	GN_042	<i>Pseudomonas aeruginosa</i>	ATCC 27853	PSR00152	TP00476-08C	M13	0.65	1.09	32.00	ug/mL
C0334779	ST10	P0529	FG_001	<i>Candida albicans</i>	ATCC 90028	PSR00152	TP00476-20F	M13	9.08	-1.20	32.00	ug/mL
C0334779	ST10	P0529	GN_042	<i>Pseudomonas aeruginosa</i>	ATCC 27853	PSR00152	TP00476-07C	M13	9.86	-0.24	32.00	ug/mL
C0334779	ST10	P0529	FG_001	<i>Candida albicans</i>	ATCC 90028	PSR00152	TP00476-19F	M13	5.69	-0.72	32.00	ug/mL
C0334779	ST10	P0529	GN_034	<i>Acinetobacter baumannii</i>	ATCC 19606	PSR00152	TP00476-05C	M13	-12.69	1.34	32.00	ug/mL
C0334779	ST10	P0529	GN_034	<i>Acinetobacter baumannii</i>	ATCC 19606	PSR00152	TP00476-06C	M13	-11.37	1.19	32.00	ug/mL
C0334779	ST10	P0529	GN_001	<i>Escherichia coli</i>	ATCC 25922	PSR00152	TP00476-01C	M13	-72.65	14.00	32.00	ug/mL
C0334779	ST10	P0529	GN_001	<i>Escherichia coli</i>	ATCC 25922	PSR00152	TP00476-02C	M13	-50.89	9.69	32.00	ug/mL
C0334779	ST10	P0529	GN_003	<i>Klebsiella pneumoniae</i>	MDR; ATCC 700603	PSR00152	TP00476-03C	M13	-33.20	5.39	32.00	ug/mL
C0334779	ST10	P0529	FG_002	<i>Cryptococcus neoformans</i>	H99; ATCC 208821	PSR00152	TP00476-17F	M13	1.91	-3.12	32.00	ug/mL
C0334779	ST10	P0529	FG_002	<i>Cryptococcus neoformans</i>	H99; ATCC 208821	PSR00152	TP00476-18F	M13	33.25	-2.97	32.00	ug/mL
C0334779	ST10	P0529	GP_020	<i>Staphylococcus aureus</i>	MRSA; ATCC 43300	PSR00152	TP00476-16V	M13	47.39	-4.58	32.00	ug/mL
C0334779	ST10	P0529	GP_020	<i>Staphylococcus aureus</i>	MRSA; ATCC 43300	PSR00152	TP00476-15V	M13	28.12	-1.81	32.00	ug/mL
C0334779	ST10	P0529	GN_003	<i>Klebsiella pneumoniae</i>	MDR; ATCC 700603	PSR00152	TP00476-04C	M13	-25.91	3.42	32.00	ug/mL

Method Analysis

Abbr Code	Name	Description	Strain	Organism	Type
Sa	GP_020 <i>Staphylococcus aureus</i>	MRSA	ATCC 43300	Bacteria	G+ve
Ec	GN_001 <i>Escherichia coli</i>	FDA control	ATCC 25922	Bacteria	G-ve
Kp	GN_003 <i>Klebsiella pneumoniae</i>	MDR	ATCC 700603	Bacteria	G-ve
Ab	GN_034 <i>Acinetobacter baumannii</i>	Type strain	ATCC 19606	Bacteria	G-ve
Pa	GN_042 <i>Pseudomonas aeruginosa</i>	Type strain	ATCC 27853	Bacteria	G-ve
Ca	FG_001 <i>Candida albicans</i>	CLSI reference	ATCC 90028	Fungi	Yeast
Cn	FG_002 <i>Cryptococcus neoformans var. grubii</i>	Type strain	H99; ATCC 20882	Fungi	Yeast

Antibacterial data collection

Inhibition of bacterial growth was determined measuring absorbance at 600 nm (OD600), using a Tecan M1000 Pro monochromator plate reader. The percentage of growth inhibition was calculated for each well, using the negative control (media only) and positive control (bacteria without inhibitors) on the same plate as references.

Antifungal data collection

Growth inhibition of *C. albicans* was determined measuring absorbance at 530 nm (OD530), while the growth inhibition of *C. neoformans* was determined measuring the difference in absorbance between 600 and 570 nm (OD600-570), after the addition of resazurin (0.001% final concentration) and incubation at 35 °C for additional 2 h. The absorbance was measured using a Biotek Synergy HTX plate reader. The percentage of growth inhibition was calculated for each well, using the negative control (media only) and positive control (bacteria without inhibitors) on the same plate as references.

Inhibition

Percentage growth inhibition of an individual sample is calculated based on Negative controls (media only) and Positive Controls (bacterial/fungal media without inhibitors). Please note negative inhibition values indicate that the growth rate (or OD600) is higher compared to the Negative Control (Bacteria/fungi only, set to 0% inhibition). The growth rates for all bacteria and fungi has a variation of $\pm 10\%$, which is within the reported normal distribution of bacterial/fungal growth. Any significant variation (or outliers/hits) is identified by the modified Z-Score, and actives are selected by a combination of inhibition value and Z-Score.

Z-Score

Z-Score analysis is done to investigate outliers or hits among the samples. The Z-Score is calculated based on the sample population using a modified Z-Score method which accounts for possible skewed sample population. The modified method uses median and MAD (median average deviation) instead of average and sd, and a scaling factor [Iglewicz, B. & Hoaglin, D. C. Volume 16: How to Detect and Handle Outliers. The ASQC Basic Reference in Quality Control: Statistical Techniques, 1993]: $M(i) = 0.6745 * (x(i) - \text{median}(x))/\text{MAD}$. $M(i)$ values of $> |2.5|$ (absolute) label outliers or hits.

Quality Control

All screening is performed as two replica (n=2), with both replicas on different assay plates, but from single plating and performed in a single screening experiment (microbial incubation). Each individual value is reported in the Table (see ..1 and ..2). In addition, two values are used as quality controls for individual plates: Z'-Factor [$1 - (3 * (sd(NegCtrl)+sd(PosCtrl))/(average(PosCtrl)-average(NegCtrl)))$] and Standard Antibiotic controls at different concentrations (>MIC and < MIC). The plate passes the quality control if Z'-Factor >0.4 and Standards are active and inactive at highest and lowest concentrations, respectively. Data not supplied.

Selection of Actives

A - [Active] Samples with inhibition values equal to or above 80% and abs(Z-Score) above |2.5| for either replicate (n=2 on different plates) were classed as active.

P - [Partial Active] compounds with inhibition values between 50.9% - 79.9% or abs(Z-Score) below |2.5|.

I - Inactive compounds with inhibition values below 50% and/or abs(Z-Score) below |2.5|.

Act_XX

Act_XX: Indicates if a compound is active in any of the assays against a specific organism (Sa, Ec, Kp, Pa, Kp, Ca or Cn), or organism classes (GN: Gram-negative, GP: Gram-positive). Please note that the flag indicates single activities even if the average Inhibition values suggests otherwise, in which case a manual adjustment of the flag might be appropriate.

Act

Act: Indicates the number of organism-classes (GN,GP and FG) the compound has been found active against, 0 = no activity.

Sel

Sel: Indicates compounds that have been selected for further dose response studies, Hit-Confirmation. The selection includes all active as well as compounds with ambiguous results requiring confirmation of activity or inactivity.

APPENDIX2 Docking Results

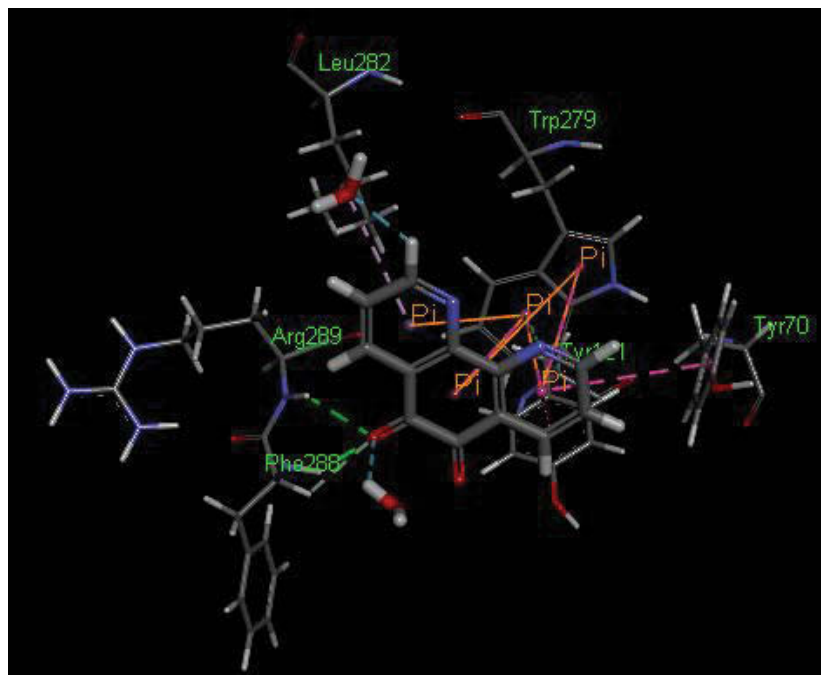


Figure 91: Binding interactions of the highest scoring pose of ST-01 with 2xi4 protein

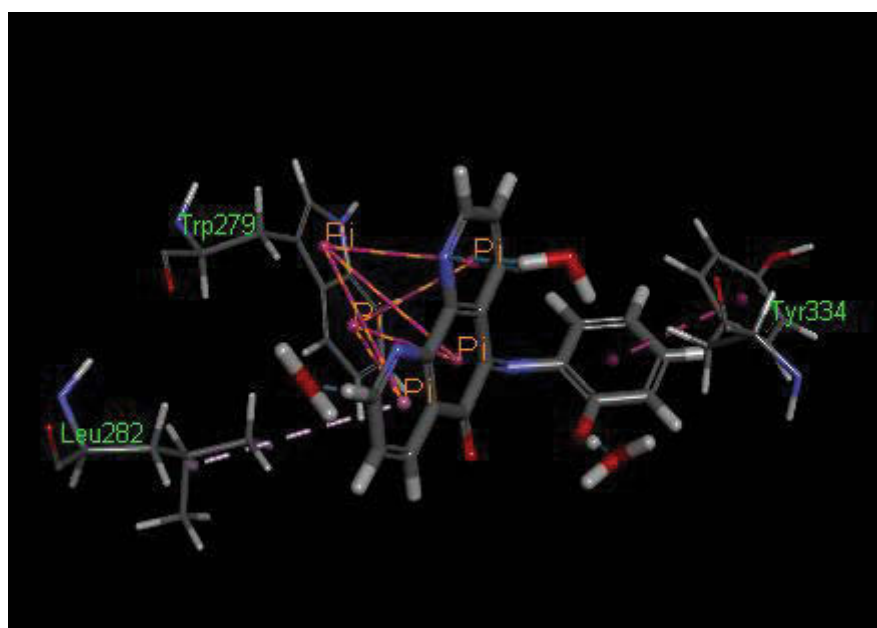


Figure 92: Binding interactions of the highest scoring pose of ST-02 with 2xi4 protein

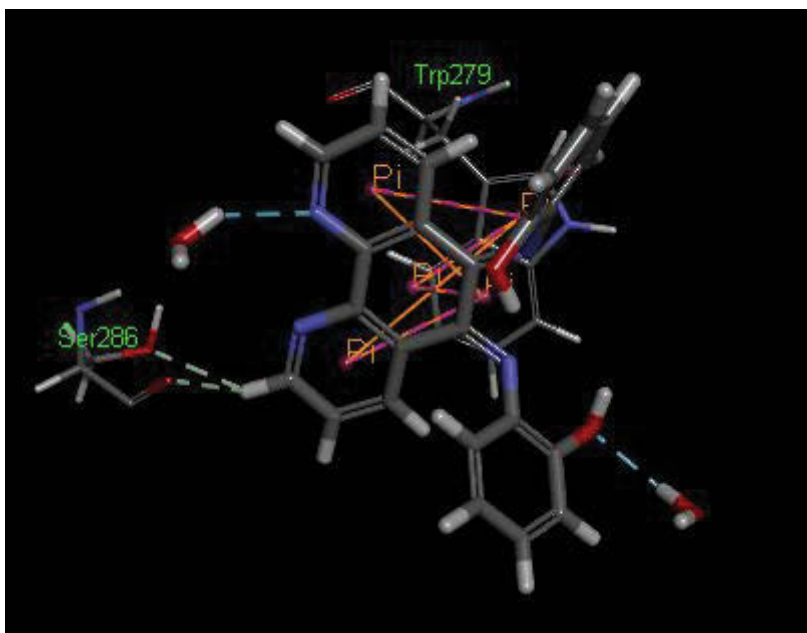


Figure 93: Binding interactions of the highest scoring pose of ST-03 with 2xi4 protein

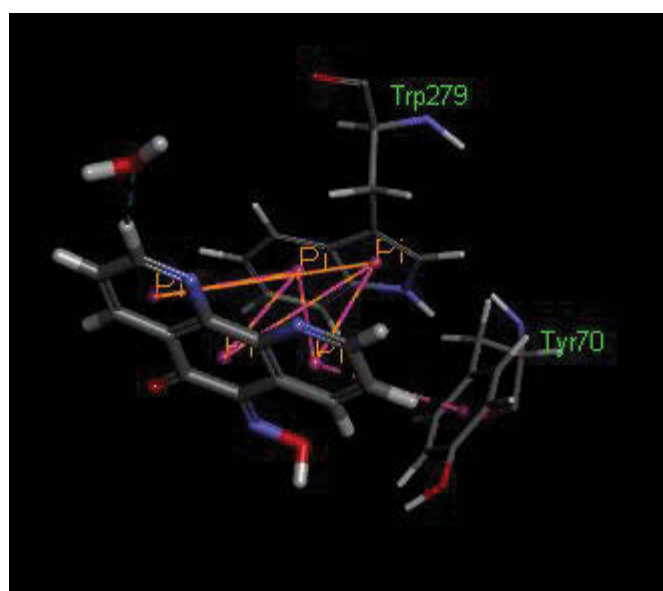


Figure 94: Binding interactions of the highest scoring pose of ST-04 with 2xi4 protein

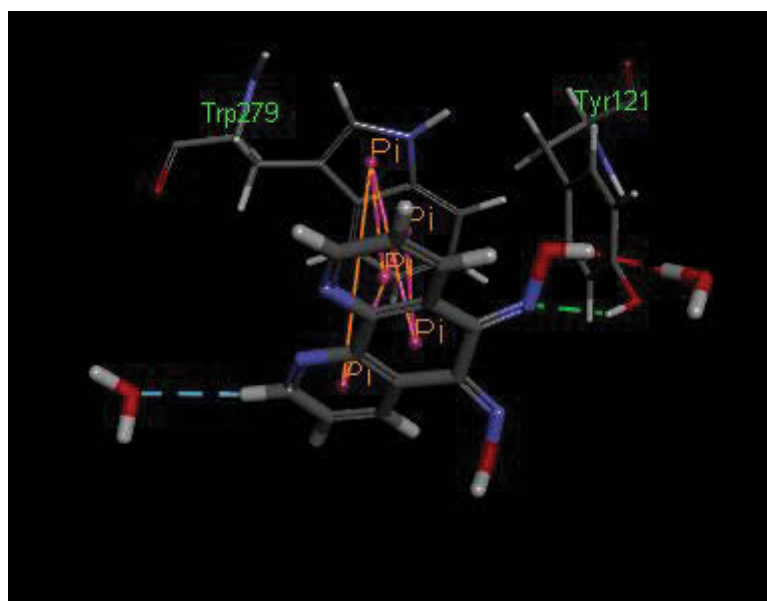


Figure 95: Binding interactions of the highest scoring pose of ST-05 with 2xi4 protein

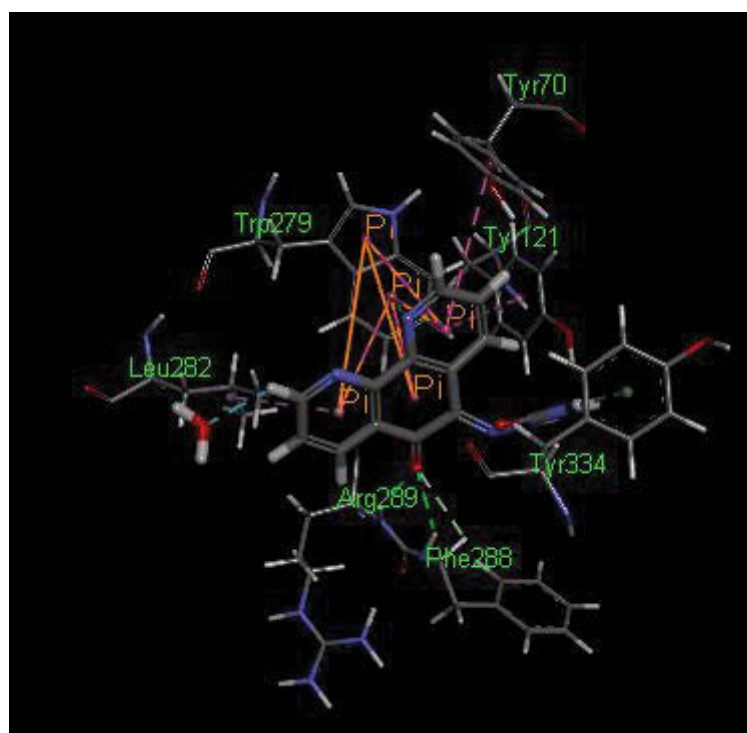


Figure 96: Binding interactions of the highest scoring pose of ST-06 with 2xi4 protein

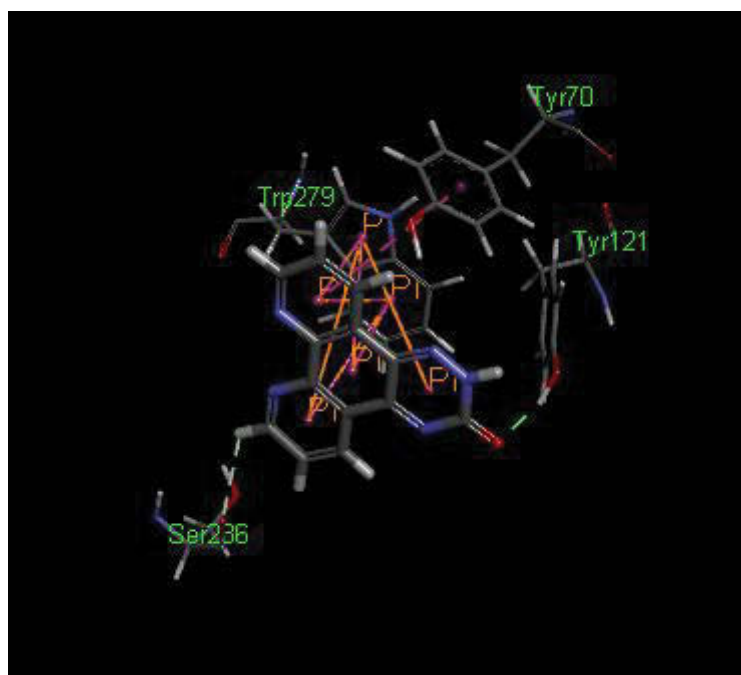


Figure 97: Binding interactions of the highest scoring pose of ST-07 with 2xi4 protein

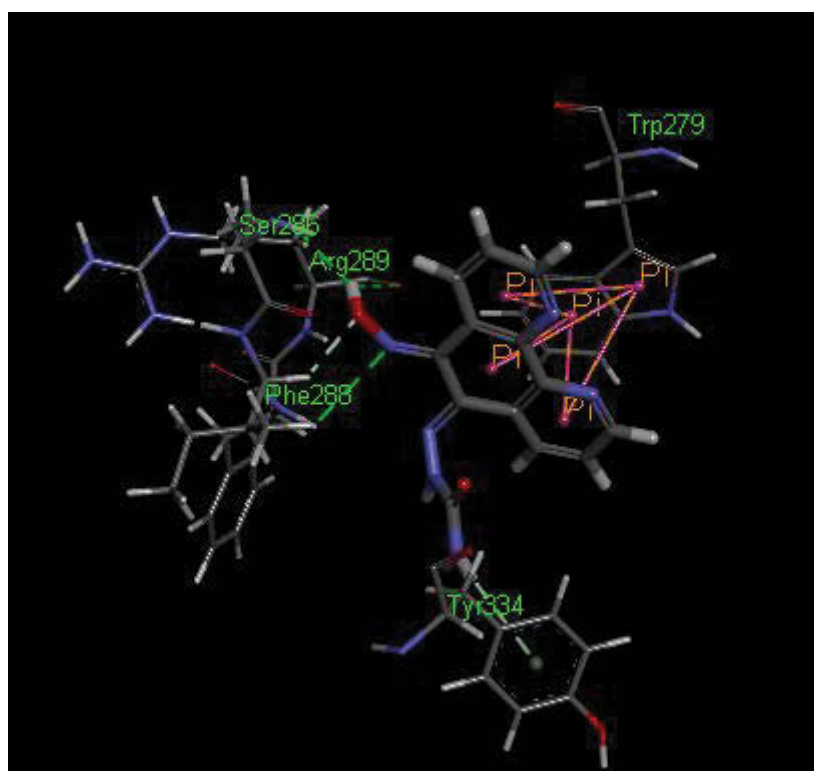


Figure 98: Binding interactions of the highest scoring pose of ST-08 with 2xi4 protein

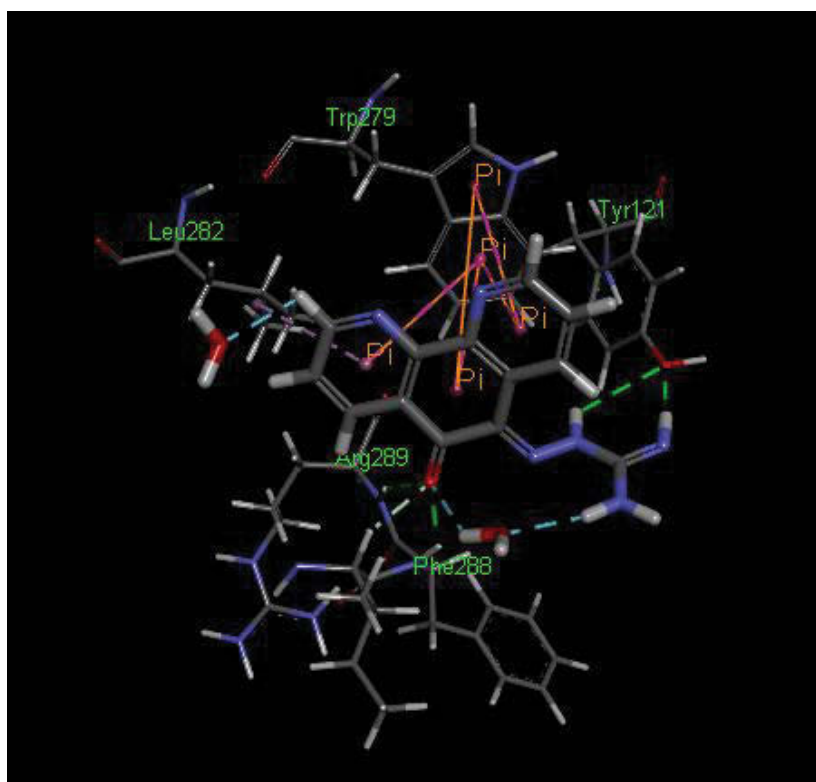


Figure 99: Binding interactions of the highest scoring pose of ST-09 with 2xi4 protein

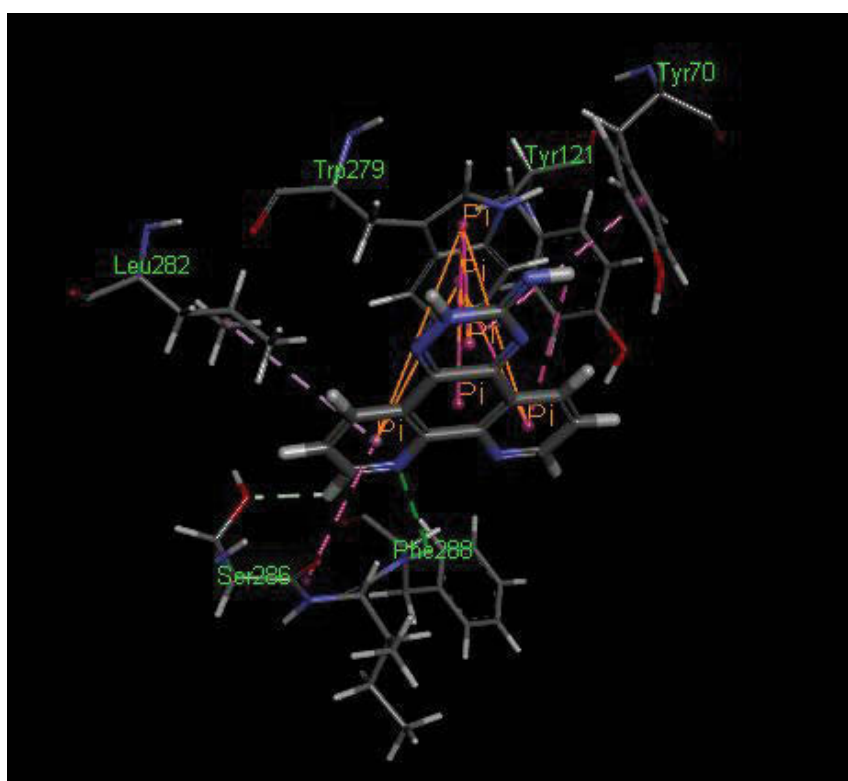


Figure 100: Binding interactions of the highest scoring pose of ST-10 with 2xi4 protein

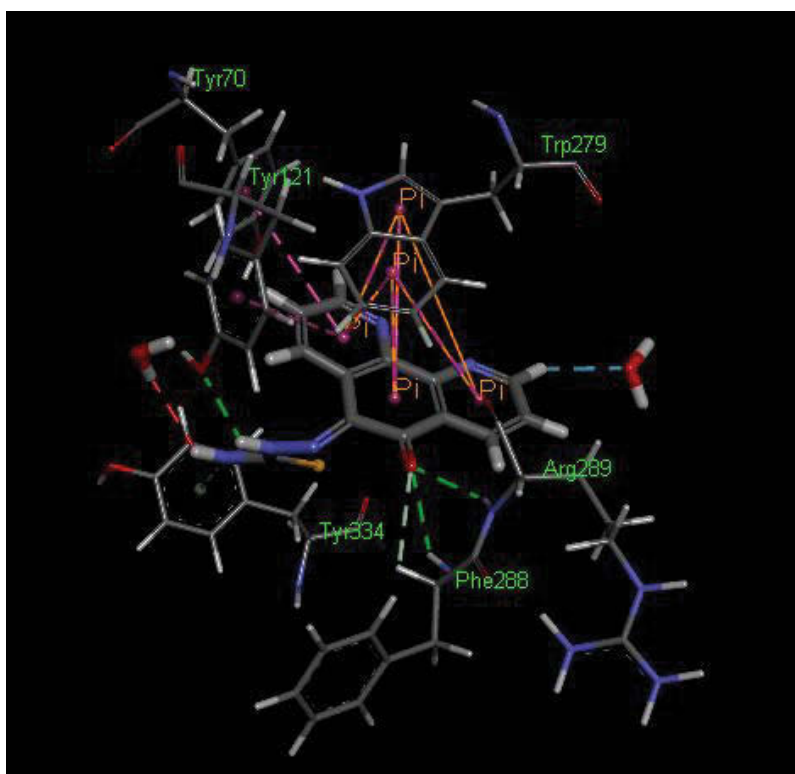


Figure 101: Binding interactions of the highest scoring pose of ST-11 with 2xi4 protein

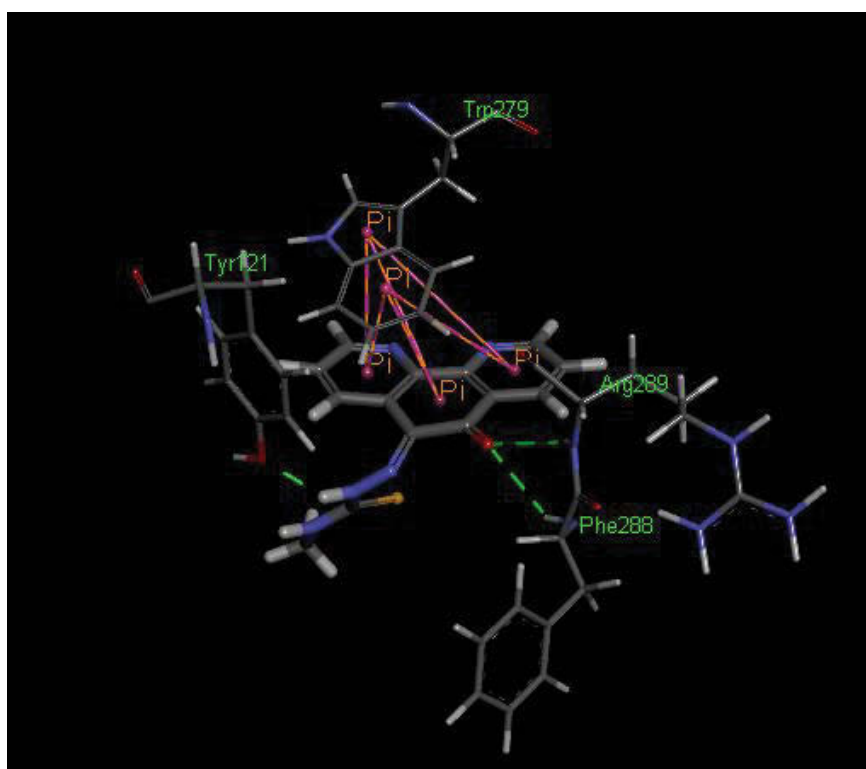


Figure 102: Binding interactions of the highest scoring pose of ST-12 with 2xi4 protein

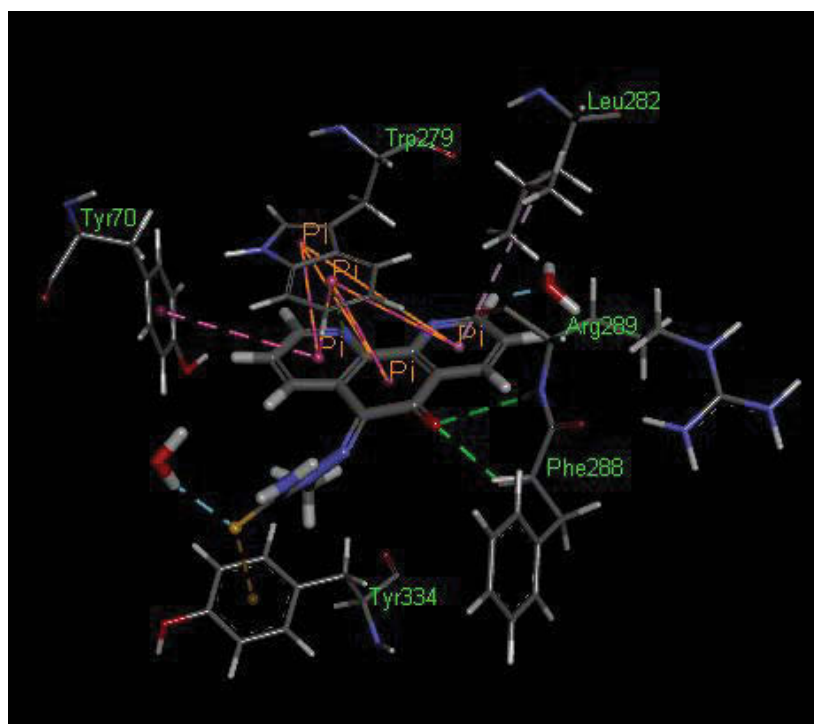


Figure 103: Binding interactions of the highest scoring pose of ST-13 with 2xi4 protein

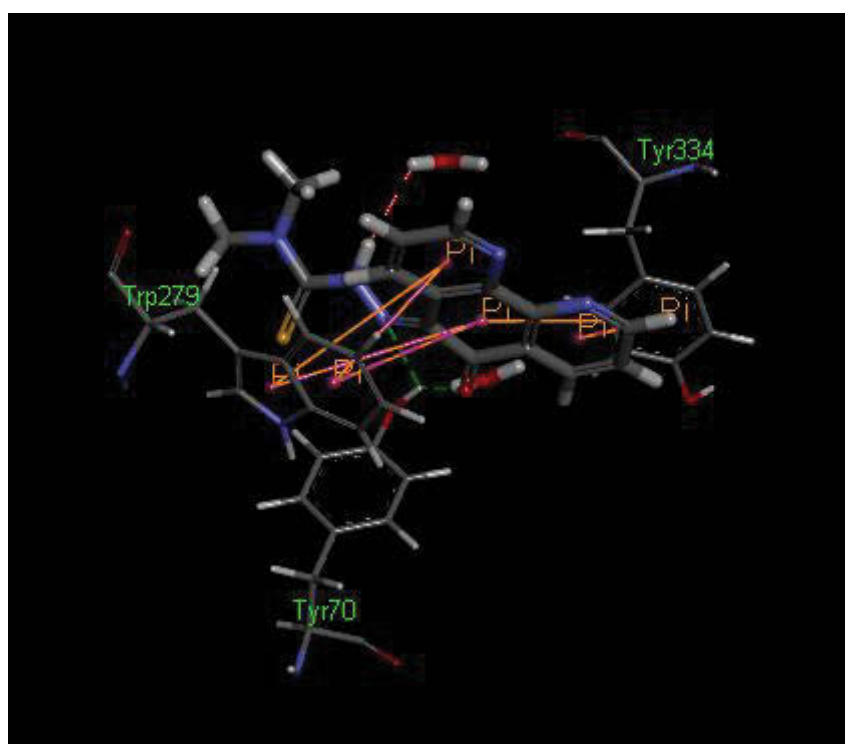


Figure 104: Binding interactions of the highest scoring pose of ST-14 with 2xi4 protein

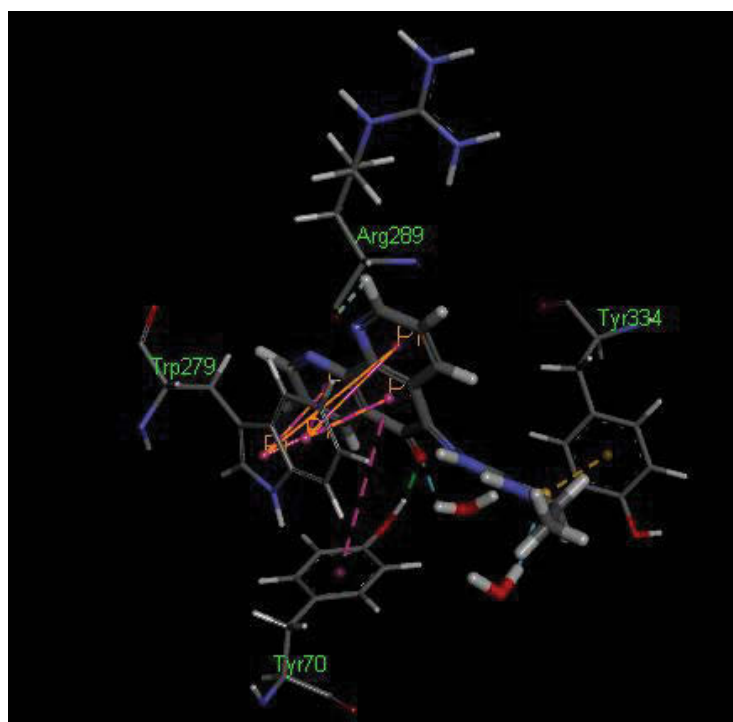


Figure 105: Binding interactions of the highest scoring pose of ST-15 with 2xi4 protein

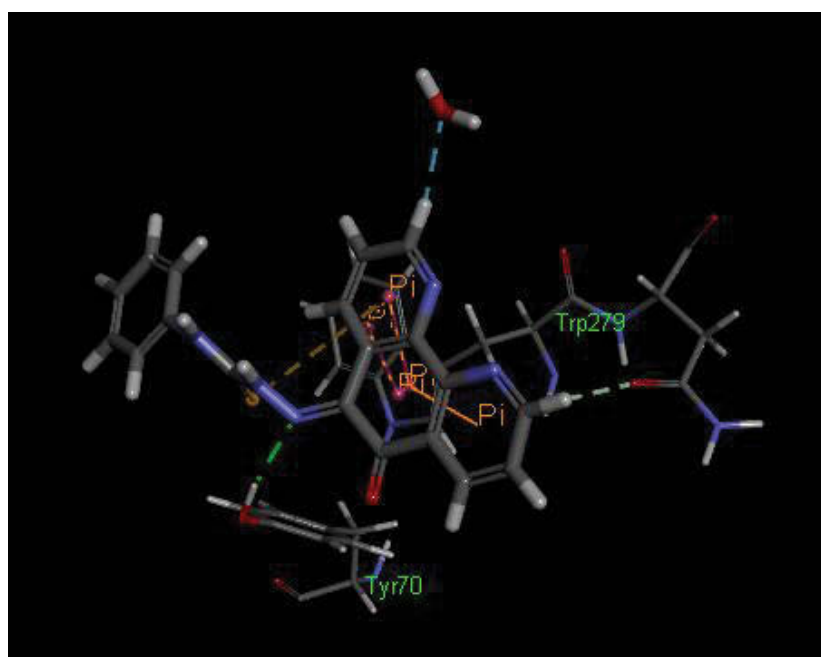


Figure 106: Binding interactions of the highest scoring pose of ST-16 with 2xi4 protein

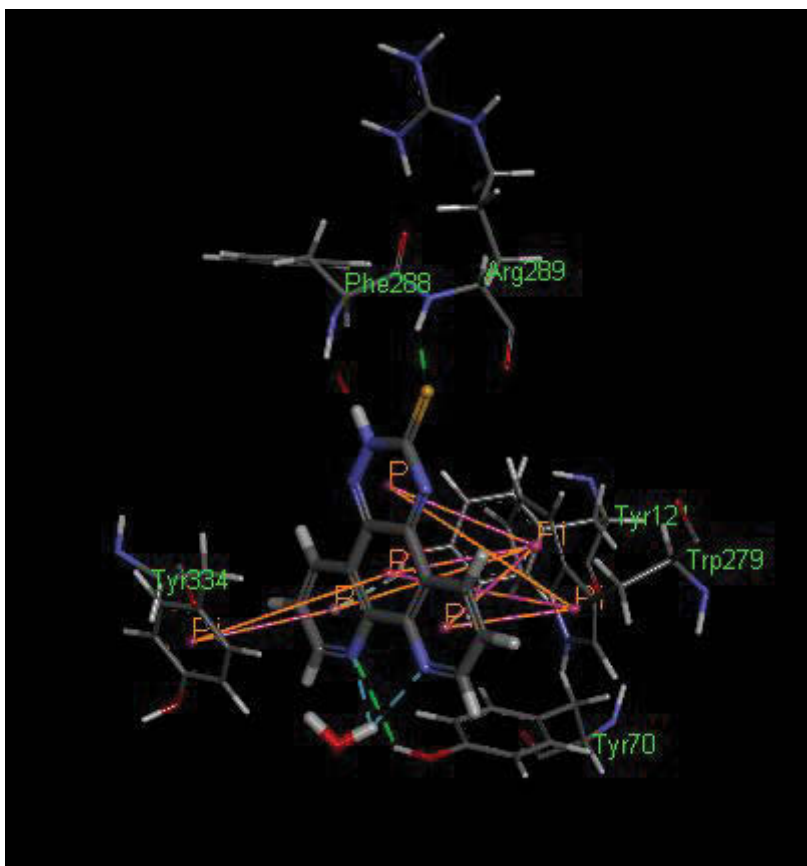


Figure 107: Binding interactions of the highest scoring pose of ST-17 with 2xi4 protein

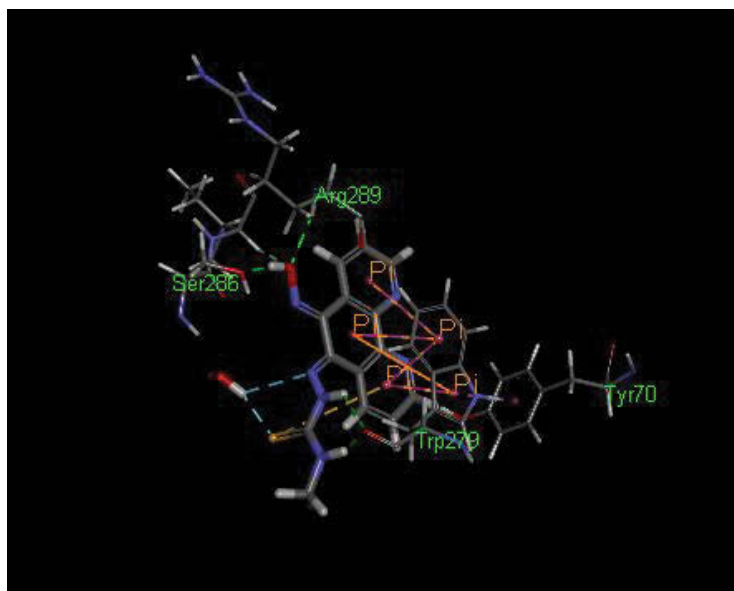


Figure 108: Binding interactions of the highest scoring pose of ST-18 with 2xi4 protein

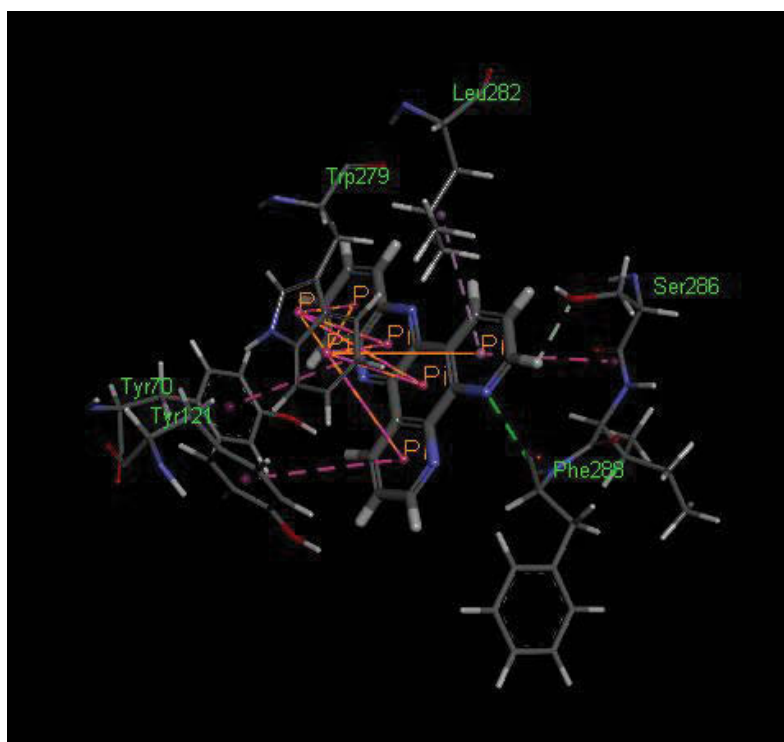


Figure 109: Binding interactions of the highest scoring pose of ST-19 with 2xi4 protein

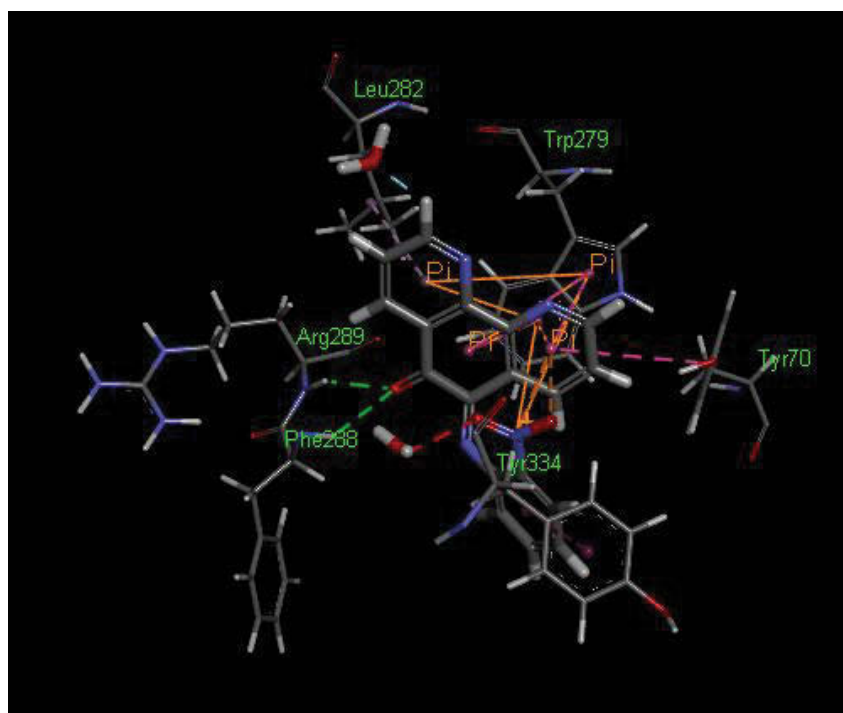


Figure 110: Binding interactions of the highest scoring pose of ST-20 with 2xi4 protein

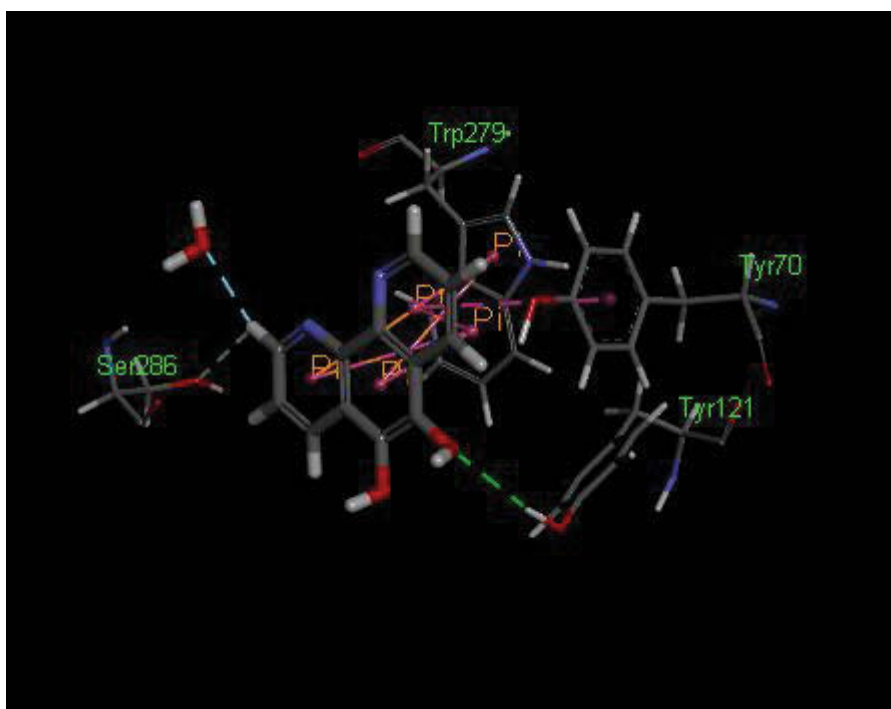


Figure 111: Binding interactions of the highest scoring pose of ST-21 with 2xi4 protein

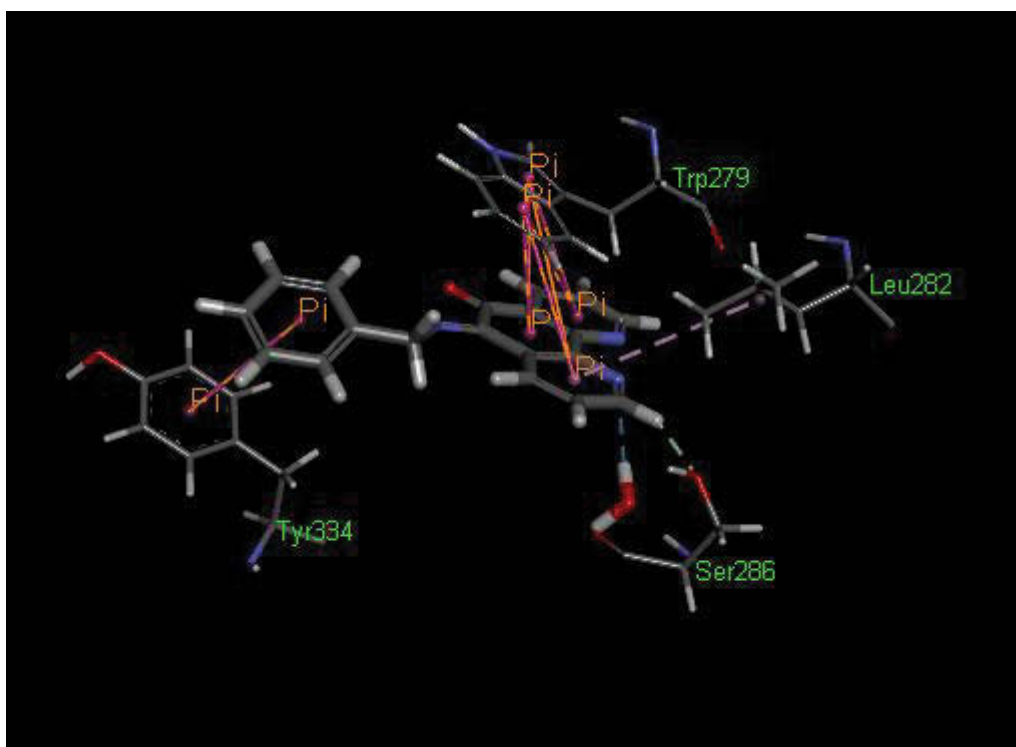


Figure 112: Binding interactions of the highest scoring pose of ST-22 with 2xi4 protein

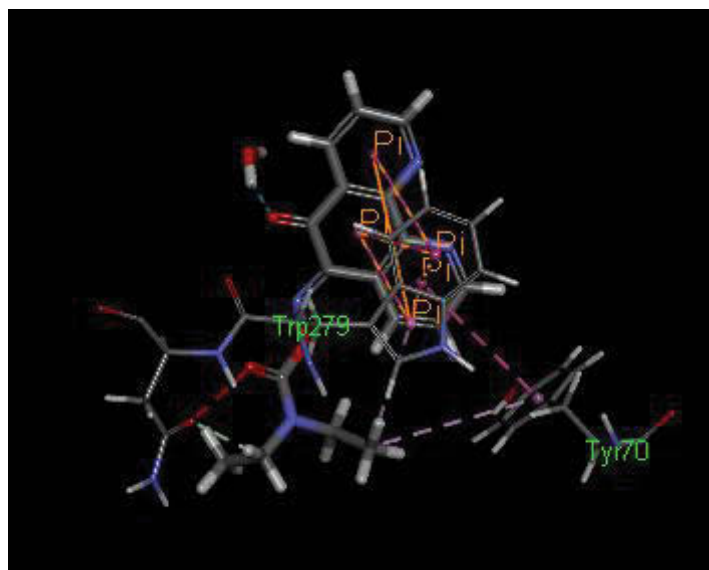


Figure 113: Binding interactions of the highest scoring pose of ST-23 with 2xi4 protein

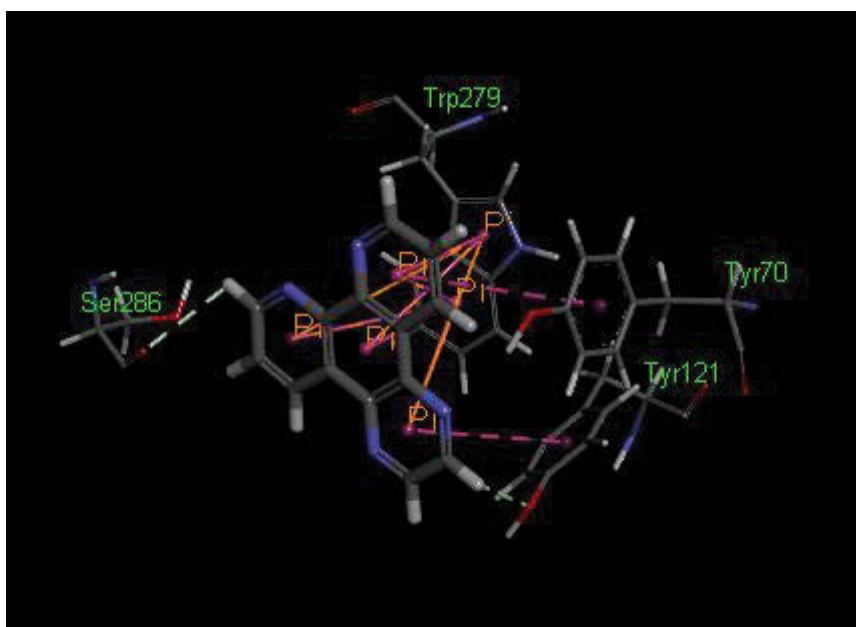


Figure 114: Binding interactions of the highest scoring pose of ST-24 with 2xi4 protein

Docking

--- GOLD DOCKING RUN (GOLD v4.5) ---

GOLD is Genetic Optimisation for Ligand Docking.

GOLD is the result of a collaborative project between Sheffield University, the CCDC and Glaxo Wellcome. GOLD is a proprietary product for which the copyright is held by the Cambridge Crystallographic Data Centre (CCDC)

Please forward any comments, bugs, or queries to CCDC Software Support:

Cambridge Crystallographic Data Centre

12 Union Road

Cambridge CB2 1EZ

tel: (44) (1223) 336022

email: support@ccdc.cam.ac.uk

Input Parameters

Fitness Function	Goldscore
GA Parameters	Automatic
Number of Dockings	100
Detect Cavity	False
Solvate All	False
Generate Diverse Solutions	False
Early Termination	False
Force Constraints	False

Explore Ring Conformations	Rigid
Flip Amide Bonds	False
Flip Planar R-NR1R2	Flip all
Flipping Pyramidal Nitrogens	False
Intramolecular Hydrogen Bonds	False
Protonated Carboxylic Acids	Flip
Fix Rotatable Bonds	None

 --- Parameter setting overview (user-defined or automatic) ---

maxops	automatic setting
popsiz	automatic setting
select_pressure	automatic setting
n_islands	automatic setting
niche_siz	automatic setting
pt_crosswt	automatic setting
allele_mutatewt	automatic setting
migratewt	automatic setting
start_vdw_linear_cutoff	defined by user
initial_virtual_pt_match_max	defined by user

 --- Parameter settings ---

* Population settings

maxops : auto

popsiz : auto
select_pressure : auto
n_islands : auto
niche_siz : auto

* GA settings

pt_crosswt : auto
allele_mutatewt : auto
migratewt : auto

* Search settings

start_vdw_linear_cutoff : 3.000
initial_virtual_pt_match_max : 4.000

* Cavity detection

Cavity detection algorithm : off
Cavity radius : 10.700
Cavity origin : 88.49 49.47 83.21

* Solvent Accessibility

Solvate all H bond donors and acceptors : off

* Ligand treatment

Internal ligand hydrogen bonds : ignored
Flexible ligand ring corners : fixed
Ligand carboxylic OH groups : flip
Ligand amide bonds : fixed

Ligand pyramidal nitrogen groups : fixed

Ligand bond to planar nitrogen groups : allow 180 degrees flip

Ligand planar nitrogen bonds (Ring-NH-R) : can flip

Ligand planar nitrogen bonds (Ring-NRR') : can flip

Flatten amide and trigonal nitrogens : yes

Torsional distributions : are used

Calculating torsional energy of ligand : yes

Ligand energy : relative wrt best tors+vdw+hbond

: reported fitness is adjusted

Post-process ligand bonds : yes

* Protein treatment:

Protein carboxylic OH groups : flip

* Algorithm Settings (from parameter file):

VDW potential (external) : 4-8 LJ potential (no. 1)

VDW potential (external) : 4-8 2-4 split potential (no. 2)

VDW potential (external) : 4-8 1-2 split potential (no. 3)

VDW potential (internal) : 6-12 LJ potential (no. 1)

VDW potential (internal) : 4-8 LJ potential (no. 2)

VDW potential (internal) : slot 3 not used

Weighting for distance matching : squared

Weighting for angle matching : squared

Mapping, second pass results : taking best three

Internal energy : on absolute scale

External energy weight : 1.375

Internal energy weight : 1.000

Length of H bond : 2.900
Angle coding : binary coded
Angle bit length : 8 bits
Allow duplicates in chromosome mappings : yes
Parameter scaling : on
Simplex minimisation after every GA run : yes
Infer hetatm types from residue names : yes
Ligand relaxation : on
Maximum relax distance : 2.000
Maximum relax angle : 60.000
Ionisation dispersion term : external

* Geometric parameters for Fitness Function (from parameter file)

Initial Virtual pt dist max : 4.000
Final Virtual pt dist max : 2.000
Virtual point distance min : 0.500
Virtual point angle min : 60.000
Virtual point angle max : 160.000
Cone virtual point angle min : 120.000
Cone virtual point angle max : 160.000
Contact distance : 10.000
D/A vdw contact weighting : 1.000
Minimum neighbour weighting : 0.200
Mapping second pass distance : 2.000

* Lone pair parameters

Planar LP: minimum angle with plane : 20.000

Planar LP: maximum angle with plane : 90.000

Protein planar acceptors : need only one lp solvated

Solvated point distance : -0.200

* VDW parameters

Border round vdw grid : 4.000

VDW cutoff fraction : 1.500

VDW cutoff distance : 20.000

Number of bins in VDW lookup : 10000

* Specific metal-coordination types

* Other settings

Write statistics : off

Current parameters file :

C:\Program Files (x86)\CCDC\goldsuite-5.3.0\GOLD\gold\gold.params
